Studies aimed at improving the properties of conjugative pCURE plasmids

by

Akram Bakht M Sultan

A thesis submitted to the University of Birmingham for the degree of DOCTOR OF PHILOSOPHY

Institute of Microbiology and Infection
School of Biosciences
College of Life and Environmental Sciences
University of Birmingham

January 2024

Abstract

In recent years, the escalating issue of microbial antibiotic resistance has become a global concern. To reduce this challenge and tackle this problem, we need to act quickly by finding and developing new ways of treating infections different from the usual antibiotics. One promising strategy involves addressing multidrug-resistant infections by displacing the resistance plasmid from bacteria exhibiting resistance. This PhD thesis focuses on the concept of antimicrobial resistance plasmid curing (displacement) through incompatibility, aiming to improve the technology for displacing antibiotic resistance plasmids from bacterial strains. The primary objective was to make a derivative of plasmid pUB307, the basis for the curing plasmid pCURE-F-307, that is resistant to suppression of its conjugative transfer (Fertility Inhibition) by competitor plasmids. Initial results showed that when *traG*, the target gene for the inhibition, was provided on a multi-copy plasmid, Fertility Inhibition was reduced. Based on this finding *traG* was deleted from pUB307 and reinserted at a new location with its own strong promoter. The new plasmid was able to transfer much more efficiently without suppression by other plasmids. This solution is more general than isolating point mutations in *traG* because not all Fertility Inhibition proteins interact with TraG in the same way. This progress could help to increase efficiency of plasmid curing strategies and thus help reduce the spread of antimicrobial resistance plasmids.

Acknowledgments

First of all, I am glad to pass on my deepest gratitude and thanks to God for the support of those who made this work possible. Then, I want to acknowledge everyone who has assisted me and made efforts to help me reach my goal of finishing this thesis.

I extend my appreciation to my supervisor, Prof. Christopher M. Thomas. Prof. Thomas always had an open door, offering support whenever I faced challenges or had questions about my research or writing. He allowed this paper to be my own work while offering guidance whenever needed.

My sincere thanks also go to Dr. Georgina Lloyd, Elton Stephens and all my Colleagues in the S101 lap for the support, insightful discussions, and collaborative spirit.

In conclusion, I want to convey my deep gratitude to my parents, wife, siblings, and friends for their unwavering support and constant encouragement during my years of study and the journey of researching and writing this thesis. This achievement would not have been possible without their steadfast presence.

Table of Contents

List of Figures

Chapter 1

Chapter 2

Chapter 3

Chapter 4

Chapter 5

Chapter 6

List of Tables

Chapter 1

Chapter 2

Chapter 3

Chapter 4

Chapter 5

List of Abbreviations

Amp	Ampicillin
Blast	Basic Local Alignment Search Tool
BSA	Bovine Serum Albumin
Cm	Chloramphenicol
DNA	Deoxyribonucleic Acid
E. coli	*Escherichia coli*
EDTA	Ethylenediamine-Tetra-Acetic Acid
His-tag	Histidine Tagged
ICU	Intensive Care Unit
IPTG	Isopropyl β-D-1-thiogalactopyranoside
Kan	Kanamycin
L-agar	Luria-Bertani agar
L-broth	Luria-Bertani broth
Mpf	Mating Pair Formation
mRNA	Messenger RNA
Nal	Nalidixic Acid
NCBI	National Centre for Biotechnology Information
Nucleotides - A, T, C, G	Adenine, Thymine, Cytosine, Guanine
OD	Optical density
oriT	Origin of transfer
oriV	Origin of vegetative Replication
PCR	Polymerase Chain Reaction

PSKs	Post-segregational Killing Systems
Rif	Rifampicin
SDS	Sodium Dodecyl Sulfate
SDS-PAGE	Sodium Dodecyl Sulfate Polyacrylamide Gel Electrophoresis
SDW	Sterile distilled water
Stm	Streptomycin
T4CP	Type IV Coupling Protein
T4SS	Type IV Secretion Systems
TE	Tris-EDTA
Tet	Tetracycline
Tm	Melting Temperature
Trm	Trimethoprim
WT	Wild-type

Chapter 1: Introduction

1.1 The problem of antibiotic resistance

1.1.1 Antibiotics

Antibiotics are compounds generated by various microorganisms, including fungi, actinomycetes, and bacteria (Ben et al., 2019). The first antibiotic (penicillin) was discovered in 1928 by Alexander Fleming at St Mary's Hospital in London. From 1950 to 1960 was marked a pivotal "golden age" in the realm of antibiotic discovery. During this period, scientists discovered a diverse array of antibiotics belonging to various classes, including cephalosporins and macrolides. This breakthrough significantly broadened the spectrum of bacterial infections that could be successfully treated. The identification of the first instance of a penicillin resistant microorganism occurred around 1960, marking a span of approximately 32 years from discovery to appearance of resistance (Davies and Davies, 2010).

The natural environment contains over two hundred types of antibiotics, categorized into ten primary groups distinguished by their diverse functional and chemical structures (Perry et al., 2016). These groups include aminoglycosides, β-lactams, lincosamides, macrolides, polypeptides, quinolones, sulfonamides, tetracyclines, chloramphenicols, and various others. The initiation of clinical antibiotic use occurred in 1940 (Perry et al., 2016).

Antibiotics could be divided also into two categories: bacteriostatic, which inhibit bacterial replication and growth without necessarily causing cell death, and bactericidal, which directly kill bacterial cells. The optimal antibiotic should target specific functions crucial for the maintenance and reproduction of bacteria (Blair et al., 2015).

Antibiotics exert their mechanisms of action through various processes, including halting the synthesis of the microorganism's cell wall, influencing DNA and RNA metabolism, inhibiting

protein formation, and inducing the loss of the bacterial cell wall (Zhang et al., 2020a). Research on antibiotics is conducted globally to address diseases affecting humans, animals, plants, and other organisms (Zhang et al., 2020a).

1.1.2 Antibiotic resistance

Antibiotics have saved millions of lives and taken a revolutionary role in medicine. However, the rising threat of bacterial resistance to antibiotics, which is the ability of bacteria to live in concentrations of antibiotics which could kill or prevent growth of others of the same species, has reduced the effectiveness of these drugs (Alos, 2014). Bacteria have been on Earth for around three billion years and are skilful at protecting themselves against toxic chemicals (Bennett, 2008).

Microbial antibiotic resistance is one of the most life-threatening issues in recent years, a time bomb waiting to explode, and the repercussions will be dire to all human life if we do not deal with it rapidly and wisely. The United Nations Environment Programme (UNEP) classified antibiotic resistance as one of the top six emerging topics of concern. It mentions that antibiotic resistance should be considered as one of the worldwide challenges that humans face in this century (Tiedje et al., 2019).

The quantity of microbial resistance has increased dramatically in the last 50 years, an effect of using a large amount of antibiotics for various reasons including, medical, agriculture and aquaculture (Bennett, 2008). The number of antibiotic-resistant pathogenic bacterial species and strains is increasing, and many antibiotics are no longer useful in antimicrobial therapy (Llor and Bjerrum, 2014).

The risks associated with human antibiotic use are categorized into significant and minor risks. First, the major risk begins when antibiotics enter the human body, they could interact with the body normal flora, which contains 95% of beneficial bacteria. It might inhibit 800 – 1000 different beneficial bacterial species and this could allow the harmful and pathogenic bacteria to infect the body. The minor risks are that the antibiotic causes metabolic perturbations and alteration of immunological development, which may harm adiposity and bone growth (Cho et al., 2012).

Microbial antibiotic resistance has become a medical issue and Llor and Bjerrum (2014) pointed out that resistant microorganisms are found in hospitals even in intensive care units (ICU) (Llor and Bjerrum, 2014). The number of people who die yearly due to antimicrobial resistance is seven million in the worldwide and the number is predicted to rise to ten million per year in 2050 if people and governments do not deal with it urgently (O'Neill, 2016). Around 25,000 people die every year in Europe due to infections with antibiotic-resistant bacteria (Zhang et al., 2020a). The number of humans who die daily of cancer, diabetes, cholera, measles, and diarrheal diseases amalgamated is lower than the number of people who die from antibiotic resistant bacteria (O'Neill, 2016). As fast as researchers discover new antibiotics, more powerful antibiotic resistant bacteria will occur, making the treatment by antibiotics more difficult (Zhang et al., 2020a).

According to Lerminiaux et al. (2020), the highest number of infections from antibacterial resistant bacteria happened in hospitals and the epidemic is particularly difficult in long term acute care facilities, where over 25% of healthcare associated infections are caused by antibiotic-resistant bacteria (Lerminiaux et al., 2020). Studies from the Centres of Disease Control and Prevention (CDC) in the USA reported that in 2010, 55.7% of patients

discharged from 325 hospitals were treated with antibiotics through their hospital stay while 37.2% of those antibiotic medicines were needless or could be improved (Fridkin et al., 2014).

The presence of bacteria carrying resistance genes in the environment poses not only a pollution hazard but also the potential for the transfer of resistance plasmids from innocuous microorganisms to pathogenic bacteria (Ashbolt et al., 2013). Transfer mechanisms involve mobile genetic elements like integrons, transposons, and plasmids, enabling the transmission of resistance genes to environmental microorganisms. This, in turn, facilitates the horizontal gene transfer between bacteria, as observed in many studies (Zhang et al., 2020b).

Examining the potential for bacteria to become antibiotic-resistant, COVID-19 serves as a compelling example of how microorganisms can profoundly impact the world in economic, health, educational, and social dimensions. According to World Health Organization (WHO), COVID-19 has infected more than 772,052,752 people until this moment with 6,985,278 cases of death (Chen et al., 2024). It also affects all levels of study and various countries shut down schools and universities. Over nine hundred million students were affected during the shutdown (Nicola et al., 2020). Economically, the harm of Covid-19 is expected to be about five hundred billion American dollars and more than 600,000 jobs have been lost due the Covid-19 pandemic in the UK (Goodell, 2020). The consequence to the world stems from the fact that only one untreatable microorganism spread. However, what is the repercussion if we get numerous untreatable antibiotic resistance bacteria (Goodell, 2020).

In recent years, the emergence of widespread drug resistance, pan drug resistance (resistance to all drugs), and multidrug resistance has become increasingly prevalent (Courvalin, 2016).

This trend poses a looming challenge as we anticipate encountering highly aggressive, robust bacteria that are difficult to treat. Compounding this issue is the fact that the pace of antibiotic discovery lags behind the rapid increase in strains that have developed immunity to existing antibiotics currently in circulation (Courvalin, 2016).

Addressing this critical problem involves not only the search for new antibiotics but also the exploration of innovative approaches to reduce the resistance of microorganisms. Molecular engineering, particularly involving plasmids, holds promise in mitigating resistance (Lopatkin et al., 2017). To tackle the global dilemma of antibiotic resistance, decisive actions are imperative, including the development of alternative therapies to antibiotics (Czaplewski et al., 2016a). One proposed solution involves regulating multidrug-resistant infections by displacing the resistance plasmid from the resistant bacteria (Hale et al., 2010).

1.2 Bacterial plasmids

Plasmids are genetic elements within a cell that are able to reproduce freely and normally and have their own mechanisms to regulate their copy number, guaranteeing a stable inheritance through cellular division (Carattoli, 2009). They are relatively small circular or linear DNA strands within the cytoplasm of a bacterium and some have the ability to move between bacteria of various genera and kingdoms by employing a conjugation mechanism (Bennett, 2008). Plasmids lack essential genes crucial for the basic growth and multiplication of cells. However, they prove beneficial under specific environmental conditions (Bennett, 2008). Moreover, they can impart functional advantages to the host, including degradative functions, enhanced virulence, and resistance to antibiotics (Bennett, 2008).

The year 1952 saw Joshua Lederberg making a significant breakthrough by discovering plasmids. The term "plasmid" was introduced to properly classify these entities that were deemed contributors in different capacities - as parasites, symbionts, and organelles. By 1970, they had gained widespread usage in biotechnology and molecular genetic research, marking a significant milestone in the field (Lederberg, 1998). Plasmids play a crucial role in the development of bacterial resistance and the emergence of pathogenic bacteria. By 1970, the usage of the term "plasmid" had surged, with approximately three thousand research articles being published each year on the subject (Lederberg, 1998).

Plasmids typically consist of a genetic "backbone" encompassing genes essential for various genetic functions necessary for replication, transfer, and partitioning, as illustrated in Figure 1.1. These genes exhibit variability among different plasmids and play a crucial role in influencing factors such as host-range, copy number control, and partitioning methods (Del Solar et al., 1998).

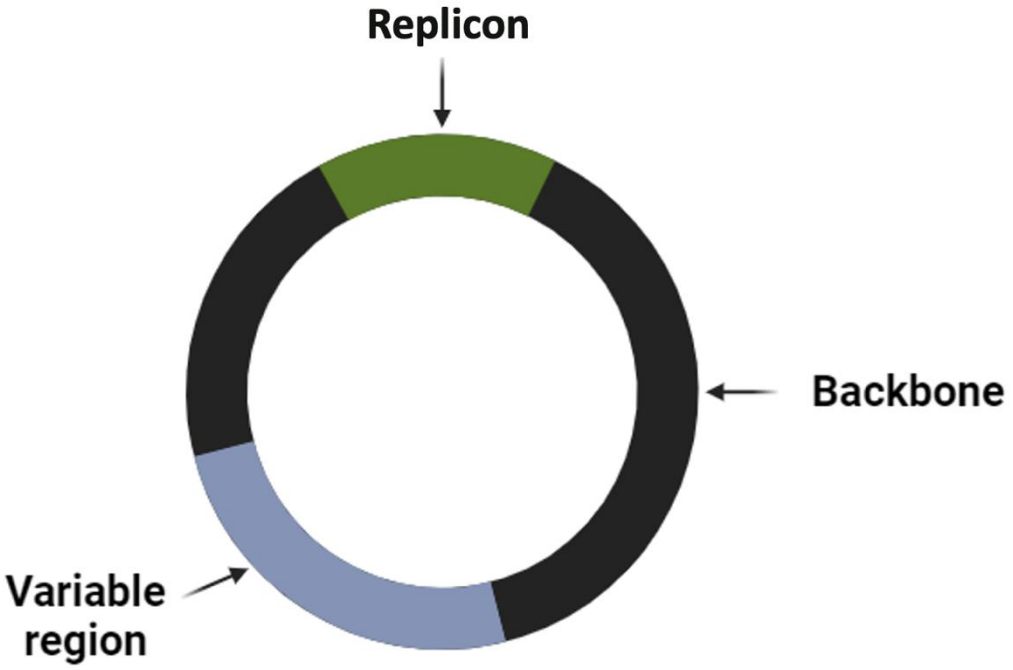

Figure 1. 1 Schematic overview of circular plasmids.

A typical plasmid structure consists of a conserved backbone region containing genes essential for stable inheritance, replication, and, if applicable, transfer or mobilization. In contrast, the variable region contains accessory genes, which often include resistance markers and transposable elements, imparting traits such as antibiotic resistance.

1.2.1 Different mechanisms for plasmid replication

Plasmids are categorized into three primary groups based on their replication mechanisms: rolling circle, strand-displacement and theta (θ) replication (Del Solar et al., 1998). The replicon is a DNA segment that contains one or multiple replication origins and genes necessary for replication control. In addition to managing plasmid functions, replicons also contribute to the coordination of host functions (Rosenfeld and Grover, 1993).

Rolling circle replication is predominantly observed in plasmids carried by Gram-positive hosts. These plasmids, which typically range from 8-30 kbp in size but are usually less than 10 kbp, have a moderate copy number (10-30 copies/chromosome) (Khan, 2005). Replication in these plasmids begins with a site-specific nick, caused by a plasmid-encoded Rep protein, at a specific site known as the double-strand origin (dso) within the *ori*. This nick exposes a 3'OH end that serves as a primer for leading strand synthesis (Ruiz-Masó et al., 2015). After the replication of the leading strand, the original template strand, which has been used for replication, is displaced. This replication leads to the formation of a circular ssDNA molecule that is then released. The release of this newly formed ssDNA molecule is a unique feature of rolling circle replication. The newly released ssDNA molecule then acts as a template for the replication of the lagging strand, which takes place at the single-strand origin (*sso*). The replication of the lagging strand is catalyzed by replication enzymes that are encoded by the host (Ruiz-Masó et al., 2015)

Switching to strand-displacement replication, this process is primarily associated with a specific group of plasmids (such as IncQ) encoding three proteins: RepA, RepB, and RepC (Del Solar et al., 1998). It's worth noting that while these three proteins are commonly found in this group, there may be other plasmids with different protein compositions facilitating similar replication mechanisms (Del Solar et al., 1998).

Theta replication was the subject of comprehensive research in prototypical plasmids commonly found in Gram-negative bacteria. This replication process involves several key steps: the initial melting of the double-stranded parental DNA, the formation of an RNA primer, and the initiation of DNA replication through covalent extension from the RNA primer. Theta replication can occur in either a uni- or bidirectional manner and may originate

from one or multiple origins. The term "theta" is derived from the shape of the replication intermediates, which resemble the Greek letter θ (Del Solar et al., 1998). Theta replication is further classified into four distinct classes (A-D).

Plasmids belonging to Class A, such as RK2, pSC101, F, and R1, rely on Rep proteins for replication initiation. These Rep proteins usually bind to direct repeats, known as iterons, located within the replicon. The binding of Rep proteins to iterons results in initial DNA melting, which is a prerequisite for plasmid replication. Additionally, Rep proteins can interact with DnaA, a replication initiation factor protein that promotes DNA unwinding. Upon recruitment of DnaA, the DnaB helicase protein is also recruited, leading to the opening of the replication fork and assembly of the replisome. Once initiated, replication of theta plasmid strands is coordinated, involving continuous leading strand synthesis and discontinuous lagging strand replication, which predominantly leads to the formation of Okazaki fragments (Lilly and Camps, 2015). It's important to note that while Okazaki fragments are primarily associated with lagging strand synthesis, they may also arise from other aspects of the replication process (Lilly and Camps, 2015).

Class B plasmids, such as ColE1, function similarly to theta replicating plasmids. They do not encode Rep proteins for initial strand melting, but instead rely on host replication and expression factors to transcribe a pre-primer called RNA II. Once RNA II is expressed, it forms a stable RNA-DNA hybrid with the leading strand DNA template in the plasmid ori, resulting in the formation of an R-loop. This R-loop formation allows for the recruitment of RNAseH, which produces a free 3’ OH end that primes the initiation of leading strand synthesis by PolI. PolIII then replicates the lagging strand, as described by (Camps, 2010).

Hybrids of class A and B plasmids are known as class C and D plasmids. ColE2 and ColE3 are examples of class C plasmids, while larger low-copy number plasmids such as pIP501 and pAMβ1 found in Streptococci or Enterococci belong to class D. Class C and D plasmids encode Rep proteins like class A, but their roles are slightly different. In class C, Rep proteins exhibit primase activity, whereas in class D, Rep proteins bind within the *ori* site, allowing the formation of an open complex. Just like class B, both class C and D plasmids use PolI to catalyze leading strand synthesis, which is initiated by the extension of a free 3'OH. According to Lilly and Camps (2015), this is how class C and D plasmids function (Camps, 2010).

1.2.2 Regulation of plasmid replication

In order to prevent overburdening the host and ensure consistent replication and vertical transmission, it is crucial to have methods for tightly controlling plasmid replication. Replicons contain elements that regulate and maintain the replication rate at an average of one event per plasmid copy and cell cycle, by adjusting for deviations from the average copy number in individual cells (Bingle and Thomas, 2001). The mechanisms for controlling copy number in plasmids rely on a negative regulatory system encoded within the plasmid itself. This system employs an inhibitor that can gauge the concentration of plasmid copies in the cell and adjust the rate of replication initiation accordingly. There are three main strategies that plasmids use for this purpose: anti-sense RNA inhibition, anti-sense RNA and protein inhibition, and initiator protein binding sites (Konieczny et al., 2015).

The process of using antisense RNA to regulate copy number involves the utilization of complementary RNA that binds to the 5' end of the target transcript or rep mRNA, also known as counter-transcribed RNA (ctRNA). RNA I, produced from a constitutive promoter,

is inherently unstable due to an RNase E cleavage site. Its expression is directly linked to the plasmid's copy number. This mechanism was elucidated previously and provides a fundamental understanding of plasmid copy number regulation (Wagner and Simons, 1994). In the IncFII plasmid R1, anti-sense RNA is utilized for replication control. The regulation of R1's copy numbers relies on the RepA synthesis level, a process governed by the copA and copB genes. CopA, an RNA molecule prone to instability, complements a specific leader region of the repA mRNA known as CopT. This association is named to align with the regulatory elements' nomenclature within the context of plasmid R1. Contrary to prior understanding, CopT acts as the target for CopA, representing the leader RNA segment of the rep gene that interacts with CopA. When CopA and CopT hybridize, they form a complex that impedes RepA synthesis. The strength of interaction between these components directly influences copy-number regulation, with a weaker interaction leading to higher copy numbers. Additionally, CopB plays a crucial role in maintaining a consistent low-level repression of repA, only being relieved in instances of low copy numbers or during host shifts lacking basal CopB levels (Konieczny et al., 2015).

The second major approach to regulate replication involves the use of anti-sense RNA and a transcriptional repressor. The role of CopB in controlling the copy number of plasmid R1 has been previously discussed, and while CopB does function as a transcriptional repressor, its impact is limited. In plasmid pMV158, CopG suppresses the transcription of *copG* and *repB* by binding to a single promoter. A small ctRNA, RNA II, which is also involved in the copy number control of pMV158, is complementary to a segment of the cop-rep mRNA situated between genes *repB* and *copG*. This method of copy-number control has been observed in theta-replicating plasmids as well (Del Solar et al., 1998).

The third major approach to regulate replication initiation and control copy number involves modulating the interaction between the initiator protein (Rep) and its target sites, such as iterons. While the traditional view may suggest a simple prevention of Rep binding, it is important to note that Rep binding to iterons can exert both positive and negative effects on replication initiation. The outcome is significantly influenced by the dynamic interplay between Rep monomers and dimers. Therefore, effective regulation requires a nuanced understanding of these interactions to finely tune replication control mechanisms. These sites, known as iterons, are directly repeated DNA sequences approximately 20 base pairs in length. The iteron sequences are unique to each plasmid and specifically bind the corresponding initiation protein, Rep (Chattoraj, 2000). The most widely accepted model for explaining copy-number control in iteron-containing plasmids is the handcuffing model. In this model, monomeric Rep proteins bind to iterons located at the origin and saturate them, initiating replication when the copy number is low. As the copy number increases, iteron-bound Rep proteins interact with similar complexes formed on other regions, leading to plasmid pairing through Rep-iteron bound Rep interaction, causing handcuffing and blocking the functions of the origins of the bound plasmids (Chattoraj, 2000)

1.2.3 Plasmid Partitioning

Different plasmids have different methods to ensure even partitioning. High-copy-number plasmids such as ColE1 exist in significant numbers within the host and can usually rely on random distribution to ensure that each daughter cell receives at least one plasmid copy (Wang, 2017). However, low-copy-number plasmids like F or RK2 cannot depend on random distribution and instead employ active partitioning systems that move plasmid copies to opposite ends of the dividing cell, ensuring proper plasmid segregation (Baxter and Funnell,

2015). These segregation systems are similar to the mitotic apparatus of eukaryotic cells and are coded by plasmid gene cassettes called *par*. The *par* cassette normally encodes two proteins, commonly known as ParA and ParB, which act on *parC* and *parS*, two centromere-like elements. The regulation of the Par proteins is essential to prevent irregular partitioning. Homologs of ParA and ParB have been identified in many plasmids, and they function similarly with a tightly controlled mechanism and sites on the plasmids that interact with the encoded proteins (Lu et al., 2013).

1.2.4 post-segregational killing (PSK) systems

Post-segregational killing (PSK) or couple-cell death systems is a phenotype determined by plasmids using a toxin and an antitoxin gene. This mechanism employed by plasmids to ensure their own survival within a bacterial population (Hayes and Van Melderen, 2011), These systems are a form of toxin-antitoxin (TA) system, where the toxin is lethal to the host cell, and the antitoxin counteracts the toxin's effects. The key feature of coupled-cell death systems is if a cell carrying a plasmid undergoes division and the resulting daughter cell fails to inherit a copy of the plasmid, the toxin will persist longer than the antitoxin, leading to the demise of the plasmid-deprived cell (Hayes and Van Melderen, 2011).

Post-segregational killing (PSK) systems are classified into five types (Mruk and Kobayashi, 2014). These systems typically comprise a pair of genes: one encoding a toxin, often a protein that interferes with essential cellular processes, and the other encoding an antitoxin, a molecule that counteracts the toxin's activity. This dynamic interplay between toxin and antitoxin regulates various cellular functions and is crucial for maintaining cellular homeostasis. Toxin-antitoxin systems come in different types, depending on how the antitoxin neutralizes the toxin. Type I systems rely on complementary base-pairing between antitoxin RNA and toxin mRNA. For example, the *hok-sok* system in some gram-negative

bacteria uses this type of mechanism (Gerdes et al., 2005). Type 2 systems involve a labile proteic antitoxin that tightly binds and inhibits the activity of a stable toxin. The CcdA-CcdB system found on the F plasmid of *Escherichia coli* is an example of this type (Lawley et al., 2003). In type 3 systems, the antitoxin RNA directly binds and neutralizes the toxin protein. The ToxI-ToxN system, described in Fineran et al. (2009), is a type 3 system. Type 4 systems, such as *socAB*, are type VI toxin-antitoxin systems discovered in *Caulobacter crescentus*. In this type, the antitoxin, SocA, promotes the degradation of the toxin, SocB, by the protease ClpXP (Fineran et al., 2009). Finally, type 5 systems, including *hha*/*tomB*, *tglT*/*takA*, and *hepT*/*mntA*, neutralize toxin activity by chemically modifying amino acid residues post-translationally (Wang et al., 2012). These different types of toxin-antitoxin systems highlight the adaptability of these systems in ensuring plasmid maintenance and bacterial survival.

1.2.5 Plasmid incompatibility

During the late 1960s, researchers noticed that sometimes when two plasmids were introduced into a bacterial strain, they could not coexist stably. Instead, one of the plasmids would eventually be lost, leaving only the other plasmid in the cell. This phenomenon was not caused by any selective pressure or competition for resources, but rather due to an inherent incompatibility between the plasmids if they were closely related (Novick, 1987).

Plasmid incompatibility is generally defined as the inability of two plasmids present within the same bacterial host to be stably and efficiently inherited in the absence of external selection (Novick, 1987) . Generally, incompatibility is due to plasmids sharing elements of plasmid replication control or partitioning and thus competing with each other for correcting and maintaining normal copy number.

Further experiments involving the introduction of plasmids into bacterial cells provided additional evidence for plasmid incompatibility. Researchers observed that introducing two plasmids from the same incompatibility group into a bacterial strain resulted in the eventual loss of one of the plasmids. However, plasmids from different incompatibility groups could be introduced and stably coexist within the same cell without being lost (Hedges and Datta, 1973).

Incompatibility among plasmids can either be symmetric or asymmetric (Novick, 1987). Asymmetric incompatibility is when one plasmid has a much higher probability of being lost exclusively or at much higher rate, than another incompatible co-resident plasmid. Symmetric incompatibility is when either of the co-resident incompatible plasmids is lost with equal probability, as is generally seen among single replicons that share the same essential maintenance and replication function. In other words, Reciprocal incompatibility may occur when both plasmids face an equal likelihood of being eliminated from a cell line that initially contains both. Alternatively, incompatibility can take a unidirectional form if one of the plasmids possesses additional features that confer a competitive advantage (Thomas, 2021). The classification groups for plasmids in *E. coli* includes: IncF, IncP, IncN, IncW, IncX, IncY, IncZ, IncHI, IncL/M and IncQ (Van Embden et al., 1978)

In general, the discovery of plasmid incompatibility was a significant milestone in the field of molecular biology, as it shed light on the mechanisms of plasmid replication and stability within bacterial cells.

1.2.5.1 Plasmid IncP-1 group.

IncP-1 plasmids constitute a class of self-transmissible plasmids with a moderately low copy number. Their remarkable adaptability is underscored by their ability to replicate across a broad range of hosts, facilitated by highly efficient conjugative transfer mechanisms (Shintani et al., 2010). These plasmids ensure their stability through various mechanisms, including dynamic partitioning, an efficient framework for conjugative exchange, and selective elimination of plasmid-free segregants.

A defining characteristic of IncP-1 plasmids is the presence of a central control operon encoding global regulators that finely modulate gene expression crucial for conjugative transfer, stable maintenance, and vegetative replication (Adamczyk and Jagura-Burdzy, 2003).

1.2.5.1.1 Subgroup Classification and Distribution

IncP-1 plasmids are further classified into six subgroups -α, -β, -γ, -ε, -δ, and ξ, distinguished by the sequence variations in the TrfA protein (Figure 1.2). This diversity reflects the evolutionary adaptations of these plasmids to diverse environmental and ecological niches.

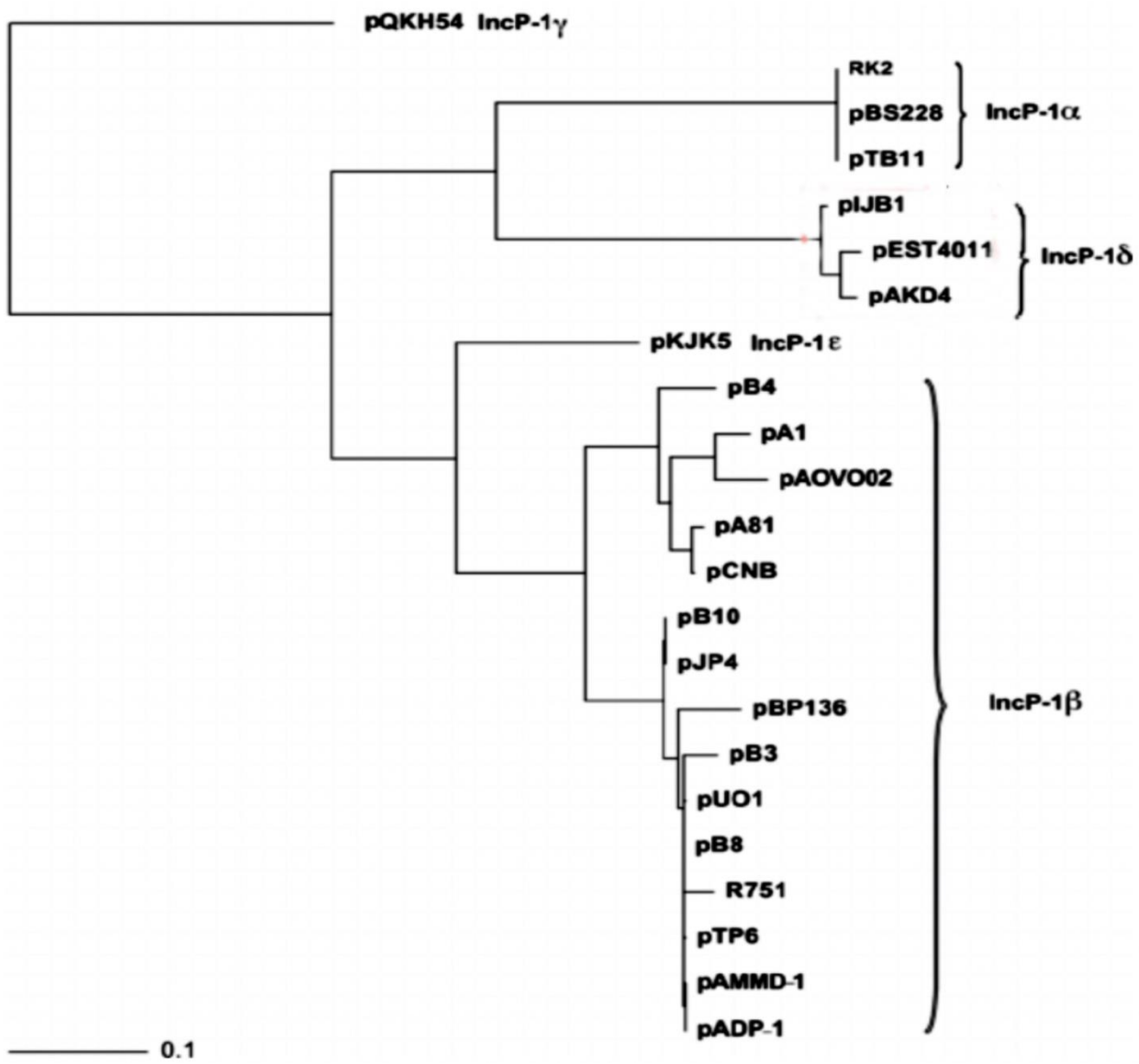

Figure 1. 2 phylogenetic tree depicting the diversity of 55 IncP-1 plasmids (Sen et al., 2010).

The tree is constructed based on the analysis of the conserved region spanning 819 bp within the replication gene *trfA2*. The tree was generated utilizing the maximum-likelihood method and aligning sequences via the muscle program, with the Kimura–Nei method applied for assessment in mega5.

1.2.5.1.2 Functional Architecture and Replication Mechanisms

The genomic architecture of IncP-1 plasmids encompasses regions dedicated to replication, control, and conjugative transfer. The Tra1 region harbors three operons - the relaxase operon, the primase operon, and the leader region operon - orchestrating the intricate processes of DNA processing during conjugative transfer (Pansegrau et al., 1994)

For replication initiation, the *oriV* locus and *trfA* genes are indispensable, with TrfA proteins serving dual roles: activating *oriV* and exerting negative control as (Toukdarian and Helinski, 1998). While TrfA monomers are essential activators, TrfA dimers regulate replication negatively. Importantly, the role of DnaA protein in IncP-1 plasmid replication contrasts with its function in chromosomal replication; here, DnaA acts as a facilitator, aiding in DNA unwinding at the replication origin (Konieczny and Helinski, 1997).

1.2.5.1.3 IncP conjugative transfer and horizontal dissemination.

IncP-1 plasmids employ the conjugation machinery to facilitate horizontal transfer between bacterial hosts, enabling their widespread dissemination across diverse microbial communities (Heinemann and Sprague, 1989). Detailed insights into the mechanisms underlying conjugative transfer are elaborated in Sections 1.3, 1.4, and 1.5.

1.3 Conjugative plasmids

Conjugative plasmids are self-transmissible plasmids capable of horizontally transferring genes through a process called conjugation. Typically, these plasmids consist of four primary gene modules: replication, propagation, stability, and adaptation. The module responsible for the transfer of genes through conjugation is known as the "adaptation" module. All those genes together are accountable for plasmid transfer and maintenance (Norman et al., 2009). The plasmid replication mechanism determines the host range for conjugative plasmids. It is

required to possess the ability to duplicate within all hosts that it passes through (Norman et al., 2009).

Conjugative plasmids employ a specialized machinery for the horizontal transfer of genetic material among bacteria as shown in Figure 1.3. This machinery, important for conjugative DNA replication, forms a nucleoprotein complex. The initiation of transfer involves the cleavage of the phosphodiester bond at a specific position, *nic*, within *oriT*. This reaction is facilitated by a tyrosine residue of the relaxase, leading to the formation of a covalent tyrosinyl-DNA adduct. The relaxase's nicking activity prepares a single strand of plasmid DNA, designated as the T-strand, for transfer (Lanka and Wilkins, 1995).

Subsequently, the single strand of plasmid DNA is recognized by the Type IV Coupling Protein (T4CP), which acts as an adapter or coupling protein. T4CP links the DNA substrate to the Type IV Secretion System, establishing a connection vital for the efficient and specific transfer of genetic material. Upon receiving contact-dependent initiation signals, the relaxase-linked transferred DNA (T-DNA) is likely to be actively pumped through the transport apparatus (Zechner et al., 2012).

In the context of the transfer process, replication in the donor cell occurs concurrently as part of the transfer mechanism. Post-transfer, in the recipient cell, the nicking reaction is reversed, leading to the reformation of the original circular plasmid molecule and the release of the relaxase enzyme. This process is followed by the stabilization of the original plasmid DNA strands through conjugative replication in both the donor and recipient cells (Zechner et al., 2012).

As indicated in section **1.2.5.1.3** the IncPα plasmids are one of the widely studied model systems for conjugative transfer. They have two distinct regions, Tra1 and Tra2, that play key roles. The Tra1 region encompasses both the *oriT* and *tra* genes, responsible for encoding the relaxosome which is essential for initiating the transfer process and DNA processing during transfer (Zechner et al., 2012). This region is organized into two opposing transcriptional units. The first unit includes *traK*, *traL*, and *traM*, while the second unit comprises *traJ*, *traK*, *traI*, *traH*, *traG*, *traF*, *traE*, *traD*, *traC*, *traB*, and *traA* (Pansegrau et al., 1994).

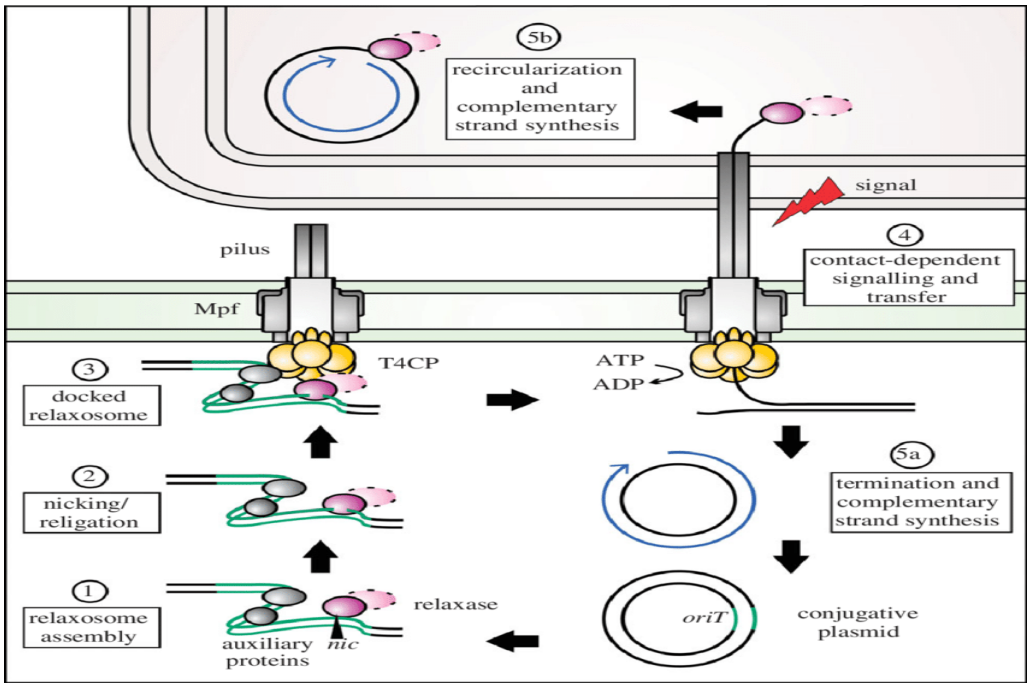

Figure 1. 3 General mechanism of plasmid transfer (Zechner et al., 2012).

The general mechanism of plasmid transfer involves conjugative plasmids equipped with an origin of transfer (*oriT*) and proteins responsible for various functions. These proteins include those for: formation of pili, the multi-protein complex spanning the cell envelope known as the type IV secretion system (T4SS); a coupling protein (T4CP) depicted in yellow; as well as the components of the secretion initiation complex (relaxosome) and the relaxase enzyme responsible for substrate secretion and DNA nicking, shown in pink. Some relaxases may possess bifunctional properties, being fused with helicase or primase domains (illustrated within a dotted oval) to aid in the processing of conjugative DNA. During this process, the transferred DNA (T-DNA) is processed into single-stranded DNA (ssDNA), while its complementary plasmid strand remains circular. The plasmid DNA processing, depicted in stages 1–4, is illustrated with linear DNA fragments for simplification.

1.4 The role of plasmids in the spread of antimicrobial resistance.

Plasmids play a crucial role in the propagation of antimicrobial resistance (AMR) as they enable the transfer of genetic material between bacteria through various mechanisms (Carattoli, 2009).

Among the different mechanisms, conjugation is the most common one, which involves direct cell-to-cell contact, facilitating the exchange of plasmids containing AMR genes from one bacterium to another. This is particularly alarming as it can occur between different bacterial species, which could lead to the widespread dissemination of AMR across a broad spectrum of bacteria (Carattoli, 2013).

Another way that plasmids could spread AMR is through transformation. In this process, bacteria can take up free DNA from their environment, including plasmids carrying AMR genes. Given the potential for plasmids to transfer AMR genes within and between bacterial species, it is essential to remain vigilant in monitoring the spread of AMR to prevent or mitigate the consequences of antibiotic resistance (Partridge et al., 2018).

Transduction is a less common mechanism for plasmid transfer and involves the transfer of genetic material via bacteriophages, which are viruses that infect bacteria. In this process, a bacteriophage infects a bacterium and incorporates the plasmid containing AMR genes into its genome. When the bacteriophage infects another bacterium, it can transfer the plasmid and its AMR genes to the new host (Partridge et al., 2018).

1.5 TraG coupling protein.

The TraG coupling protein is a pivotal component in bacterial conjugation, facilitating the transfer of genetic material, usually in the form of plasmids, between bacteria. Integral to the process are Type IV coupling proteins (T4CPs), of which TraG is one. It is situated within the primase operon and orchestrates the initial interaction between donor and recipient cells, marking a crucial step in conjugation.

The significance of TraG extends beyond mere plasmid transfer; its interaction with TraJ, a membrane protein, is essential for efficient DNA transfer. Although the precise mechanism of this interaction remains incompletely understood, genetic and biochemical evidence strongly supports the physical association between TraG and relaxosome components (Schoder et al., 2002).

Further studies, such as those by Nicholas and Audette (2022), delve into TraG's molecular intricacies. Through a combination of structural and functional analyses, researchers have uncovered specific roles played by TraG within the Type IV Secretion System (T4SS). The N-terminal domain of TraG drives the assembly and stability of conjugative pili, crucial conduits for DNA transfer, while its C-terminal domain coordinates essential components of the T4SS machinery, ensuring fidelity and efficiency in genetic exchange (Nicholas and Audette, 2022).

Such comprehensive understanding underscores TraG's multifaceted importance, not only in bacterial conjugation but also in broader contexts such as bacterial pathogenesis. Additionally, in the context of fertility inhibition, TraG's involvement in the recognition of

inhibitory plasmids is highlighted, further underscoring its significance in microbial genetic exchange.

Researchers have employed a diverse array of approaches, including biochemical assays, genetic studies, and structural analyses, to elucidate TraG's roles and mechanisms, exemplified by the study by Santini and Stanisich (1998). This integrative approach has provided insights into how TraG and associated proteins like PifC achieve inhibition, shedding light on the intricate processes governing bacterial genetic exchange.

AlphaFold, a protein structure prediction method, has been developed by DeepMind - a subsidiary of Alphabet Inc. AlphaFold deploys a neural network architecture known as a transformer to predict the 3D structure of a protein based on its amino acid sequence. It is important to note that the predictions made by AlphaFold are not experimental structures, and therefore should be interpreted with caution (Senior, 2020). A TraG coupling protein structure from *traG* gene was found in AlphaFold Protein Structure Database and with PDB Q5ZHE1. The protein structure shown in Figure 1.4. The AlphaFold Protein Structure is an alternative because X-ray crystal structures for the TraG gene were not available.

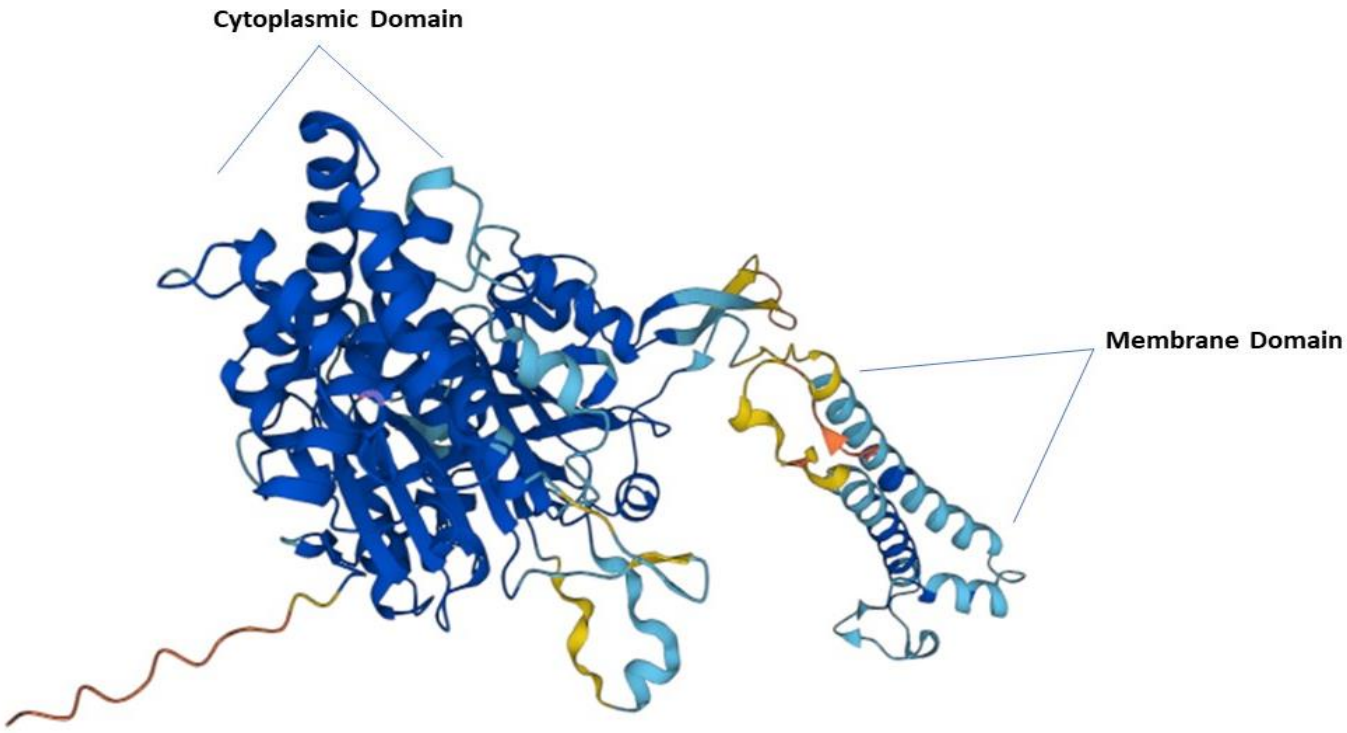

Figure 1. 4 TraG coupling protein Structure (Jumper, 2021).

A structure of TraG coupling protein that has made by AlphaFold. The neural network architecture utilized by AlphaFold to predict the 3D structure of a protein from its amino acid sequence is known as a transformer. However, it is essential to keep in mind that the structures predicted by AlphaFold aren't experimental and should be interpreted with caution, as stated by Senior in 2020.

The phylogenetic tree in Figure 1.5 illustrates the evolutionary relationships among various TraG proteins and their associated proteins. Bootstrap values, indicating the percentage of replicate trees in which the associated taxa clustered together (based on 1000 replicates), are shown next to the branches. The tree is drawn to scale, with branch lengths representing the evolutionary distances computed using the p-distance method, measured as the number of amino acid differences per site. This analysis involved 12 amino acid sequences, with all ambiguous positions removed for each sequence pair using the pairwise deletion option. The final dataset comprised 636 positions. Evolutionary analyses and the construction of the phylogenetic tree were conducted using MEGA11.

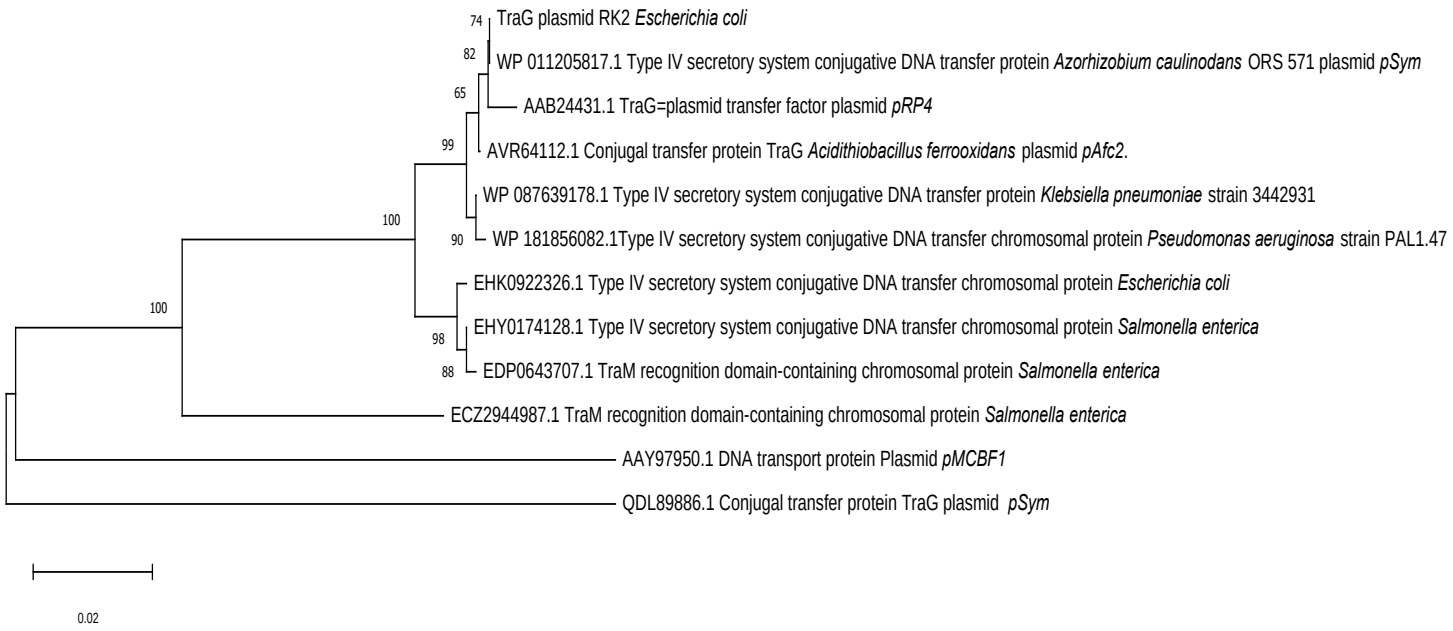

Figure 1. 5 Phylogenetic tree of TraG neighbourhood from RK2 plasmid.

The percentage of replicate trees in which the associated taxa clustered together in the bootstrap test (1000 replicates) are shown next to the branches. The tree is drawn to scale, with branch lengths in the same units as those of the evolutionary distances used to infer the phylogenetic tree. The evolutionary distances were computed using the p-distance method and are in the units of the number of amino acid differences per site. This analysis involved 18 amino acid sequences. All ambiguous positions were removed for each sequence pair (pairwise deletion option). There was a total of 636 positions in the final dataset. Evolutionary analyses were conducted in MEGA11.

1.6 F-like plasmids

In the 1940s, Lederberg and Tatum reported a sexual mating determined by the *E. coli* F "fertility" factor. This led to the discovery and definition of "plasmids" (Lederberg, 1998) as well as the first conjugation system. Nowadays, conjugation is recognised as a primary mechanism of gene transmission that has played a vital role in bacterial evolution (Hu et al., 2019). Plasmids carrying all or part of the same conjugation system as F were grouped together as F-plasmids or F-like plasmids. These plasmids belong to a range of Inc groups FI, FII, FIII etc that are often conjugative and frequently encode antibiotic resistances genes. They contain two entry exclusion systems. They also employ a fertility inhibition system to regulate their own transfer between bacteria (Gubbins et al., 2003). The sizes of these plasmids typically range from 80 to 150 kb and they contain one or more replicons, namely RepFIA, RepFIB, and RepFIC (Mulec et al., 2002). The prevalence of F-like plasmids was studied and showed that in both *E.coli* and *Salmonella*, about 15% of the strains contain F-like plasmids (Boyd et al., 1996).

1.7 Plasmid transfer inhibition.

There are various methods to inhibit the transfer of plasmids, and this study will explore several of them, with a particular focus on fertility inhibition.

1.7.1 Restriction systems

Bacterial defense mechanisms against foreign DNA, such as plasmids, are crucial for preventing the spread of harmful genetic material. Restriction systems play a key role in this regard, consisting of restriction endonucleases that identify specific DNA sequences and cut the DNA at or near those sequences, effectively hindering plasmid transfer between bacteria (Wilson and Murray, 1991).

In addition, all bacteria have a modification system alongside their restriction system that adds methyl groups to specific bases within the bacterial DNA, protecting them from cleavage by the restriction endonucleases. If the same methylation pattern is present on plasmid DNA from the same bacterial strain, the plasmid can be protected. However, if a plasmid from a different bacterial strain enters the host, it may lack the appropriate methylation pattern, making it vulnerable to restriction cleavage (Wilson and Murray, 1991).

1.7.2 CRISPR-Cas system

The CRISPR array is a segment of the bacterial genome consisting of repetitive DNA sequences known as "repeats," interspaced with unique DNA sequences called "spacers." These spacers are acquired from foreign genetic elements encountered by the bacterium, such as viruses or plasmids. The Type II CRISPR-Cas system, exemplified by *Streptococcus pyogenes*, employs the Cas9 protein as its primary effector (Tan et al., 2015).

In the functioning of the Type II CRISPR-Cas system, upon encountering foreign DNA like a virus or plasmid, the bacterium integrates a small segment of that DNA into its CRISPR array through a process known as "acquisition." This segment becomes a new spacer in the array and serves as a molecular memory of past encounters (Makarova et al., 2011).

Subsequently, the CRISPR array is transcribed into a molecule of RNA known as "CRISPR RNA" or crRNA. This crRNA contains a sequence complementary to the spacer acquired from the foreign DNA and acts as a guide to direct the Cas9 protein to the target DNA.

Once bound to the crRNA, the Cas9 protein forms the CRISPR-Cas9 complex, which then scans the bacterial genome and seeks out DNA sequences matching the crRNA. Upon finding a complementary sequence, Cas9 induces a site-specific double-strand break in the target DNA, ultimately leading to the destruction of the foreign genetic element (Makarova et al., 2011).

1.7.3 Fertility inhibition

Plasmid F is derepressed for transfer and many F-like plasmids were found to repress the transfer of F because their control system was intact. These control functions were therefore referred to a Fertility Inhibition (Fin) functions. Further analysis has shown that the transfer of F-like plasmids is controlled through the FinOP fertility inhibition system (Frost et al., 1994). Fertility inhibition (FI) more generally refers to a system capable of diminishing the conjugation capability of plasmids, with numerous mechanisms identified for this purpose (Norman et al., 2009).

The control of expression of the gene for the F positive regulatory protein, TraJ, is controled by the antisense RNA, FinP, and the RNA-binding protein FinO. FinO protects FinP from degradation, facilitating the formation of a structure between FinP and *traJ* mRNA. This interaction leads to the repression of both *traJ* expression and the F conjugative transfer mechanism (Gubbins et al., 2003).

This system, known as the FinOP system, specifically regulates the conjugative transfer of the F plasmid through the control of *traJ* (Garcillán-Barcia and de la Cruz, 2008). Its impact is primarily on the transfer of the F plasmid itself and not on unrelated co-resident plasmids. Several instances have been documented where the conjugative transfer of the F plasmid is hindered by the presence of a second, unrelated plasmid within the same bacterial cell. Six distinct types of fertility inhibition of the F plasmid by various co-resident plasmids have been identified (Willetts and Skurray, 1980a). This highlights the specificity of the FinOP system in regulating the transfer of the F plasmid and its limited effect on non-related co-resident plasmids (Willetts and Skurray, 1980b).

Fertility Inhibition (FI) can serve as both a competitive strategy for limiting the colonization of new hosts and as a defense mechanism against potentially harmful invading genomes. In the context of competition, FI involves inhibiting the transfer of rival plasmids within bacterial populations, thereby reducing their ability to establish in new hosts. This competitive interference aids in maintaining the stability of plasmid populations within bacterial communities (Getino et al., 2017).

Furthermore, FI can function as a defensive response by recipient bacteria against potentially harmful invading genomes. Similar to the concept of restriction-modification systems, where bacterial cells protect themselves against foreign DNA by restricting its replication, FI acts as a safeguard mechanism. By halting the spread of exogenous plasmids that enter a cell within a population, FI helps mitigate the risk posed by these potentially detrimental genetic elements to the bacterial community as a whole (Getino et al., 2017).

1.7.3.1 Fertility inhibition against IncP-1

In the context of IncP-1 plasmids, the mechanism of fertility inhibition involves the orchestrated action of specific genes, notably *pifC* and *osA*, as reviewed by (Getino et al., 2017) . The discovery of these genes and their roles in fertility inhibition represents a significant milestone in understanding the intricate dynamics of plasmid interactions within bacterial populations (Getino et al., 2017). Prior to the work of Getino et al. (2018), seminal studies such as Miller et al. (1985) laid the foundation for unraveling the mechanisms underlying fertility inhibition towards IncP plasmids. Miller et al. (1985) provided crucial insights into how the F plasmid, through its *pifC* gene, selectively inhibits the fertility of plasmid RP4, a member of the IncP incompatibility group (Miller et al., 1985).

The findings of Miller et al. (1985) paved the way for further exploration into the molecular intricacies of fertility inhibition in IncP plasmids. By employing mutagenesis approaches and gene expression analyses, Miller et al. (1985) elucidated the mechanisms by which the F plasmid, specifically the *pifC* gene, targets coupling proteins involved in T-DNA transfer. Notably, their work highlighted the specificity of *pifC* in targeting TraG, a key coupling protein crucial for facilitating T-DNA transfer.

In subsequent studies, such as Getino et al. (2018), the roles of additional genes like *osA* were delineated, further enriching our understanding of the complex network governing fertility inhibition in IncP plasmids. The comprehensive investigation undertaken by Getino et al. (2018) shed light on the interplay between various genes and proteins involved in the regulation of plasmid transfer dynamics. By elucidating the molecular mechanisms underlying fertility inhibition, these studies contribute invaluable insights into the co-

evolutionary arms race between bacteria and mobile genetic elements, shaping microbial communities and their ecological niches (Getino et al., 2017).

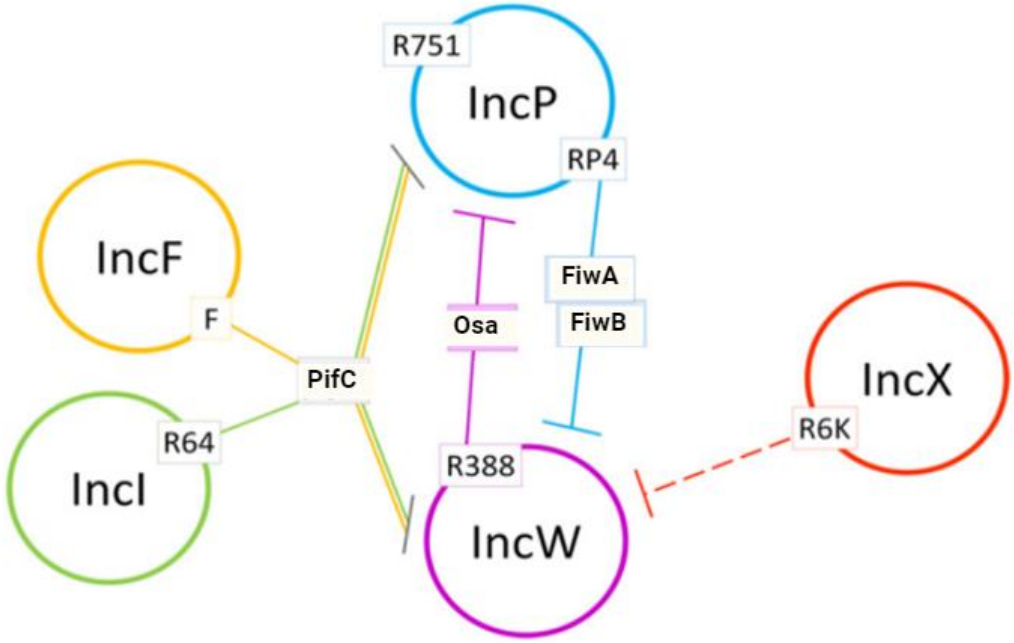

Figure 1. 6 Plasmid interactions between plasmid incompatibility groups (Getino et al., 2017).

The plasmid incompatibility groups are represented by colored circles, while continuous lines indicate identified fertility inhibition systems from plasmids in white boxes. Dashed lines, on the other hand, indicate fertility inhibition systems caused by unidentified genes from plasmids in white boxes.

1.8 RK2 plasmid

RK2 was identified in 1969 at Birmingham Hospital's Burns Unit in the United Kingdom, RK2 originating from *Klebsiella* species, but associated with an outbreak of *Pseudomonas aeruginosa* infections as detailed by Ingram et al. (1973). The RK2 plasmid, part of the IncP incompatibility group, ranks as one of the most extensively studied plasmids within this category (Thomas, 1981) . The size of RK2 is 60,096 base pairs, a self-transmissible plasmid, and carries ampicillin (*bla*), tetracycline (*tetAR*), and kanamycin resistance genes (*aph*) as

shown in Figure 1.7. RK2 possesses a notable ability to replicate in a diverse range of bacteria, making it highly advantageous for applications in genetic engineering (Blatny et al., 1997).

Additionally, RK2 possesses a set of genes known as *kil* genes, which have the potential to be harmful to the cell. Controlling these *kil* genes are a group of transcriptional repressor genes called *kor* (short for "*kil*-override") genes, designed to deactivate the *kil* genes. The coordinated action between these *kil* and *kor* genes is believed to be pivotal in RK2's ability to infect a wide range of host organisms. This intricate genetic interplay likely ensures RK2's adaptability across diverse bacterial hosts by neutralizing any cytotoxic effects that could impede its survival and propagation. The existence of this dual genetic system underscores the complexity of RK2's regulatory mechanisms, emphasizing the need for further investigation into its molecular intricacies to gain a comprehensive understanding of its biological functions (Kornacki et al., 1993).

The broad host compatibility and functional adaptability establish the RK2 Plasmid as a valuable tool in molecular biology, offering researchers a reliable platform for genetic manipulation and experimentation across various bacterial species (Blatny et al., 1997).

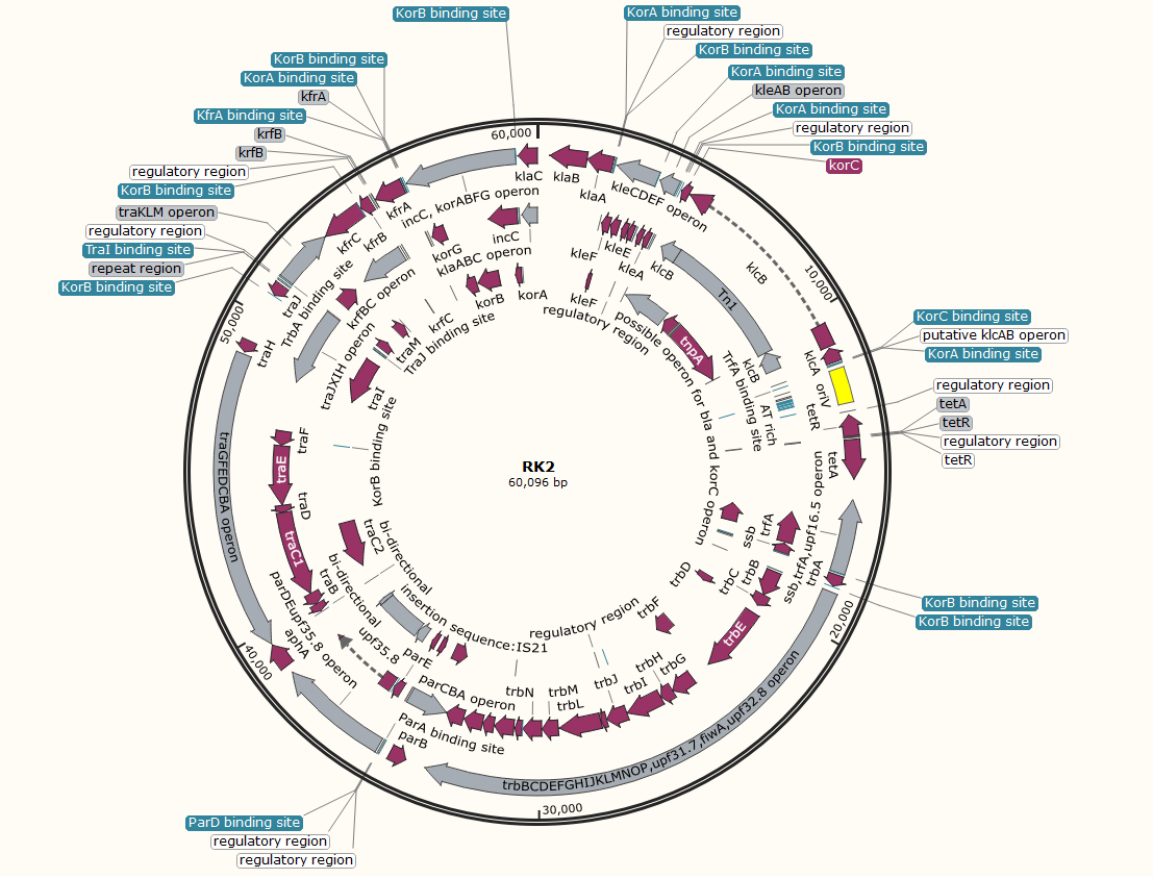

Figure 1. 7 Map of RK2.

The figure displays a schematic representation of the RK2 plasmid generated using SnapGene software and based on the sequence obtained from NCBI. Key features depicted include gene locations, promoters, restriction sites, the *tra* operon responsible for conjugation, and the replication origin (*oriV*). This visualization aids in understanding the organization and function of RK2. Notable features include its role in conjugation between bacterial cells facilitated by the *tra* operon and replication maintenance via *oriV*.

1.9 Plasmid Displacement

Plasmid curing refers to the process of displacing a specific plasmid species from a bacterial population. A promising strategy for overcoming microbial antibiotic resistance involves the elimination of resistance plasmids from the host bacteria. This approach holds significant potential, it can help reduce infections caused by these bacteria by applying previously discovered and used antibiotics, as the bacteria would have lost their resistance to these treatments (Hale et al., 2010).

There are various approaches available for plasmid curing such as, growing cells at a temperature higher than their optimal temperature until they reach the late log phase (Trevors, 1986). Also, another method for curing entails the utilization of chemical agents that affect elements crucial for plasmid replication and maintenance, resulting in the displacement of the plasmid (Hooper et al., 1984). For example, Sodium dodecyl sulfate (SDS) can eliminate certain plasmids from specific bacterial strains. They effectively induced the loss of the virulence plasmid, pSLT, in Salmonella (García-Quintanilla et al., 2006).

While there are various methods for eliminating plasmids from bacteria, it is essential to recognize that these approaches often lack specificity. This lack of specificity raises concerns about unintended mutations, which could potentially harm the bacterial host, as highlighted by Hale et al. (2010). This emphasizes the significance of consideration and optimization when utilizing plasmid displacement techniques to avoid the unintended consequences within bacterial populations (Hale et al., 2010).

Curing plasmids from bacteria through the principle of plasmid incompatibility serves as an alternative approach to chemical or drug-based strategies (Bringel et al., 1989).
The primary benefit of employing this method is the reduced risk of chromosomal mutations and potential toxicity often linked to chemical curing agents (Hovi et al., 1988).
Furthermore, curing based on incompatibility is specific to plasmids belonging to the targeted incompatibility group (Ni et al., 2008).

An effective method for eliminating resistance plasmids involves utilizing an unrelated plasmid replicon as a vector to carry genes capable of inhibiting the replication of the targeted antibiotic resistance plasmid. This approach is particularly useful in avoiding

plasmids that may harbour post-segregational killing systems (PSKs), wherein proteins encoded by these systems impede the growth of bacteria that have lost the plasmid, as observed by (Hale et al., 2010).

Hale and colleagues proposed a strategy that involves blocking each replication system and neutralizing each PSK system. Their research suggests that this comprehensive approach could be highly effective in displacing such plasmids from a bacterial population without inducing unnecessary stress. By leveraging the interference with replication mechanisms and addressing the post-segregational killing systems concurrently, this method offers a potentially more targeted and less disruptive means of plasmid removal, providing a valuable contribution to the ongoing efforts to combat antibiotic resistance (Hale et al., 2010).

The complexity and variability of bacterial populations in clinical settings is a major concern. These populations are highly diverse and can evolve rapidly in response to selective pressures like antibiotic treatment. As a result, new resistance mechanisms can emerge that may not be effectively targeted by plasmid displacement alone (Lopatkin et al., 2017).

On top of that, the process of plasmid displacement itself presents significant challenges. It involves introducing a foreign plasmid into bacterial cells. Additionally, the effectiveness of plasmid displacement can vary depending on the bacterial strain and the infection's conditions, which further complicates its use in clinical settings (Lopatkin et al., 2017). Although plasmid displacement shows promise as a potential treatment for antibiotic-resistant infections, several challenges and limitations must be addressed before it can be effectively used in a medical context. It is crucial to undertake a critical evaluation of the existing literature, including publications such as Hale et al. (2010) and Lopatkin et al. (2017), to

identify and address these challenges. Only then can safe and effective strategies be developed for using plasmid displacement in clinical settings.

Professor Chris Thomas and his lab have used a conjugative pCURE plasmid that is self-transmissible and is compatible with the target F plasmid. The pCURE contains sections of each IncF replicon (multiple binding sites for Rep protein for FIA and FIB replicons and the transcriptional repressor CopB and the antisense RNA for the FIC replicon). At that point, the cell will respond as if F had replicated several times and turn off F replication. pCURE also encodes genes that provide the antidotes for each PSK system in the target plasmid (Lazdins et al., 2020).

1.10 Development of pCURE plasmids

Originating from Professor Chris Thomas's laboratory, pCURE is a plasmid established in 2005 (www.plasgene.com). The principle of this work is based on curing by provision of plasmid replication control elements with the additional benefit of supplying components to neutralise the addiction systems of the targeted plasmid system (Hale et al. 2010). The second generation of pCURE plasmids are self-transmissible plasmids that are able to replicate at low copy numbers, and they are based on a broad-host-range plasmid.

This conjugative pCURE is classified as an IncP-1 plasmid, and it has been used as a vector for curing IncF and IncK plasmids. However, the historical journey leading to the creation of this plasmid unfolded through the process described below. This process represents a significant chapter in the development of the plasmid, marking a crucial milestone in its evolution (Hale et al., 2010).

The initial plasmid in the pCURE series, designated as pCURE1, was conceived with the specific purpose of displacing pO157 from its host, *E. coli*. The strategy involved the identification, amplification, and cloning of curing functions tailored for the target plasmids as listed in Table 1.1. These functions were then combined into a curing cassette. The resulting cassette was integrated into pAKE604, encoding kanamycin and ampicillin selectable markers, along with *sacB*, giving rise to the pCURE1 plasmid, as illustrated in Figure 1.8. The *sacB* gene encodes levan sucrase, responsible for polymerizing fructose from sucrose which is lethal for bacteria. This process induces sucrose sensitivity in Gram-negative bacteria, simplifying the isolation of plasmid-free segregants (Ried and Collmer, 1987).This experimental approach served as a rigorous test for the displacement strategy, particularly noteworthy due to the presence of multiple replicons and PSK in pO157 (Hale et al., 2010).

Table 1.1 pCURE1 Segment

System	Function
Strategies for blocking replication	Antisense RNA, CopA, to indirectly block translation of the repFIIA *rep* gene. Combination of the FIB rep associated iterons (Rep binding sites) for controlling replication.
Strategies for blocking PSK systems	Control/antidote regions from identified PSK systems, including sok of the hok/sok system and letA from the letAB system.
Replicons	repFIIA - repFIB
PSK systems	ccdAB (letAB) - parB (hok/sok)

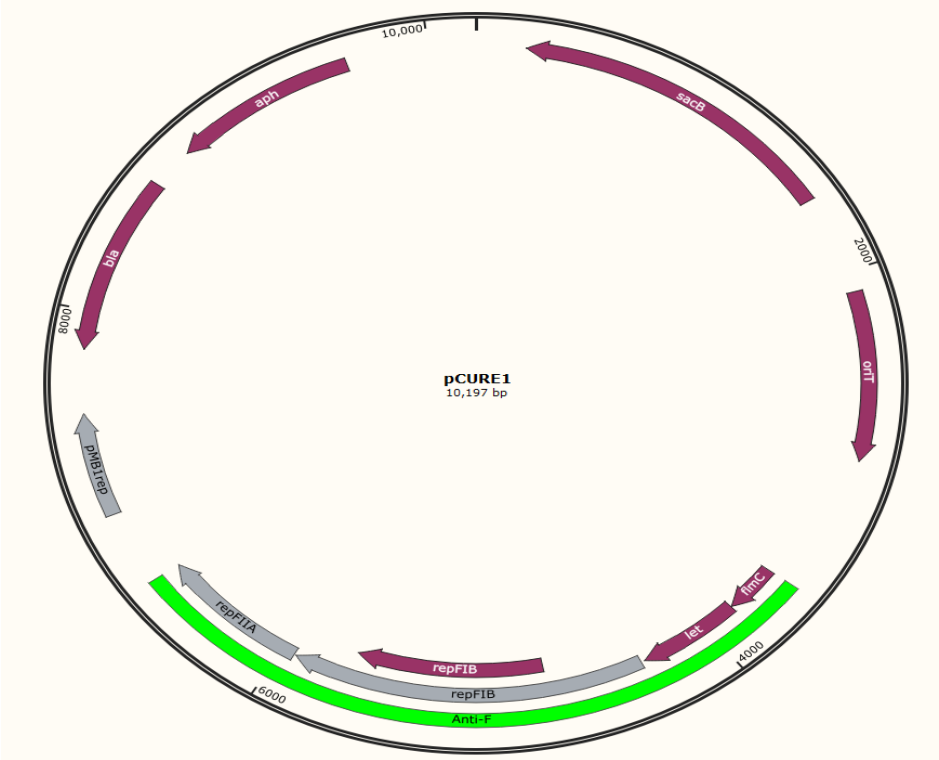

Figure 1. 8 Map of pCURE1.

The genetic structure of pCURE1, constructed on a pAKE604 backbone with *sacB*, inducing sucrose sensitivity in the host organism. pCURE1 includes anti-F cassettes containing repFIIA, repFIB, *sok* from the hok'sok system, and *letA* from the letAB system. These components collectively inhibit replication of the pO157 plasmid and counteract its addiction functions.

Derived from pCURE1, pCURE2 has an anti-F cassette enriched with supplementary elements, specifically (repFIC/FIIA, repFIA, and repFIC) as listed in Table 1.2. The increased complexity of pCURE2 plays a crucial role in effectively blocking the replication of IncF plasmids. It includes anti-toxins that are specifically selected to neutralize common toxins found in various IncF plasmids. This design not only enhances the effectiveness of pCURE2, but also provides a strong safeguard against the intricate processes involved in IncF plasmid replication, as illustrated in Figure 1.9 (Hale et al., 2010).

Table 1.2 Anti-F cassette of pCURE2 Segments.

System	Cloned component	Function
Replicon targets		
repFIA	incC repeats	Five 22bp repeats to which initiator protein RepE binds to, blocking replication.
repFIB	Iterons and repA	Overproduction of RepA interferes with plasmid replication. Iterons titrate Rep proteins.
repFIC	copA/B	ctRNA encoded by copA/repB blocks replication initiation protein RepA
repFIC/FIIA	copA/B	ctRNA encoded by copA/repB blocks replication initiation protein RepA
Toxin-Antitoxin targets		
srnB/srnC (hok/sok)	*srnC*	srnC/flmB are short-lived RNA molecules complementary to the srnB/flmA toxin mRNAs.
flmA/flmB (hok/sok)	*flmB*	
pemI/pemK	*pemI*	*pemI* encodes the PemI antitoxin protein that neutralises the PemK ribonuclease toxin
letA/letB (ccdA/ccdB)	*letA*	*letA* encodes the LetA antitoxin protein that neutralises the LetB gyrase inhibitor.

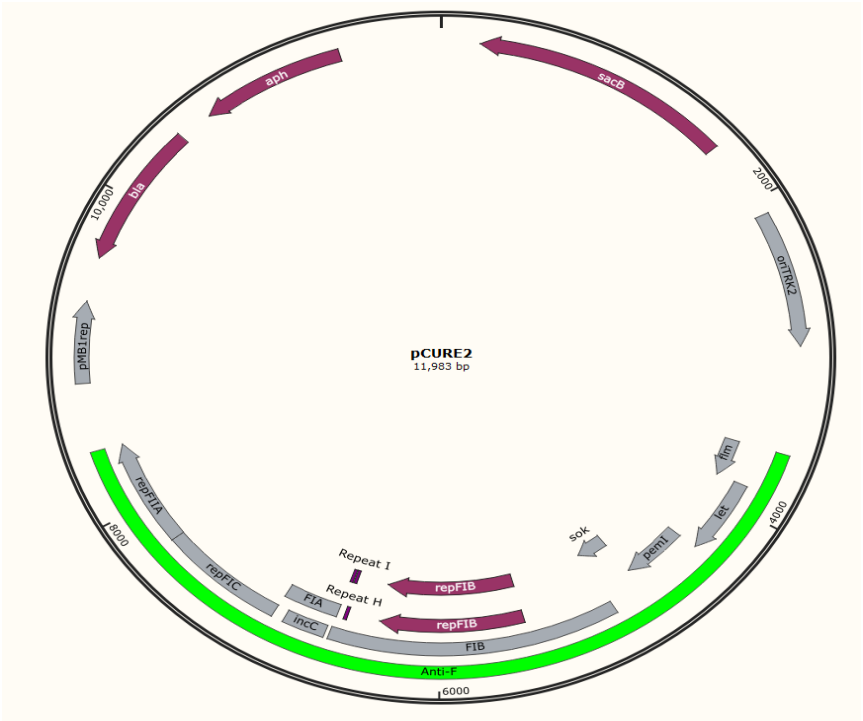

Figure 1. 9 Map of pCURE2

The genetic arrangement of pCURE2, built on a pAKE604 backbone containing *sacB*, leading to sucrose sensitivity in the host. pCURE2 integrates anti-F cassette containing repFIC/FIIA, repFIA, and repFIC elements, which inhibit the replication of IncF plasmids. Additionally, the construct incorporates anti-toxins effective against common toxins found in various IncF plasmids.

Subsequently, pCURE-K was developed to displace IncK plasmids which are known to carry antibiotic resistance genes and contribute to the spread of antibiotic resistance in bacterial populations. The design of pCURE-K involved the cloning a segment containing the ctRNA (inc RNA) from the single replicon of plasmid R387 into pAKE604 as listed in Table 1.3. By introducing pCURE-K into bacterial strains carrying IncK plasmids, researchers aimed to disrupt the replication and maintenance of these harmful plasmids, ultimately reducing the prevalence of antibiotic resistance in bacterial populations. The development of pCURE-K represents a promising approach to combating antibiotic resistance and highlights the potential of genetic engineering in addressing global health challenges (Hale et al., 2010).

Table1.3 Anti-K cassette from pCURE-K Segments

System	Cloned component	Function
Replicon targets		
Col1b-P9- like replicon	ctRNA repZ	Anti-sense RNA that represses the translation of RepZ, the Rep protein required for initiation of plasmid replication.
Col1b-P9- like replicon	repY	Protein functioning as a positive regulator for RepZ expression, but inhibited by ctRNA of repZ.

A novel iteration of the pCURE series, pCURE-F-RK2, was designed with the specific objective of curing IncF plasmids. It is based on a low-copy-number, broad-host-range, self-transmissible IncP-1 plasmid RK2, constructed by integration of the anti-F cassette from pCURE2 (see Table 1.2), as illustrated in Table 1.4 and Figure 1.11.

While pCURE-F-RK2 is proficient in sustaining the unidirectional displacement of F-like plasmids, its efficiency is somewhat lower compared to when carried by the high-copy-number pCURE2 plasmid (>40 copies per chromosome) based on the pMB1 replicon. Removal of the *oriV* segment with the TrfA (Rep) binding site i10 amplifies the curing potential (Lazdins et al., 2020). By eliminating the transposon and flanking backbone sequences from pCURE-F-RK2, this modified plasmid demonstrates exceptional efficacy in causing the displacement of IncF plasmids. This culmination of advancements results in the latest version of the pCURE plasmid, named pCURE-F-307, as depicted in Figure 1.10. The capabilities of this updated plasmid extend to neutralizing the action of PSK systems encoded by the target plasmid.

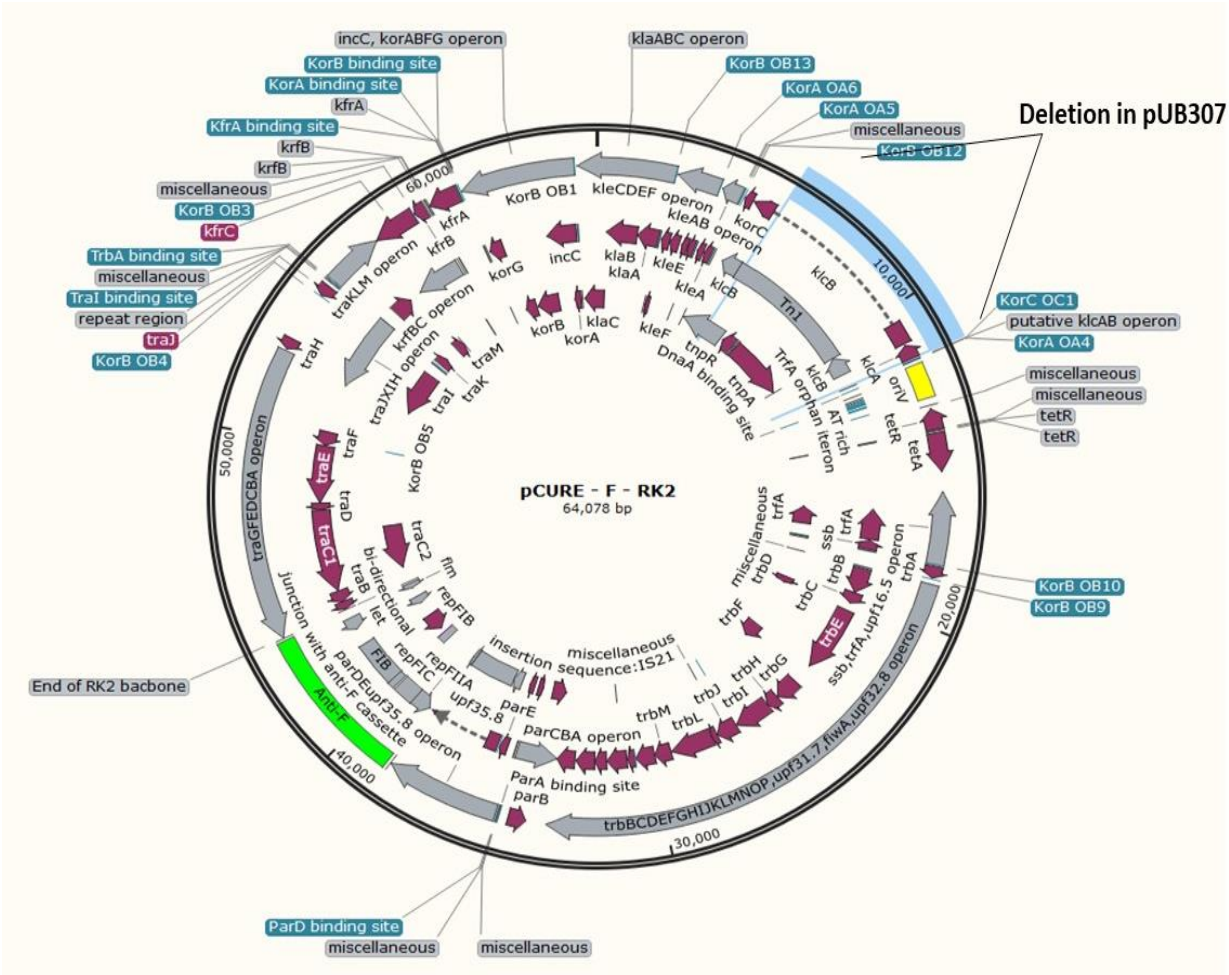

Figure 1. 10 Gene map of pCURE-F-RK2 and pCURE-F-307.

The anti-F cassette included in the pCURE-F-RK2 and 307 has the same functions as in pCURE2.

1.11 The importance of having pCURE able to escape F plasmid inhibition

IncF plasmids are recognized for harbouring a diverse range of genes that provide resistance to multiple antimicrobial classes, such as β-lactams, aminoglycosides, tetracyclines, chloramphenicol, and quinolones. Notably, extended-spectrum β-lactamases (ESBLs), markedly those belonging to the CTX-M type, are often associated with plasmid-mediated quinolone resistance (PMQR) and aminoglycoside resistance genes. IncF plasmids, specifically, have emerged as key vectors for these resistance determinants, as documented in the study by (Boyd et al., 2004). This underscores the crucial role of IncF plasmids in the

spread of antibiotic resistance genes, presenting a significant hurdle in the effective management of bacterial infections.

In a study conducted by Stephens et al. (2020), faecal samples were collected from healthy human subjects, and commensal *E. coli* strains were isolated. Molecular techniques were then employed to analyse these strains for the presence of F plasmids and antibiotic resistance genes (ARGs). The findings of the study revealed that F plasmids were the primary carriers of ARGs in the commensal *E. coli* strains. Furthermore, the F plasmids harbouring ARGs exhibited a high degree of diversity, indicating their potential to transfer between different strains of *E. coli* (Stephens et al., 2020). These results underscore the significant role of F plasmids in disseminating antibiotic resistance among human-associated E. coli strains.

The initial objective of developing pCURE is to eliminate F-like antibiotic resistance plasmids from the human gut. Given that F plasmids were previously known to hinder the fertility of IncP plasmid RP4/RP1/RK2, it was crucial to try to ensure that pCURE-F-307 could transfer without being impeded by F plasmids.

1.12 Aims of this research and objectives.

The primary aim of this doctoral project was to enhance the functionality of the pCURE conjugative plasmid, ensuring its ability to transfer without being suppressed by other plasmids, especially the F plasmid. The specific goal was to create a derivative of the conjugative pCURE-F-307 that would allow transfer without susceptibility to inhibition by the F plasmid.

The first objective of this study was to check the fertility inhibition phenotype against RK2 when the F plasmid is present in the donor. Additionally, it aimed to define the consequences of starting with fewer donors, having the F plasmid in the recipient, and having two sources of inhibition on pCURE transfer.

The second goal was to obtain a mutant conjugative pCURE that could transfer without being suppressed by other plasmids. During the process of obtaining the mutant, we discovered that increasing the expression of the *traG* gene could enable the plasmid to escape inhibition without any mutation. This discovery was established as the final objective of this PhD project.

Chapter 2: Materials and Methods

2.1 Bacterial strains used in this study, growth media and culture conditions.

Bacteria used in the work are listed in Table 2.1. Most of the strains mentioned here are based on derivatives of *E. coli* K12. Strains were cultured in L-broth (Bertani, 1951), that was made by the Central Services of the School of Biosciences, University of Birmingham, UK. The recipe of the LB consists of yeast extract (10 g/l), tryptone (5g/l) and 5g/L NaCl. To produce L-agar, 15g/L of agar wad added. Before starting transfer experiments, the M9-minimal medium was used to check the presence of F'prolac in the donor strains. An autoclave was used at 121°C for 20 minutes to sterilise all bacterial media. Antibiotics were added to L-broth and L-agar, as indicated in Table 2.2. Growth conditions for all *E. coli* strains used in this study were 37°C, and aeration with shaking at 200 rpm for liquid growth.

For long-term storage of bacterial strains, 750 µL of overnight culture was mixed with 750 µL of 50:50 mix of glycerol and LB broth and stored at -80°C.

Table 2.1 *Escherichia coli* strains used in this study

Abbreviation	Description	Source/Reference
BL21(DE3)	*F^- ompT hsdSB (r_B^-, m_B^-) dcm gal λ(DE3)*	Invitrogen
C600	*F^- tonA21 thi-1 thr-1 leuB6 lacY1 glnV44 rfbC1 fhuA1 λ^-*	Appleyard (1954)
DH5α	*F^- endA1 glnV44 thi-1 recA1 relA1 gyrA96 deoR nupG Φ80d*lacZ*ΔM15 Δ(lacZYA-argF)U169, hsdR17(r_K^- m_K^+), λ^-*	Hanahan (1983)
E. coli Nissle 1917 (EcN)	*Probiotic E. coli strain*	Grozdanov et al., (2004)

HB101	*F- mcrB mrr hsdS20(r_B^-, m_B^-) recA13 leuB6 ara-14 proA2 lacY1 galK2 xyl-5 mtl-1 rpsL20(Sm^R) glnV44 λ^-*	Boyer and Roulland-Dussoix (1969)
JM109	*endA1 glnV44 thi-1 relA1 gyrA96 recA1 mcrB+* Δ(*lac-proAB*) e14- [F' *traD36 proAB+ lacIq lacZΔM15*] *hsdR17($r_K^-m_K^+$)*	Yanisch-Perron et al., (1985)
JM109C	*endA1 glnV44 thi-1 relA1 gyrA96 recA1 mcrB+* Δ(*lac-proAB*) e14- *hsdR17($r_K^-m_K^+$)*	Thomas lab after displacing the F'with pCURE2
MV10-Nal^R	*F- tonA21 thi-1 thr-1 leuB6 lacY1 glnV44 rfbC1 fhuA1 ΔtrpE5 gyrA*(Nal^R) λ^-	Hershfield et al., (1974)
S17-1	*recA1 thiE1 pro-82 hsdR17* RP4-2(Tc::Mu-1, Km::Tn7)	Simon et al. (1983)

Table 2.2 Antibiotics used

Antibiotic	Abbreviation	Stock concentration mg/ml	Working concentration µg/ml	Solvent
Ampicillin	Amp	100	100	SDW
Chloramphenicol	Cm	10	25	100% Ethanol
Kanamycin	Kan	50	50	SDW
Nalidixic Acid	Nal	10	30	SDW
Rifampicin	Rif	100	40	DMSO
Streptomycin	Stm	50	25	SDW
Tetracycline	Tet	10	15	70% Ethanol
Trimethoprim	Trm	100	100	SDW

To prepare M9 minimal medium, a mixture of M9 X2 salts ($Na_2HPO_4 \bullet 7H_2O$, KH_2PO_4, NaCl, NH_4Cl), as shown in Table 2.3, was combined with 3% water agar. To this mixture, 400 µL of 1M $MgSO_4$, 400 µL of 100mM $CaCl_2$, 1ml of 4% thiamine, and 2ml of 40% glucose were added. The necessary amino acids were included to achieve a final concentration of 50µg/ml, and antibiotics were incorporated as needed (Miller, 1972).

Table 2.3 Preparation of M9 X2 salts

Na_2HPO_4-$7H_2O$	64g
KH_2PO_4	15g
NH_4Cl	5.0g
Adjust to 1000ml with distilled H_2O	
Sterilize by autoclaving	

2.2 Plasmid isolation

Plasmids were isolated using a Plasmid Mini kit (Bioline, London, UK) and all isolated plasmid DNA solutions were stored at -20°C. The Plasmid Mini kit works on the basis of a modified alkaline lysis technique (Birnboim and Doly, 1979). The protocol, in short, is as follows.

Using bacterial cultures grown overnight with selection, cells were spun down at 3000g by centrifugation. Cells were lysed with alkaline sodium hydroxide/SDS in order to release the cell components and denature the DNA. The next step was adding a neutralising solution, allowing the plasmid DNA to re-nature and remain in the solution. The mixture was left at room temperature for 7 minutes and then centrifuged at speed, around 11.000 x g for 10 minutes at 4 °C temperature. 750 µL of the supernatant solution was moved to a filter column

containing silica membranes, incubated for 1 minute, and then centrifuged. Washing the sample with ethanol is required to eliminate salts and other residues. Lastly, elution buffer for elution as supplied by the manufacturer was used to elute the plasmid DNA in a clean and sterile microfuge tube 1.5 ml, and it was stored at -20°C for future use.

Table 2.4 List of plasmids used in this work

Plasmid	Source/Reference
pACYC184	(Chang and Cohen., 1978)
pACYC184-*traG*	This Study
pACYC184-*traG-oriT*	This Study
pACYC184- His_6-*traG-oriT*	This Study
pET28a	Novagen
pET28a-His_6-traG	This Study
pGBT30	(Jagura-Burdzy et al., 1991)
pGBT30-*pifC*	This Study
pGEM-T	Promega
pLAZ2	(Lazdins et al., 2020)
pLAZSOE1	This Study SOEd arms for RK2 deletion. Cloned into HindIII and SalI sites; CmR.
pLAZSOE2	This Study

	traG with SOEd arms for traG restore. Cloned into HindIII and SalI sites; CmR.
pLAZSOE3	This Study xylE with SOEd arms for traG replacement in RK2. Cloned into HindIII and SalI sites; CmR.
pLAZSOE4	This Study xylE with SOEd arms for traG replacement in pUB Δ+. Cloned into HindIII and SalI sites; CmR.
pUB307	(Grinsted et al., 1977)
pUBΔtraG	This Study
pUBΔ+	This Study
pUBΔ :: xylE	This Study
pUBΔ+ **::** xylE	This Study
RK2	(Pansegrau et al., 1994)
R388	(Llosa et al., 1994)

2.3 Chemically competent cells

Competent cells were used in DNA transformation and were made in our lab using Calcium chloride $CaCl_2$ (Cohen et al., 1972). The protocol for making competent cells starts with making 5ml of overnight culture with a selectable antibiotic where necessary. The following day, 500µL of the culture was used to inoculate 50ml (100-fold dilution) of LB broth medium in a 250ml conical flask (Figure 2.1).

The culture was grown at 37°C with shaking at 200 rpm until the OD 600nm reached between 0.4-0.6. Cultures were spun down at 3000g for 7 min at 4°C, then the supernatant was discarded, and cells were re-suspended in 20 ml of chilled 100 mM $CaCl_2$ and placed on ice for 20 minutes. The cells were centrifuged again, and the supernatant was removed. At the final stage, cells were gently re-suspended in 5ml of chilled 100mM $CaCl_2$. Competent cells that had been made were stored for up to 1 week at 4˚C.

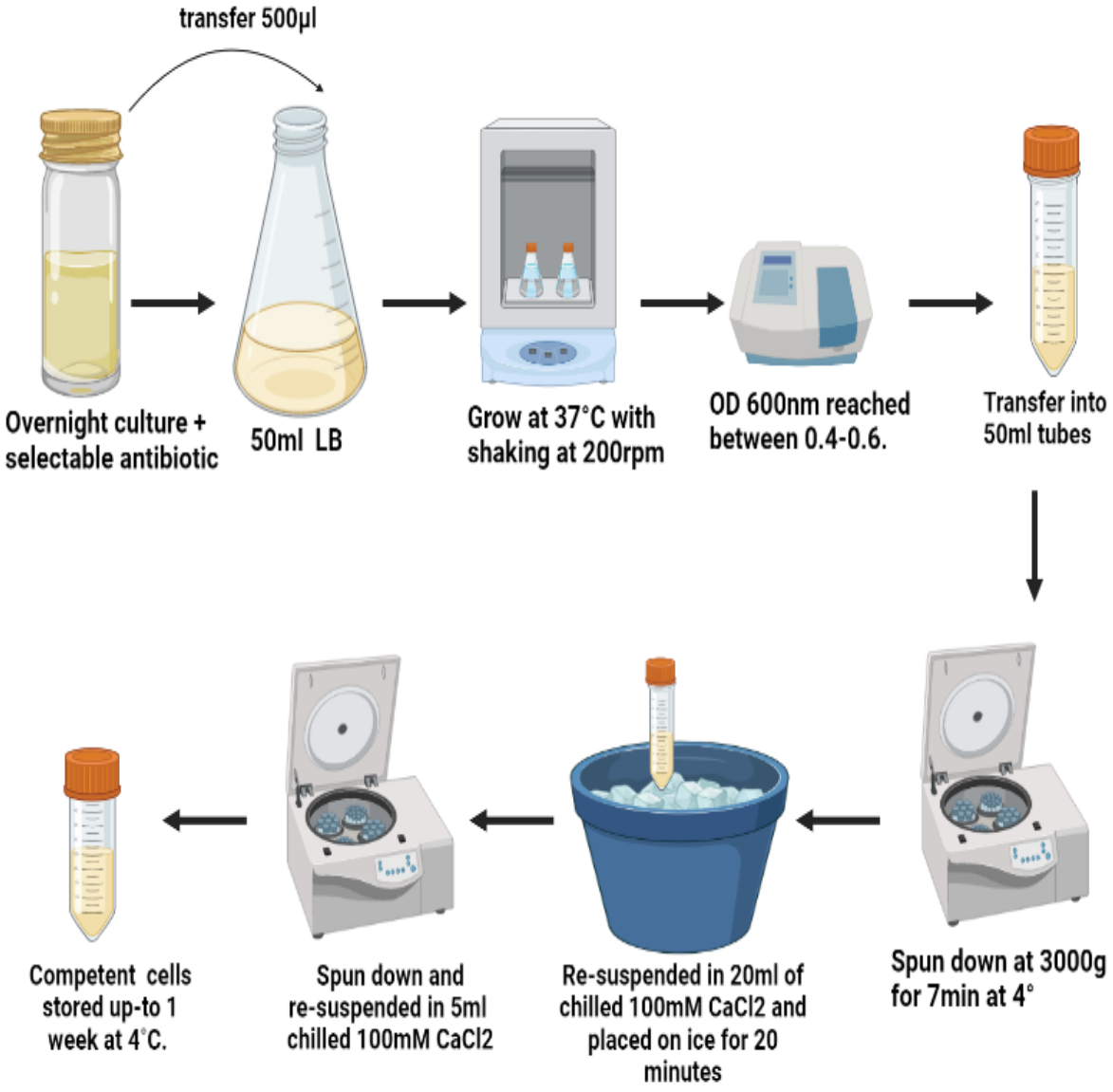

Figure 2.1 Summary of the protocol of making chemically competent cells.

The competent cells generated through this protocol retain their functionality for a limited period, typically ranging from a few days to a maximum of one week following preparation. During this time window, their effectiveness for transformation purposes may diminish.

2.4 DNA transformation

Competent cells were transformed with DNA using a heat shock method (Chang and Cohen,

1978). Initially 100µL of competent cells was introduced into a sterile 1.5ml microfuge tube.

Subsequently, 1µL to 10 µL of plasmid DNA was added and gently mixed. The cell-DNA

mixture was kept on ice for 30 minutes, followed by a heat shock at 42°C for 45 seconds. Afterwards, the mixture was returned to ice for an additional 5 minutes. To facilitate recovery, 900 µL of fresh LB broth was added, and the cells were allowed to recuperate at 37°C for 1 hour. Post-recovery, typically 100µL of the revived cells were plated on LBA and the remaining cells were centrifuged to pellet, the supernatant was discarded, and the pellet was resuspended in 100µ of LBA. The resuspended cells were then spread on a plate. A negative control was established by including the same strain without the addition of any DNA. All plates were incubated at the required temperature.

2.5 Conjugation Studies

Conjugation is a crucial process in bacterial genetics, facilitating the transfer of genetic material, particularly plasmids, between bacterial cells. This section details the methodologies employed to investigate plasmid transfer capabilities between different bacterial strains and the assessment of transfer efficiencies over specific time intervals.

2.5.1 General Plasmid Conjugation

The primary objective of general plasmid conjugation is to transfer plasmids from one bacterial strain to another. This process is fundamental in bacterial genetics, allowing for the exchange of genetic material and the study of various genetic traits. In this study, plasmid conjugation aimed to transfer plasmids containing oriT sequences between strains, such as RK2, R388, and others.

Additionally, the capability of traG to facilitate transfer without inhibition by F plasmids was assessed. The conjugation experiments involved mixing 10 µL of donor culture with 100 µL of recipient culture, resulting in a 1:10 ratio. Subsequently, 15 µL of the mixture was spotted

on Luria-Bertani agar (LBA) and incubated for 4 hours under optimal conditions for the recipient strain. After incubation, the mixture spot was streaked out on LBA supplemented with antibiotics to select for transconjugants. Negative controls, consisting of donor and recipient streaked on LBA with antibiotics, were also included for comparison.

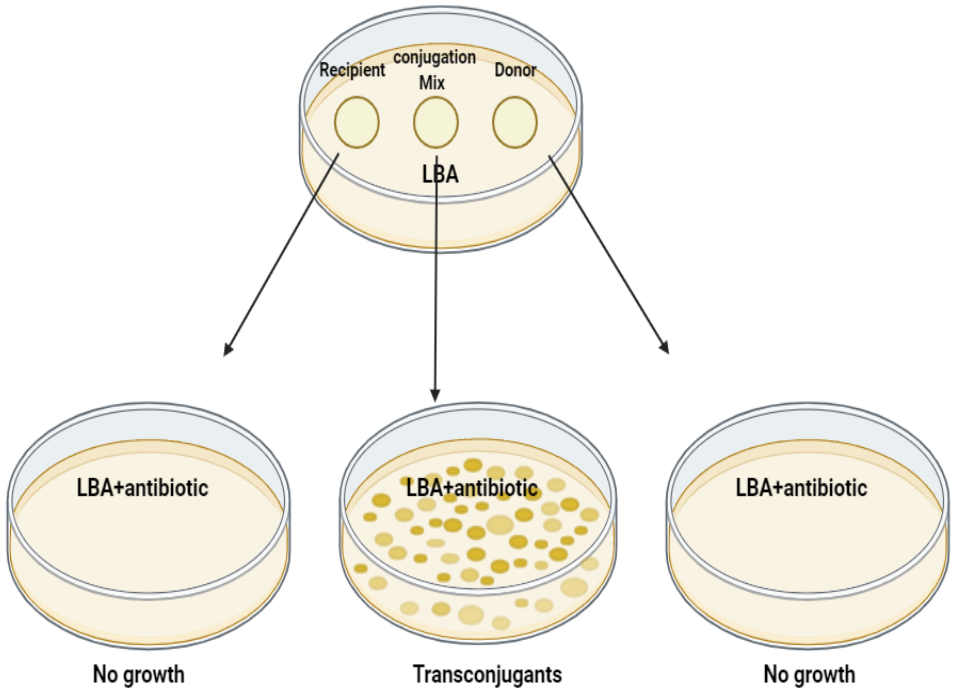

Figure 2.2 General plasmid Conjugation

A total of 10µL of donor, recipient and donor-recipient mixture were placed on LBA and incubated for four hours. The spots were then streaked out onto selective media.

2.5.2 Plasmid Conjugation for Specific Time Points

This method aims to compare the transfer abilities of different plasmids at specific time intervals. Strains were cultured separately overnight in Luria-Bertani broth (LB) at 37°C. Subsequently, 1:10 mixtures of donor and recipient cultures were prepared. Five 20 µL spots of the mixture were placed on LB agar for control and time-point assessments

2.6 PCR

All primers used in PCR reaction were designed using Snapgene software (SnapGene, Chicago, USA) and listed in Table 2.5. The annealing temperatures were checked with Primer Analysis Software Netprimer (Premier Biosoft, Palo Alto, USA). PCR was used to amplify the needed gene using DNA prepared isolated by Plasmid Mini Kit (Bioline, London, UK), as mentioned in section 2.2 or boiling as mentioned in section 2.6.3 of this chapter.

Table 2.5 List of PCR primers used in this study

Lab Name	Purpose	Tm, ˚C	Sequence (5'-3')
pifC Ins- F	To clone *pifC* into pGBT30	60	GCATGAGAATTCATGCTAAGCCAGCTTAACCTGC
pifC Ins- R	To clone *pifC* into PGBT30	61	GCATGATCTAGAATTACAGATCTCCGTACAGGCAGC
pGBT30 Seq-F	To sequence part of pGBT30	64	GTATTTTCCCGACCGGCACG
pGBT30 Seq-R	To sequence part of pGBT30	65	CCACGCGGTGTCAAGAAGGC
Del RK2 arm1-F	To make a deletion in RK2	66	CACGGTCGACAGGCCCGAAGTAGCGGC
Del RK2 arm1-R	To make a deletion in RK2	69	TTGCAGATGGCCGCTTCCAGCGCCTCACC
Del RK2 arm2-F	To make a deletion in RK2	71	GCCGTCTGGATCCGTATCTGTGGCCCCACGGC
Del RK2 arm2-R	To make a deletion in RK2	68	CACGAAGCTTGCGAGCGCTGTCCCAACTC
traG Ins- F	To clone *traG* into pACYC184	65	GCATGAGTCGACCGGCTCATATCGTGATCCCCTC
traG Ins- R	To clone *traG* into pACYC184	70	CGATAAGCTTTAACCGTGACCCCGCGAGGCTC

oriT Ins- F	To clone *oriT* into pACYC184-*traG*	71	GCATGAAAGCTTATCGATGATAAGCTGT CAACAGCCTCGCAGAGCAGGATTCCC
oriT Ins- R	To clone *oriT* into pACYC184-*traG*	70	GCATGATCTAGAGCTGCATAACCCTGTTTCGGGGTC
traG Res- pUBΔ arm1 F	To restore *traG* into pUBΔ arm1	63	GCTAAGCTTCGATGAATCGCTCACGATCATG
traG Res- pUBΔ arm1 R	To restore *traG* into pUBΔ arm1	62	CTATTAAAGCTGATCGATGATAAGCTG TCAATCATAACGAGGCCCACACCAC
traG Res- pUBΔ arm2 F	To restore *traG* into pUBΔ arm2	65	CGATATGAGCCCAGAGGCGCAGATGAAAAAGC
traG Res- pUBΔ arm2 R	To restore *traG* into pUBΔ arm2	66	GCATGAGTCGACAGGAGGCCGAGACGGAACAG
traG Res- pUBΔ traG F	To restore *traG* into pUBΔtraG	61	ACAGCTTATCATCGATCAGCTTTAATAGCGTCCATCCCGCTA ACTACCCGAGGTAGCTAGATGAAGAACCGAAACAACGC
traG Res- pUBΔ traG R	To restore *traG* into pUBΔtraG	60	GCGCCTCTGGGCTCATATCGTGATCCCCTC
traG mid seq F	To sequence middle of *traG*	63	AGATGAGGTAGCACTTGATGCCG
traG mid seq R	To sequence middle of *traG*	63	TGGTGTCAGGCAAACACCCG
traG GTG- F	To attenuate the *traG* promoter	60	GTGAAGAACCGAAACAACGCCG
traG GTG- R	To attenuate the *traG* promoter	59	CTACTCCTACCTCGGGTAGTTTTAAG
traG TTG - F	To attenuate the *traG* promoter	60	TTGAAGAACCGAAACAACGCCG
traG TTG - R	To attenuate the *traG* promoter	59	CTACTCCTACCTCGGGTAGTTTTAAG
osA Ins- F	To amplify *osA* gene	62	GCATGATCTAGACACGCCCTAGATCTTCCTGC
osA Ins- R	To amplify *osA* gene	62	GCATGAGAATTCGAGCATGGGAGCTAACGATGC

traG-His F	To tag *traG* with His_6	63	CATCACCATTGAGCCGGTCGACCGATG
traG-His R	To tag *traG* with His_6	63	GTGATGGTGTATCGTGATCCCCTCCCTTC
traG-His F 1	To tag *traG* with His_6	64	CATCACCATAAGAACCGAAACAACGCCGTG
traG-His R 2	To tag *traG* with His_6	63	GTGATGGTGCATCTACTCCTACCTCGGGTAGTTTTAAG
traG-His Ins- F	To clone His_6 *traG* into pET28a	63	TCGCCATGGGTCACCATCACCATCACCATAAGAAC
traG-His Ins- R	To clone His_6 *traG* into pET28a	62	TCGCATATGGCGTTGAAGGCTCTCAAGGGCATC
xylE Rep 307 F	To replace *xylE* instead of *traG* in pUB307 arm1	66	ACGAAGCTTGCGAGCGCTGTCCCAACT
xylE Rep 307 R	To replace *xylE* instead of *traG* in pUB307 arm1	59	CATTACACCTTTGTTCATCTACTCCTACCTCGGGTAG
xylE Rep 307 F	To replace *xylE* instead of *traG* in pUB307 arm2	60	GTAGGAGTAGATGAACAAAGGTGTAATGCGACC
xylE Rep 307 R	To replace *xylE* instead of *traG* in pUB307 arm2	66	TCGCTCGAGGACAGGCCCAGAAGTAGCGGC
xylE Rep 307 F	To replace *xylE* instead of *traG* in pUB307*xylE*	60	GTAGGAGTAGATGAACAAAGGTGTAATGCGACC
xylE Rep 307 R	To replace *xylE* instead of *traG* in pUBΔ *xylE*	64	CTGGAAGCGGCTCAGGTCAGCACGGTCATGAATC
xylE Rep pUBΔ+ F	To replace *xylE* instead of *traG* in pUBΔ+ arm1	63	GCTAAGCTTCGATGAATCGCTCACGATCATG
xylE Rep pUBΔ+ R	To replace *xylE* instead of *traG* in pUBΔ+ arm1	60	CATTACACCTTTGTTCATCTAGCTACCTCGGGTAGTTAGC
xylE Rep pUBΔ+ F	To replace *xylE* instead of *traG* in pUBΔ+ arm2	61	GTGCTGACCTGACAGAGGCGCAGATGAAAAAGC
xylE Rep pUBΔ+ R	To replace *xylE* instead of *traG* in pUBΔ+ arm2	64	TCGCACGTGCCCTTGCGCTCTACGTGCAG

xylE Rep pUBΔ+ F	To replace *xylE* instead of *traG* in pUBΔ+ *xylE*	60	GGTAGCTAGATGAACAAAGGTGTAATGCGACC
xylE Rep pUBΔ+ R	To replace *xylE* instead of *traG* in pUBΔ+ *xylE*	61	CGCCTCTGTCAGGTCAGCACGGTCATG
xylE Rep pUBΔ+ F	To replace *xylE* instead of *traG* in pACYC184	60	TCGAAGCTTTAATACCGTGACCCCGCGAGGCTCCCTTAAAACT ACCCGAGGTAGGAGTAGATGAACAAAGGTGTAATGCGACC
xylE Rep pUBΔ+ R	To replace *xylE* instead of *traG* in pACYC184	60	CTCGAGCTCTGCAATAAGTCGTACCGGAC

Table 2.6 List of Oligonucleotides used in this study

Lab Name	Purpose	Tm, ˚C	Sequence (5'-3')
osA-1	Oligo 1 to create *osA* gene and clone it into pGBT30	100	GACACGCCCTAGATCTTCCTGCATTGCTCACGCAGCTTTGAAA CCTGAATCGGCGCTGCTACGCCCACGTGTTCTGCCAACATAAC GGCGGATGCTTCATCACGGGAAAGCACCG
osA-2	Oligo 2 to create *osA* gene and clone it into pGBT30	101	CTTCATCACGGGAAAGCACCGGAAACACGGCGACCTC ATGGGCCAAAAGCCACATTGAACGGGTCATGCCATCAG GAAACACACCGCGAAATGGCCCAGAATCATGGTCGGGC
osA-3	Oligo 3 to create *osA* gene and clone it into pGBT30	103	GCCCAGAATCATGGTCGGGCTTACGTCAGCAAGCGGAAC GGGGCTGTCGATGCCCACGGCAAAATGCGCGGCGCTCGAC GGATATTTCCGGTCTTTAGGCATGTCCTGCTTCAACGGGCA
osA-4	Oligo 4 to create *osA* gene and clone it into pGBT30	98	CATGTCCTGCTTCAACGGGCAGGCTTGAGAATCCTCGAC GCCTAACGCCAACCACGCTCGATAGAAAGCCAAGCCATT CACATACACAATGAAATCGGACTGTGCGGCATTTGAAGC
osA-5	Oligo 5 to create *osA* gene and clone it into pGBT30	101	GGACTGTGCGGCATTTGAAGCTGTCATAAAGGCGTCAGG ATGGTTCGGCACGGGCAGCCGCCAAACAACCTCATTCCA AGCATTCGGCACGATTTGAGGCAATTCGAGGGGCAACC
osA-6	Oligo 6 to create *osA* gene and clone it into pGBT30	101	GGCAATTCGAGGGGCAACCCGCTCGACTGCGCAAGCTC TTTATCAAGCCGCCGAATTTCCAGCCAAGCGCGACACCG CCGCCGTAGCAACATCAGCATCGTTAGCGCCCATGCTC

2.6.1 PCR using Velocity Taq polymerase.

The Velocity polymerase from (Bioline, London, UK) was used and each 50 µL PCR reaction was mixed in a PCR tube as follows: 10 µL of 10X Standard Taq Reaction buffer, 5 µL of 10 mM dNTPs, 1.5 µL of 5% DMSO, 0.5 µL Taq DNA polymerase, 1 µL of each 10 µM primer, 1 µL template and 30 µL water. The initial reaction was at 94°C for 2 minutes,

denaturation was at 94°C for 30 seconds, annealing was done for thirty seconds, and the determination of the annealing temperature was accomplished through the utilization of NetPrimer software that predicted the melting temperature (Tm) of the primers based on their sequence. Extension at 72°C was carried out for a time period based on the size of the product expected – normally 1 minute per kb and a final extension at 72°C for 10 minutes. The standard programme used 30 cycles.

2.6.2 PCR using SimpliFi HS Mix.

The SimpliFi HS Mix from (Meridian Bioscience, London, UK) was used and each 50 µL PCR reaction was mixed in a PCR tube as follows: 25 µL of Simplifi HS Mix 2X, 1 µL of each 10 µM primer, 1 µL template and 22 µL water. All subsequent steps in the process are similar to the Velocity Taq polymerase.

2.6.3 Template preparation by boiling.

Pure plasmid DNA was not necessary to prepare a template for PCR reactions; instead, boiling samples was sufficient (Figure 2.3). A single colony was selected from a fresh agar plate with a sterile toothpick and combined into 1.5ml Eppendorf tubes containing 50 µL of SDW. The samples were heated up to 100°C for 10 minutes, then spun down at 11,000x g for 5 minutes in a MiniSpin. The supernatant was used as the template for PCR reaction directly.

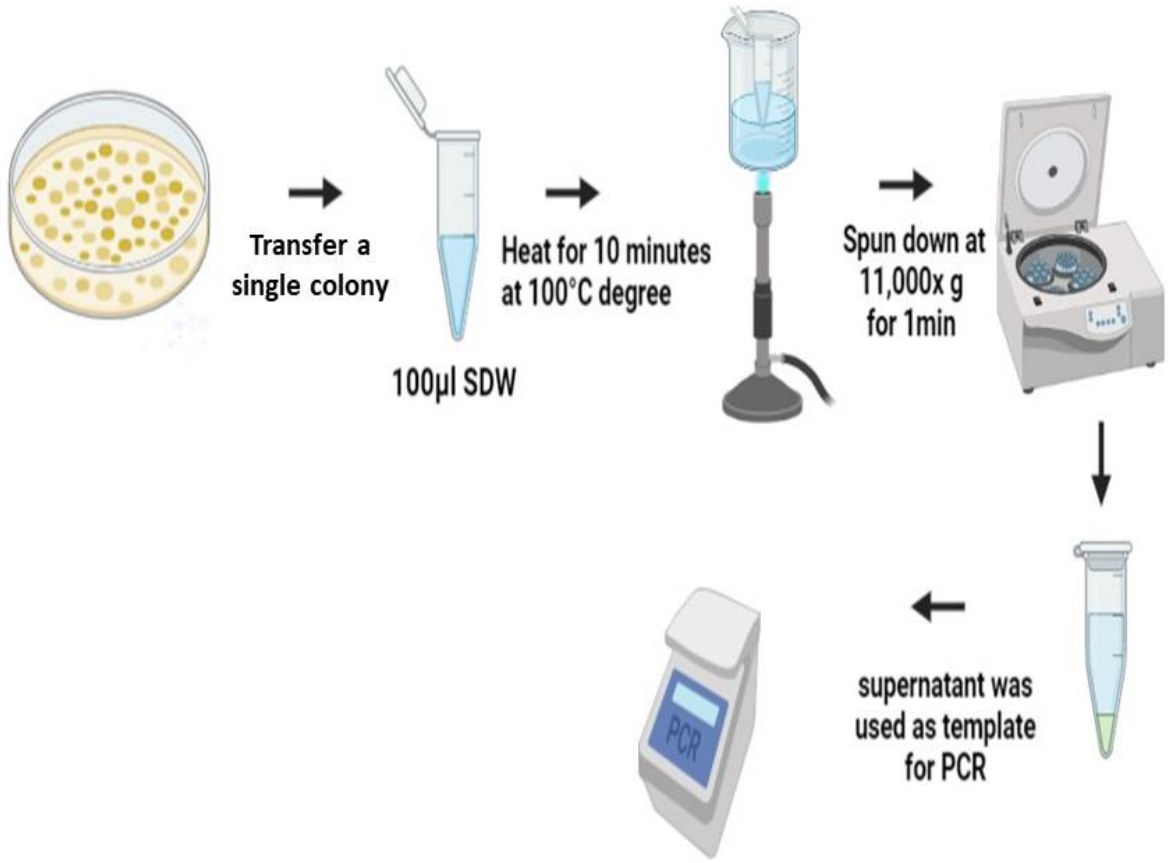

Figure 2.3 The protocol of preparation template by boiling.

To prepare a template for PCR reactions, select a single colony from a fresh agar plate using a sterile toothpick and combine it with 50 µL of SDW in 1.5ml Eppendorf tubes. Heat the samples up to 100°C for 10 minutes, then spin them down at 11,000x g for 1 minutes. Finally, use the supernatant directly as the template for PCR reactions.

2.7 DNA Sequencing reactions

Most of the sequencing was done using Sanger Sequencing by the Genomics Laboratory at the University of Birmingham, run on an ABI 3730 DNA Analyser (Applied Biosystems, Foster City, USA). We are required to create a mixture consisting of template DNA, primer, and sterile distilled water (SDW) for sending it to the Genomics Laboratory. The mixture should contain 200-500ng of the template DNA or 10ng for PCR sequencing were mixed with 3.2pmol primer for DNA sequencing. The mixture final volume was 10µL, and it was topped up with SDW. Data analyses were done with SnapGene software.

Full-length plasmid sequencing was done by plasmidsNG (Birmingham, United Kingdom). 15µL of purified plasmid DNA at a concentration of 25 ng/µL were placed into PCR strip tubes, and samples were placed into jiffy bags and sent for sequencing. To check the concentration of the DNA, a Nanodrop Spectrophotometer was used. Data analyses were done with SnapGene software.

2.15 Splicing Overlap Extension (SOE) PCR

Splicing Overlap Extension (SOE) PCR was employed to facilitate the joining of DNA fragments with the objective of introducing changes, such as deletions or insertions, utilizing homologous recombination. The SOE PCR protocol, as introduced by (Zarghampoor et al., 2020), involves several key steps. Firstly, primer pairs flanking approximately 600 bp regions within the target plasmid are designed. These primers are utilized to amplify the two arms of the target region separately by PCR, using template DNA extracted from the desired plasmid.

The PCR reactions are then purified to remove any remaining primers or nucleotides. Subsequently, the purified PCR products are utilized as templates in a second PCR reaction, where primers are omitted. This PCR reaction is conducted for three cycles under standard conditions to allow the overlapping regions of the PCR products to anneal and extend, facilitating the formation of hybrid DNA molecules. After three cycles, outer primers complementary to the ends of the target region are added to the PCR mixture, and the reaction is continued for an additional 30 cycles to amplify the desired product.

Finally, the resulting PCR product is analysed by agarose gel electrophoresis to confirm its size and integrity. Upon verification, the targeted product is excised from the gel and purified, yielding the final desired DNA construct. The detailed procedure for SOE PCR is illustrated in Figure 2.4.

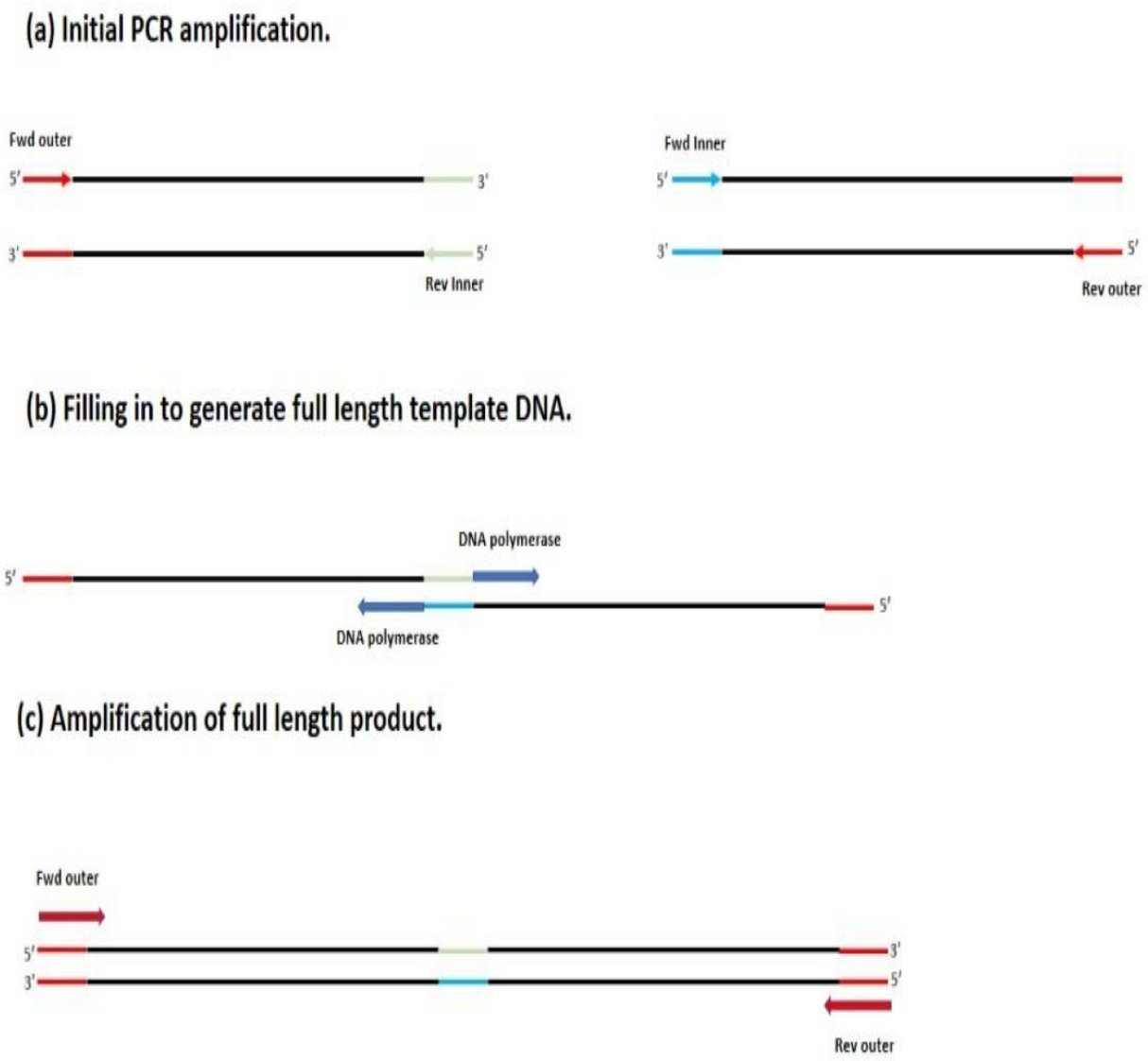

Figure 2.4 Overlap extension PCR, used to generate primer-dictated modification.

(a). Using overlapping primers to amplify PCR products. The inner primer coloured with green, and blue are overlapped and complementary to each other.
(b). After purifying the PCR products, they serve as templates for each other using overlap extension PCR. Three PCR cycles were performed to combine complementary PCR products. This allows the DNA polymerase to extend the 3' end of the DNA fragment using the other fragment as a template. The desired modified full-length product becomes available in the reaction mixture.
(c). Outer primers were added, and 30 cycles of PCR were performed to amplify the full-length product.

2.16 Recombineering via homologous recombination to insert or delete segments of a conjugative plasmid.

Homologous recombination was used to insert or delete a particular gene, as shown in Figure 2.5. First, amplifying homology arms that are specific for the target plasmid was done, and both sides of the region that need to be inserted or deleted were linked together by SOEing-PCR and cloned into non-mobilisable recombineering (shuttle) vectors. Plasmid pLAZ2, which contains the chloramphenicol resistance gene, was the vector used in this work. The shuttle vector was then transformed into a recombination-proficient strain (MV10-Nal^R) containing the target conjugative plasmid. In this study, the target plasmid was always either pUB307, pUBΔtraG or pUBΔ+. Selection of the target plasmid and the vector resistance markers (kanamycin and chloramphenicol) was done for the transformants. Six 5ml LB with kanamycin and chloramphenicol overnight cultures were made from the transformant colonies. Also, overnight culture of 5ml LB with Rifampicin was made from a fresh Nissle Rif plate which was used as the recombination-proficient recipient. The following day, conjugation between donors and recipients was done, as shown previously, and a conjugation spot was made on LBA for two hours. After incubation, conjugation spots were streaked out onto LBA with Rifampicin, kanamycin, and chloramphenicol to select for conjugated co-integrants. Individual streaks of donors and recipients were done on (Rifampicin, kanamycin and chloramphenicol) LBA selective media as a control, and left to grow overnight at 37˚C. The next day, ten transconjugant colonies from the conjugation were selected and streaked out on LBA with Kanamycin and Rifampicin to get single colonies. Then, a patch of the single colony was plated on LBA with chloramphenicol and 5% sucrose. The plates were allowed to grow overnight, and any resulting colonies were expected to have lost the shuttle vector. Screening for deletion or insertion was done by picking 30 colonies and patching them on LBA with chloramphenicol and then on LBA with kanamycin. The desired colony

should be chloramphenicol sensitive and kanamycin resistant. DNA was isolated from such colonies, and PCR was used to confirm gene insertion or deletion.

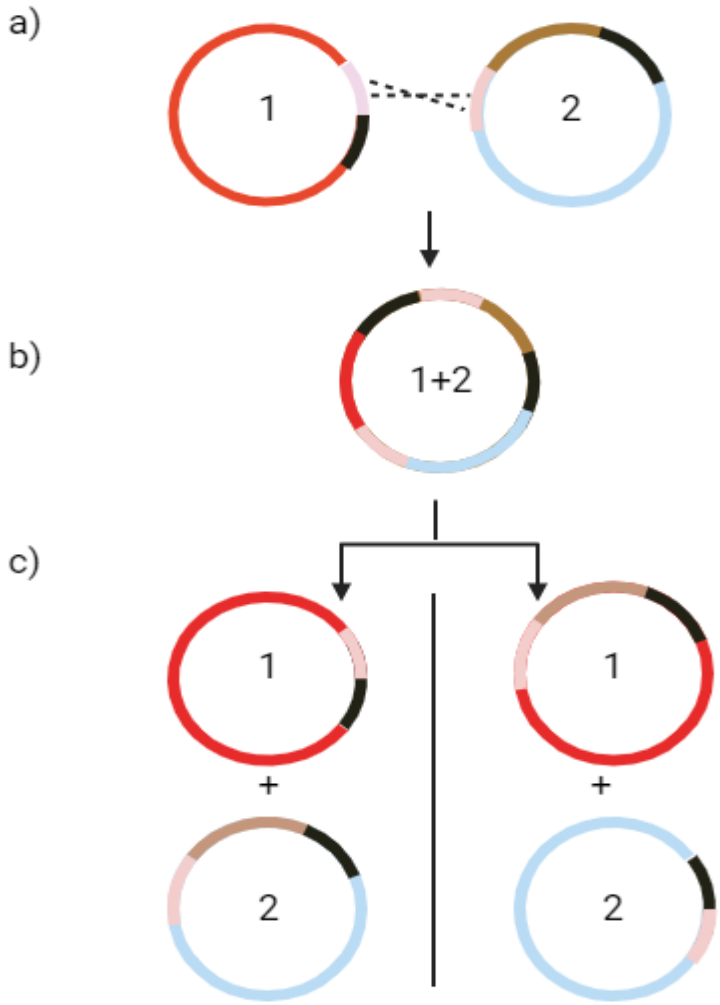

Figure 2.5 Homologous recombination to insert into or delete a segment from a conjugative plasmid.

1. Plasmid 2 is the non-mobilisable recombineering plasmid. (a) The two plasmids are placed in a recombination proficient host. The recombineering plasmid has been designed to have two homology arms (pink and black) able recombine with the same sequences in the target plasmid. (b) Conjugative transfer of both plasmids to a new host selects for the products of recombination creating a cointegrant. (c) The cointegrant can also break down by homologous recombination, the result of which is either the plasmids returned to the original structures (shown on the left part), or it could produce two new plasmids (shown on the right part).

2.17 XylE assay

XylE assays were conducted using standard methods as outlined by Zukowski (1983). In the XylE assay, the response, typically measured as the rate of change in absorbance over time, can vary depending on several factors, including the strength of the promoter driving XylE expression, the efficiency of transcription and translation processes, and the stability of the XylE enzyme itself. The strength of the promoter is a key determinant of the level of XylE expression and, consequently, the intensity of the assay signal (Zukowski et al., 1983).

2.17.1 Sample preparation for XylE assay.

The protocol of XylE assay starts with setting up a 5ml overnight culture of the sample. The following day, in 50 ml conical flasks, 10 ml of LB broth with selectable antibiotics were prepared and inoculated with 100 µL of the overnight culture. Flasks were incubated at 37^{o}C in the shaking incubator until OD_{600nm} reached ~0.5. Then, 5 ml of the culture was transferred to a 15 ml Falcon tube and harvested by centrifugation at 5000g for 10 min. The supernatant was discarded, and pellets were resuspended in 500 µL 9:1 mixture of 0.1M Na phosphate: acetone buffer. The cell suspension was transferred to microfuge tubes and sonicated for 15 seconds in three 5 second burst in ice in the cold room. To pellet cell debris, sonicated samples were spun for 15 minutes at 10,000g at 4°C. The cleared lysate was transferred into a microfuge tube, kept on ice to do the XylE assays. Samples can be frozen at -70^{o}C after adding 50µL of 50% glycerol solution (Zukowski et al., 1983).

2.17.2 Conducting the XylE assay.

First, a catechol solution was prepared by adding 4.5 mg catechol to 12.5 ml 0.1M Na phosphate buffer pH 7.4. A spectrophotometer was used to do the assay, and the blank assay was made by adding 100 µL 9:1 Na phosphate: acetone solution to the cuvette. To do the assay, 100 µL of the clear lysate solution was added to a cuvette that contained 2.8 ml

phosphate buffer + 200 µL catechol solution. The Spectra Analysis program was used to calculate the increase in absorbance over time, and the biuret assay was used to calculate the protein concentration of the samples (Zukowski et al., 1983).

The Spectra Analysis program in a spectrophotometer is a software tool used for analyzing the spectral data obtained from the instrument. Spectrophotometers are scientific instruments that measure the absorption or transmission of light by a sample at different wavelengths. The Spectra Analysis program used in this study is Jasco Spectra Manager, (Tokyo, Japan) and it allows to visualize and analyze the spectral data obtained from the instrument. In the analysis conducted, the program presents the spectral data as a graph or spectrogram, where the horizontal axis denotes time and the vertical axis represents the change in absorption over time. This means that instead of the wavelength of light, the analysis tracks variations in absorption against time intervals. The program also allows users to apply various filters and corrections to the spectral data to improve the accuracy of the measurements.

To calculate the XylE activity, the following equation is used.

$$\frac{OD_{374nm}\ min^{-1} \times \text{dilution factor}}{\text{Protein concentration (mg/ml)}}$$

(Dilution factor = 1000 ÷ volume of lysate used in assay)

(OD_{374nm} min^{-1} = increase in absorbance at 374 nm over 1 minute).

2.17.3 Biuret assay.

Biuret assays were conducted following the standard methods outlined by (Gornall et al., 1949), for protein concentration determination. The biuret assay is a biochemical test utilized to quantitatively measure protein concentrations in a solution. The protocol began by preparing a series of protein standards using Bovine Serum Albumin (BSA) with known concentrations. For sample preparation, 200 µL (50 µL cleared lysate + 150 µL water) was combined with 800 µL of Biuret reagent in 1 ml cuvettes. A blank cuvette was prepared with 150 µL water, 50 µL phosphate buffer, and 800 µL Biuret reagent. After gentle mixing, the samples were incubated in the dark at room temperature for 30 minutes. Protein concentrations were then measured using a spectrophotometer at OD550nm (Gornall et al., 1949).

2.18 Agarose gel electrophoresis

The protocol of electrophoresis starts with making a 50x (TAE, Tris Acetate EDTA) buffer stock solution. In order to produce a 50x buffer stock solution, 242g Tris base is dissolved in 200 ml of distilled water, followed by 57.1 ml of Glacial Acetic Acid and 100 ml of 500 mM of EDTA (pH 8.0). The solution is brought to the final volume (1 L) before autoclaving.
To prepare a gel 1 g of Hi-Res Standard Agarose from (Cambridge Reagents) was mixed with 100 mL 1xTAE, and the mixture was heated for 2 minutes (approx) in a microwave until the agarose was completely dissolved. The mixture was allowed to cool slightly before adding 2 µL ethidium bromide (10 mg/ml). The solution was poured into the gel tray with a comb, and the gel was allowed to solidify at room temperature for a duration of 30 minutes. Preparation of samples involved mixing each sample with 2µL of 6x Purple gel loading dye (NEB) for every 10 µL of the sample. The 1kb molecular weight ladder (N3232L) shown in

Figure 2.6 was used when the gel was run in the gel tank with 1xTAE buffer. Samples were normally run at 100V for about 1 hour. The samples were then visualised in a Gel Doc XR UV transilluminator (Bio-Rad Laboratories, Hercules, USA) and investigated via Image Lab (Bio-Rad Laboratories).

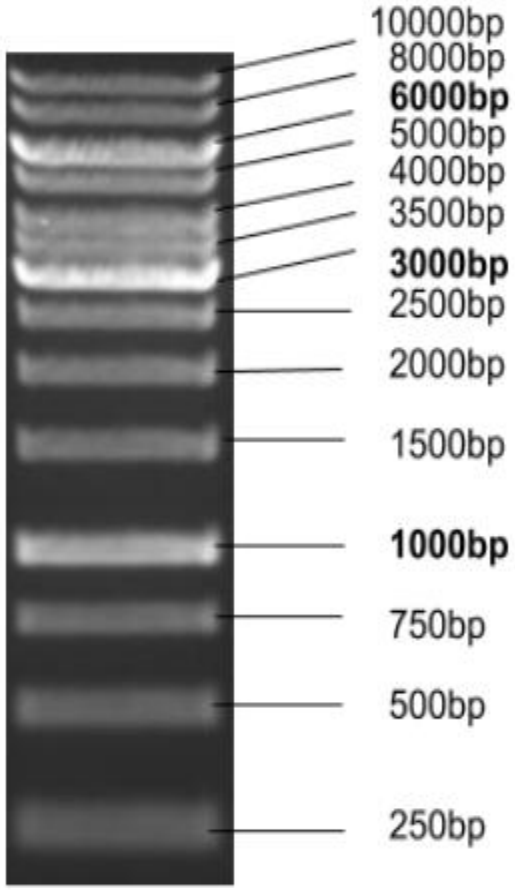

Figure 2.6 The GeneRuler 1kb DNA ladder.

This ladder was utilized in this study to to assess the size of DNA fragments within the gel. The ladder was sourced from Thermo Scientific, located in Oxford, United Kingdom.

2.19 Gel purification

The protocol for purifying DNA from standard agarose gel that was made using the protocol in 2.18 starts with ensuring that all buffers and tools used in agarose gel are fresh and clean to avoid contamination. The bands that showed the needed fragment of interest were cut out of the gel by razor under UV light and placed in a 1.5 ml microfuge tube. Gel Band Purification

Kit (GE Healthcare, Chalfont, UK) was used to purify the DNA from the gel, and it was normally eluted in 30 µL (2x15µL) elution buffer and stored at -20°C.

2.20 Standard T4 ligation

T4 DNA ligase was always used to prepare a mixture when ligations were required, as shown in Table 2.7. The molar ratio should be 1:3 vector to insert.

Table 2.7 T4 DNA ligase mixture as recommended by New England Biolabs

COMPONENT	20 µL REACTION
T4 DNA Ligase Buffer (10X)	2 µL
Vector DNA (eg 4 kb)	50 ng (0.020 pmol)
Insert DNA (eg 1 kb)	37.5 ng (0.060 pmol)
Nuclease-free water	to 20 µL
T4 DNA Ligase	1 µL

2.21 Analysing gene expression using western blotting.

2.21.1 Sample Preparation

The protein sample was released by sonication. Specifically, 15 µL of bacterial culture with an optical density (OD_{600nm}) of 0.6 was combined with 5 µL of Bio-Rad Laemmli Sample Buffer (4X). The loading buffer serves to denature proteins, disrupt disulfide bonds, and apply a negatively charged dye to the proteins. This process aids in enhancing protein visualization during electrophoresis (Schägger and Von Jagow, 1987). This mixture was placed on ice and sonicated for 15 seconds in 5-second bursts. In addition, an alternative method for lysing the sample cells involved boiling the sample at 100°C for 5 minutes. Half

the material was then loaded onto an SDS-PAGE gel, while the remaining sample was stored at -20 °C.

2.21.2 Making an SDS-PAGE gel

The protocol starts with preparing a 10%, separation gel as shown in Table 2.8. The gel was poured immediately after adding TEMED and APS. A space of 2 cm below the bottom of the comb was left for the stacking gel. After pouring the separation gel, isopropanol was pipetted onto the top to eliminate bubbles and exclude air. The gel was left to set for 30 minutes and then washed with distilled water after removing isopropanol. The next step is pouring the stacking gel, as shown in Table 2.9, on top of the separation gel and combs were added to form wells. After setting the gel on the bench for 30 minutes, the gel was ready to use. The gel was placed into a gel tank and filled up with the running buffer 1X, as mentioned in Table 2.10. Protein samples were loaded into the wells after removing the combs, and the gel was run at 180 volts.

Table 2.8 Preparing of the separation gel (10% w/v)

H_2O	4.1 ml
Acrylamide/bis (30% 37.5.1 Bio-Rad)	3.3 ml
Tris-HCI (1.5M, pH 8.0)	2.5
SDS 10% (w/v)	100 µL
TEMED(Bio-Rad)	10 µL
Ammonium persulfate (APS) 10% (w/v)	32 µL

Table 2.9 Preparing of the stacking gel (4% w/v)

H_2O	6.1 ml
Acrylamide/bis (30% 37.5.1 Bio-Rad)	1.3
Tris-HCI (0.5M, pH 6.8)	2.5
SDS 10%	100 µL
TEMED(Bio-Rad)	10 µL
Ammonium persulfate (APS) 10%	100 µL

Table 2.10 Preparing of the 1X running buffer

Tris base	25mM
Glycine	192 mM
SDS	0.1%
pH	8

2.21.3 Gel Staining

Coomassie Blue stain (Quick Coomassie Stain) that contains (Coomassie Blue dye Coomassie Brilliant Blue R-250, Methanol, Acetic acid, Distilled waterwas) used to stain the SDS-PAGE gel. The gel was covered with 400mL of Coomassie for 4 hours with gentle agitation at room temperature. To destain the gel, the gel was covered with SDW and incubated at room temperature with gentle agitation to remove excess dye for two hours. The gel is ready for Gel Imaging.

2.21.4 Western blotting

To do the Western blotting, a protocol from Bio-Rad was used. After separating the target protein(s) by SDS-PAGE the Proteins were transferred from the gel to a nitrocellulose

membrane using the Trans-Blot Turbo Transfer System by Bio-Rad, employing the Trans-Blot® Mini Nitrocellulose Transfer Packs. The transfer was conducted following the preprogrammed 'Mixed MW' protocol on the Trans-Blot Turbo Transfer System, applying a voltage ranging from 1.3 V to 25 V for a duration of 7 minutes. The second step was to add the 6xHis monoclonal antibody (Clontech, Oxford, UK) primary antibody. Goat Anti-Mouse IgG Antibody [HRP] (2BScientific, Oxfordshire, UK) secondary antibody to the blocking buffer (PBST) 1:1000. To prepare the PBST blocking buffer, combine 5% skim milk powder with phosphate-buffered saline (PBS) in distilled water at a ratio of 1 tablet per 100 mL. Additionally, include 0.1% Tween 20 (Thermo-Fisher Scientific, Loughborough, UK) in the solution. The membrane was washed in 20ml blocking buffer for 30 min. Then, the membrane was subjected to a washing process using PBST (Phosphate-Buffered Saline with Tween 20) washing buffer for 10 minutes, repeating the wash three times. The secondary antibody diluted in blocking buffer was added, and the membrane was incubated for three hours. The membrane was washed again to remove excess secondary antibodies, and the membrane was placed on a plastic surface with the protein side up. To image the membrane, a GE ImageQuant instrument was used and 2 ml of the activated ECL reagent (Thermo-Fisher Scientific, Loughborough, UK) was added to the membrane and incubated for 1 minute. The membrane was then placed on a tray and into the GE ImageQuant to image the protein.

2.22 Restriction digests

In this study restriction digests were used for gene cloning to cut a plasmid vector and target gene of interest at specific sites. It was also, used to check the size of a DNA fragment by cutting a DNA sample with a restriction enzyme that recognizes sites on either side of the target fragment. Restriction digests were done using enzymes and buffers from New England

Biolabs, as can be observed in Tables 2.11 and 2.12. In this study I have used lot of restriction enzymes such as EcoRI, HindIII, BamHI, XhoI, SalI, XbaI, NdeI, BsaI, XhoII, AgeI, and SmlI.

Table 2.11 Cloning 50µL Digest

Restriction enzyme	1 µL
10x Buffer	5 µL
plasmid prep	The volume ranges from 2µL to 10µL, and this is depending on the DNA concentration
SDW	42 µL to 34 µL as required
Total	50 µL

Table 2.12 Diagnostic 25µL Digest

Restriction enzyme	0.5 µL
10x Buffer	2.5 µL
plasmid prep	4 µL
SDW	18 µL
Total	25 µL

2.23 Site directed mutagenesis (SDM)

Site-directed mutagenesis typically involves designing primers to amplify the entire plasmid with back-to-back primers that introduce the desired mutation. When using Q5 polymerase

for this purpose, the elongation time should be adjusted according to the size of the plasmid and is usually longer than 30 seconds.

The PCR mixture consists of 12.5 µL of 1X Q5 Hot High-Fidelity 2X Master Mix (New England Biolabs, Ipswich, USA), 1.25 µL each of forward and reverse primers, 1 µL of DNA template, and 9.0 µL of sterile distilled water (SDW). PCR cycling begins with denaturation at 98 °C for 30 seconds, followed by annealing at 67°C for 30 seconds, primer extension for a duration appropriate for the plasmid size at 72°C, and a final extension at 72°C for three minutes.

Following PCR, the next step is the Kinase, Ligase, and DpnI (KLD) treatment. The KLD enzyme mix from New England Biolabs (Ipswich, USA) is used in this step. The reaction mixture comprises 1 µL of PCR product, 5 µL of 2X KLD reaction buffer, 1 µL of 10X KLD enzyme mix, and 3 µL of SDW. After incubating the mixture for 5 minutes at room temperature, 10 µL of it is used for transformation.

2.24 Hydroxylamine mutagenesis:

The protocol used was based on (Amberg et al., 2006). The hydroxylamine solution was be prepared and stored on ice until use. To prepare the hydroxylamine solution, 0.35 g hydroxylamine HCl and 0.09g NaOH were dissolved in 5 ml ice-cold H_2O. The pH was adjusted to 7. Then 5 µL of purified plasmid DNA pACYC184-traG-oriT was added to 250 µL of hydroxylamine solution in a microfuge tube. Samples were incubated at 37^{o}C, and different periods (2, 4, 8, 14, 20, 30 and 40 h) were tested. To stop the reaction, 5 µL of 5 M NaCl, 25 µL of bovine serum albumin (BSA, 1 mg/ml), and 0.5 ml of ethanol were added, then samples were spun down for 10 minutes, and the supernatant was removed. Treated

DNA was resuspended in 50 μL of TE (10 mM Tris [pH 8), 5 μL of 3M Sodium Acetate and 125 μL of 100% ethanol. Samples were incubated at 70^{o}C for 10 minutes, and 800 μL of the DNA was moved into the silica membrane spin columns from the Plasmid Mini kit (Bioline, London, UK). The sample was incubated for 1 min at room temperature and spun down. The bound DNA was washed using wash buffer from the same kit, and purified DNA was eluted in 30 μL.

2.25 Statistical Analysis

To compare means between two different conditions, a statistical analysis was conducted using the t-test tool in GraphPad Prism version 10.0.0 for Windows, developed by GraphPad Software, Boston, Massachusetts, USA. Alongside the mean values, standard error (SE) values were also calculated and reported. The means represented the average measurements of three replicates and acted as reference points for comparison between the two conditions.

The standard error (SE) values were used to determine the variability or precision associated with each mean estimate. The SE value indicated how much the individual data points spread or dispersed around the mean and reflected the degree of uncertainty in estimating the true population mean based on the sample data. In this study, the standard significance level is typically set at $\alpha = 0.05$.

Chapter 3: Checking the fertility inhibition phenotype of plasmid F against RK2.

3.1 Background

Plasmids are powerful agents for transferring antibiotic resistance genes between bacterial populations, and this frequently endures even in the absence of any selection. Antibiotic resistance is a pressing issue that is on the rise, particularly in the Enterobacteriaceae family, as discussed in the Chapter 1, Section 1.1 (Nordmann et al., 2011).

Fertility inhibition, as mentioned earlier in the introduction of Chapter 1 Section 1.3, refers to systems capable of inhibiting the conjugation capacity of plasmids. There are a variety of mechanisms for this inhibition (Norman et al., 2009), and donors can employ it to regulate the conjugative transfer of plasmids (Garcillán-Barcia and de la Cruz, 2008). It may also influence the conjugation status of unrelated co-residual plasmids. Based on a study conducted by (Getino et al., 2017), it has been shown that the conjugation of the R388 that is belongs to IncW plasmids, can be strongly inhibited by a particular groups of other plasmids. This system is found in IncF plasmids such as F and IncI plasmids like R64, which both carry a responsible gene called *pifC*. This gene is known to play a role in the fertility inhibition of IncP plasmids. Additionally, the presence of the R388 gene has been found to inhibit the conjugation of IncP plasmids with the responsible gene being *osa* (Getino et al., 2017).

Our lab investigated the idea of using a pCURE vector to displace IncF plasmids, as described in Chapter One, section 1.5. pCURE-F-307 is a self-transmissible plasmid that is able to replicate in higher copy number than its parent plasmid RK2 and has a broad-host-range (Lazdins et al., 2020). The functioning principle of the pCURE plasmid relies on blocking the replication and neutralising addiction systems of the target plasmids using a curing cassette. This principle worked very well in the laboratory population. However, the

efficiency of the plasmid spread and displacement of IncK plasmids in the mouse model could have been more efficient (Lazdins et al., 2020).

A potential limitation on spread of pCURE-F-307 could be due to the interaction between IncF plasmids and IncP plasmids. IncF plasmids contain the *pifC* gene, whose product targets the TraG coupling protein of IncP plasmids, which is responsible for the formation of the pilus and the transfer of DNA from the donor bacterium to the recipient bacterium during conjugation (see Chapter 1 section 1.4). The binding of PifC to TraG hinders its proper functioning. Consequently, this will inhibit the spread of IncP, as confirmed in previous studies (Getino et al., 2017).

Another mechanism involves surface exclusion proteins that prevent donor cells from binding to the surface of recipient cells. These proteins can physically obstruct the entry of the donor cell or inhibit the formation of stable conjugative bridges necessary for DNA transfer (de Oliveira et al., 2016). It is possible that the effectiveness of plasmid transfer through pCURE-F-307 could be affected by the recipient cell, which may pose a potential limitation in its distribution.

3.2 Aims and hypotheses.

The overall aim of this first block of work was to confirm and become familiar with the Fertility Inhibition phenotype of F plasmids against IncP plasmids. I therefore started this work using RK2 as the model plasmid before it became clear that using the related plasmid pUB307 (that is related to RK2 by loss of the segment including the whole of the Ap^R transposon Tn1, Figure 1.11) for the further work, described in Chapters 4 and 5, would be

more sensible. Plasmid pUB307 is the basis for the effective pCURE-F-307 (Lazdins et al., 2020) but also has the advantage of not conferring Ap^R.

The first objective of the work in this chapter was to determine the optimal donor to recipient ratio for the transfer of RK2. The second objective was to confirm that strain JM109 has the F' prolac and that the JM109-cured strain does not, using growth on M9 minimal medium as a critical test. This aim derives from the genotype of JM109, in which additional genetic material carried by the F' element allows it to produce the proline amino acid, which is not present in the minimal medium (Lazdins et al., 2020).

RK2, as discussed in the Chapter 1 section 1.4, is an IncP plasmid, and several reports have shown that F plasmids can inhibit plasmids transfer in IncP plasmids (Miller et al., 1985). The main aim of this chapter is to confirm the effect of F when present in the same strain as RK2.

Recipient bacteria have the ability to encode natural mechanisms that act as defence systems against potentially harmful invading genetic material (Wilkins, 2002). From the previous principal and others, it was essential to consider the impact of the presence of F in the recipient strain. One of this chapter's objectives is to check the consequences of having F plasmid in the recipient strain on the transfer of RK2.

The final aim of this chapter was to assess the impact of having two sources of inhibition in the donor strain on the transfer of RK2. The presence of multiple inhibition sources could affect plasmid transfer either positively or negatively. This is due to interactions involving the plasmid, as indicated in a study by (Getino et al., 2017).

3.3 Results

3.3.1 Investigating the effect of donor to recipient ratio on RK2 conjugative transfer.

The central process studied in this project was the ability of IncP plasmids RK2/pUB307 to spread by conjugative transfer and how different factors influenced this. It was, therefore, essential to determine the optimal donor to recipient ratio to get efficient transfer for RK2. Three different donor to recipient ratios were tested as follows: 1-1, 1-10 and 1-100. The JM109 cured strain was used as a donor, and HB101 was used as a recipient. The experimental design is summarised in Figure 3.1.

The results showed that the best donor to recipient ratio to do a RK2 transfer is a 1-10 ratio, then a 1-100 ratio, and the least efficient is a 1-1 ratio, as shown in Table 3.1 and Figure 3.2.

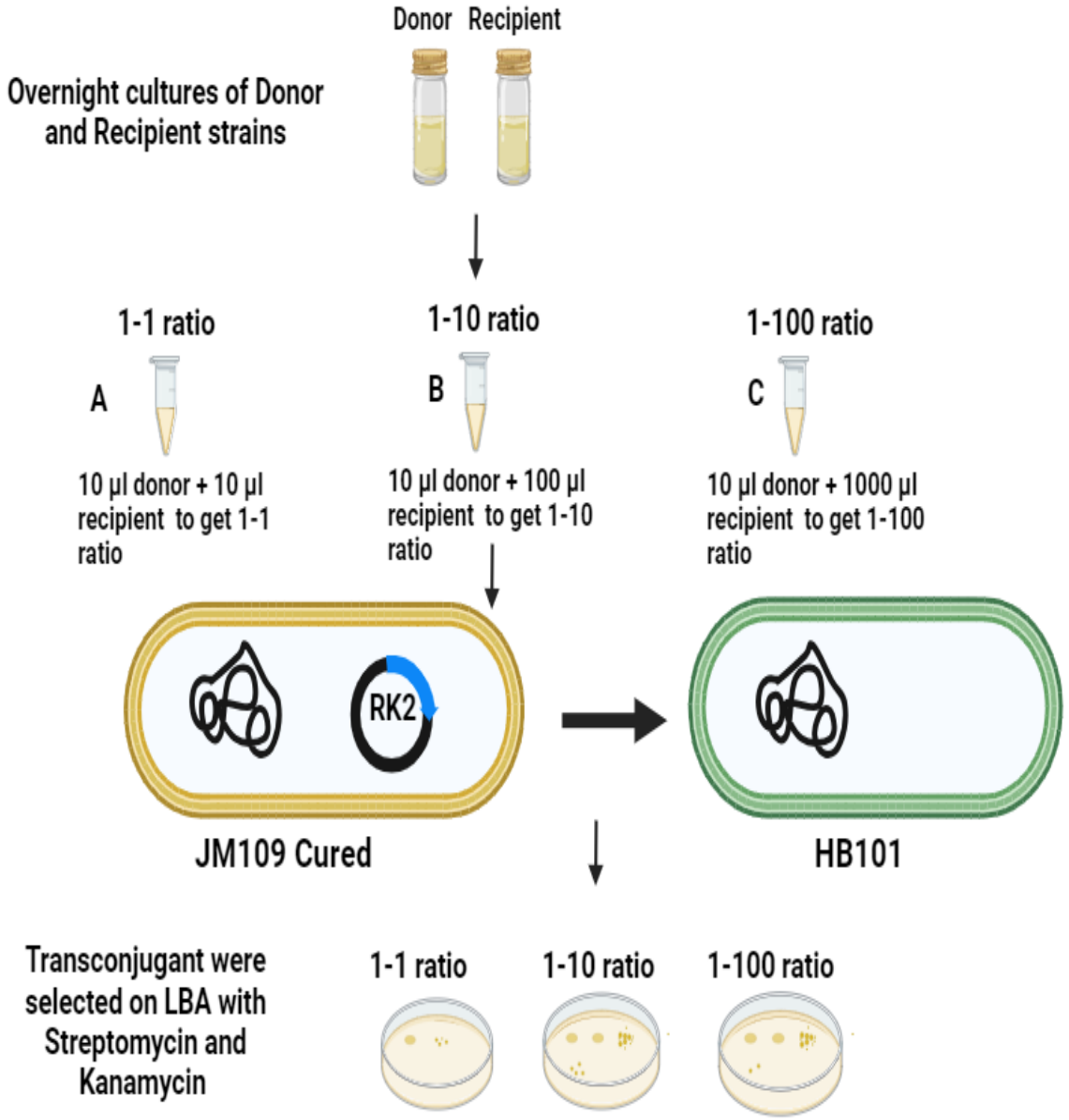

Figure 3.1 Checking the best donor to recipient ratio to do RK2 transfer.

Cultures of donor and recipient were made in 5 ml LB with selectable antibiotics, and cultures were incubated in the shaking incubator at 37°C. To prepare different donor to recipient ratios, 10 µL donor and 10 µL recipient were mixed to get a 1-1 ratio, 10 µL donor and 100 µL recipient were mixed to get a 1-10 ratio, and 10 µL donor and 1000 µL recipient were mixed, to get 1-100 ratio. Mating was terminated after 10, 30, 50, 180 and 240 minutes by cutting out the LB agar with the spot and suspending in 1 ml of 0.85% (w/v) saline. Serial dilutions were made from 10-1 to 10-7. 20 µL of each dilution was spotted on selective plates, which were then incubated overnight at 37ºC, and the number of colonies was counted.

Table 3.1 Determining the best donor to recipient ratio to do RK2 transfer.

	1 to 1		1 to 10		1 to 100		1 to 1 & 1 to 10	1 to 1 & 1 to 100	1 to 10 & 1 to 100
Time (minutes)	**Mean**	**SD**	**Mean**	**SD**	**Mean**	**SD**	**P value[a]**		
10	**43**	**11**	**148**	**17**	**103**	**20**	**0.001**	**0.012**	**0.046**
30	**766**	**152**	**2333**	**404**	**1300**	**264**	**0.003**	**0.039**	**0.021**
60	**15000**	**2645**	**32666**	**3055**	**27666**	**1154**	**0.002**	**0.002**	**0.057**

a. $p < 0.05$: Statistically significant $p < 0.01$: Highly statistically significant $p < 0.001$: Extremely statistically significant. Statistical significance determined using t-test in GraphPad.

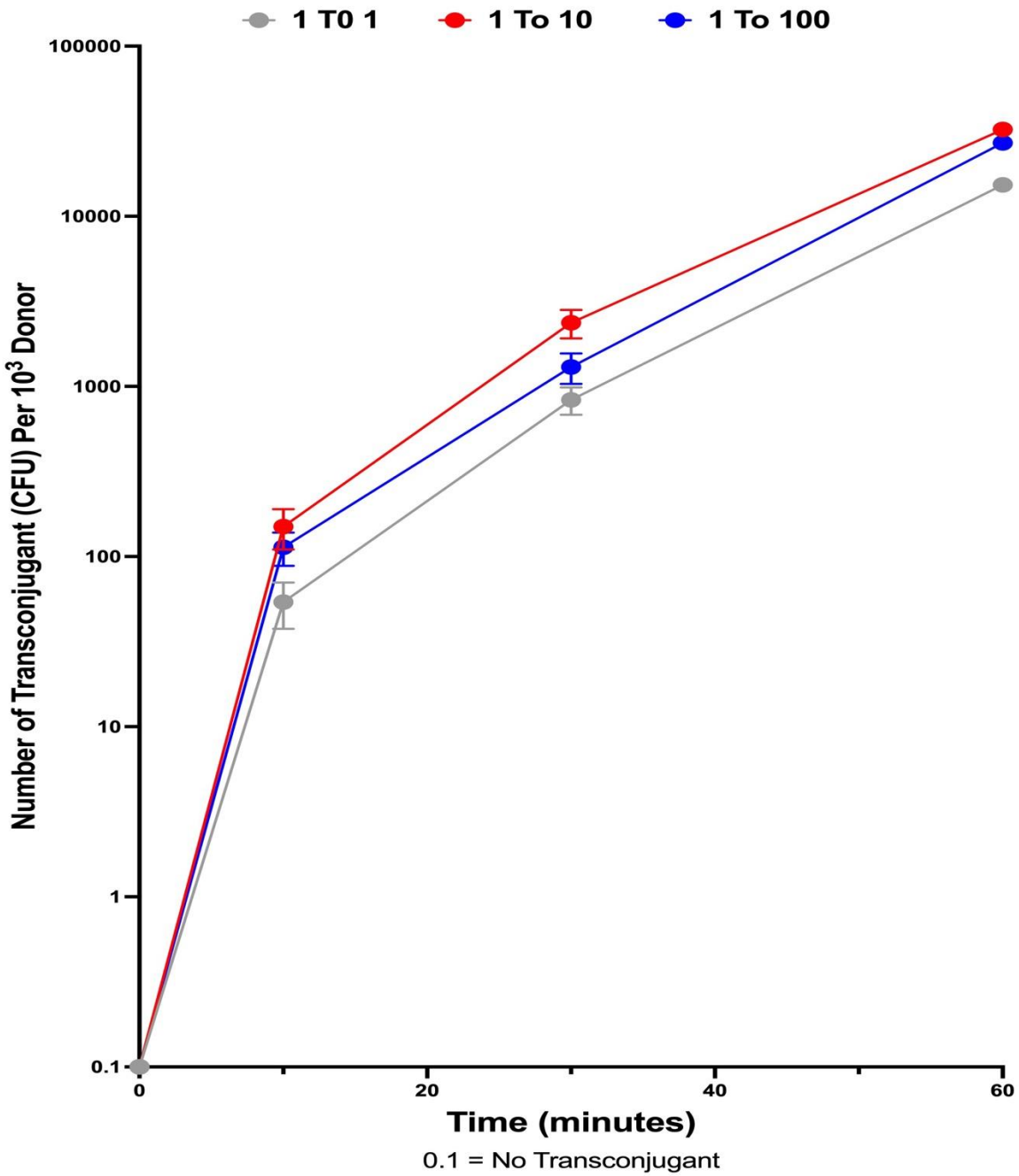

Figure 3.2 Finding out the best donor to recipient ratio to do RK2 transfer.

Three different donor to recipient ratios were tested as follows: 1-1, 1-10 and 1-100. The JM109 cured strain was used as a donor, and HB101 was used as a recipient. The graph drawing package was set to show the error bars for each point but due to the log scale on the y axis these are sometimes not visible. For this reason, the data is also shown in Table 3.1 which includes means, standard deviations and tests of significance where relevant.

3.3.2 To confirm that strain JM109 has the F' plasmid and JM109-cured has not.

The genotypes of JM109 and JM109-cured were described in Chapter Two, section 2.1. The original F plasmid does not carry a selectable marker so F' derivatives that carry part of the chromosome are often used to allow selection of the F-plasmid in a strain that has lost part of the chromosome because the genes on the F' complement the defect. In JM109 the F' critically carries a chromosomal segment that includes the *lac* and *pro* genes. To confirm that strain JM109 has the F' plasmid and JM109 cured strain has not, M9 minimal medium was used to culture the bacteria under controlled conditions. Basically, M9 medium has only a carbon source, several salts that are inorganic and water without the presence of any amino acid (Collins and Thune, 1996). Thiamine was added to the M9 minimal medium because it is essential for growth of both JM109 and JM109-cured. To check the phenotype of JM109 and JM109-cured, both strains were grown on M9 minimal medium (Figures 3.3 and 3.4). This showed that JM109 grows well on M9 minimal medium, confirming that it contains F'prolac plasmid, and that JM109-cured does not.

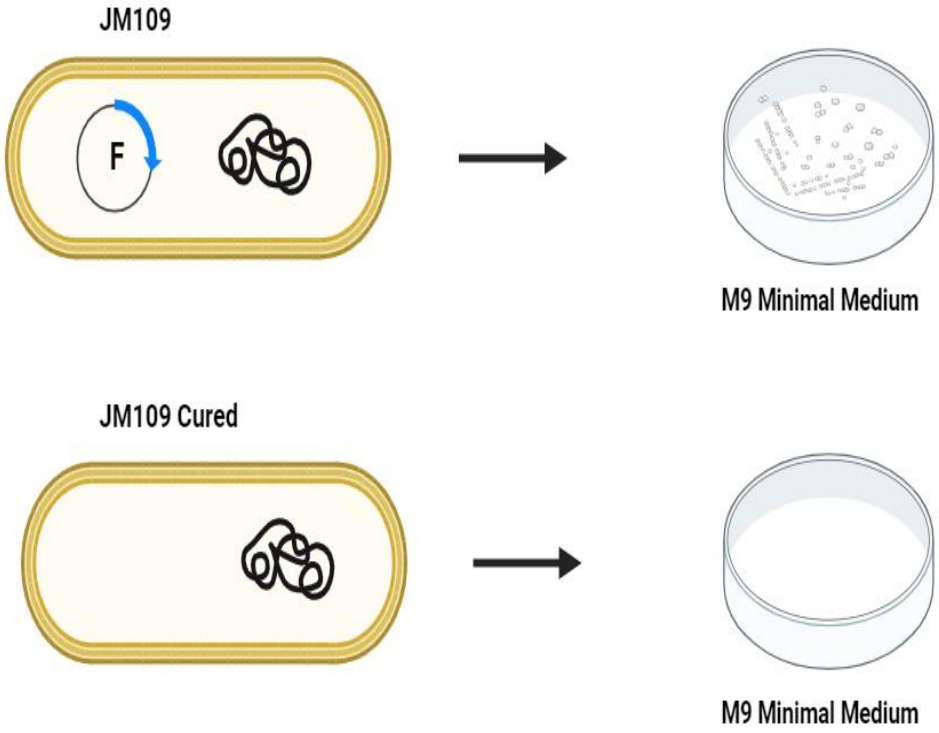

Figure 3.3 Outline of the experiment to test the growth of JM109 and JM109-cured on M9 minimal medium.

The objective of this experiment is to validate the essential role of the F' plasmid, carrying the *lac* and *pro* genes, in facilitating the growth of JM109 strains on M9 minimal medium. Additionally, we aim to demonstrate the incapacity of JM109 Cured strains to proliferate, attributable to the absence of the F' plasmid.

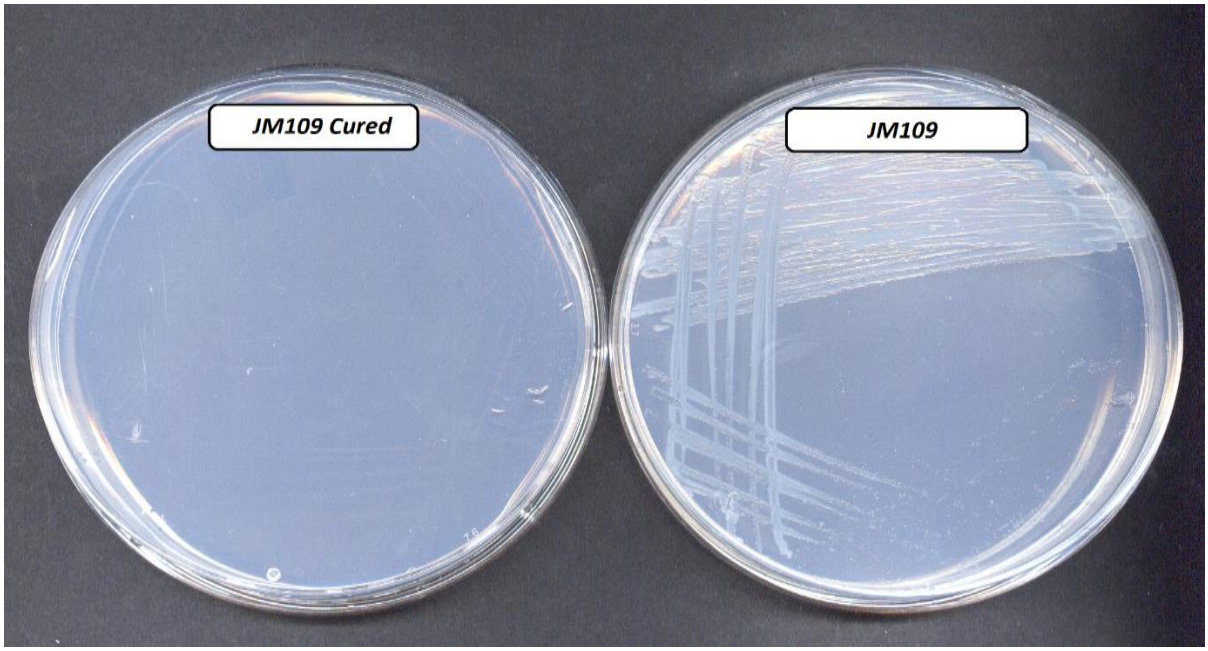

Figure 3.4 Comparison of the growth of JM109-cured and JM109 on M9 minimal medium.

The noticeable difference in growth between the two plates serves as compelling evidence supporting the hypotheses under examination.

3.3.3 To confirm the F' fertility inhibition phenotype against RK2.

The most essential group of experiments involved determining the effect of the F' plasmid when it was present in the same strain as the IncP-1 plasmid. Therefore, RK2 was introduced into JM109 and JM109-cured, and the effect of having F'prolac present on the ability of the IncP-1 plasmid to transfer was determined (Figure 3.5). The standard conditions for observing plasmid transfer involve having a 10-fold excess of recipients (HB101) over donors (JM109 or JM109 cured), so the initial experiment was set up in this way, as shown in Figure 3.5.

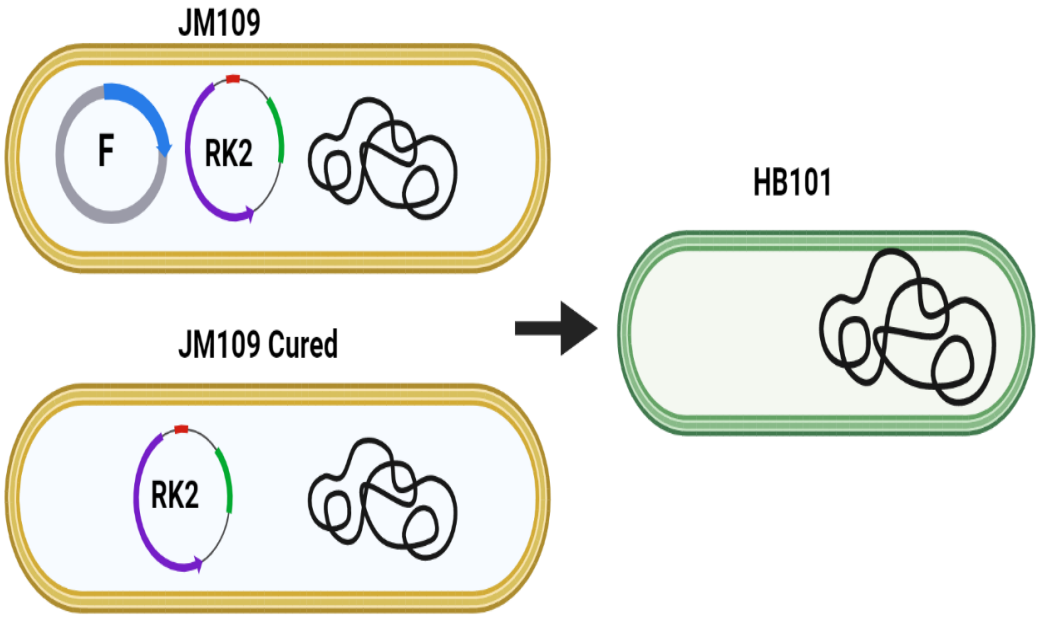

Figure 3.5 Determining the effect of the F' plasmid on RK2 conjugative transfer.

RK2 was transformed to JM109 and JM109 Cured then the transfer of RK2 was compared in the presence of F' in JM109 and in the absence of F' in JM109-cured.

As reported in previous studies, F plasmid negatively affects IncP-1 plasmid transfer (Miller et al., 1985). In my experiments, at the first time-point (after 10 minutes of mating) the number of transconjugants was zero with JM109, while hundreds were observed for JM109-cured (Table 3.2). Moreover, a similar difference between the number of transconjugants from JM109 and JM109-cured was observed at 30 and 60 minute time-points, which confirms that F plasmid inhibits conjugation of RK2. However, at 180 minutes and 240 minutes, the difference between the number of transconjugants from JM109 and JM109 cured transfer were not statistically significant. A possible explanation for the relative increase in transconjugants number from JM109 at these last two time-points could be that the number of potential recipients in the JM109-cured mating becomes limiting when most of these bacteria have received RK2, so the transconjugants count will plateau allowing the JM109 mating mix to "catch up" (Figure 3.6). Also, the F' in JM109 is defective in conjugation due to the

traD36 mutation and therefore does not transfer to HB101, so once some transfer of RK2 to HB101 has occurred, it will no longer be inhibited and will be increasingly able to transfer to other HB101 which have not yet received the plasmid. These results are also presented in Table 3.2, which shows the inhibition factors of F plasmids on RK2 transfer. Because of the plateau in transfer from the Cured strain the inhibition factors of F plasmids on RK2 decrease gradually over time.

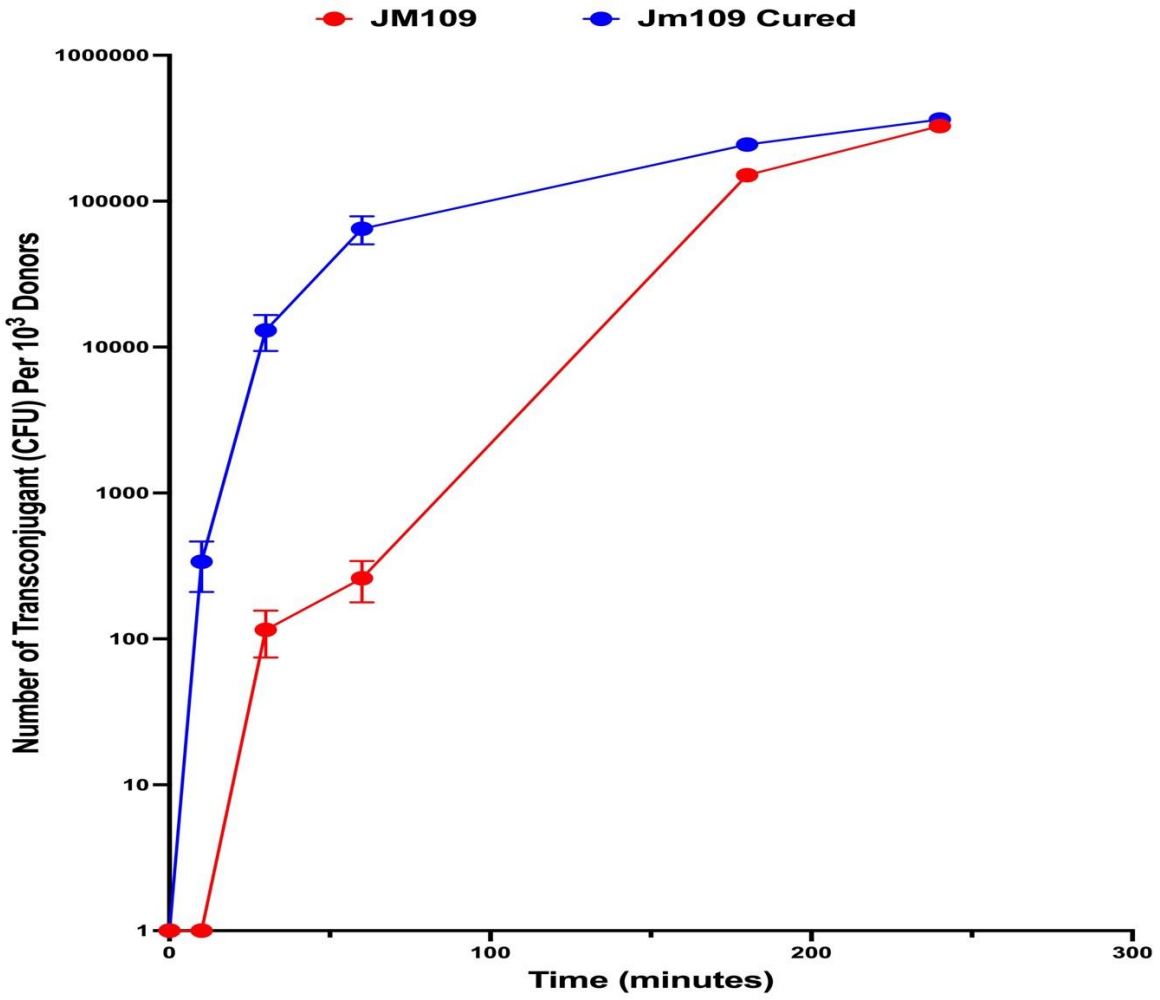

1 present the zero transconjugant

Figure 3.6 RK2 conjugative transfer from JM109 and JM109 Cured to HB101 to check the effect of F' in the donor strain.

The graph drawing package was set to show the error bars for each point but due to the log scale on the y axis these are sometimes not visible. For this reason, the data is also shown in Table 3.2 which includes means, standard deviations and tests of significance where relevant.

Table 3.2 Inhibition factors of F plasmids on RK2 transfer at various time intervals.

	JM109		JM109 Cured			
Time (minutes)	**Mean**	**SD**	**Mean**	**SD**	**P value[b]**	**Inhibition Factor[c]**
10	**<1[a]**	**0**	**337.7**	**128**	**0.010419**	**403**
30	**115.3**	**31**	**13000**	**1000**	**0.000024**	**286**
60	**260.0**	**81**	**65667**	**577**	**<0.000001**	**285**
180	**150667**	**4932**	**244693**	**2309**	**0.000007**	**49**
240	**326867**	**642**	**363367**	**305**	**<0.000001**	**1.42**

a. Number <1 represents 0 colonies.
b. $p < 0.05$: Statistically significant $p < 0.01$: Highly statistically significant $p < 0.001$: Extremely statistically significant. Statistical significance determined using t-test in GraphPad.
c. To calculate the inhibition factor, the following equation was used: Inhibition factor = (Transfer frequency without F plasmid) / (Transfer frequency with F plasmid). To the transfer frequency, the following equation was used: Transfer frequency = The number of transconjugant colonies / The number of donor colonies.

3.3.4 To check the effect of having two sources of inhibition on RK2 conjugation transfer.

A strong relationship between F plasmid presence and inhibiting RK2 transfer has been confirmed in section 3.3.3 above. Most studies in the field of fertility inhibition have only focused on the relationship between pairs of plasmids (ie two plasmids at a time) – one whose transfer is being measured and one whose effect on transfer of the second is being determined. However, in the real-world application of pCURE, the plasmid may encounter more than one plasmid carrying fertility inhibition genes, so it is important to explore the potential outcomes stemming from the presence of two sources of inhibition on the conjugative transfer of the target plasmid. In this section, RK2 transfer was examined in the presence of two sources of inhibition, either (F and R64) or (F and R388).

The experiment was planned first to test the effect of R388, R64 and F on RK2 conjugative transfer separately, as shown in Figure 3.7. Following these studies, experiments to understand how R388 or R64, in combination with F, affects RK2 conjugation transfer were carried out, as shown in Figure 3.8. In order to prepare strains for the experiment, R388 and R64 were transformed into JM109 and JM109-cured, which contain RK2. JM109 Cured containing RK2 was used as a positive control, and the transfer experiments were performed.

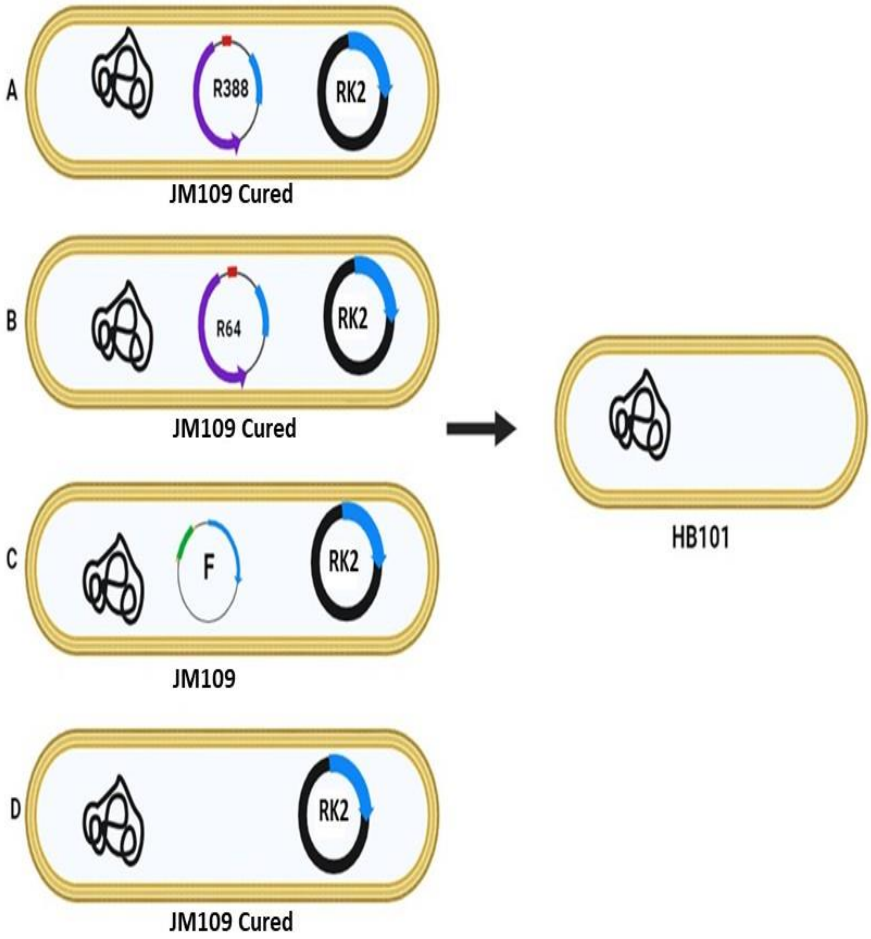

Figure 3.7 Checking the effect of R388, R64 and F on RK2 conjugative transfer separately.

Strain A was used to check the effect of R388 on RK2 transfer.
Strain B was used to check the effect of R64 on RK2 transfer.
Strain C (JM109) was used to check the effect of F on RK2 transfer.
Strain D (JM09-cured containing RK2) was used as a positive control.

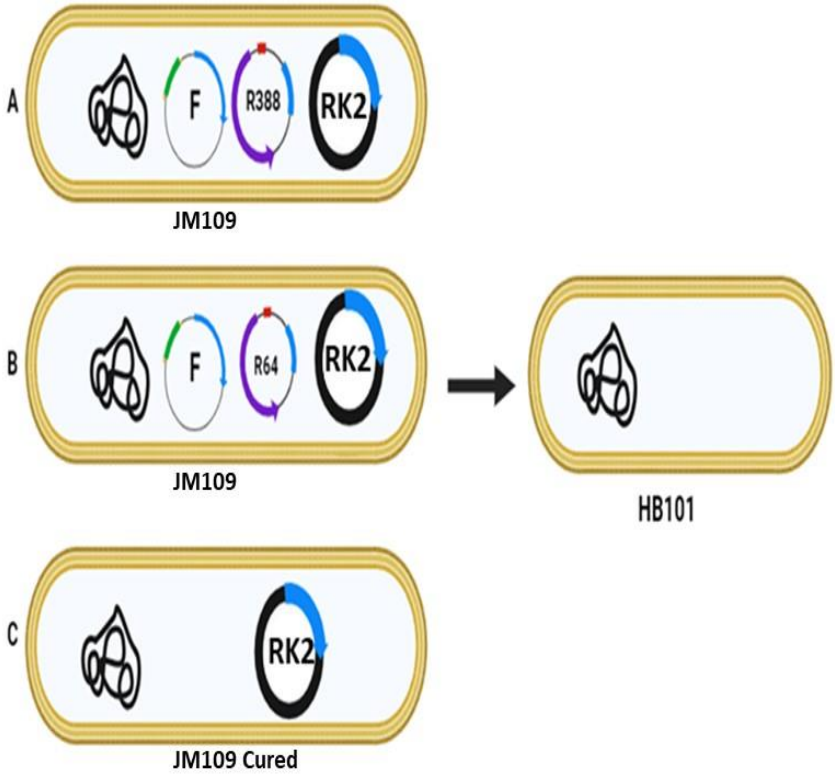

Figure 3.8 Checking how R388 or R64, in combination with F, affect RK2 transfer.

Strain A was used to check the effect of F and R388 on RK2.
Strain B was used to check the effect of F and R64 on RK2.
Strain C (JM109-cured containing RK2) was used as a positive control.

After careful analysis of the data presented in Table 3.3 and Figure 3.9, we can see that R388 has the most significant inhibitory effect on RK2 conjugation transfer when R388, R64 and F'prolac were tested individually. Indeed, no RK2 transfer was observed at 30-minute or 60-minute intervals and only 11 transconjugants were observed at 90 minutes in the presence of R388. Turning now to R64, the inhibitory effect of R64 was clearly present throughout the time course. While it has a much stronger inhibitory effect than F, it is somewhat less powerful than the inhibitory effect of R388 on RK2 transfer. In contrast, the inhibitory effect of F on RK2 is significantly lower than that of R388 and R64, as demonstrated by the 106 transconjugants present after 30 minutes and 263 transconjugants present after 60 minutes,

which is considerably higher than the six transconjugants present with R64 and zero present with R388 after the 30 minutes. However, the inhibition of RK2 by F is still pronounced compared to the control.

The story changes when we simultaneously compare two inhibitors in one strain. When R64 and R388 were added with F, a significant difference in RK2 transfer was detected. In general, the number of transconjugants was reduced significantly in (F+R388) and (F+R64) compared to having only F in the donor strain, as shown in Table 3.4 and Figure 3.9.

First, looking at R388, the most striking result from the data in Figure 3.9 is that the effect of R388 with F on RK2 transfer is slightly weaker than that of R388 individually. After 30 minutes, the number of the transconjugants was 15 when R388 was present with F, while it was zero when R388 was alone. Also, at 60 and 90 minutes, the number of transconjugants was higher when R388 was placed alone.

Having R64 with F positively impacts (ie strengthens) R64 and F inhibition, where the number of the transconjugant after 30 minutes was zero compared to 6 with R64 and 106 with F when they were tested individually. The positive effect continued at all time-points, which confirms that the effect of R64 with F is positive and is stronger than the effect of either alone, as depicted in Figure 3.9.

To see the results from the F plasmid side, the effects of having F with R64 or F with R388 positively impact the inhibition of RK2. The impact of F with R64 on inhibiting the transfer ability of RK2 was more significant than that of F with R388 across all time course points, as shown in Table 3.4 and Figure 3.9.

Table 3.3 Checking the effect of single inhibitor encoded by R388, R64 or F on RK2 conjugation transfer

	F			R64			R388			Control RK2 alone)	
Time (minutes)	**Mean**	**SD**	**P value[b]**	**Mean**	**SD**	**P value[b]**	**Mean**	**SD**	**P value[b]**	**Mean**	**SD**
30	**96**	**20**	**0.000294**	**6**	**8**	**0.000222**	**<1[a]**	**0**	**0.000218**	**1400**	**190**
60	**254**	**50**	**0.000005**	**20**	**21**	**0.000004**	**<1[a]**	**0**	**0.000004**	**23111**	**1170**
90	**1966**	**305**	**<0.000001**	**130**	**128**	**<0.000001**	**8**	**2**	**<0.000001**	**55222**	**1346**

a. Number <1 represents 0 colonie

p < 0.05: Statistically significant p < 0.01: Highly statistically significant p < 0.001: Extremely statistically significant. Statistical significance determined using t-test in GraphPad.

Table 3.4 Checking the effect of multiple inhibitors encoded by R388, R64 or F on RK2 conjugation transfer

	F + R64			F + R388			Control (RK2 alone)	
Time (minutes)	**Mean**	**SD**	**P value[b]**	**Mean**	**SD**	**P value[b]**	**Mean**	**SD**
30	**<1[a]**	**0**	**0.000218**	**15**	**4**	**0.000227**	**1400**	**190**
60	**10**	**3**	**0.000004**	**101**	**24**	**0.000004**	**23111**	**1170**
90	**52**	**11**	**<0.000001**	**536**	**130**	**<0.000001**	**55222**	**1346**

a. Number <1 represents 0 colonies.

b. $p < 0.05$: Statistically significant $p < 0.01$: Highly statistically significant $p < 0.001$: Extremely statistically significant. Statistical significance determined using t-test in GraphPad.

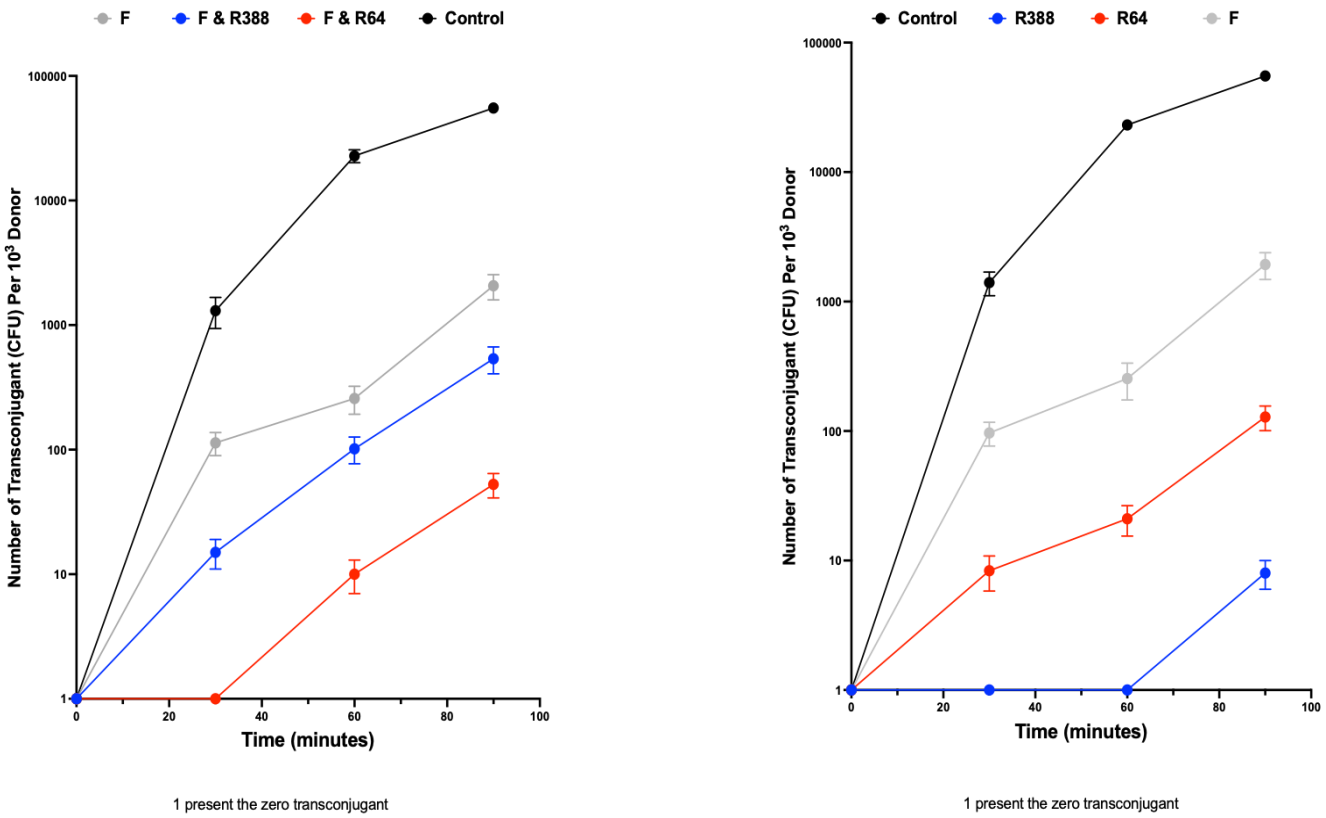

Figure 3.9 Checking the effect of single and multiple inhibitors on RK2 transfer.

The graph drawing package was set to show the error bars for each point but due to the log scale on the y axis these are sometimes not visible. For this reason, the data is also shown in Tables 3.3 and 3.4 which includes means, standard deviations and tests of significance where relevant.

3.3.5 To check the consequences of having F plasmid in the recipient strain.

To determine the optimal conditions of RK2 conjugative transfer, it was essential to evaluate the effect of the presence of F in the recipient strain. The experiment was planned: JM109 and JM109 Cured was used as a recipient, and HB101 containing RK2 was used as a donor, as seen in Figure 3.10.

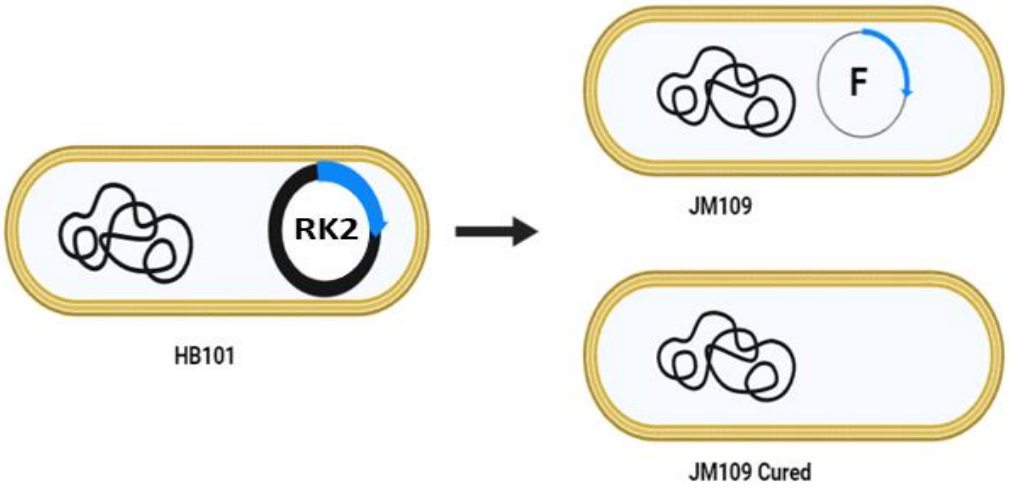

Figure 3.10 Transfer Experiment: Transferring RK2 from HB101 to JM109 and JM109 Cured.

The objective of this experiment is to assess the influence of F' plasmid presence in the recipient strain when using JM109 and JM109-cured as recipients. We anticipate that the transfer efficiency to JM109 Cured will surpass that of JM109 due to the absence of F' in JM109-cured.

The results demonstrate an F plasmid effect on RK2 once F is placed in the recipient strain. The difference in the number of transconjugants when JM109 and JM109 Cured were used as recipients was slight at 10 minutes, while the number of transconjugants started to increase steadily in JM109 Cured until it reached 1200 at 30 minutes and 3100 at 60 minutes. By contrast, with JM109 as a recipient, it was only 400 after 30 minutes and 900 at 60 minutes (Figure 3.11).

Table 3.5 To check the consequences of having F plasmid in the recipient strain when HB101(RK2) is the donor.

	JM109		JM109-cured		
Time (minute)	**Mean**	**SD**	**Mean**	**SD**	**P value[a]**
10	**390**	**40**	**416**	**37**	**0.448870**
30	**676**	**65**	**1233**	**152**	**0.004375**
60	**966**	**125**	**3100**	**200**	**0.000098**

a. $p < 0.05$: Statistically significant $p < 0.01$: Highly statistically significant $p < 0.001$: Extremely statistically significant. Statistical significance determined using t-test in GraphPad.

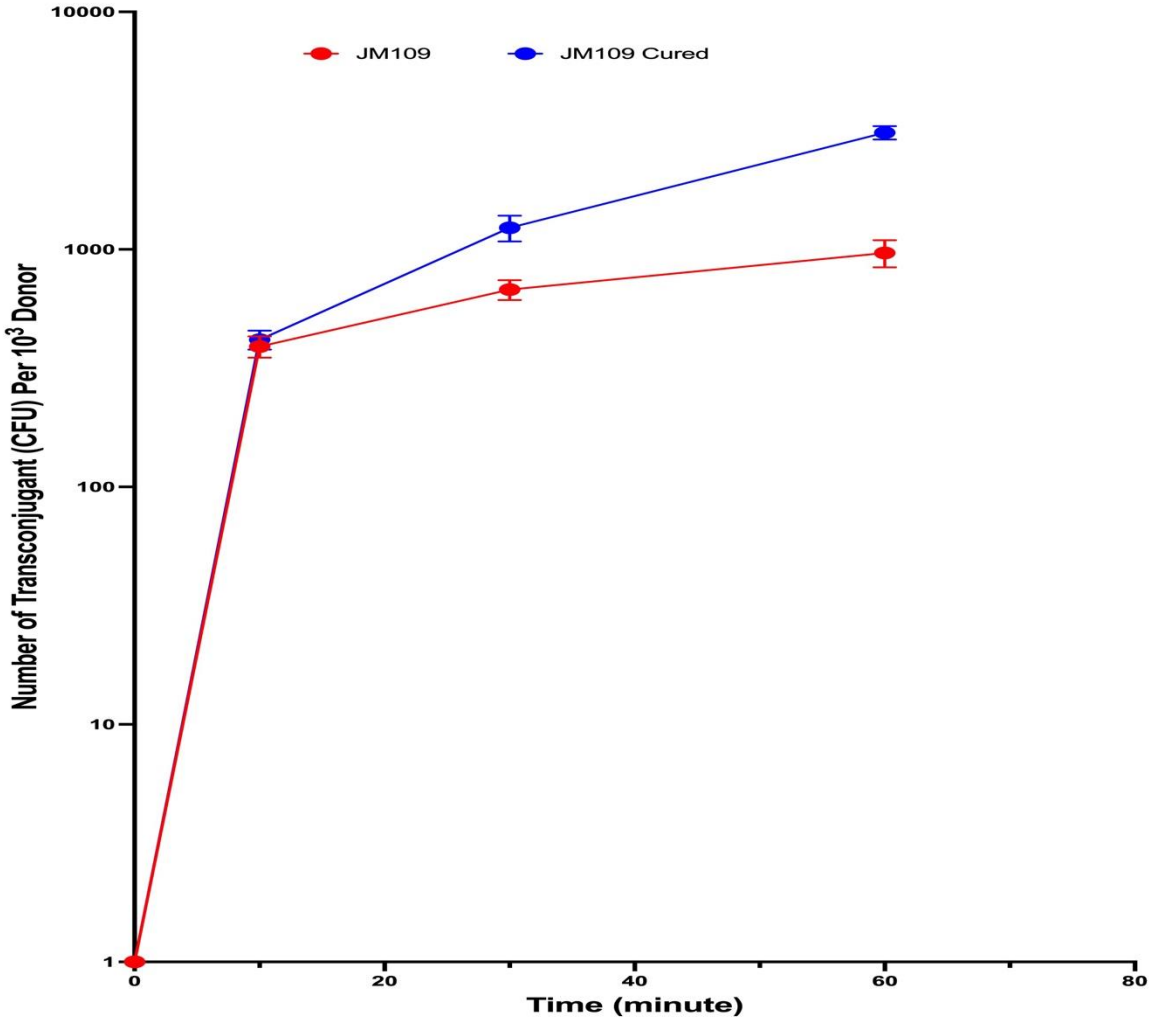

Figure 3.11 RK2 conjugative transfer from HB101 to JM109 and JM109 Cured to check the effect of F in the recipient strain.

The graph drawing package was set to show the error bars for each point but due to the log scale on the y axis these are sometimes not visible. For this reason, the data is also shown in Table 3.5 which includes means, standard deviations and tests of significance where relevant.

3.4 Discussion

The primary aim of this chapter was to check the F' fertility inhibition phenotype against RK2 transfer. This aim included exploring different donor to recipient ratios for RK2 conjugative transfer, confirming the presence of F'prolac in the JM109 strain but not in the JM109-cured strain, and determining the effect of F fertility inhibition on RK2.

The second aim of the study was to look at the effects of a donor strain with multiple inhibitory sources, such as F with R64 or F with R388, on RK2 conjugative transfer, as well as how the presence of F in the recipient strain affected RK2 transfer.

The findings of this study show that the best donor to recipient ratio of those tried for RK2 transfer was 1 to 10 although 1 to 100 had the advantage that a plateau was not reached so quickly. The study also emphasized that the presence of the F plasmid in the donor strain negatively influences RK2 conjugation transfer, consistent with previous studies (Czaplewski et al., 2016b).

3.4.1 Investigating the effect of donor to recipient ratio on RK2 conjugative transfer.

The results of this study highlight the critical role of the donor to recipient ratio in plasmid transfer, consistent with findings by (Alderliesten et al., 2020). However, it is essential to consider that in some systems, transfer dynamics may be influenced by factors produced by both the donor and recipient. These factors could potentially stimulate or inhibit transfer, and their concentrations may vary as the donor to recipient ratio changes.

In our study, the number of transconjugants varied across the three ratios tested. Interestingly, the best donor to recipient ratio observed was 1 to 10 across all time-points tested (10, 30, and 60 minutes). This finding contradicts the results of (Lampkowska et al., 2008) who reported an ideal 1:1 ratio for conjugation transfer between two model lactococcal strains. However, our results align with those of Sasaki (Sasaki et al., 1988), who found that a 1:10 donor to recipient ratio was optimal when transferring pAMß1 from *E. faecalis* to *Lactobacillus plantarum*.

Considering the complex interplay of factors involved in plasmid transfer, further investigation into the specific mechanisms underlying the observed donor to recipient ratio effects is warranted. Future studies could explore how the concentrations of factors produced by both donor and recipient cells dynamically change with varying ratios, influencing the efficiency and dynamics of plasmid transfer.

The observed outcomes of this study may be attributed to the donor to recipient ratio's influence on successful conjugations. In a 1:10 donor to recipient ratio, there are more recipient cells available to receive the gene from the donor, increasing the likelihood of successful conjugations and consequently yielding more transconjugants per donor. However, the plateauing of transconjugant numbers at later time-points, as depicted in Figure 3.6, suggests a saturation effect, where most recipient cells have already acquired the plasmid.

At a 1:100 donor to recipient ratio, the abundance of recipient cells surpasses that of donor cells, potentially leading to a slight decrease in the total number of transconjugants. This decrease may be attributed to the statistical likelihood of each recipient cell interacting with a donor cell diminishing when recipient cells greatly outnumber donor cells.

However, at longer time-points such as 180 and 240 minutes, the optimal donor to recipient ratio appears to be 1:100 rather than 1:10, as illustrated in Figure 3.6. This shift may be explained by the need to ensure an adequate supply of potential recipient cells to sustain ongoing transfer events. It's worth noting that almost all recipient cells may have received the plasmid at this stage, limiting further increases in transconjugant numbers except through growth and cell division.

In hindsight, determining the total number of recipient bacteria alongside transconjugant counts could provide a clearer understanding of the saturation effect and its impact on transfer dynamics.

At a 1:1 ratio, there are similar numbers of donor and recipient cells, which could result in more competition between donor bacteria and recipient cells. In other words, not all donor cells will be able to find suitable recipients, which will cause lower transfer efficiency.

3.4.2 To confirm the F’ fertility inhibition phenotype against RK2.

To confirm the F’ fertility inhibition phenotype against RK2, it was first essential to verify that JM109 has the F’ plasmid and that JM109 Cured not. This was conducted using M9 minimal medium to grow both strains. As expected, JM109 grew satisfactorily, and JM109 cured showed no growth confirming that the F’prolac in JM109 carries the genes that allow JM109 to make proline and grow on M9 minimal medium.

The current investigation confirms that F’ plasmid has a negative impact on IncP plasmid conjugative transfer, as observed in prior studies (Miller et al., 1985). The ability of RK2 to

transfer was higher and faster in the absence of F'than in its presence. The difference between the number of transconjugants of JM109 that contain F and JM109 Cured that do not have F was consistently observed, which underlines the fact that the F plasmid inhibits RK2 conjugation. However, the number of JM109 transconjugants increased sharply after 3 and 4 hours and approached the number of JM109 cured transfectants. The reason for the dramatic rise in transconjugants count from JM109 at these last two time-points could be due to the limited number of recipient bacterium (HB101) in JM109 Cured mating when most of these bacteria have received RK2, the transconjugants count will plateau and the other mating mix will catch up. Also, F does not transfer to HB101, so once some transfer of RK2 to HB101 has occurred, it will no longer be inhibited and will be increasingly able to transfer to HB101, which has not yet received the plasmid. In this case, using a 1:100 donor to recipient ratio might have had some advantages due to the increase in the number of recipients, so JM109-cured transfer does not get limited.

It is clear that the inhibition factors of F plasmids on RK2 transfer decrease over time during an experiment. One possible explanation for this trend is that as more transconjugants of HB101 with RK2 are produced, they can act as donors for HB101 which have not yet received RK2 without encountering any inhibitory effects on the transfer. This would also account for the increase in the number of transconjugants of JM109 observed in the later time-points.

3.4.3. To check the effect of having two sources of inhibition on RK2 conjugation transfer.

The findings of this project demonstrate that R388, R64 and F plasmids are able to inhibit RK2 transfer when they are present in the donor strain both individually and when two

plasmids are present. These findings support the findings of previous research in this field, (Getino et al., 2017).

When the three inhibitors were tested individually, the most potent inhibition effect on RK2 ability to transfer was with R388, and then R64 and F were the last. However, when I combined other inhibition sources with F, the most powerful inhibition on the transfer of RK2 was with R64 and F compared to R388 with F. One potential reason for this could be because interacting between F and R388 negatively impacts R388. The PifC produced by F not only inhibits RK2 but can also inhibit R388, as was confirmed by Getino et al., (2017) and having less of R388 means a decrease in R388 ability to inhibit RK2. However, the interaction with F with R64 positively affects R64 inhibition ability. A reasonable explanation for that is that R64 and F produce PifC, and having two of them simultaneously means increasing the amount of PifC protein products there for increasing RK2 inhibition, as illustrated in Fig. 3.9.

The result also highlighted that having another source of inhibition with F had a positive effect on F ability to inhibit RK2. The presence of either the R64 or the R388 with F decreased the transconjugants number compared to the number that was only inhibited by F as shown in Figure 3.9.

3.4.4 Assessing the impact of having F plasmid in the recipient strain on the transfer of RK2.

The results highlight the influence of the F plasmid on RK2 transfer once it is present in the recipient strain. Initially, there was only a slight difference in transconjugant count between the JM109 and JM109-cured strains, as depicted in Figure 3.11. However, over time, the

number of transconjugants from the JM109 strain gradually decreased while those from the JM109-cured strain increased. This shift suggests that early time points are dominated by transfer from the initial donor, whereas at later time points, transconjugants acting as donors become more significant contributors. One potential explanation for these findings is that transconjugants of JM109 initially acquired the F plasmid, limiting further spread, while transconjugants of JM109-cured did not possess this restriction. This aligns with previous findings in Section 3.3.3 of this chapter, where the presence of the F plasmid in the donor strain inhibited transfer due to fertility inhibition (FIR). Therefore, when JM109-cured transconjugants act as donors, they exhibit efficient transfer with no inhibition. Conversely, when JM109 transconjugants serve as donors, they demonstrate reduced efficiency in transfer due to the presence of the F plasmid.

Chapter 4: Getting a mutant of conjugative pCURE that is able to transfer without being suppressed by other plasmids.

4.1 Background

The pCURE-F-307 and pCURE-K-307 plasmids are low copy number, self-transmissible plasmid that are able to transfer among a broad range of hosts. They are based on one of the IncP-1 plasmid group and have been used to displace IncF and IncK plasmids as described in Chapter One Section 1.5. To cure IncF plasmids, pCURE-F-307 carries the anti-F curing cassette to displace the target plasmid. The principle of this cassette works with incompatibility with the additional benefit of supplying neutralising components to the aimed plasmid system. The pCURE-F-307 contains sections of each IncF replicon (multiple binding sites for Rep protein for FIA and FIB replicons and the transcriptional repressor CopB and the copA antisense RNA for the FIC replicon) (Lazdins et al., 2020).

As was confirmed in Chapter 3 Section 3.3.3, the transfer of IncP-1 plasmids can be inhibited due to fertility inhibition of IncF plasmids. One of the primase operon products essential for the transfer in conjugation plasmids is the TraG coupling protein. TraG is present in the cytoplasmic membrane and is responsible for handing the relaxosome to the Mpf (Álvarez-Rodríguez et al., 2020b). Coupling proteins are necessary for the relaxase to guide it to the exporter and then to the recipient cell as described in Chapter one, section 1.5. PifC from the F plasmid inhibits IncP-1 by targeting the TraG coupling protein (Santini and Stanisich, 1998).

To be able to use the pCURE-F-307 vector to displace IncF plasmids, it would be an advantage to have a mutant that has a modification of the *traG* sequence that may result in a mutant TraG coupling protein that allows it to overcome the PifC effect. Also, it is essential to emphasize that the sequence alteration in *traG* gene should not affect the functional status of TraG within transfer. The effectiveness of using pCURE vectors to combat antibiotic

resistance hinges on their ability to transfer autonomously without interference from other plasmids. Getting a mutant conjugative pCURE that is able to transfer without being inhibited by other plasmids could be the critical aspect of using the pCURE vector efficiently to cure antibiotic resistance plasmids.

One method for isolation of mutants is hydroxylamine mutagenesis, which has been used in biological research to induce mutations in DNA (Gross, 1985). The reason for choosing hydroxylamine mutagenesis is its ability to create single-point mutations in DNA sequences, which we aimed to do in the *traG* gene sequence. Hydroxylamine is a chemical compound that reacts with cytosine so that it is more likely to pair with adenine, resulting in a C-G to T-A transition mutation (Gross, 1985). Therefore, I chose hydroxylamine mutagenesis to produce mutant of conjugative pCURE plasmids that are able to escape fertility inhibition of F plasmids.

To select *traG* mutants, we can employ the *pifC* over-expression plasmid. The selection process would involve pooling bacteria from plates for each treated *traG* time-point after enrichment, followed by a subsequent transfer experiment using the *pifC* over-expression plasmid in the donor as a robust source of inhibition. One area to be investigated was the inhibition profile exhibited by *pifC* to optimise the selection of mutants less sensitivie to fertility inhibition. This transfer experiment allows for a 10-minute window to detect strains capable of escaping inhibition, while a wild-type strain containing non-mutant *traG* serves as a negative control. For detailed description of the method, please refer to Section 4.3.9 of this chapter.

According to Lazdins et al., (2020), pUB307 is a variation of the RP1 IncP-1 plasmid that has lost the transposon Tn1, including the *bla* gene conferring Ap^R (Grinsted et al., 1977). In our lab, prior investigation identified the boundaries of this deletion, spanning from position 5464..5466 to 12045..12047 in the IncP-1 genome sequence (accession BN000925.1) (Haines, 2001). It's worth noting that at the junction, there exist three bases that could originate from either side of the deletion hence the lack of precision about the exact coordinates of the deletion. Plasmids RP1 and RK2 came from the same outbreak of resistant *Pseudomonas aeruginosa* in 1969 and are essentially different isolates of the same plasmid (Burkardt et al., 1979). Plasmid pUB307 is used instead of RK2 in Chapters 4 and 5 because it is the basis for the effective curing plasmid pCURE-F-307 (Lazdins et al., 2020) but also because it does not confer resistance to ampicillin due to the deletion of Tn1 from pUB307. This allows a second plasmid that does confer ampicillin resistance to be used in the same bacterium. In these chapters, pGBT30-pifC, which is characterized by an ampicillin selectable marker, will be used as a source of the inhibition. Therefore, using pUB307 enabled me to select the presence of the plasmid carrying this gene.

4.2 Aims and Hypotheses

The work outlined in this Chapter aimed to make a mutation in the *traG* gene that encodes TraG coupling protein which could enable the pCURE plasmid to transfer without being inhibited by F plasmids. It was necessary to construct a very clear system to isolate a mutant that is able to escape fertility inhibition. The chosen methodology begins with the cloning of the *pifC* gene from the F plasmid, sourced from the JM109 strain as outlined in Table 2.1 of Chapter Two, because this gene is essential for the observed fertility inhibition. Detailed instructions for this cloning process are provided in sections 4.3.1 and 4.3.2. Subsequently, the *pifC* gene was inserted into the pGBT30 expression vector. The resulting construct, called

pGBT30-pifC, was then utilized to evaluate the pCURE mutant's ability to evade fertility inhibition.

The plan also involved cloning of the *traG* gene from RK2 in the pACYC184 vector, mutating it by hydroxylamine mutagenesis, sequencing the mutants and determining the basis for the effect. Our hypothesis was that the gene encoding TraG coupling protein can be altered by mutating it in this way to the create a mutant that is able to overcome the fertility inhibiting of IncF plasmids and still perform its function during the conjugative transfer.

4.3 Results

4.3.1 Cloning the *pifC* gene from F plasmid.

As described in the hypothesis, we thought at the start of this project that cloning the *pifC* gene from the F plasmid into the pGBT30 expression vector was important to create strong enough selection to isolate a mutant that can escape fertility inhibition. To clone *pifC* from F plasmid, primers were designed with restriction sites EcoRI and XbaI using SnapGene software (as shown in Chapter two, Table 2.6). Gene maps of pGBT30 before and after *pifC* insertion are shown in Figure 4.1. The *pifC* gene was amplified using PCR. The PCR product was purified after separating the bands by gel electrophoresis as shown in Figure 4.2. The purified *pifC* gene was stored at -20°C to use in future work.

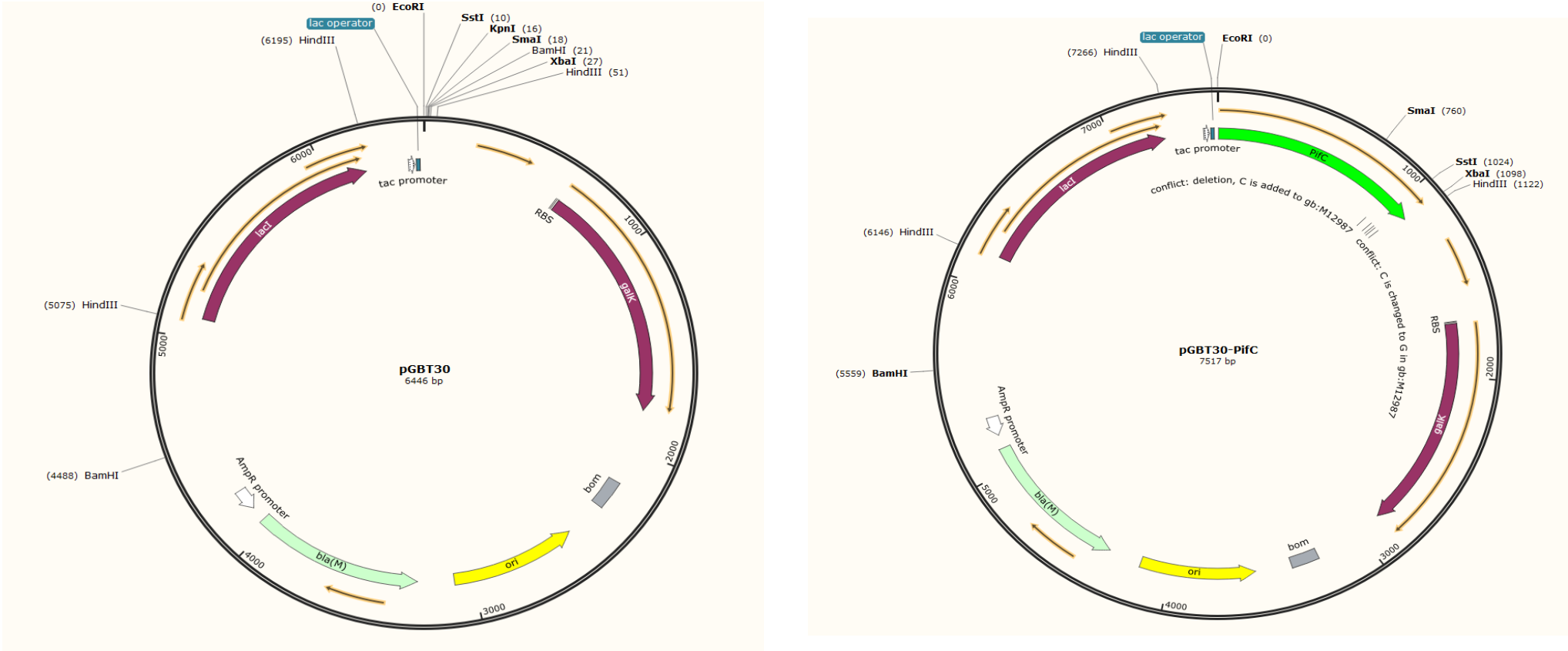

Figure 4.1 Gene map of pGBT30 gene before and after the *pifC* insertion.

A gene map was constructed to clarify the strategy for inserting *pifC* into pGBT30. This gene map includes information on the restriction enzymes employed in the process, as well as the size of the vector before and after the insertion. By detailing these aspects, the gene map provides a clear visualization of the genetic manipulation performed on pGBT30, facilitating a better understanding of the experimental design.

Figure 4.2 Gel electrophoresis of PCR product of the *pifC* gene.

Gel electrophoresis was conducted to verify the size of the *pifC* gene, revealing a band of 1092 base pairs, consistent with the expected size of the *pifC* gene.

4.3.2 Inserting *pifC* gene into the pGBT30 expression vector.

To insert the *pifC* gene into the pGBT30 vector, the purified *pifC* gene and the pGBT30 vector were digested with EcoRI and XbaI restriction enzymes for two hours at 37 °C. Subsequently, the digested fragments were ligated and transformed following the protocol in Chapter two sections 2.4 and 2.20. Plasmid DNA was isolated for the ten transformants and digested with EcoRI and XbaI, and then a gel was run to check the insertion (Figure 4.3).

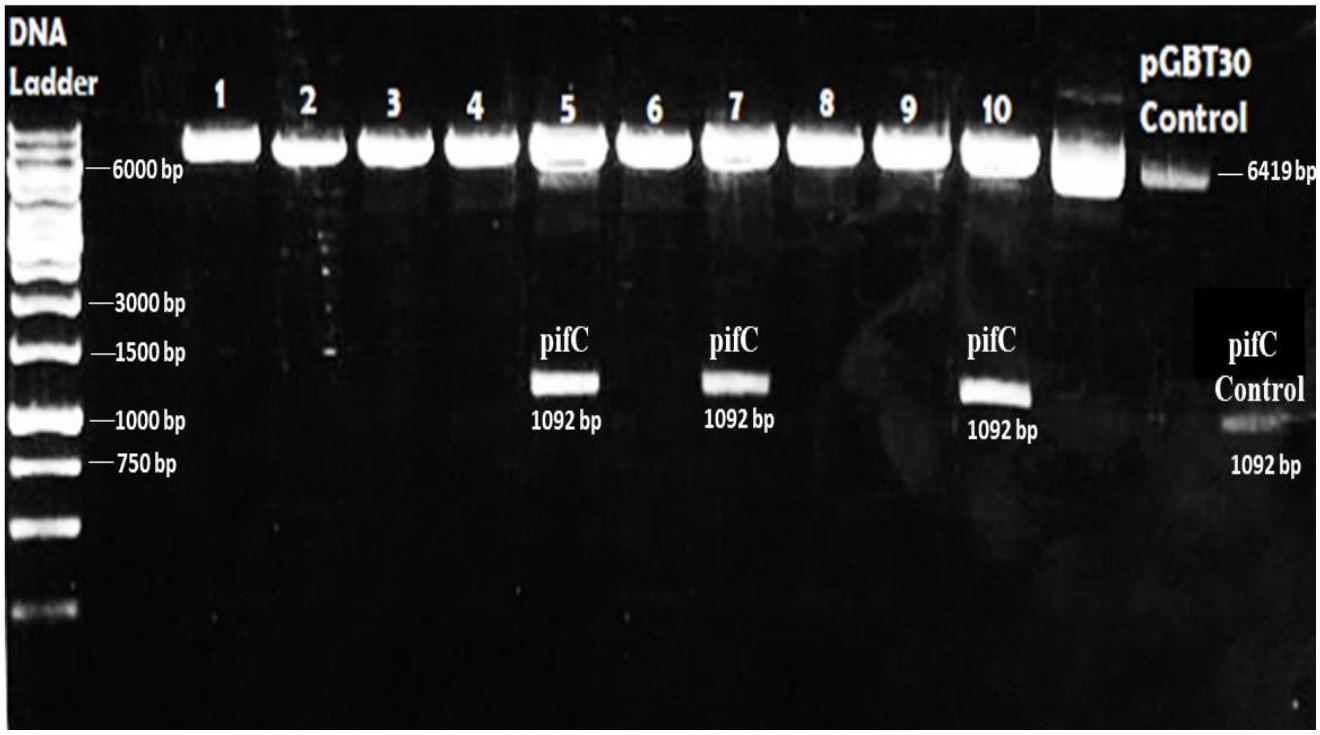

Figure 4.3 Gel electrophoresis of PCR product *pifC* gene inserted in the pGBT30 and digested with EcoRI and XbaI.

Only samples 5, 7, and 10 contain the *pifC* gene. This can be observed from the appearance of a second band with a size of approximately 1100 bp, which is the size of the *pifC* gene. The strains were stored at -20°C for future use.

4.3.3 Checking the effect of *pifC* on pUB307 conjugative transfer.

A conjugative transfer experiment was done to check if pGBT30-pifC can block the transfer of pUB307. The donors in the experiment were DH5α containing pUB307 with pGBT30-pifC and DH5α containing pUB307 with pGBT30, which was used as a control. HB101 was used as the recipient with a ratio of 1 to 10 donor to recipient ratios by the visual representation in Figure 4.4.

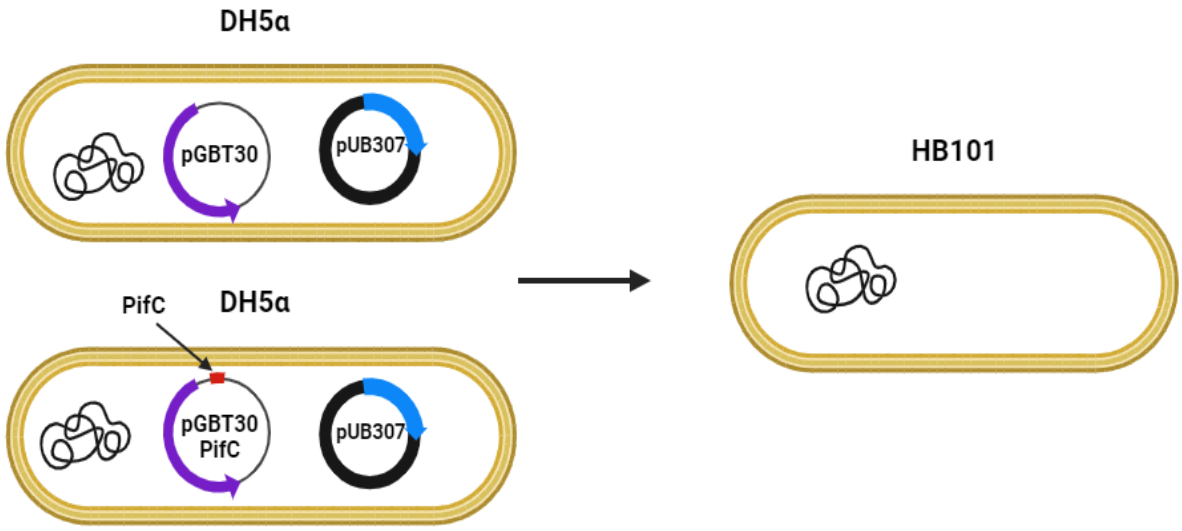

Figure 4.4 Outline of the experiment to determine the effect of *pifC* on transfer of pUB307.

The figure illustrates the experimental setup aimed at evaluating the influence of pGBT30-pifC on the transfer of pUB307. The experiment predicts that the presence of *pifC* will hinder the transfer of pUB307 compared to when *pifC* is absent. Plasmids pGBT30-pifC and pUB307 harbor distinct selectable markers facilitating their identification during transfer. pGBT30-pifC carries an Ampicillin resistance gene, whereas pUB307 carries a Kanamycin resistance gene. The recipient strain HB101 also contains Streptomycin as its own set of selectable markers on the chromosome.

The results demonstrate a strong inhibitory effect of *pifC* on the conjugative transfer process as shown in Figure 4.5, Figure 4.6 and Table 4.1 align with the objectives of the project. The impact of PifC is clear, as there were no observable transconjugant colonies after 10, 30, and 60 minutes in strains containing *pifC*. In contrast, the strain without *pifC* exhibited a significant increase, with the number of transconjugants reaching 6,000 after 30 minutes and 12,000 after 60 minutes.

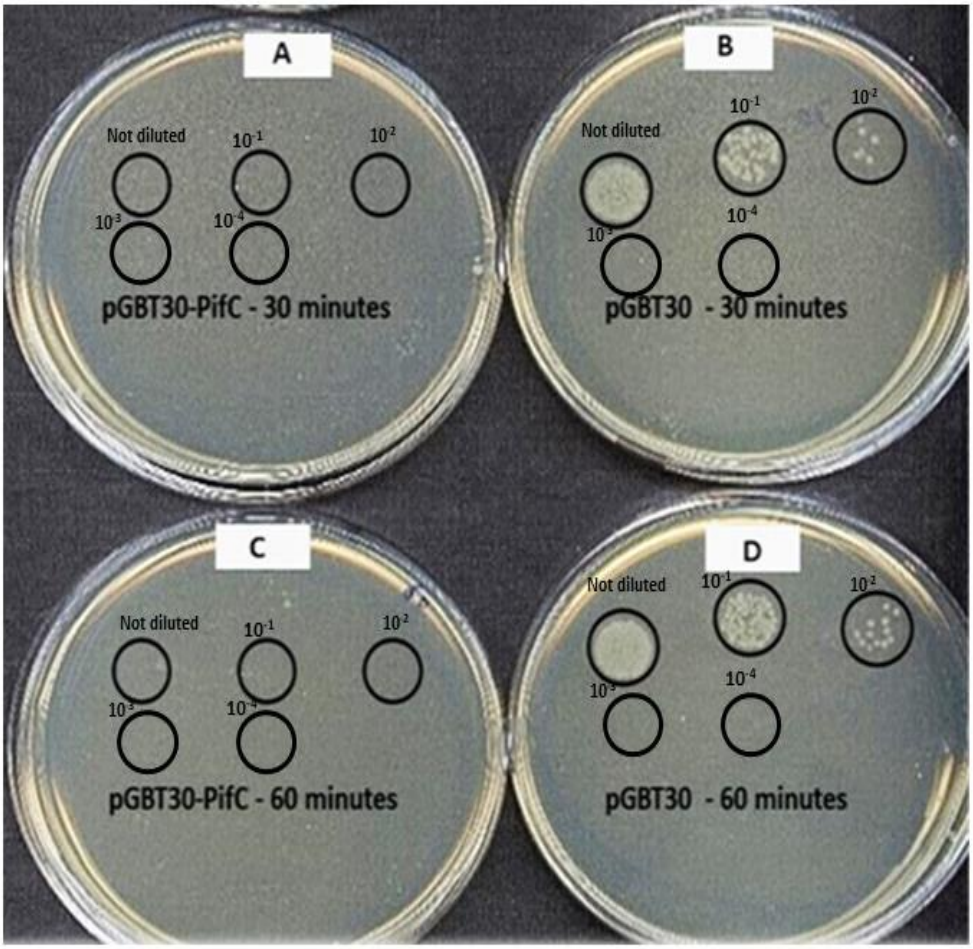

Figure 4.5 Plates from two of the time points in the experiment to check the effect of pGBT30-pifC on pUB307 conjugative transfer.

The plates show transfer analysed after 30 minutes and 60 minutes. Serial dilutions allowed determination of number of transconjugants.

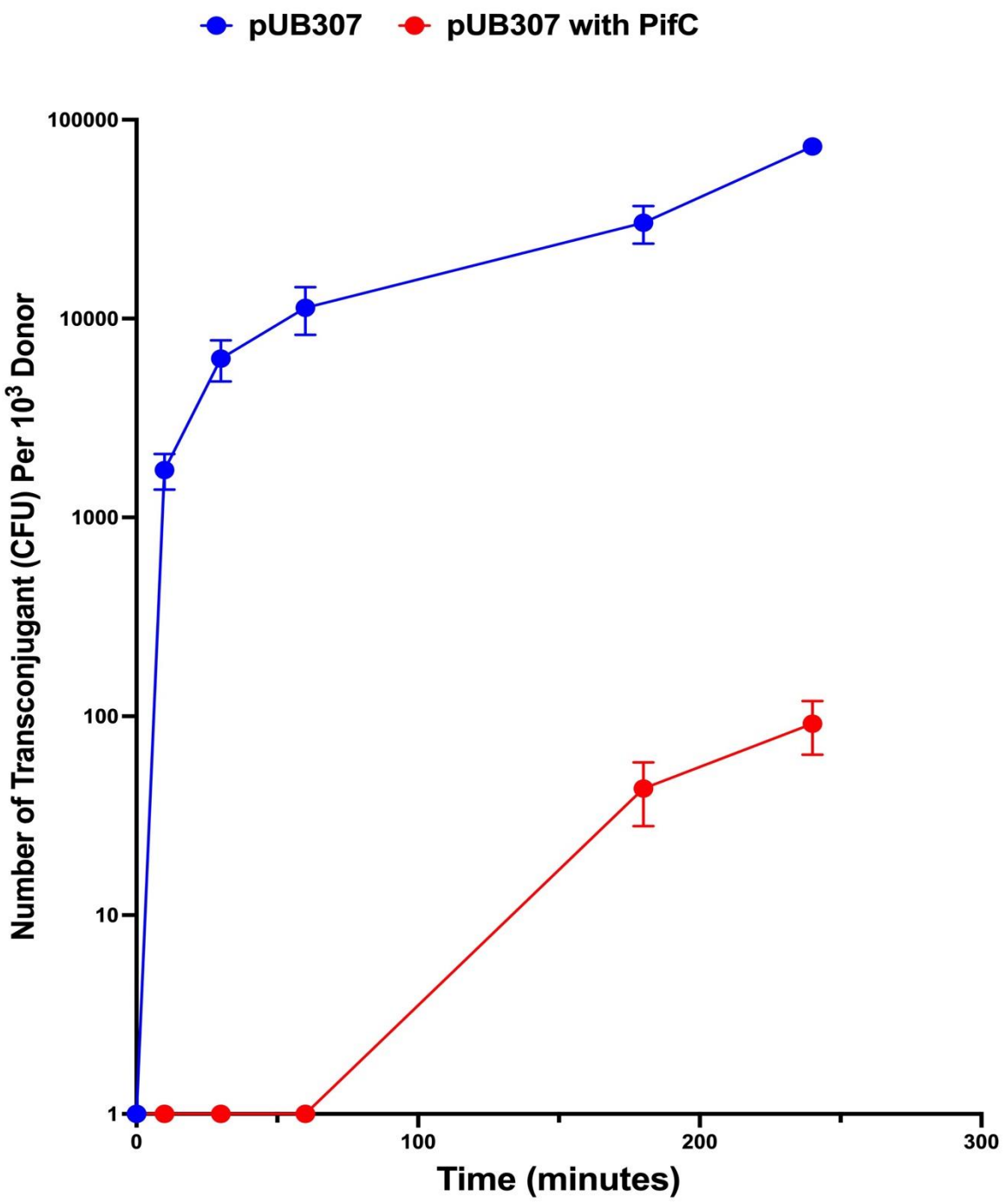

Figure 4.6 Results of the experiment outlined in Fig 4.4 to check the effect of pGBT30-pifC on pUB307 conjugative transfer to *E. coli* HB101.

The graph drawing package was set to show the error bars for each point but due to the log scale on the y axis these are sometimes not visible. For this reason, the data is also shown in Table 4.1 which includes means, standard deviations and tests of significance where relevant.

Table 4.1 Transfer conjugation experiment to check the effect of pGBT30-pifC on pUB307 conjugative transfer

	pUB307		pUB307+PifC		
Time (minute)	**Mean**	**SD**	**Mean**	**Standard Deviation**	**P value[b]**
10	**1733**	**351**	**<1[a]**	**0**	**0.001030**
30	**6300**	**1473**	**<1 [a]**	**0**	**0.001773**
60	**11333**	**3055**	**<1 [a]**	**0**	**0.003017**
180	**30333**	**6506**	**43**	**15**	**0.001285**
240	**73333**	**4163**	**91**	**27**	**0.000007**

a. Number <1 represents 0 colonies.

b. $p < 0.05$: Statistically significant $p < 0.01$: Highly statistically significant $p < 0.001$: Extremely statistically significant. Statistical significance determined using t-test in GraphPad.

4.3.4 Checking the impact of IPTG on ability of *pifC* to inhibit pUB307 transfer.

In the pGBT30-pifC construct (Fig. 4.1), *pifC* expression is driven by the *tac* promoter, regulated by the Lac repressor encoded within the plasmid. The effect of *pifC* on pUB307 conjugative transfer was initially confirmed in section 4.3.3. To further investigate the role of *pifC* and its regulation, the transfer experiment was repeated with pGBT30-pifC present, both with and without IPTG induction.

Unexpectedly, the data presented in Figure 4.7 and Table 4.2 revealed that the addition of IPTG had a slight negative effect on the inhibition process. When *pifC* was tested without IPTG, the mean number of transconjugants was 54 at 180 minutes and 106 at 240 minutes. However, upon IPTG addition, the number of transconjugants decreased to 40 at 180 minutes and 60 at 240 minutes, although only the decrease at 240 minutes was statistically significant.

It is important to consider that the observed difference may not solely reflect a weaker effect of *pifC* induced by IPTG. Instead, the addition of IPTG may increase the metabolic burden associated with harboring the pGBT30-pifC plasmid, potentially favoring bacterial subpopulations that have lost the plasmid. Thus, the observed decrease in transconjugants may be attributed, at least in part, to plasmid loss rather than a diminished effect of *pifC*. This underscores the complexity of interpreting the effects of inducers on plasmid-mediated processes and emphasizes the need for further investigation into the underlying mechanisms.

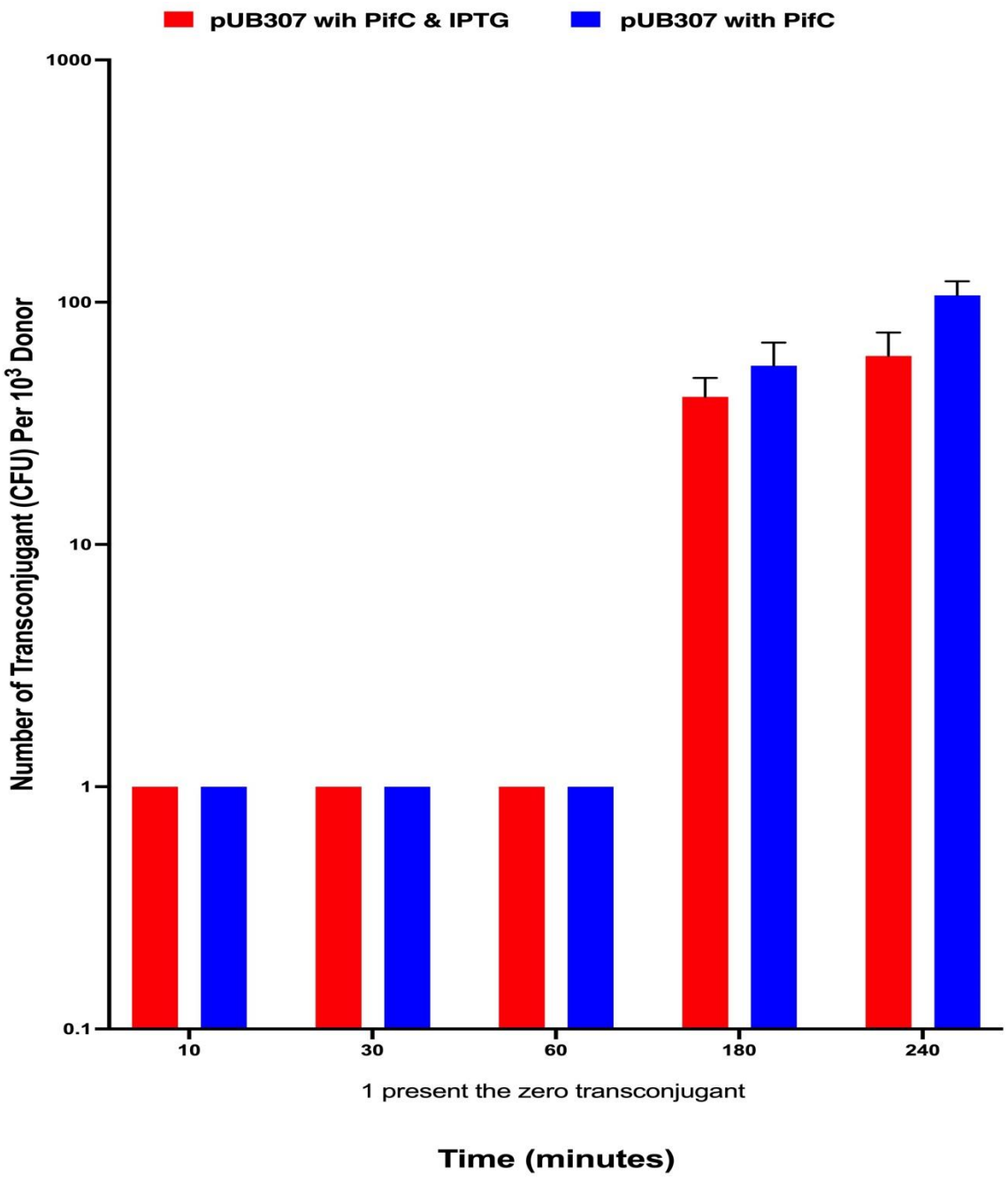

Figure 4.7 Transfer conjugation experiment to determine the effect of IPTG on pGBT30-pifC inhibition ability.

The graph drawing package was set to show the error bars for each point but due to the log scale on the y axis these are sometimes not visible. For this reason, the data is also shown in Table 4.2 which includes means, standard deviations and tests of significance where relevant.

Table 4.2 Transfer conjugation experiment to determine the effect of IPTG on pGBT30-pifC inhibition ability

	pUB307 with pGBT30-pifC		pUB307 with pGBT30-pifC & IPTG		
Time (minutes)	**Mean**	**SD**	**Mean**	**Standard Deviation**	**P value[b]**
10	**<1[a]**	**0**	**<1[a]**	**0**	**0**
30	**<1[a]**	**0**	**<1[a]**	**0**	**0**
60	**<1[a]**	**0**	**<1[a]**	**0**	**0**
180	**54**	**13**	**40**	**3**	**0.153086**
240	**106**	**15**	**60**	**5**	**0.007339**

a. Number <1 represents 0 colonies.

b. $p < 0.05$: Statistically significant $p < 0.01$: Highly statistically significant $p < 0.001$: Extremely statistically significant. Statistical significance determined using t-test in GraphPad.

4.3.5 Cloning the *traG* gene from RK2 in pACYC184 vector.

To allow mutagenesis of just *traG* from RK2, primers to amplify *traG* gene were designed with HindIII and SalI restriction sites using SnapGene software (as shown in Chapter two Table 2.5). A gene map of the pACYC184 before and after the *traG* insertion has been generated as shown in Figure 4.8 in order to facilitate the cloning of the *traG* gene into pACYC184 plasmid. The *traG* gene was amplified using PCR under the following conditions. The annealing was done for thirty seconds at 67°C and the extension at 72°C for 2 minutes because the size of the *traG* gene fragment is 1908 bp. The gene was purified after separating the bands by gel electrophoresis as shown in Figure 4.9. The purified *traG* gene was stored at -20°C to use in future work.

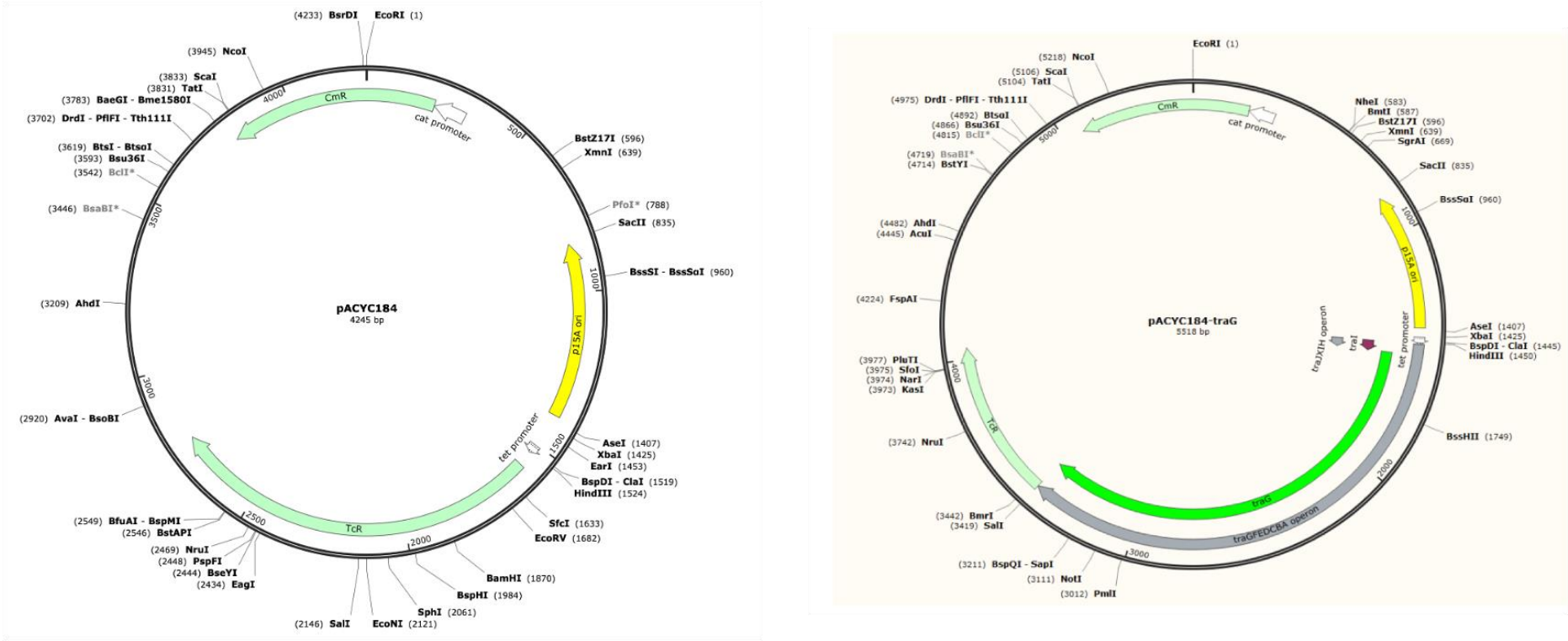

Figure 4.8 Gene map of pACYC184 plasmid before and after the *traG* insertion.

A gene map was constructed to clarify the strategy for inserting *traG* into pACYC184. This gene map includes information on the restriction enzymes employed in the process, as well as the size of the vector before and after the insertion. By detailing these aspects, the gene map provides a clear visualization of the genetic manipulation performed on pACYC184, facilitating a better understanding of the experimental design.

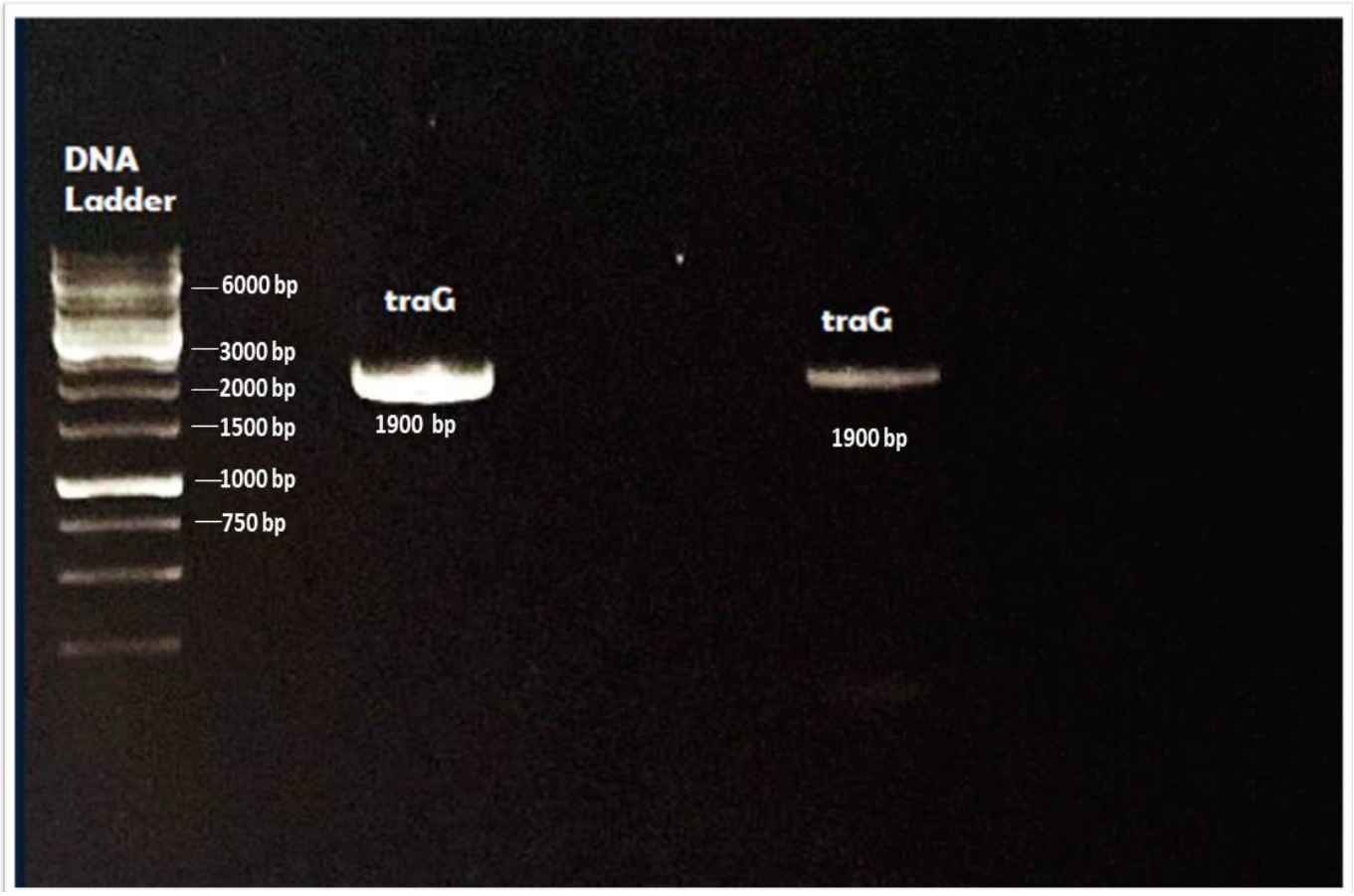

Figure 4.9 Gel electrophoresis of *traG* gene PCR product from RK2.

Gel electrophoresis was conducted to verify the size of the *traG* gene, revealing a band of 1900 base pairs, consistent with the expected size of the *traG* gene.

The *traG* gene was inserted into the pACYC184 vector after digesting the purified PCR product and pACYC184 with HindIII and SalI restriction enzymes for two hours at 37 °C. Subsequently, they were ligated following the protocol in Chapter two sections 2.4 and 2.20. In order to confirm that the insertion was successful, the plasmid DNA was subjected to transformation and isolation processes. Afterward, it was digested with HindIII and SalI, and a gel was run as shown in Figure 4.10.

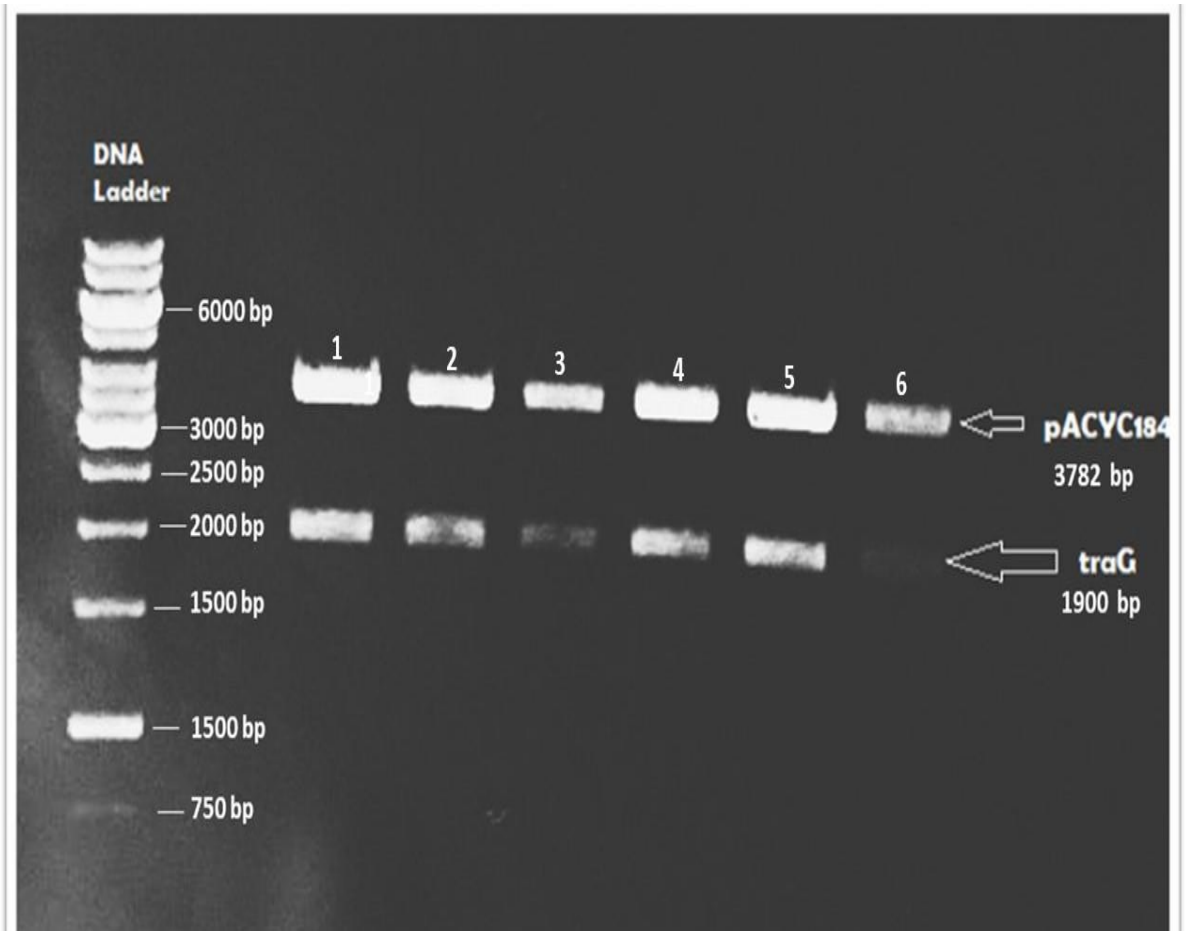

Figure 4.10 Gel electrophoresis of *traG* gene PCR product inserted into pACYC184 and digested with HindIII and SalI.

The gel confirms that the insertion of *traG* was successful in sample 1 to 5, as confirmed by two distinct bands of correct sizes observed in the gels. The lower fragment, about 1900bp in size, corresponds to the *traG* gene, while the upper fragment, measuring 3782bp, represents the digested pACYC184 size.

4.3.6 Inserting *oriT-traG* into the pACYC184 vector.

To allow the selection of *traG* mutants that had escaped *pifC* inhibition, *oriT* from RK2 was inserted into the plasmid to allow it to transfer. To clone *oriT* into the pACYC184-traG vector, primers were designed with specific HindIII and XbaI restriction sites using SnapGene software (as shown in chapter two Table 2.6). A gene map of the pACYC184-traG before and after the *oriT* insertion has been generated as shown in Figure 4.11 in order to facilitate the cloning of the *oriT* gene into pACYC184-traG plasmid. The protocol used in

this chapter, section 4.3.2 to clone the *traG* gene from RK2 in the pACYC184 vector was employed to clone the *oriT* fragment into pACYC184-traG.

To confirm *oriT* insertion, a transfer experiment was done from DH5α strains containing pACYC184-traG and pACYC184-oriT-traG to HB101 strain. The results validate that strains containing pACYC184-oriT-traG were capable of transfer, whereas those with pACYC184-traG did not.

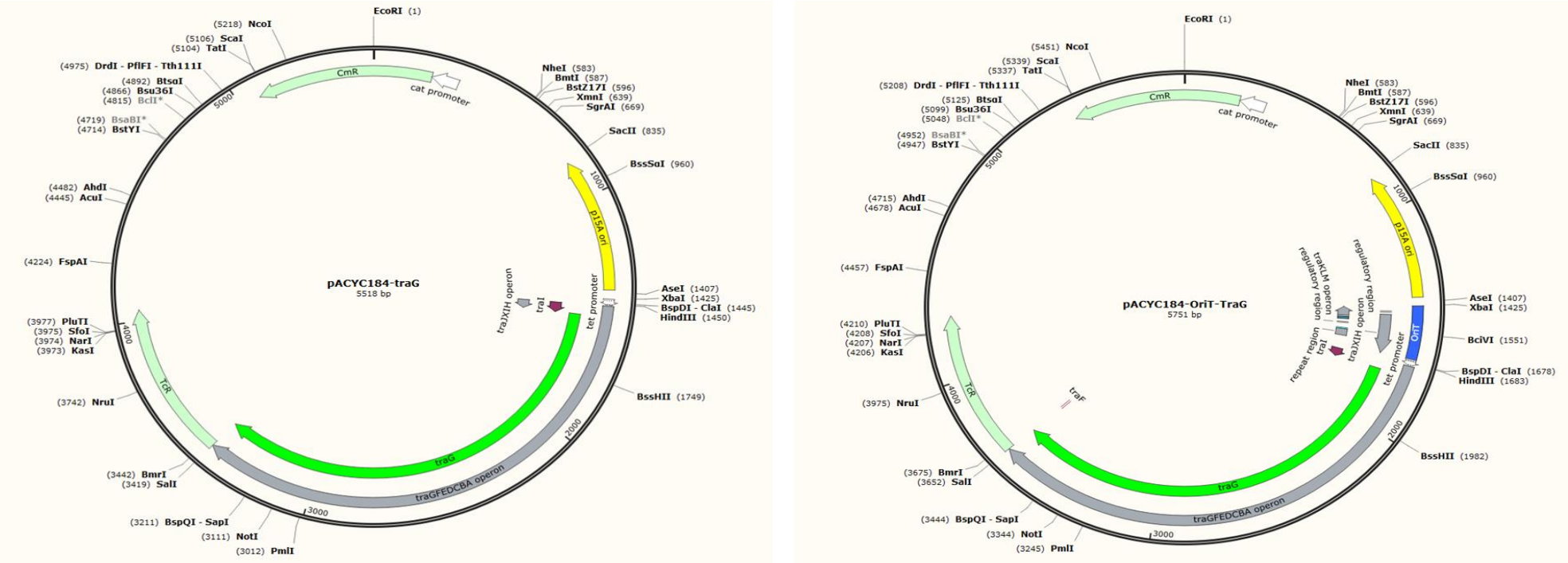

Figure 4.11 The gene map of plasmid pACYC184-traG before and after *oriT* insertion.

A gene map was constructed to elucidate the strategy for inserting *oriT* into pACYC184-traG. This gene map includes information on the restriction enzymes employed in the process, as well as the size of the vector both before and after the insertion. By detailing these aspects, the gene map provides a clear visualization of the genetic manipulation performed on pACYC184-traG, facilitating a better understanding of the experimental design.

4.3.7 Making a mutant of pUB307.

4.3.7.1 Deleting *traG* gene from pUB307 using homologous recombination.

To initiate homologous recombination to delete *traG* from pUB307, homology arms specific to the target pUB307 were amplified using PCR. Subsequently, the individual homology arms were joined through SOEing PCR, as shown in Figure 4.12. The homology arms product was cloned into pLAZ1 and digested with HindIII and SalI to check the insertion, as can be seen in in Figure 4.13. The gene map of pLAZ1 before and after cloning the homology arms product was made as shown in Figure 4.14. To force homologous recombination to delete *traG* from pUB307, the protocol in Chapter two Section 2.16 was utilized. To screen for potential deletion, PCR with recombination homology arms outer primers (as shown in Chapter two, Table 2.6) was used to identify the colonies that had lost *traG*.

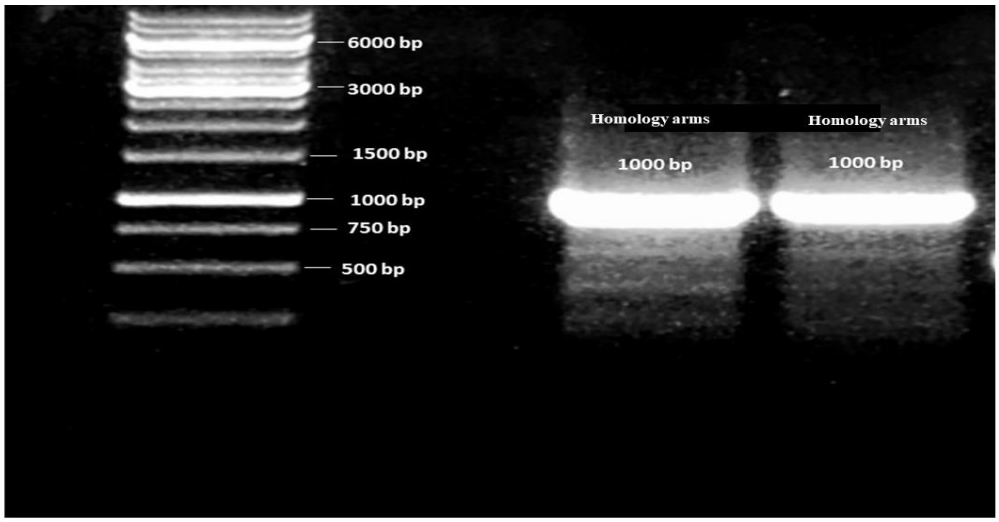

Figure 4.12 Homology arms specific to delete *traG* from pUB307 were joined together through SOEing PCR.

Gel electrophoresis was conducted to verify the size of the Homology arms, revealing a band of 1000 base pairs, consistent with the expected size of the PCR product.

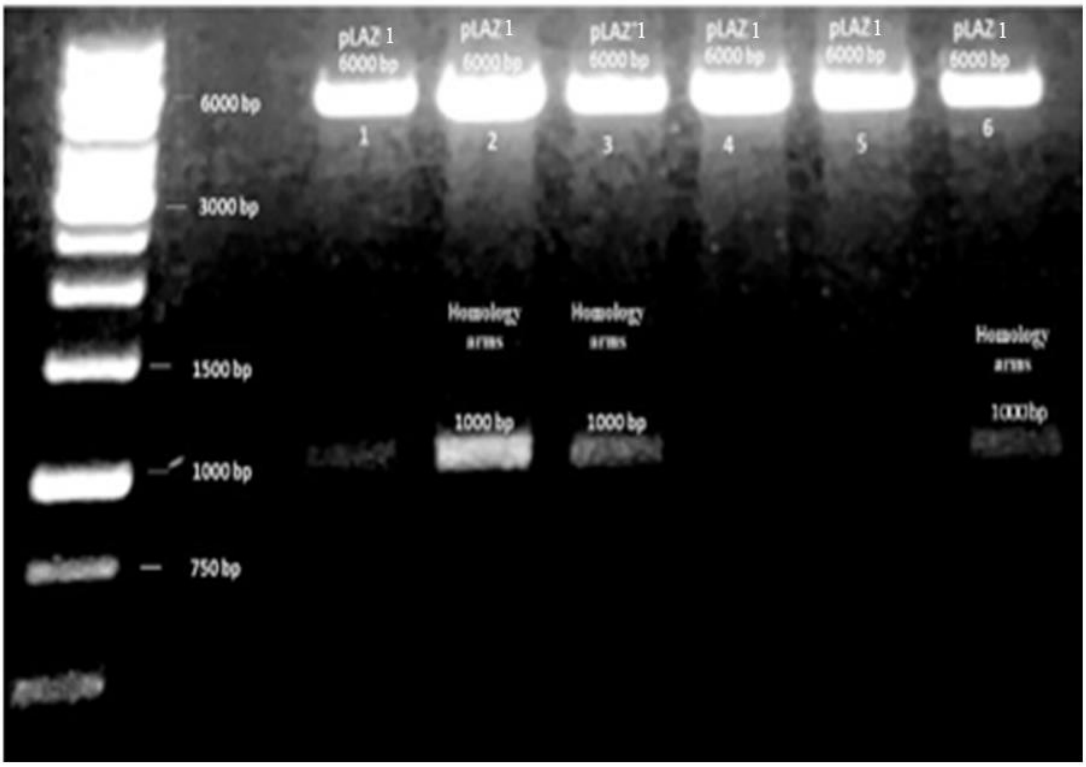

Figure 4.13 Digested pLAZ1+ SOEd product with HindIII and SalI to check the insertion of arm1 and arm2 SOEd.

The data in this Figure confirms that the insertion of arm1 and arm2 SOEd was successful in samples 2,3 and 6, as confirmed by two distinct bands of correct sizes observed in the gels. The lower fragment, about 1000bp in size, corresponds to the arm1 and arm2 SOEd PCR product, while the upper fragment, measuring 6000bp, represents the digested pLAZ1 size.

Figure 4.14 The gene map of pLAZ1 before and after cloning the homology arms product.

A gene map was constructed to elucidate the strategy for inserting the homology arms product into pLAZ1. This gene map includes information on the restriction enzymes employed in the process, as well as the size of the vector both before and after the insertion. By detailing these aspects, the gene map provides a clear visualization of the genetic manipulation performed on pLAZ1, facilitating a better understanding of the experimental design.

4.3.7.2 Confirming the *traG* deletion.

To verify the deletion of the *traG* gene, a conjugation transfer experiment was done to confirm that strain MV10-Nal^R -pUB307ΔtraG samples 29-8 and 34-8 are unable to transfer due to the lack of *traG*. In parallel, pACYC184-traG-oriT was added into MV10-Nal^R (pUB307ΔtraG) samples 29-8 and 34-8, and then the transfer experiment was done. HB101 was used as a recipient, and transconjugants were selected on LBA with Kanamycin and Streptomycin.

The result established that MV10 containing pUBΔtraG samples 29-8 and 34-8 could not transfer, whereas the same strains were transferred successfully when pACYC184-traG-oriT was added as shown in Table 4.3. This result can be taken as solid evidence of deletion of the *traG* gene in strain MV10-pUB307ΔtraG samples 29-8 and 34-8 because *traG* is responsible for DNA transport in conjugation as demonstrated previously (Álvarez-Rodríguez et al., 2020a). The strain were stored at -20°C for future use.

Table 4.3 Comparing the transfer in MV10-pUB307ΔtraG samples 29 and 34 in the presence or absence of pACYC184-traG-oriT.

Sample	pUB307ΔtraG transfer status
HB101 (pUB307ΔtraG #29)	**–**
HB101 (pUBΔ307traG + pACYC184-traG-oriT#29)	**+**
HB101 (pUB307ΔtraG #34)	**–**
HB101 (pUB307ΔtraG + pACYC184-traG-oriT#34)	**+**

4.3.8 Testing the effect of pGBT30-pifC on pUB307ΔtraG :: pACYC184-traG.

It was demonstrated in Chapter three that the transfer of plasmid pUB307 is inhibited due to the presence of *pifC* from F. The purpose of this experiment was to confirm that pGBT30-pifC is able to inhibit plasmid pUBΔtraG with pACYC184-traG as well because this will be the basis for selecting mutants resistant to fertility inhibition. A transfer experiment was performed comparing pUB307 and (pUBΔtraG with pACYC184-traG). Initially, pGBT30-pifC was transformed separately into DH5α containing pUB307 and pUBΔtraG. The pACYC184-traG was also transformed with pUBΔtraG. The standard conditions for observing plasmid transfer involve having HB101as recipient and DH5α (pGBT30-pifC, pUB307) and DH5α (pGBT30-pifC, pUBΔtraG, pACYC184-traG) as donors. The transfer experiment was set up as presented in Figure 4.15.

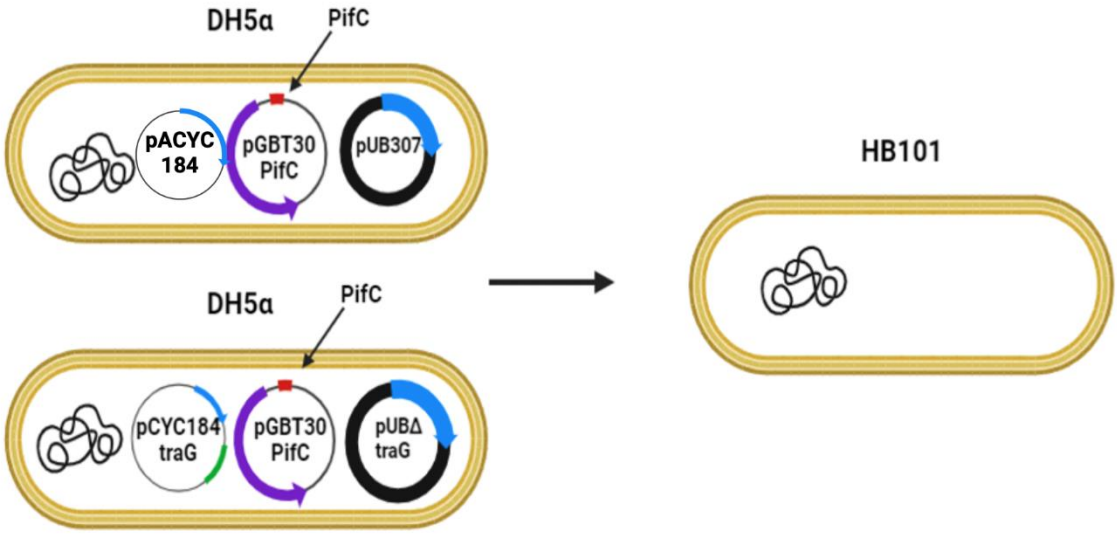

Figure 4.15 Comparing the transfer of pUB307 and (pUBΔtraG with pACYC184-traG) in the presence of *pifC*.

We anticipated that the transfer of pUB307 would be impeded, while there would be comparatively less inhibition for pUBΔtraG with pACYC184-traG. This expectation stems from the upregulation of traG expression facilitated by pACYC184-traG, which could potentially mitigate the inhibitory effects observed in the transfer of pUB307.

As expected, the pUBΔtraG complemented by pACYC184-traG plasmid demonstrated transfer but escaped *pifC* inhibition within the initial 30-minute time course. In contrast, pUB307 exhibited very little transfer, even after 180 and 240 minutes as depicted in Figures 4.16 and 4.17. The results are summarized in Table 4.4. The count of transconjugants for pUBΔtraG with pACYC184-traG consistently surpassed the count for pUB307 across all time-points, indicating a significant difference.

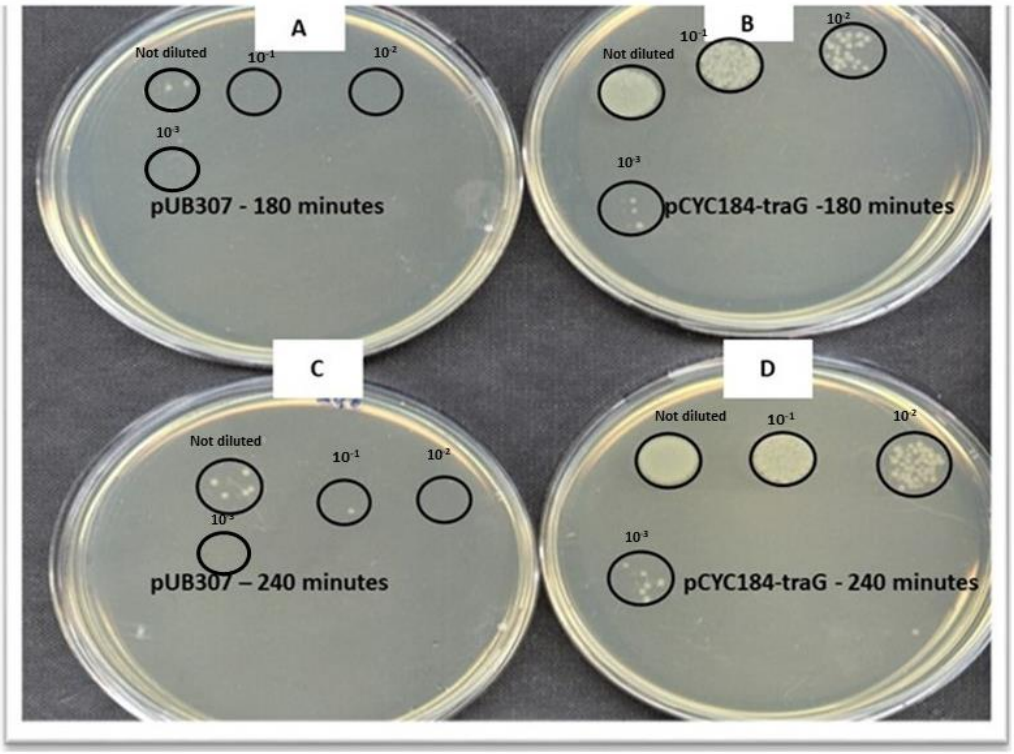

Figure 4.16 Comparison of the conjugative transfer of pUB307 with that of (pUBΔtraG + pACYC184-traG) in the presence of PifC produced by pGBT30-pifC.

Here, only the time-points at 180 and 240 minutes are shown, yet the complete time course is illustrated in Figure 4.17. The donor host utilized is DH5α, while the recipient is HB101.

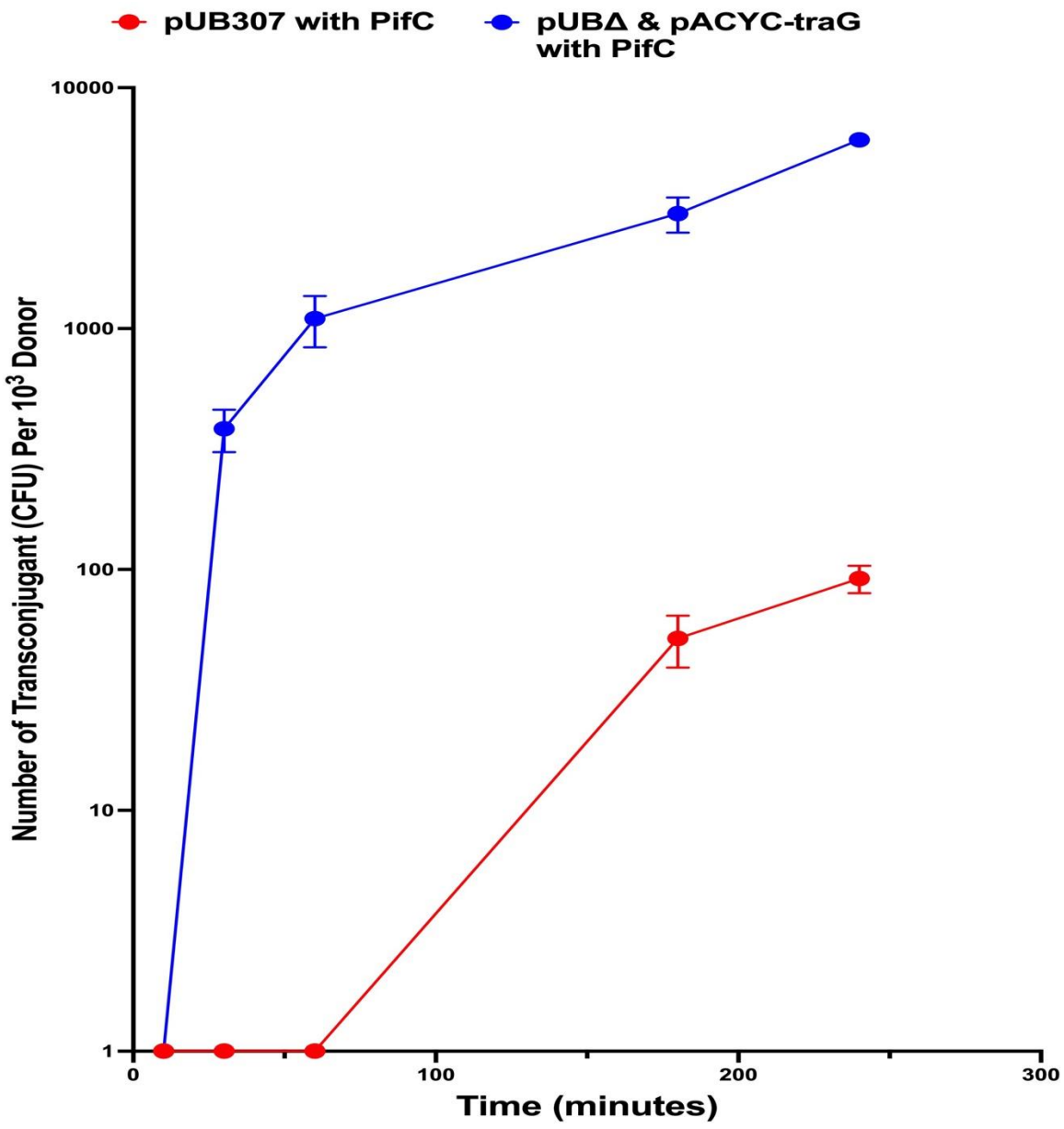

Figure 4.17 The effect of PifC on the conjugative transfer of pUB307 and (pUBΔtraG with pACYC184-traG) from DH5α to HB101.

The graph-drawing package was set to show the error bars for each point but due to the log scale on the y axis these are sometimes not visible. For this reason, the data is also shown in Table 4.4 which includes means, standard deviations and tests of significance where relevant.

Table 4.4 The effect of pGBT30-pifC on the conjugative transfer of pUB307 and (pUBΔtraG with pACYC184-traG) from DH5α to HB101.

	pUB307, pGBT30-pifC		pUBΔtraG, pACYC184-traG, pGBT30-pifC		
Time (minutes)	**Mean**	**Standard Deviation**	**Mean**	**Standard Deviation**	**P value[b]**
10	**<1[a]**	**<1[a]**	**<1[a]**	**<1[a]**	
30	**<1[a]**	**<1[a]**	**383**	**76**	**0.000974**
60	**<1[a]**	**<1[a]**	**1100**	**264**	**0.001978**
180	**51**	**12**	**3000**	**500**	**0.000519**
240	**91**	**11**	**6066**	**115**	**<0.000001**

a. Number <1 represents 0 colonies.

b. $p < 0.05$: Statistically significant $p < 0.01$: Highly statistically significant $p < 0.001$: Extremely statistically significant. Statistical significance determined using t-test in GraphPad.

These unexpected results led to a new perspective on my PhD project. The strong evidence of (pUBΔtraG, pACYC184-traG) being able to escape *pifC* inhibition after 30 minutes could be due to the increase in the level of *traG* expression pACYC184 plasmid. To confirm this phenomenon, an additional experiment was added to check if restoring *traG* with a high expression from a strong promoter in pUBΔtraG could enable it to be resistant to *pifC* inhibition. Chapter 5 of this Thesis describes the testing and validation of this theory.

4.3.9 Attempting to make a mutant of *traG* able to escape fertility inhibition using hydroxylamine mutagenesis.

The planned procedure for creating a mutant of traG capable of escaping fertility inhibition of F is outlined in steps 1 to 9 in Figure 4.18, with further details provided in section 4.3.7.1. During this process, it is important to note that despite the use of pACYC184-traG, which allows escape from fertility inhibition, there appears to be a brief period during which transfer is affected. This observation underscores the complexity of the escape mechanism and highlights the need for careful analysis.

The analysis of the products of this process is summarized in steps 10 to 17 of Figure 4.18 and described in sections 4.3.8 to 4.3.10. However, it should be emphasized that the use of a short transfer period during the enrichment process is not explicitly indicated in Figure 4.18. Further clarification is needed regarding whether a short transfer period was employed solely at the final stage or also during earlier stages of the process. This distinction is crucial for understanding the dynamics of the escape mechanism and its impact on plasmid transfer efficiency.

1. Plasmid pACYC-traG was treated with hydroxylamine for different times.

2. Treated pACYC-traG was transformed into DH5α that containing pUBΔ and pGBT30-*pifC*

3. For each hydroxylamine treatment point, transformants were pooled and cultured overnight.

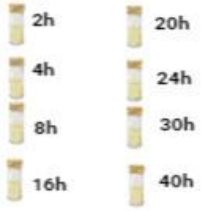

4. Transfer to HB101(pifC) to enrich mutant population (enrichment).

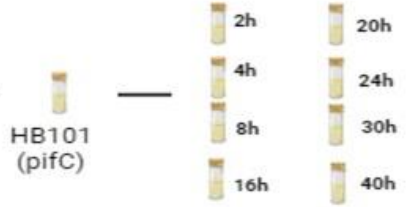

5. For each time point, transconjugants were pooled and cultured overnight.

6. For each time point, transconjugants were pooled and cultured overnight (enrichment).

7. For each time point, transconjugants were pooled and cultured overnight.

8. Transfer experiment to select the best pooled that is able to overcome PifC inhibition in 10 minutes.

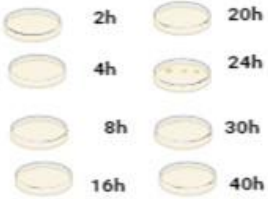

9. DNA for best pool (24h) was isolated from 12 single colonies of HB101 and sent for sequencing with traG amplifying primer

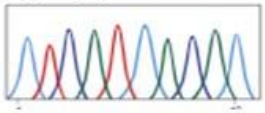

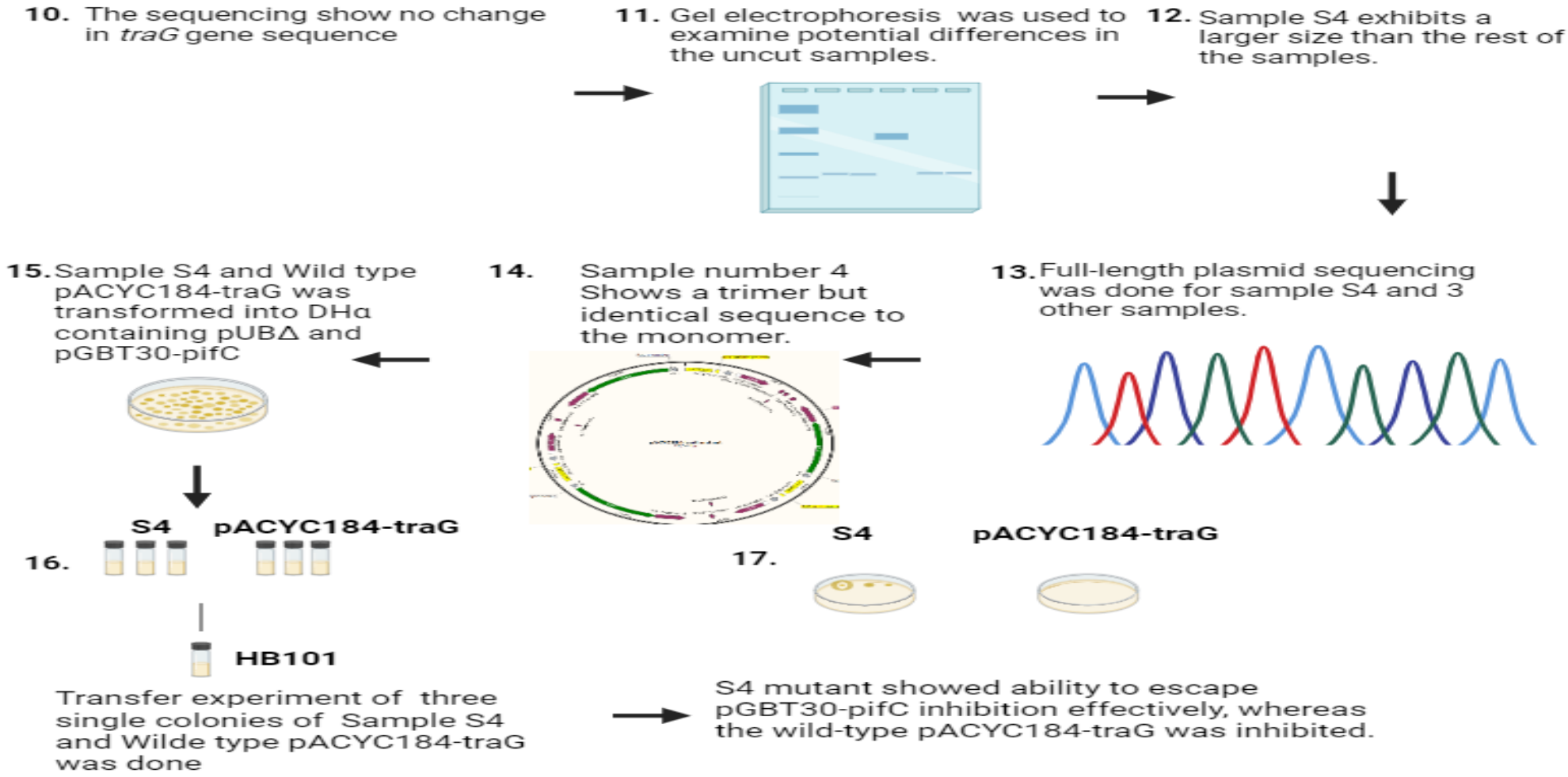

Figure 4.18 The planned procedure for creating a mutant of *traG* capable of escape fertility inhibition.

The plan includes mutagenesis, enrichment, and analysis of pACYC-traG plasmid able to overcome fertility inhibition.

4.3.9.1 Treatment of pACYC184-traG with hydroxylamine and selecting plasmids able to escape *pifC* inhibition

To apply hydroxylamine treatment to pACYC184-traG, the protocol in Chapter two Section 2.24 was used. The treatment was conducted at 37°C for varying durations, specifically 2, 4, 8, 14, 20, 30 and 40 hours. Finally, fresh DHα competent cells, carrying pUBΔ and pGBT30-pifC, were transformed with treated pACYC-traG samples collected at the various time-points. The resulting transformants were selected on LBA plates with ampicillin, kanamycin, and chloramphenicol and the number of transformants decreased as the treatment time progressed, as depicted in Table 4.5. Subsequently, transformants from plates at each time-point were pooled and cultured overnight in LB broth supplemented with ampicillin, kanamycin, and chloramphenicol.

Table 4.5. The quantification of transformations subsequent to the mutagenesis procedure.

Treatment time	Total number of transformants
2 hours	Uncountable
4 hours	Uncountable
8 hours	392
16 hours	310
20 hours	245
24 hours	121
30 hours	64
40 hours	15

To enrich for the mutants in the population, multiple transfer experiments were performed, transferring from DHα (pGBT30-pifC) to HB101 (pGBT30-pifC), and from HB101 (pGBT30-pifC) to Nissle (pGBT30-pifC), as illustrated in Figure 4.18. To select the pool most capable of overcoming PifC inhibition, plates pooled from each treatment time-point after enrichment were utilized in the next transfer experiment. The transfer experiment only allowed 10 min for the transfer, aiming to detect strains with mutants capable of escaping inhibition which was strongest at that time. To choose the best pool, a transfer experiment was run with Nissle containing pUBΔ, pGBT30-pifC and treated pACYC184-traG after enrichment served as donors, while DH5α was used as the recipient. The wild-type pACYC-traG with pUBΔtraG and pGBT30-pifC was used as a control. Transconjugants were selected on LBA supplemented with nalidixic acid and kanamycin, as depicted in Figure 4.19.

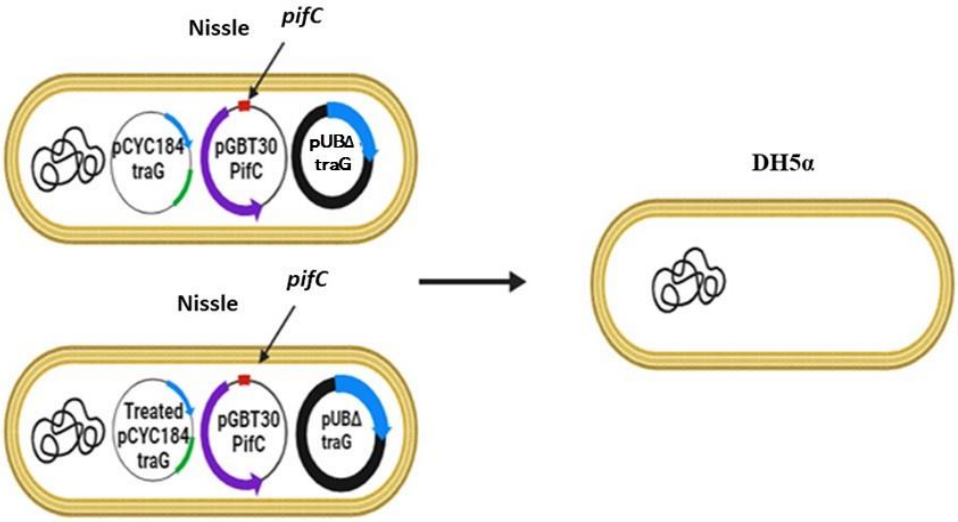

Figure 4.19 Transfer experiment to select the pool that is best able to overcome PifC inhibition.

We anticipate that the mutant will possess the ability to bypass PifC inhibition, resulting in faster transfer of the treated pACYC184-traG compared to the wild type pACYC184-traG. This expectation is based on the hypothesis that the genetic alterations in the mutant will confer resistance to the inhibitory effects of PifC, thereby facilitating a more efficient transfer process.

Based on the result in Figure 4.20, the less effective pools capable of overcoming PifC inhibition were at 0-, 2- and 4-hours treatment, where there were no observable

transconjugants, and the control wild-type pACYC-traG also showed no growth. At 16 hours, transconjugants were observed, with the value reaching 18 and 24 at 20 hours. The highest number of transconjugants was at 24 hours when transconjugants reached 65. The transfer value had decreased slightly at 30 hours with the value of 11 and back to zero at 40 hours. These results indicate that at 24 hours of treatment, the pools effectively overcame *pifC* inhibition with the greatest frequency.

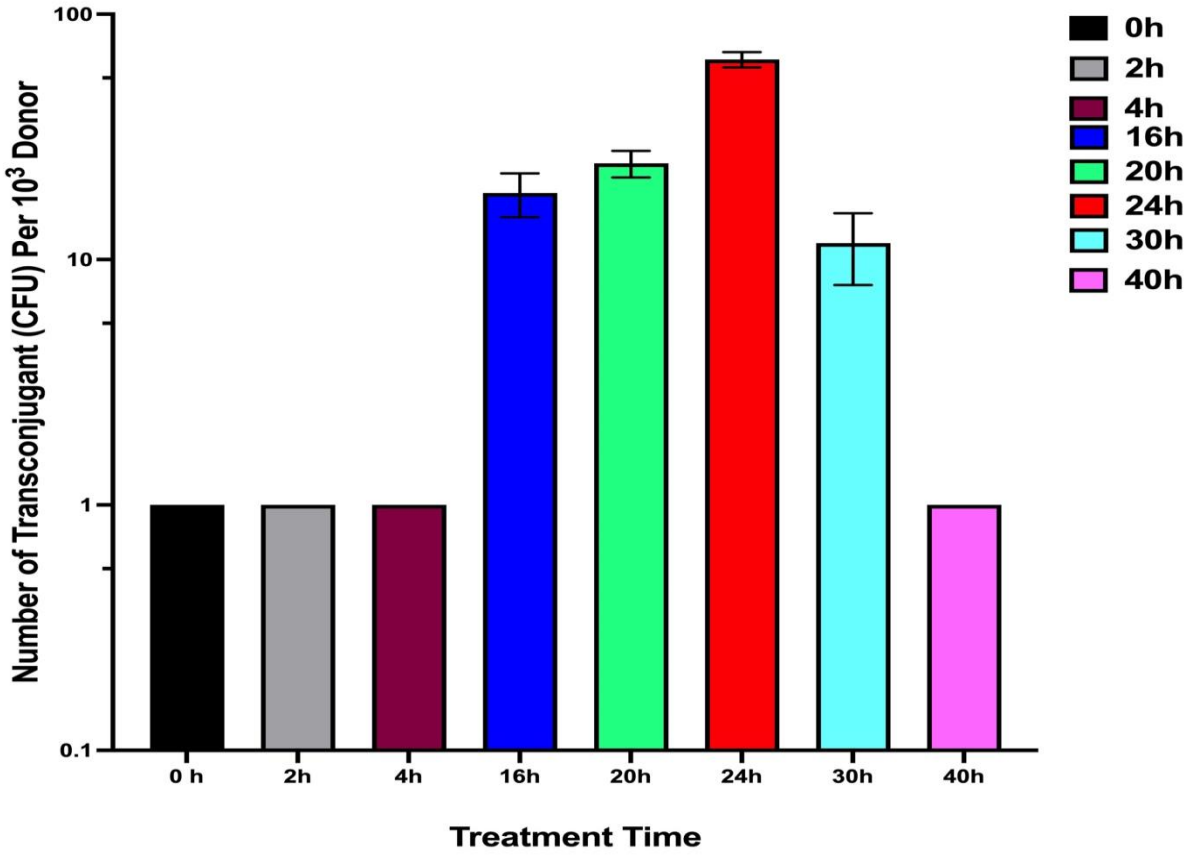

Figure 4.20 Comparing the transfer of pUB307 to DH5α in the presence of pACYC184-traG from different hydroxylamine treated periods as indicated in Fig 4.19.

The primary objective of this experiment was to identify the most effective mutant capable of escape PifC inhibition. As illustrated in the figure, the sample treated for 24 hours exhibited the highest degree of escaping ability.

4.3.10. Analysis of plasmids from the most efficient pool, capable of escaping PifC inhibition.

To identify a mutant capable of escaping inhibition, sequencing the most efficient pool of transferants that were able to transfer without inhibition was crucial. To sequence and determine the basis for the effect, twelve single colonies from the 24h pool recipient that escaped the PifC inhibition at 10 minutes were cultured and DNA was isolated. The DNA was sequenced by the Genomics Laboratory at the University of Birmingham using primers designed to cover the whole *traG* gene to identify the genotype change. Surprisingly the sequence of all the samples was identical to the wild type *traG* sequence.

Therefore, the uncut DNA extracted from the 12 individual colonies and the wild-type pACYC-traG was subjected to electrophoresis gel analysis to identify any differences. The gel results showed that sample number 4 contained a plasmid of a larger size than the other samples, as shown in Figure 4.21. Also, it looked like samples 3, 7 and 8 might have higher copy number because the bands appeared much brighter.

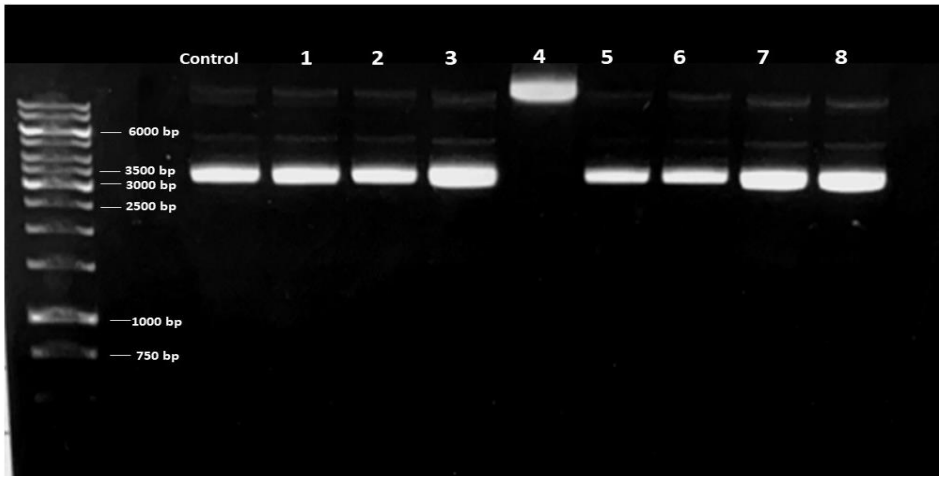

Figure 4.21 Gel electrophoresis of uncut plasmid DNA from 8 transconjugants from the most proficient pool compared to the wild type pACYC184-traG control.

The primary objective of conducting this gel electrophoresis was to assess whether there were any alterations in DNA size that could facilitate escape from PifC inhibition. Notably, sample number four displayed a notable difference, exhibiting a larger size compared to the other samples.

Since a genotypic change had not been detected in *traG* itself, full-length plasmid sequencing provided by PlasmidsNG (Birmingham, United Kingdom) was used as an alternative approach to determine whether a genotypic change had occurred elsewhere in the pACYC184 plasmid. This long-read sequencing was carried out on samples 1, 2 , 3 , 4 , 7 and 8 from the gel. The sequencing results showed once again no changes in the DNA sequence of *traG* or the rest of pACYC184. However, clone 4 was revealed as a trimer of pACYC184-traG instead of the monomer pACYC184-traG as shown Figure 4.22 while all the other samples were confirmed as monomers of pACYC184-traG.

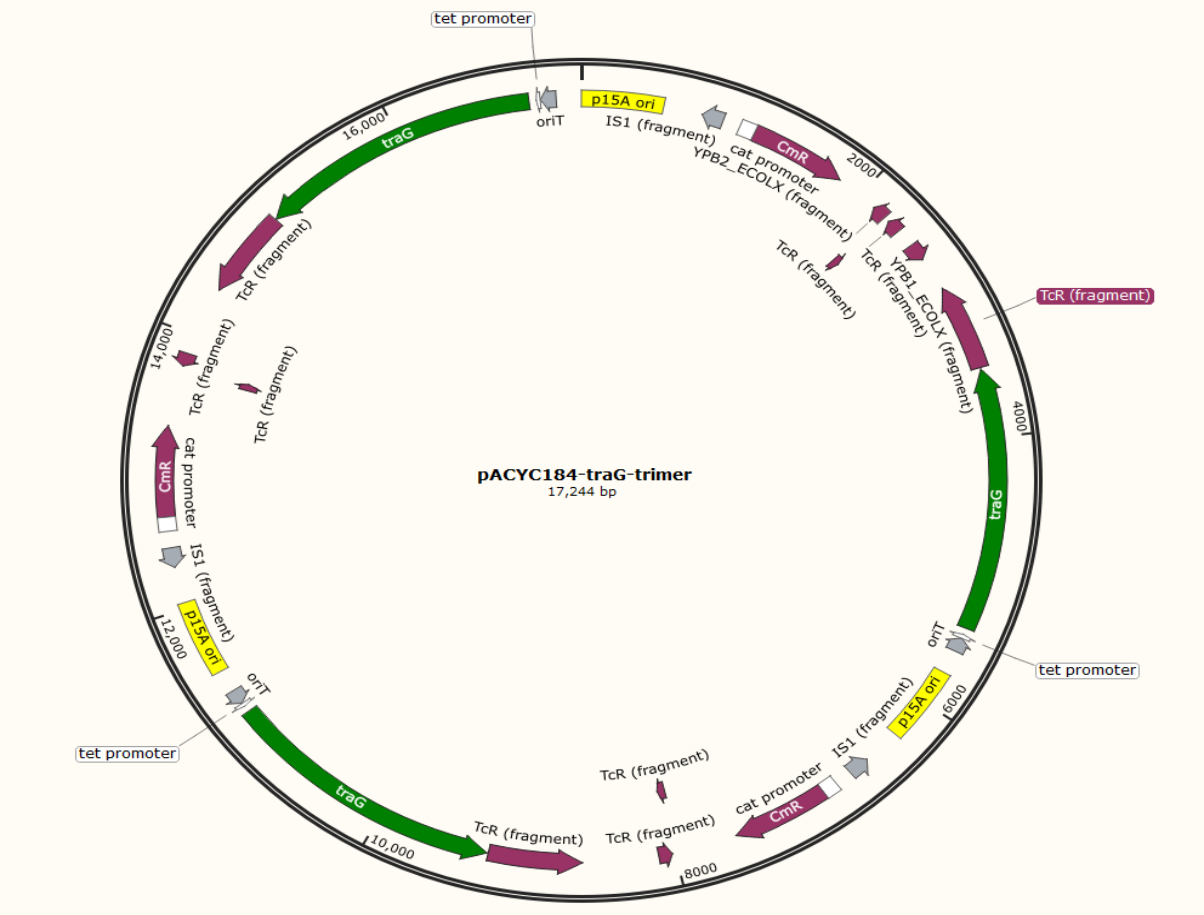

Figure 4.22 A trimer of pACYC184-traG gene map from sample four.

The comprehensive sequencing of the entire plasmid was performed by PlasmidsNG (Birmingham, United Kingdom), ensuring thorough coverage and accuracy in the analysis of the plasmid's genetic composition and structure. This detailed sequencing process provided valuable insights into the complete sequence of the plasmid, facilitating further characterization and understanding of its functional properties.

4.3.11. Checking the ability of the pACYC184-traG trimer to escape the inhibition of *pifC.*

To confirm the escape capability of the trimer in sample four from inhibition, the DNA from sample four was introduced into fresh DHα competent cells containing pUBΔtraG and pGBT30-pifC for a transfer experiment. This experiment involved a comparison between the wild type of monomer pACYC-traG and the trimer pACYC-traG. The trimer, coupled with pGBT30 but lacking *pifC*, was employed as the positive control for this experiment. The selected time-points for the experiment were 5 and 15 minutes, aiming to assess early escape specifically due to the ability to overcome inhibition. The results, shown in Figure 4.23, Figure 4.24, and summarized in Table 4.6, confirmed the trimer mutant capacity to escape pGBT30-pifC inhibition at all examined time-points. However, it is noteworthy that the quantity of trimer transconjugants was less than that of the positive control.

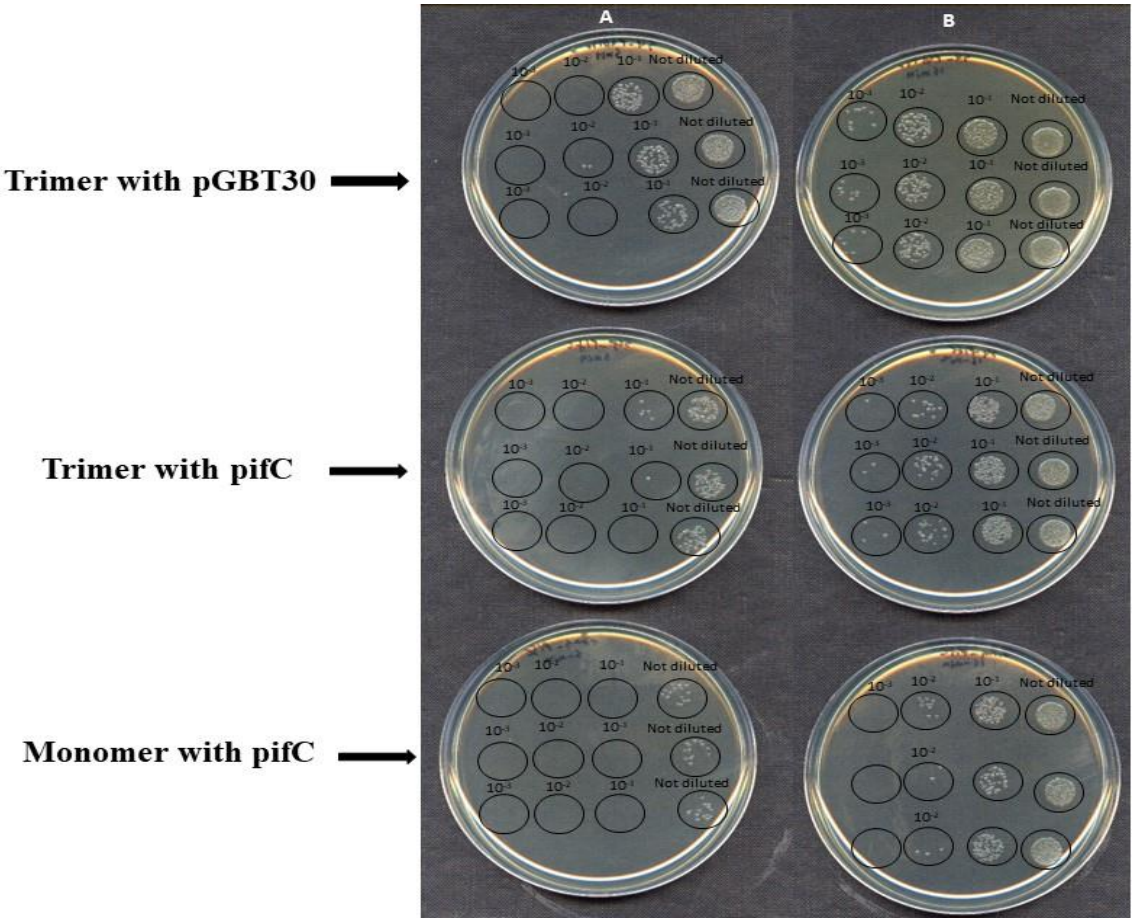

Figure 4.23 Transfer experiment to check the ability of the trimer to escape the inhibition of PifC.

The plates on the left (A) were after 5 min mating and the plates on the right (B) were after 15 min mating.

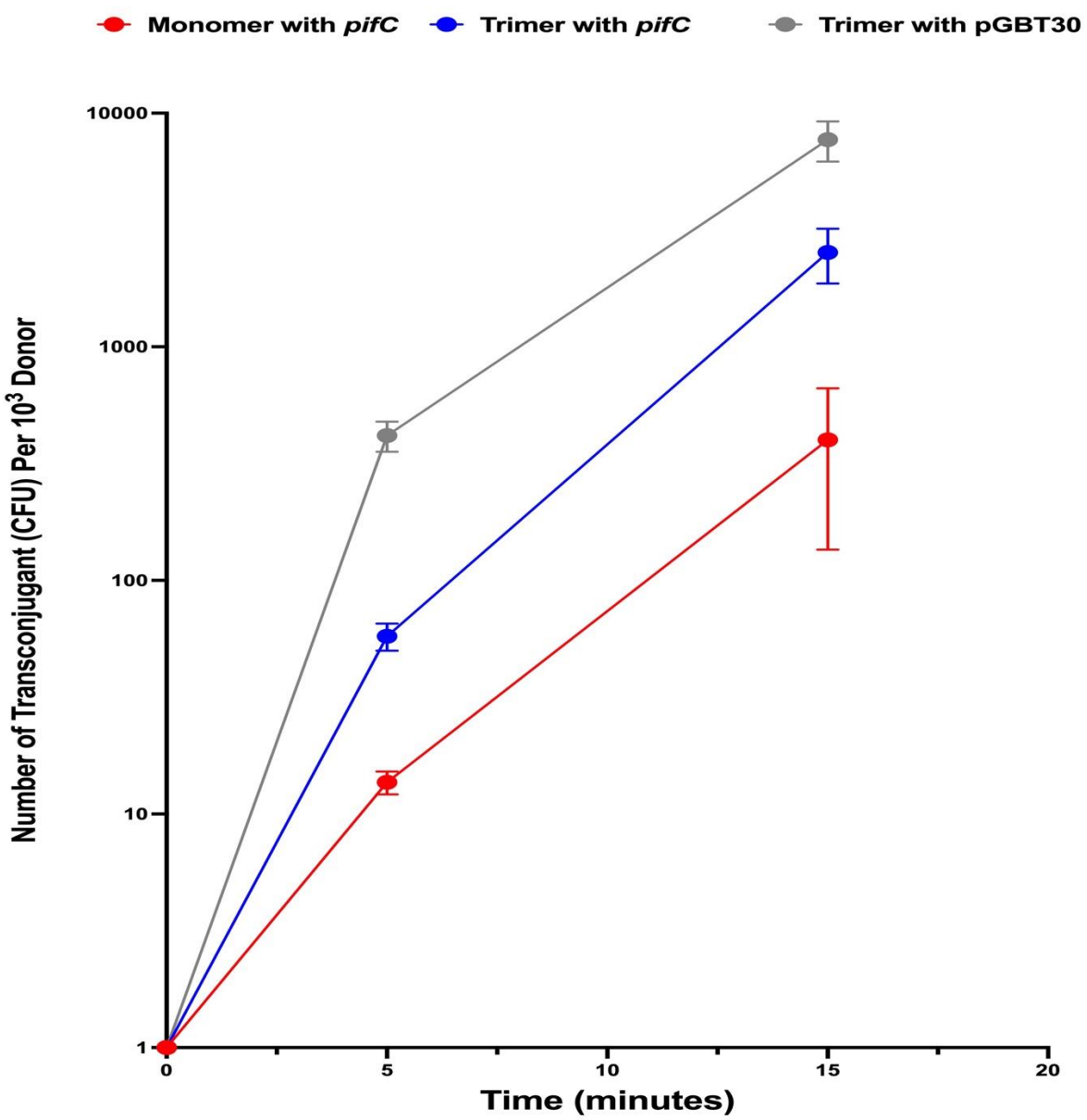

Figure 4.24 Transfer experiment to check the ability of the trimer to escape the inhibition of PifC.

The graph drawing package was set to show the error bars for each point but due to the log scale on the y axis these are sometimes not visible. For this reason, the data is also shown in Table 4.6 which includes means, standard deviations and tests of significance where relevant.

Table 4.6 Comparison of the ability of monomer and trimer pACYC-traG to overcome *pifC* inhibition

Sample	Mean	Standard Deviation	P value[a]
5 Minutes			
Monomer, pGBT30-pifC	**13.7**	**1.53**	**0.000611**
Trimer, pGBT30-pifC	**57.7**	**7.68**	
Trimer, pGBT30	**416.7**	**61.10**	**0.000541**
15 Minutes			
Monomer, pGBT30-pifC	**399.9**	**264.57**	**0.006711**
Trimer, pGBT30-pifC	**2533.3**	**665.83**	
Trimer, pGBT30	**7706.7**	**1501.51**	**0.005487**

a. $p < 0.05$: Statistically significant $p < 0.01$: Highly statistically significant $p < 0.001$: Extremely statistically significant. Statistical significance determined using t-test in GraphPad.

4.3.12. Comparing relative copy number, the pACYC184-traG monomer and trimer.

To be able to compare the plasmid DNA level in the pACYC184-traG monomer and trimer, DH5α strains containing these two plasmids individually were transformed with plasmid pGCMT1 to provide an internal standard. Plasmid DNA was isolation from overnight cultures grown from distinct single colonies of both strains. Uncut DNA samples were subjected to gel electrophoresis analysis, as shown in Figure 4.25.

Quantification of the DNA content was achieved through image analysis software, and the obtained data submit to statistical comparison using a T test, as presented in Table 4.7. The mean levels of the internal control bands were not statisitically different whereas comparison of the means for the monomer and the trimer showed an approximately twofold increase in DNA pACYC184-traG trimer compared to the monomer.

Figure 4.25 Gel electrophoresis of uncut DNA of pACYC184-traG monomer and trimer.

The main aim of this gel is to compare pACYC184-traG monomer and trimer relative copy numbers. Plasmid pGCMT1 is present as an internal control.

Table 4.7 Measuring the DNA in the pACYC184-traG monomer and pACYC184-traG trimer

Sample	Mean	Standard Deviation	P value[a]
pACYC184 :: traG monomer	**2566.02**	**345.17**	**0.000375**
pACYC184 :: traG trimer	**5155.66**	**210.14**	
pGCMT1 with pACYC184 :: traG monomermonomer	**1670.33**	**46.26**	**0.288314**
pGCMT1 with pACYC184 :: traG trimer	**1582.33**	**115.67**	

a. $p < 0.05$: Statistically significant $p < 0.01$: Highly statistically significant $p < 0.001$: Extremely statistically significant. Statistical significance determined using t-test in GraphPad.

4.4 Discussion

An initial objective of the chapter was to create a mutation in the TraG coupling protein that would allow the transfer of the pCURE plasmid without being inhibited by the F plasmid. This was planned to be achieved through hydroxylamine mutagenesis, which has been widely used in biological research to generate mutations in DNA (Gross, 1985).

4.4.1. Cloning the *piou might do difC* gene from F plasmid

The cloning of *pifC* from the F plasmid into the pGBT30 vector not only facilitated the investigation of *pifC*'s impact on pUB307 but also provided a means to identify mutants capable of escaping PifC inhibition. The insertion of *pifC* into the vector offered versatility, allowing transformation into various strains for experimentation. Our results revealed that the inhibitory effect of pGBT30-pifC exceeded that of F.

Furthermore, our findings from the *pifC*/IPTG experiment shed light on a significant observation that has raised concerns within the molecular biology community. IPTG, commonly used as an inducer of gene expression in systems regulated by the LacI repressor, was found to potentially compromise the inhibitory efficacy of PifC. This observation aligns with the research by Gomes et al. (2020), which demonstrated that IPTG supplementation could adversely affect the expression of recombinant proteins, particularly in cases involving high-copy plasmids (Gomes et al., 2020).

Understanding the mechanism proposed by Gomes et al. (2020) is crucial in interpreting our findings. Their study suggests that the interaction between IPTG and the LacI repressor could disrupt the regulatory balance, leading to unintended consequences such as reduced inhibitory efficacy. This highlights the importance of carefully considering the effects of inducers like

IPTG on gene expression systems and the potential implications for experimental outcomes (Gomes et al., 2020).

It is evident that addressing the observed impact of IPTG on inhibitory efficacy is essential for the robustness of our study. Considering this, a more thorough consideration of the potential effects of IPTG on experimental outcomes could have been beneficial during the experimental design phase. This could have involved pre-testing the IPTG induction protocol to assess its compatibility with the intended study objectives. By proactively addressing this issue, we could have ensured a more accurate interpretation of our results and potentially avoided unexpected confounding factors.

Moving forward, it would be prudent to incorporate such considerations into future experimental designs. This proactive approach can help researchers mitigate the risk of unintended influences on their experimental outcomes and ensure the reliability and integrity of their data. While our study highlights the importance of this issue, it also serves as a reminder for researchers to critically evaluate and address potential experimental variables to enhance the validity of their findings

4.4.2. Cloning the *traG* gene from pUB307 in pACYC184 vector

The primary objective of cloning the *traG* gene from pUB307 into the pACYC184 vector was to enable selective mutagenesis of the *traG* gene from pUB307 while avoiding any mutations in other regions of pUB307.

The insertion of the *oriT* region into the pACYC184-traG vector was intended to allow pACYC184-traG to transfer so that those better able to transfer could be isolated from the

rest. The results demonstrate that the pACYC184-traG vector with *oriT* was able to transfer satisfactorily, whereas the pACYC184-traG vector without *oriT* was unable to transfer. This finding confirmed that *oriT* is essential for plasmid conjugation transfer (Frost et al., 1994). In the study by Matson & Ragonese, (2005), significant insights were gained regarding the importance of *oriT* in facilitating conjugative transfer as the initiation site for the transfer process. The research highlighted the role of a relaxase, typically encoded by the plasmid, which specifically targets the *oriT*, leading to the induction of a single-strand DNA break (nick) at the *oriT* site. Furthermore, the relaxase forms a covalent attachment to the 5′ end of the nicked DNA strand through a phosphotyrosyl linkage, elucidating crucial molecular mechanisms involved in the transfer of genetic material Matson (Matson and Ragonese, 2005).

The most intriguing and significant outcome appeared while examining the *traG* that had been cloned into pACYC184 plasmid. The primary objective of the experiment was to validate the impact of the F plasmid on the *traG* in pACYC184-traG vector and subsequently compare these effects following the introduction of a mutation in pACYC184-traG. Surprisingly, the *traG* in pACYC184-traG demonstrated the ability to overcome the inhibition by the F plasmid even in the absence of any mutation. This finding was unexpected and suggests a direct connection between the expression level of *traG* and the ability to escape inhibition by the F plasmid. This phenomenon will be thoroughly investigated in Chapter five of this study.

4.4.3 Deleting *traG* from pUB307.

The main objective of this part was to produce a mutated version of pUB307 by deleting the *traG* gene from it using homologous recombination. The experiment outcome indicated that the *traG* gene was successfully deleted from pUB307, leading to the creation of pUBΔ. The

method employed to verify the deletion involved trying to transfer the pUBΔ alone and in combination with of pACYC184-oriT-traG. The results showed that pUBΔ could not be transferred independently, whereas the same strains could be transferred successfully with the addition of pACYC184-oriT-traG. This outcome can be taken as strong evidence of deletion of the *traG* gene since it is consistent with the findings of Alvarez et al. (2020), who established that the TraG coupling protein is fundamental for the transfer in conjugation plasmids.

4.4.4. Making a mutant of *traG* able to escape fertility inhibition using Hydroxylamine mutagenesis.

In this section, the objective was to use hydroxylamine mutagenesis to create a mutation in the *traG* gene that would have no impact on the function of *traG* gene but should allow it to escape inhibition from the *pifC*. The experiment gave one plasmid that was at least partially able to escape inhibition from *pifC*, but this was not due to a single base change as planned.

After full-length plasmid sequencing of the wild type pACYC184-traG and the potential mutant pACYC184-traG, it was found that the sequence of the pACYC184-traG potential mutant was a trimer identical to that of the monomer wild type. The amount of the DNA per genome in the trimer was almost double that of the monomer as shown in Table 4.6. This was an interesting observation because copy number of the P15A replicon in pACYC184 is controlled by an antisense RNA like the related replicons from plasmids ColE1, pMB1, RSF1030 and CloDF13 (Selzer et al., 1983), which should be proportional to the number of

copies of the plasmid genome, not the number of separate molecules. Therefore, we expected that plasmid genome copy number should be similar for monomer and multimer (Summers, 1998), but perhaps the fact that a single replication initiation on the trimer will produce three new copies distorts the control system. It is also interesting that the trimer seems to be so stable – when DNA from the trimer was retransformed into fresh bacteria all transformants analysed still had a trimer and this is consistent with the observation that insertion of a multimer resolution system into pACYC184 increased its segregational stability indicating that it does not already have such a system (Krause and Guiney, 1991).

The increased copy number of the trimer could provide a possible explanation for the phenotypic change. The higher amount of DNA means more copies of *traG* per cell and thus higher *traG* expression to allow escape from the inhibition. This principle is similar to the ability of pACYC-traG wild type to allow escape from *pifC* inhibition at 30 and 60 minutes when pUB037 was inhibited and provides the starting point for the work described in the next chapter which aimed to insert *traG* with high expression in pUB307 to enable it to escape PifC inhibition.

Although obtaining a plasmid multimer in this mutagenesis experiment was not what we were aiming for, the fact that this derivative was isolated indicates that it is likely that the selection process chosen was effective in enrichment for variants that were less inhibited by

PifC. Therefore, it could be advantageous to enhance the efficacy of the mutagenesis process by expanding the scope of plasmid sampling. The observed transformations that evaded inhibition suggest that our mutagenesis protocol was potentially highly effective. However, it is plausible that some mutants may have remained undetected. Additionally, the decrease in transformation numbers over time following treatment with hydroxylamine indicates its impact on DNA, potentially facilitating mutant creation.

An important aspect to consider is the effect of dimerization or trimerization on plasmid copy number. During mutagenesis, the formation of plasmid dimers or trimers can lead to alterations in copy number, potentially affecting the observed transformation rates. Further investigation into the mechanisms underlying plasmid dimerization or trimerization and their impact on mutagenesis outcomes is warranted.

To enhance our understanding and detection of mutants, future investigations could involve broader sampling of plasmids and the implementation of rigorous mutagenesis protocols. By incorporating considerations of plasmid dimerization or trimerization and their effects on copy number, we can better elucidate the mechanisms driving mutant creation and improve the accuracy of our experimental outcomes.

Chapter 5: Strategy for deriving pCURE plasmids that are resistant to fertility inhibition

5.1 Background

The main aim of the current study was to create a comprehensive solution for pCURE plasmid to overcome the F plasmid fertility inhibition (FIR) issue. Chapter 4 reported that when the pUB307ΔtraG transfer defect was complemented by pACYC-traG the sensitivity to inhibition by *pifC* was reduced. This suggested that increased expression of *traG* might reduce the sensitivity to inhibition by PifC and suggested a strategy to create a pUB307 derivative with reduced sensitivity to this inhibition.

As elucidated in Chapter 1, particularly in section 1.7.1, it is important to highlight that the transfer of IncP-1 plasmids face inhibition not only from plasmids within the F group but also from other plasmid groups. Furthermore, in the investigation of IncI and IncW plasmids, it has been established that this inhibitory effect is also through the targeting of TraG, as detailed by Getino et al. (2018).

5.2 Aims and Hypotheses

The primary focus of this chapter is twofold: firstly, to enhance *traG* expression in the pCURE plasmid by reintroducing it with a strong promoter of its own, and secondly, to evaluate the effectiveness of a high-expression *traG* pCURE plasmid in overcoming inhibition by F. To prevent unintended elevation of other transfer genes' expression due to promoter read-through, *traG* was strategically inserted at the end of the *traKLM* transcriptional unit but before the terminator following *traM*.

A secondary objective is to explore the ability of the restored high-expression *traG* pCURE plasmid to evade inhibition caused by other plasmids like R388 and R64.

Furthermore, this study aims to investigate whether the presence of pUB307 influences the expression of *traG* in its new location. The wild-type (WT) *traG*, located within the *traJ-traA* operon, possesses a promoter immediately upstream of *traG*. Its transcription is regulated by TrbA, which reppresses the *traG* promoter (Zatyka et al., 1994). Therefore, the inquiry revolves around the differential expression of *traG* genes in their original versus new locations and the extent of regulation by RK2 gene products.

5.3 Results

5.3.1 Insert *traG* along with *tet* promoter in pUBΔ to increase *traG* expression through the utilization of homologous recombination.

5.3.1.1 Combining *traG* gene with the *tet* promoter.

Primers to amplify the *tet* promoter with *traG* gene from pACYC184-traG were designed with the sticky ends that were complementary to homology arms specific to the target *traM* in pUBΔtraG using SnapGene software (as shown in Chapter Two Table 2.6). A gene map of the pUBΔ+ after the *tetp-traG* insertion was generated, as shown in Figure 5.1. The *tetp-traG* gene fragment was amplified using PCR under the following conditions: annealing at 56°C; and extension at 72°C for 2 minutes because the size of the *tetp-traG* gene fragment is 1976 bp. The PCR product was purified after separating the bands by gel electrophoresis, as shown in Figure 5.2, and stored at -20°C.

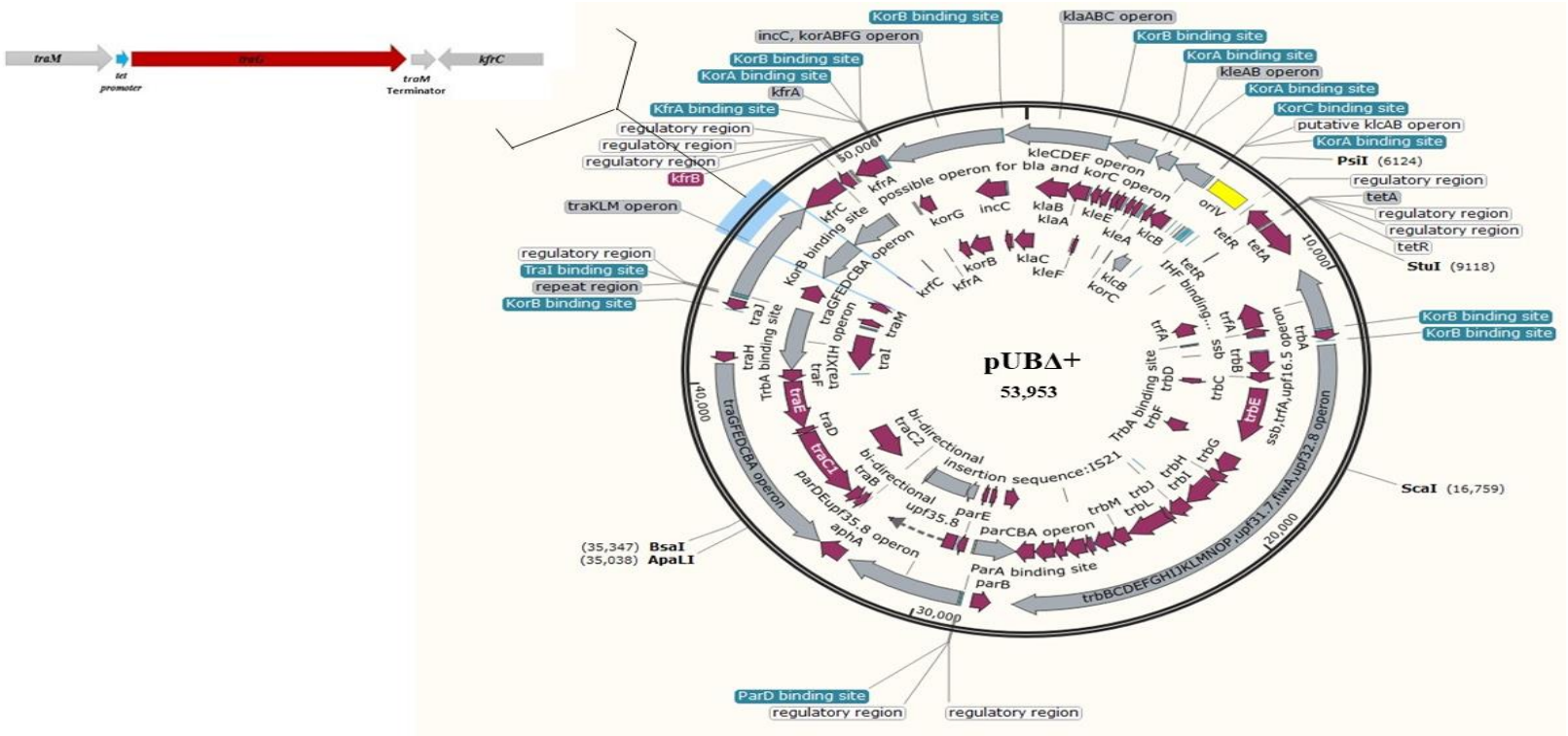

Figure 5.1 Gene map of the pUBΔ+ after the insertion of *tetp-traG*.

A gene map was constructed to elucidate the strategy for the homology arms to allow insertion into pUBΔ+. This gene map includes information on the restriction enzymes employed in the process, as well as the size of the vector both before and after the insertion. By detailing these aspects, the gene map provides a clear visualization of the genetic manipulation performed on pUBΔ+, facilitating a better understanding of the experimental design.

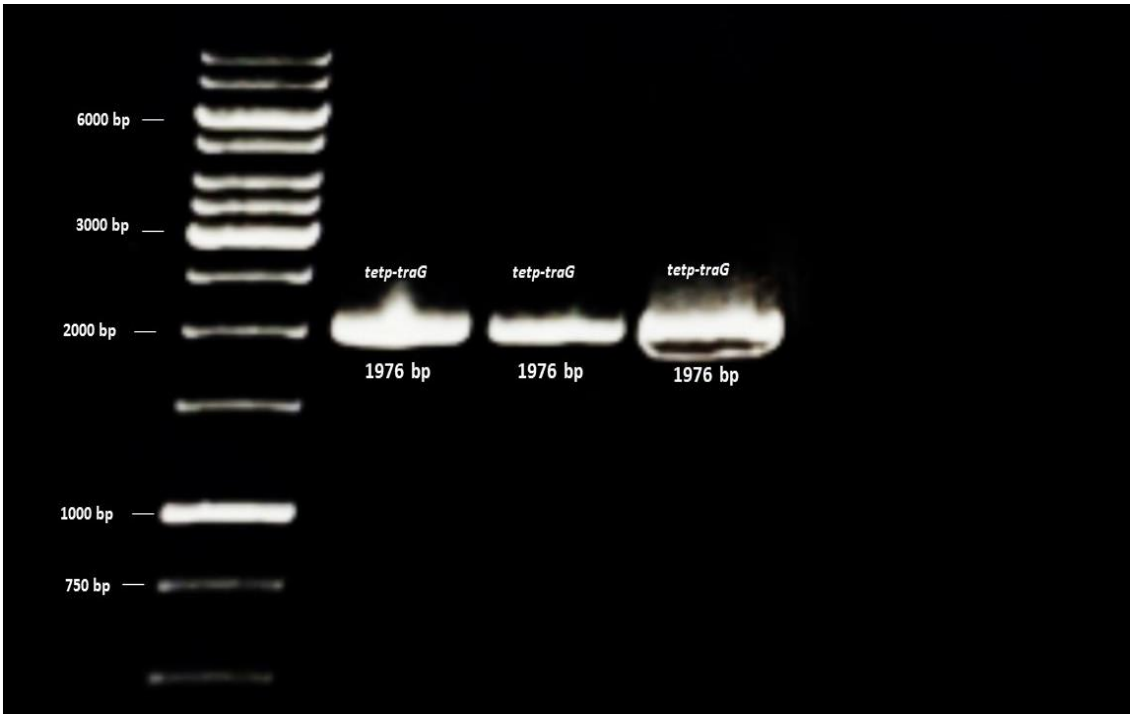

Figure 5.2 The *tetp-traG* amplicon running in an electrophoresis gel.

PCR amplification was performed to target the *tetp-traG* gene fragment, revealing a distinct band indicating successful amplification. The gel electrophoresis analysis confirms the size of the amplified *tetp-traG* gene fragment to be 1976 base pairs (bp).

5.3.1.2 Amplifying and SOEing recombination homology arms with *tetp-traG.*

To initiate homologous recombination to insert *tetp-traG* into pUBΔ, homology arms specific to the target *traM* in pUBΔ were amplified using PCR under the following conditions: annealing at 67°C and extension at 72°C for 30 seconds because the homology arms are both approximately 500 bp. Subsequently, the individual homology arms were joined with *tetp-traG* through SOEing PCR, and outer primers for the homology arms were used to amplify the *tetp-traG* flanked by homology arms. The PCR product was purified after separated by gel electrophoresis, as shown in Figure 5.3, and stored at -20°C.

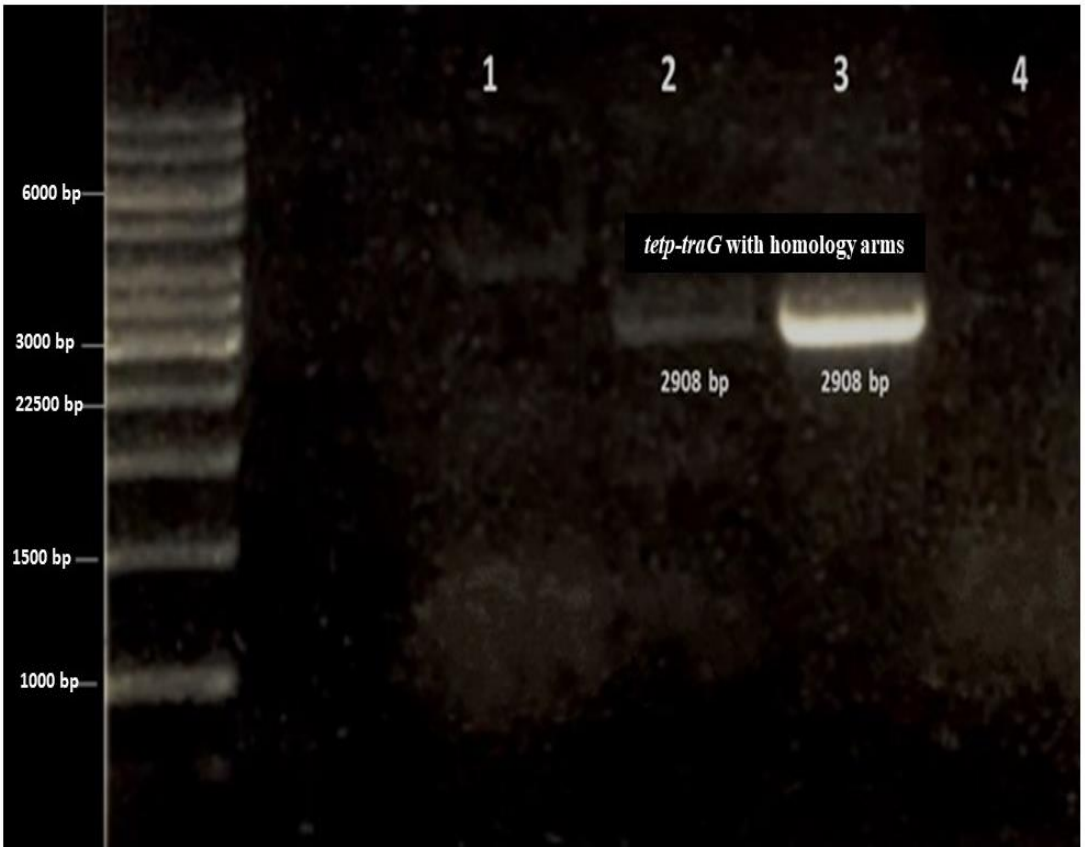

Figure 5.3 The PCR product of *tetp-traG* flanked by homology arms separated by gel electrophoresis.

Clear bands, with a size of 2908 base pairs (bp), indicate successful amplification and the presence of the desired DNA fragment.

5.3.1.3 Inserting *tetp-traG* with homology arms into pLAZ2 to create the recombineering plasmid.

A gene map of pLAZ2 before and after cloning *tetp-traG* with homology arms is shown in Figure 5.4. Inserting *tetp-traG* with homology arms into pLAZ2 was done by digesting both with HindIII and SalI restriction enzymes and ligated follow the protocol in Chapter two sections 2.4 and 2.20. In order to isolate the desired product, the ligated DNA was transformed into DH5alpha, plasmid DNA extracted from individual clones, digested using HindIII and SalI and analysed by gel electrophoresis, as shown in Figure 5.5.

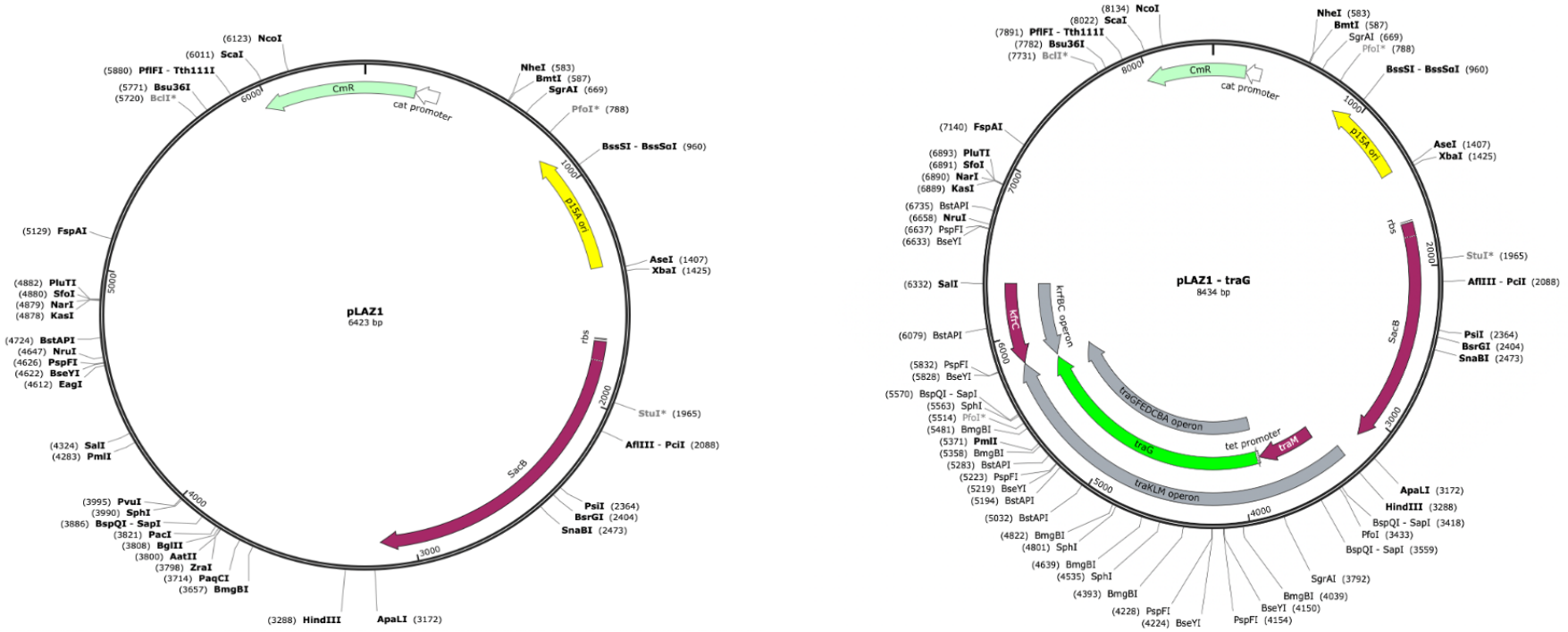

Figure 5.4 Gene map of pLAZ2 and the derivative after inserting the *tetp-traG* with homology arms.

The *traG* gene is shown in bright green and the convergent *traM* and *kfrC* coding regions in the homology arms are also labelled.

Figure 5.5 Electrophoretic analysis of six potential clones of pLAZ2 with the *tetp-traG* with homology arms digested with HindIII and SalI.

Only samples 1, 2, 3 and 4 contain the *tetp-traG* with homology arms, and these were stored at -20°C for future use. Samples 5 and 6 give a 1000 bp HindIII-SalI fragment corresponding to the Arm1+Arm2 segment in pLAZ2.

5.3.1.4 Inserting *tetp-traG* into pUBΔ*traG* through homologous recombination.

To use homologous recombination for insertion of *tetp-traG* into pUBΔtraG, the protocol in Chapter two Section 2.16 was utilized. To screen for potential insertion, PCR with recombination homology arms outer primers (as shown in chapter two, Table 2.6) was used to identify the colonies that had got *traG* and a gel was run to check the products as shown in Figure 5.6.

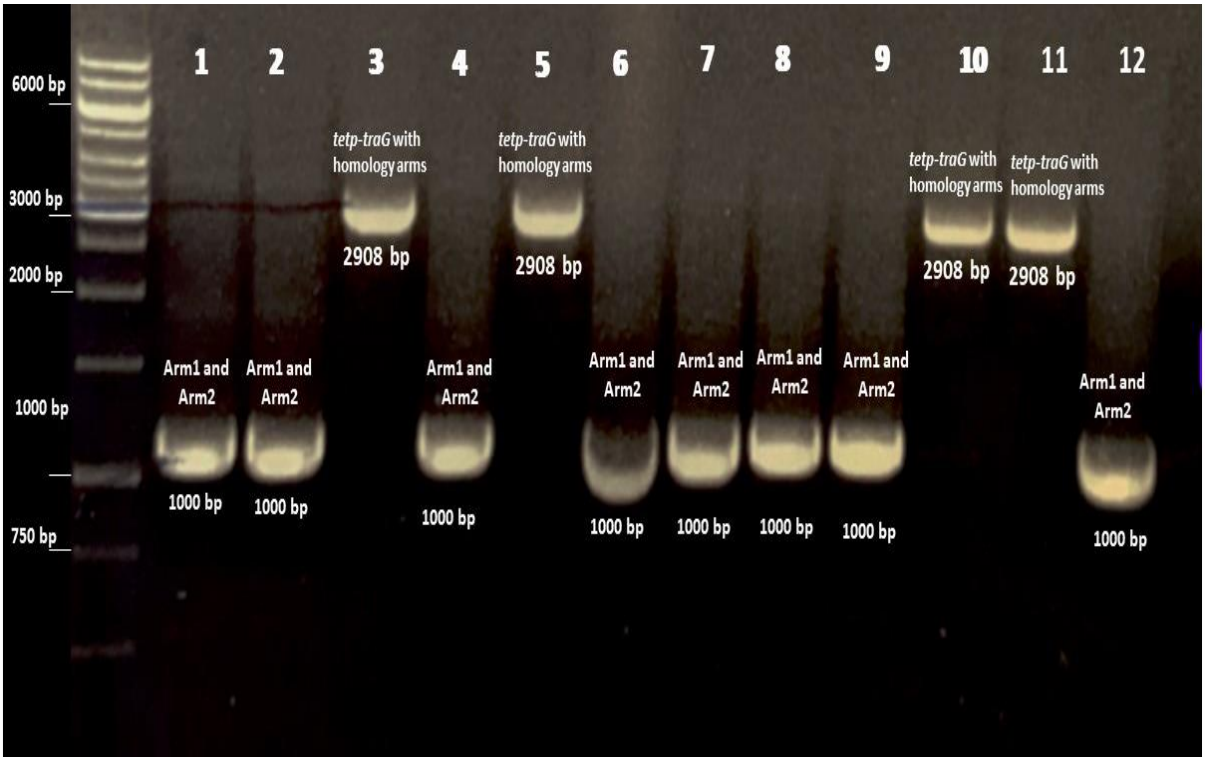

Figure 5.6 PCR to check the inserted *tetp-traG* in pUBΔ.

Only samples 3, 5, 10 and 11 contain the inserted *tetp-traG* in pUBΔ as indicated by the 2908 bp band which corresponds to the size of *tetp-traG* with homology arms. These strains were stored at -20°C, and the plasmid with reinserted *traG* was called pUBΔ+.

5.3.2 Testing the capability of pUBΔ+ to escape different sources of inhibition.

5.3.2.1 The ability of pUBΔ+ to escape F' inhibition.

Before examining pUBΔ+ capability to escape inhibition, a transfer experiment was conducted as an initial step to evaluate pUBΔ+ ability to transfer. The outcome of the experiment substantiated the ability of pUBΔ+ in successful transfer. A second transfer experiment was done to check if inserting *tetp-traG* with high expression in pUBΔ+ could confer resistance to F inhibition. The experiment compared the transfer of pUB307 with that of pUBΔ+ in the presence of F', as shown in Figure 5.7.

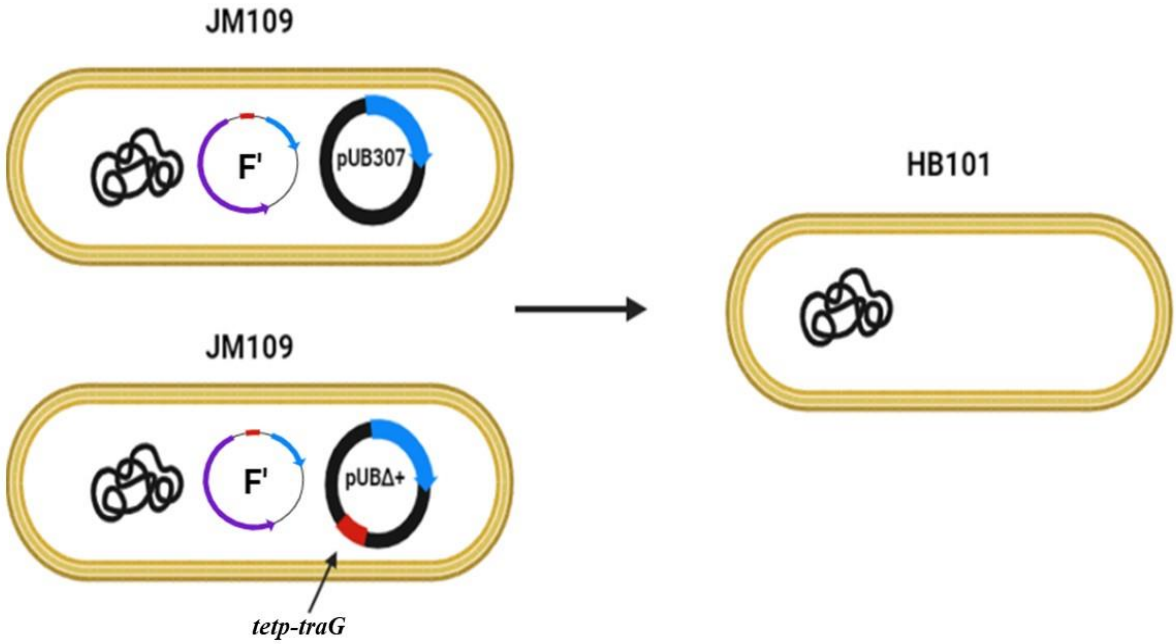

Figure 5.7 Transfer experiment to compare the transfer of pUB307 and pUBΔ+ in the presence F'prolac.

The primary goal of this experiment is to verify pUBΔ+ ability to escape the inhibition caused by the F' plasmid. We anticipate that pUBΔ+ will demonstrate a more efficient transfer compared to the wild type pUB307.

It is apparent from Table 5.1 and Figure 5.8 that inserting *tetp-traG* into pUBΔ+ shows a statistically significant improvement in the plasmid ability to transfer in the presence of F'. The number of transconjugants were higher in pUBΔ+ than pUB307 transconjugants numbers at all time-points. This finding highlights the importance of the *tetp-traG* element in enhancing the transferability of the plasmid in the presence of F'.

Table 5.1 Comparing the ability to resist the fertility inhibition (FIR) between pUB307 and pUBΔ+ in the presence of F' plasmid

	pUB307		pUBΔ+		
Time (minutes)	**Mean**	**Standard Deviation**	**Mean**	**Standard Deviation**	**P value[b]**
10	**<1[a]**	**0**	**43.010**	**11.790**	**0.003503**
30	**99.333**	**11.504**	**317.333**	**19.858**	**0.000080**
60	**207.200**	**20.998**	**665.333**	**33.855**	**0.000037**

a. Number <1 represents 0 colonies.

b. $p < 0.05$: Statistically significant $p < 0.01$: Highly statistically significant $p < 0.001$: Extremely statistically significant. Statistical significance determined using t-test in GraphPad.

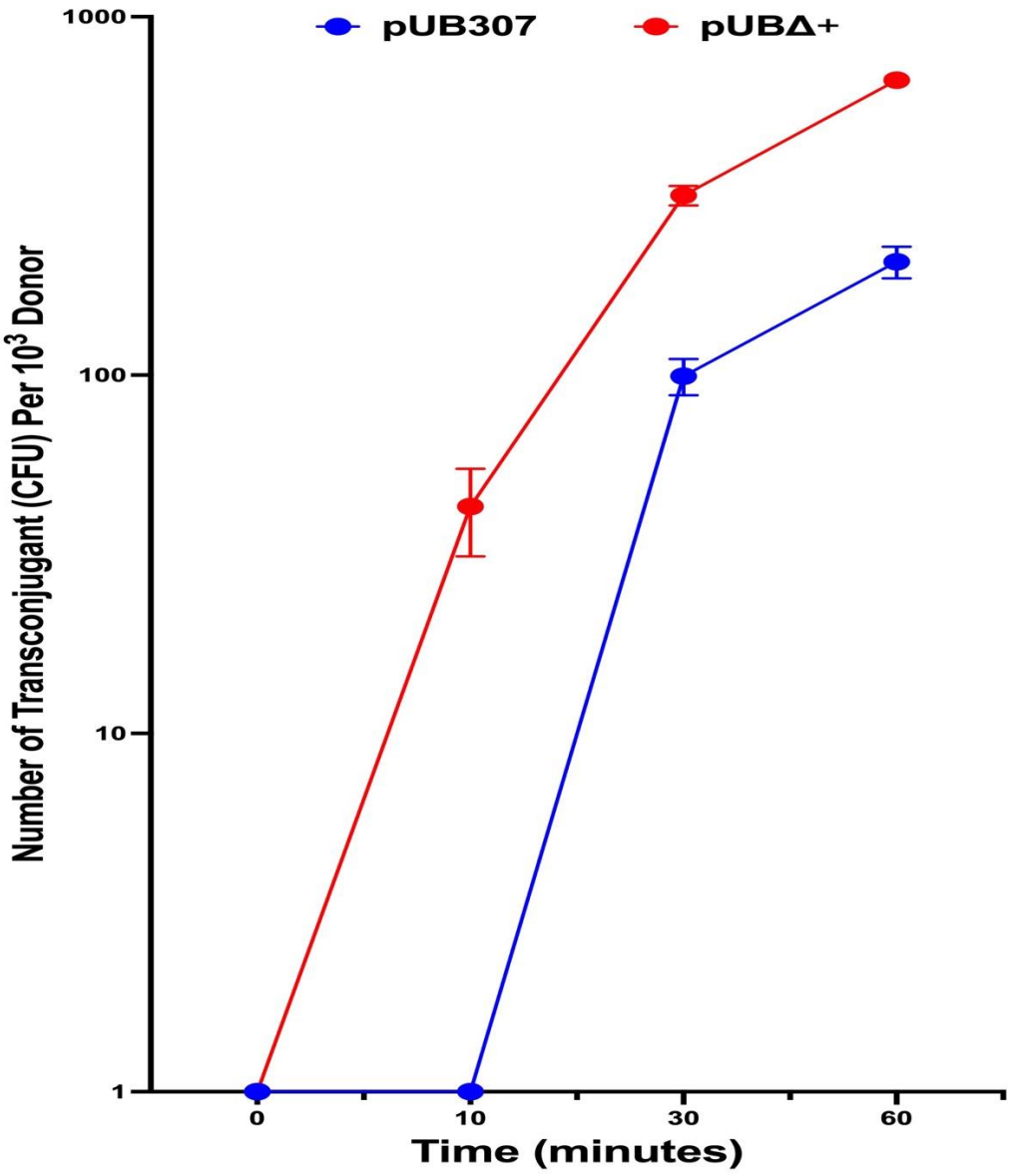

Figure 5.8 Transfer Experiment for pUB307 and pUBΔ+ Plasmid in the presence of F' plasmid.

This figure shows the increased transfer (reduced fertility inhibition resistance, FIR) of pUBΔ+ compared to pUB307 in the presence of the F' plasmid.

5.3.2.2 The ability of pUBΔ+ to escape R64 fertility inhibition.

To determine the effect of R64 on pUBΔ+ spread, a transfer experiment was conducted to determine whether inserting *traG* with high expression in pUBΔ+ could enable it to resist R64 inhibition. The experiment compared the transfer of pUB307 and pUBΔ+ in the presence of R64, as shown in Figure 5.9.

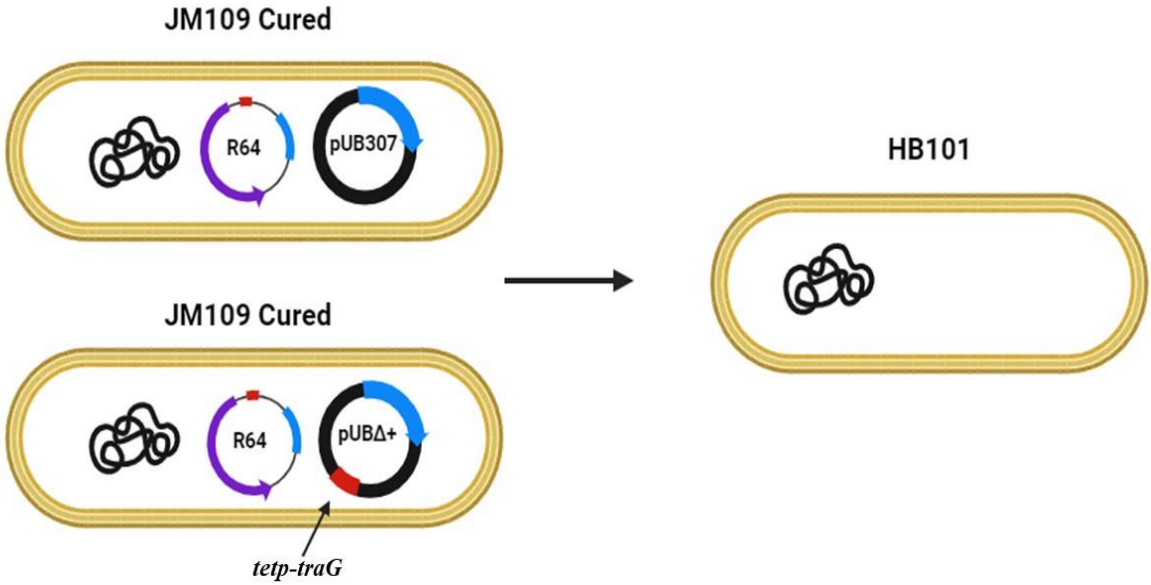

Figure 5.9 Transfer experiment to compare the transfer of pUB307 and pUBΔ+ in the presence of R64.

The primary goal of this experiment is to test pUBΔ+ ability to escape the inhibition caused by the R64 plasmid. Our hypothesis was that pUBΔ+ would demonstrate a more efficient transfer compared to the wild type pUB307.

Table 5.2 and Figure 5.10 illustrate a consistent trend where the quantity of transconjugants from pUBΔ+ consistently surpassed those from pUB307 across all observed time intervals. Additionally, the data presented in these visuals provide a comprehensive view of the comparative transconjugant numbers between the two vectors over time.

Table 5.2 Comparing the ability to resist the fertility inhibition (FIR) between pUB307 and pUBΔ+ in the presence of R64 plasmid

	pUB307		pUBΔ+		
Time (minutes)	**Mean**	**Standard Deviation**	**Mean**	**Standard Deviation**	**P value[b]**
10	**<1[a]**	**0**	**6.167**	**2.930**	**0.022**
30	**4.833**	**1.258**	**51.333**	**11.060**	**0.002**
60	**20.333**	**5.508**	**195.667**	**37.112**	**0.001**

a. Number <1 represents 0 colonies.

b. $p < 0.05$: Statistically significant $p < 0.01$: Highly statistically significant $p < 0.001$: Extremely statistically significant. Statistical significance determined using t-test in GraphPad.

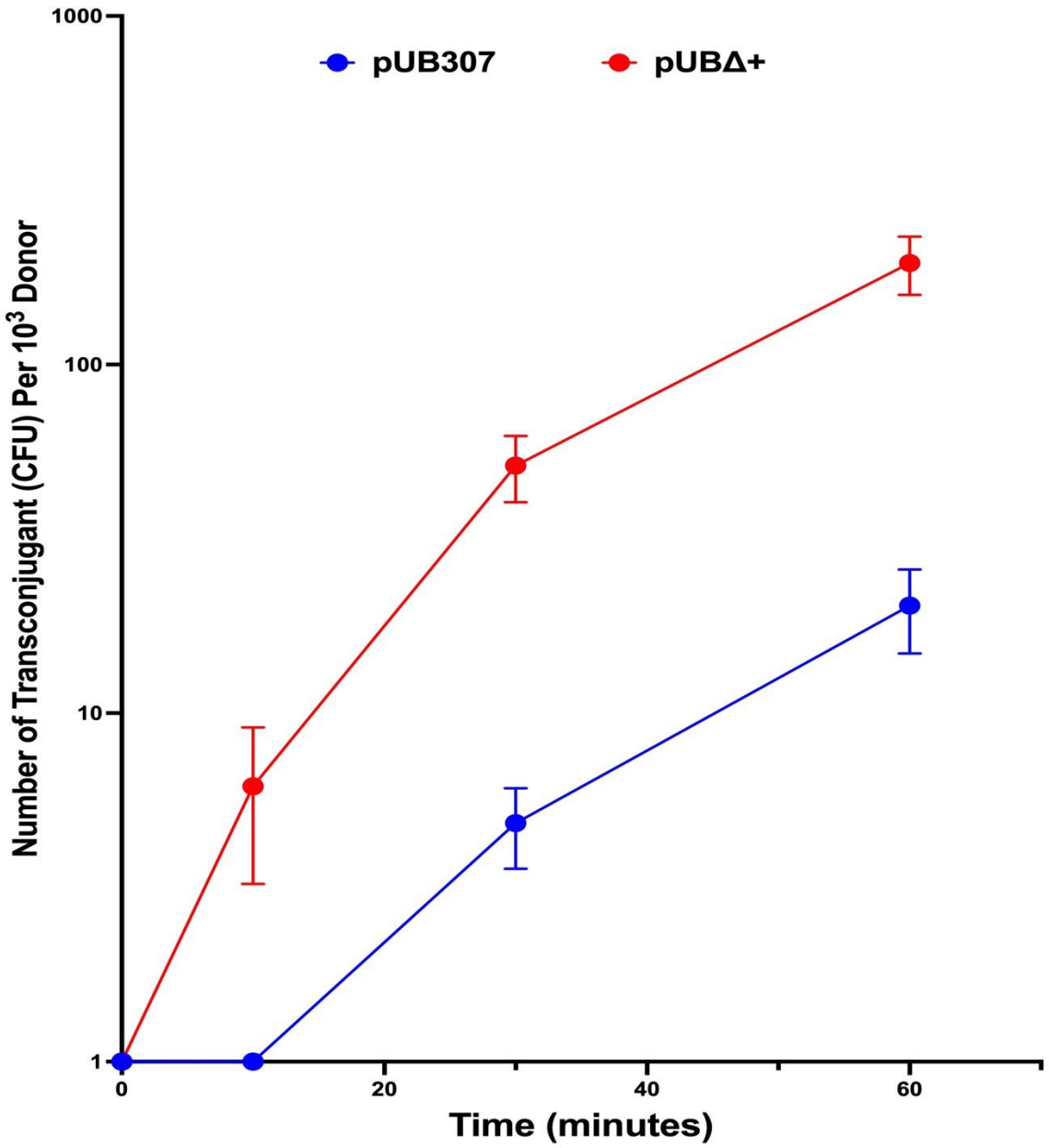

Figure 5.10 Transfer experiment for pUB307 and pUBΔ+ in the presence of R64.

This figure shows the increased transfer (reduced fertility inhibition resistance, FIR) of pUBΔ+ compared to pUB307 in the presence of the R64 plasmid.

5.3.2.3 The ability of pUBΔ+ to escape R388 inhibition.

A conjugative transfer experiment as shown in Figure 5.11, was done to investigate whether inserting *traG* with elevated expression in pUBΔ+ could confer resistance to R388 inhibition.

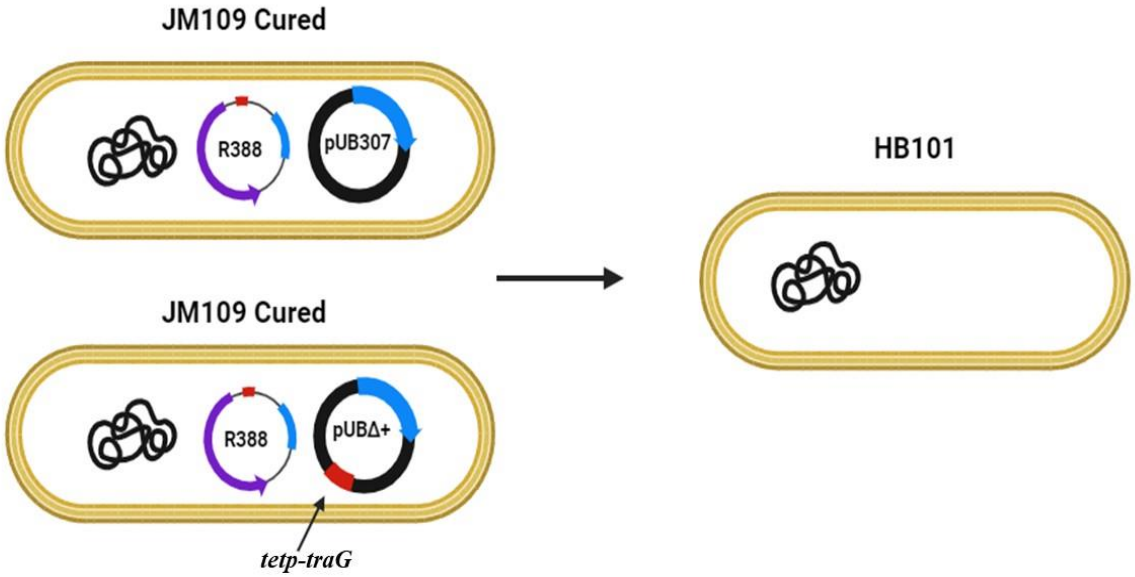

Figure 5.11 Transfer experiment to compare the transfer of pUB307 and pUBΔ+ in the presence of R388.

The primary goal of this experiment was to test pUBΔ+ ability to escape the inhibition caused by the R388 plasmid. Our hypothesis was that pUBΔ+ would demonstrate a more efficient transfer compared to the wild type pUB307.

Table 5.3 and Figure 5.12 show that the number of pUB307 transconjugants was undetectable at all time-points while the number of transconjugants of pUBΔ+ increased steadily from 10 to 60 minutes, demonstraing a statistically significant improvement of pUBΔ+ transfer in the presence of R388.

Table 5.3 Comparing the ability to resist the fertility inhibition (FIR) between pUB307 and pUBΔ+ in the presence of R388 plasmid

	pUB307		pUBΔ+		
Time (minutes)	**Mean**	**Standard deviation**	**Mean**	**Standard deviation**	**P value[b]**
10	**<1[a]**	**0**	**5.467**	**1.501**	**0.007**
30	**<1[a]**	**0**	**12.333**	**4.509**	**0.001**
60	**<1[a]**	**0**	**31.833**	**6.934**	**0.001**

a. Number <1 represents 0 colonies.

b. $p < 0.05$: Statistically significant $p < 0.01$: Highly statistically significant $p < 0.001$: Extremely statistically significant. Statistical significance determined using t-test in GraphPad.

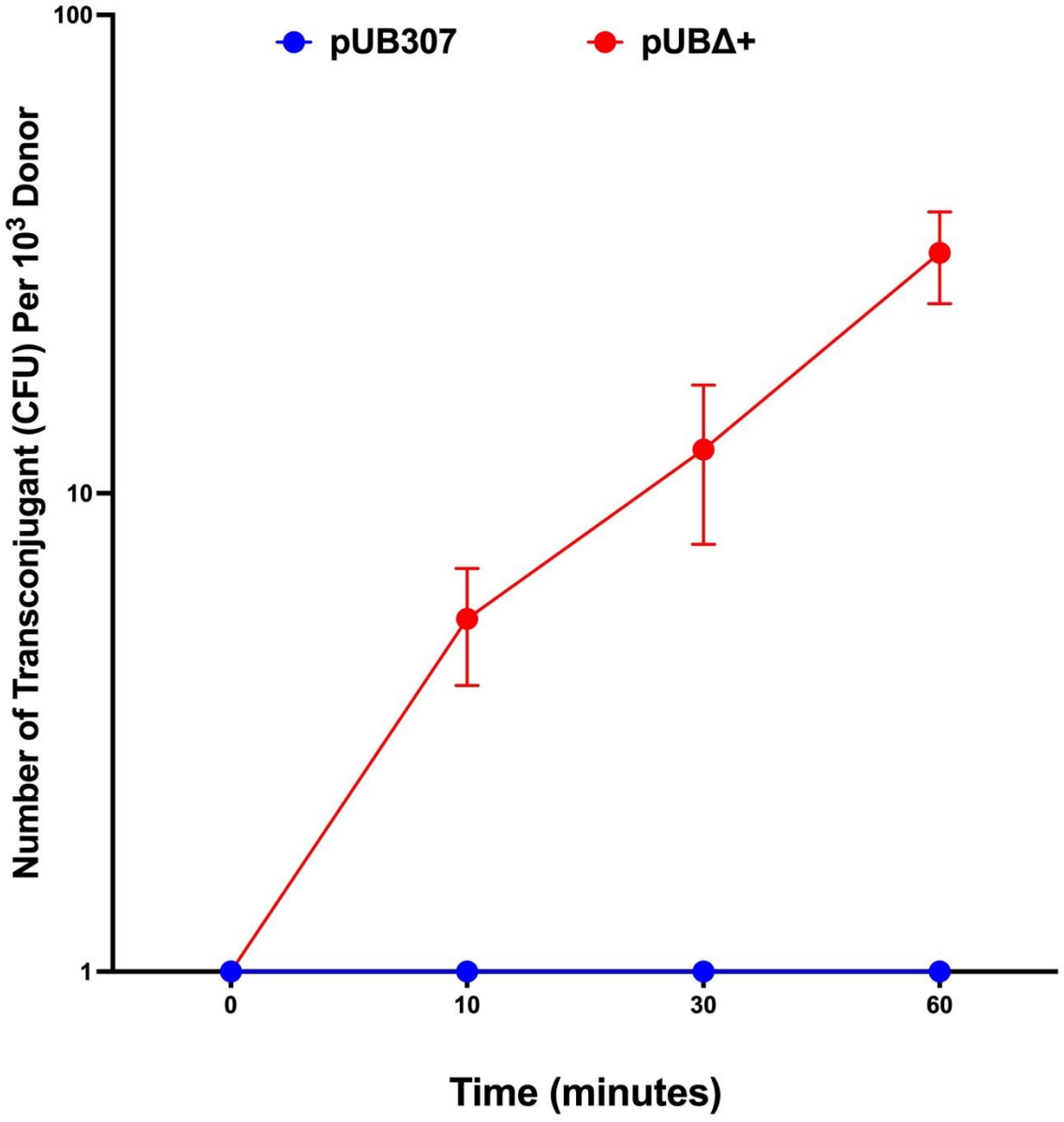

Figure 5.12 Transfer Experiment for pUB307 and pUBΔ+ in the presence of R388 plasmid.

This figure shows the increased transfer (reduced fertility inhibition resistance, FIR) of pUBΔ+ compared to pUB307 in the presence of the R388 plasmid.

5.3.3 Measuring *traG* gene expression in pUB307, pUBΔ+ and pACYC184-traG.

To assess *traG* gene expression in pUB307, pUBΔ+, and pACYC184-traG, a strategy involving introducing a histidine tag into *traG* was devised. The first phase of this strategy involved tagging *traG* within pACYC184-traG. This step aimed to assess its effectiveness in measuring *traG* expression. If successful, a similar approach would then be applied to pUB307 and pUBΔ+. The detection of expression would utilize Western blotting, with the methodology extensively described in Chapter Two, Section 2.21.4. The pACYC184-traG utilized in this experiment was constructed as part of this study, as detailed in Chapter Four, Section 4.3.5.

5.3.3.1 Site direct mutagenesis to tag TraG with a Hexa-histidine tail.

Two pACYC184-his-traG plasmids were constructed, the first being tagged at the *traG* N-terminus and the second one tagged at the C-terminus of *traG*. To introduce the His_6-tags into pACYC184-traG, primers were designed using SnapGene software to amplify the whole of pACYC184-traG, with the Histidine sequence positioned at the tail of the primers (as shown in Chapter 2 Table 2.6). The Site direct mutagenesis was done using PCR with Q5 polymerase under the following conditions. The annealing was done at 63°C and the extension at 72°C for three minutes, as recommended by the Q5 protocol of 30 seconds/kb, and the size of His tag pACYC-oriT-traG is 5769 bp. The PCR product was purified after separating the bands by gel electrophoresis as shown in Figure 5.13.

Figure 5.13 Electrophoretic analysis of PCR products after amplifying pACYC184-His-traG to insert a His6-tag at both the beginning and the end of the traG gene. "F" denotes tagging at the N-terminus of traG, while "R" denotes tagging at the C-terminus of traG.

The PCR product of pACYC184-His-traG was generated using site-directed mutagenesis with Q5 polymerase. The gel electrophoresis image displays bands which are not all consistent in mobility. Specifically, lanes 1 and 3 show a distinct band around 5769 bp, corresponding to the expected size of pACYC-oriT-traG, whereas the bands in lanes 2 and 4 run distinctly slower, indicating they may be larger than anticipated. Following amplification, the PCR products underwent purification to remove contaminants and impurities, ensuring their integrity and suitability for downstream applications. The purified PCR products were stored for future experimental use, facilitating further analyses and investigations.

The PCR product of pACYC184-His-*traG* was ligated overnight at room temperature in the presence of T4 Polynucleotide Kinase to phosphorylate the 5, ends. In order to confirm that the insertion was successful, the plasmid DNA was subjected to transformation and isolation processes. Afterward, it was sent for sequencing using primers for amplifying *traG* as shown in Chapter two Table 2.6. The results of the sequencing confirmed that pACYC184-traG has been tagged with the His_6-tail as illustrated in Figure 5.14.

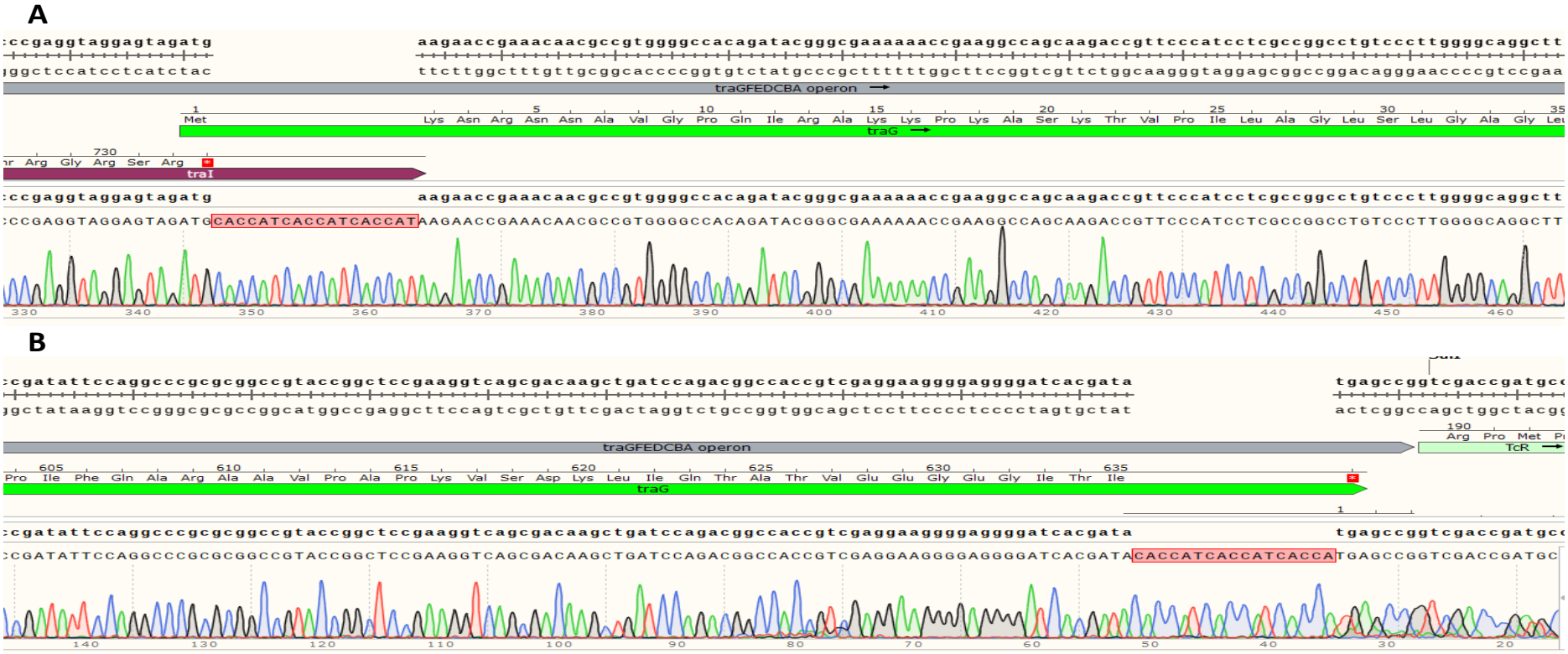

Figure 5.13 Alignment of sequencing from pACYC184-His-traG clones with the pACYC184-traG sequence.

Primers specifically designed to amplify the traG gene were utilized in this sequencing analysis. These primers enabled the precise targeting and amplification of the traG gene, ensuring accurate and efficient sequencing results.

A- The His_6 was tagged at the N-terminus of *traG* gene.

B- The His_6 was tagged at the C-terminus of *traG* gene

5.3.3.2 SDS-PAGE to check the protein.

It is important to isolate the protein from the strain DH5α that contains pACYC184 -His-*traG* for use in SDS-PAGE as well as western blotting. This will allow the evaluation of the protein quantity of the His-tagged TraG. The isolation process involved utilizing a sonication system to extract the protein sample as described in Chapter 2, Section 2.21.1. Overnight cultures of two samples of DH5α contain pACYC184-His-traG were prepared by inoculating fresh plates into 5ml of LB broth containing chloramphenicol (CM) as the selective antibiotic. The first strain contained pACYC-His-traG tagged at the N-terminus, while the second contained pACYC-His-traG tagged at the C-terminus. The next day, 500 µL of each culture was used to inoculate 50ml of LB broth medium in a 250ml conical flask (a 100-fold dilution). The cultures were incubated at 37°C with shaking at 200 rpm until they reached an OD 600nm of 0.6. A volume of 15 µL from a culture with an OD_{600} of 0.6 was mixed with 5 µL of 4X protein loading buffer. The mixture was placed on ice, and three sonication bursts, each lasting for 10 seconds, were employed. Samples were used for SDS-PAGE while the rest were stored at -20 °C. The SDS-PAGE was run using the protocol in Chapter Two, section 2.21, and the gel photo is shown in Figure 5.15.

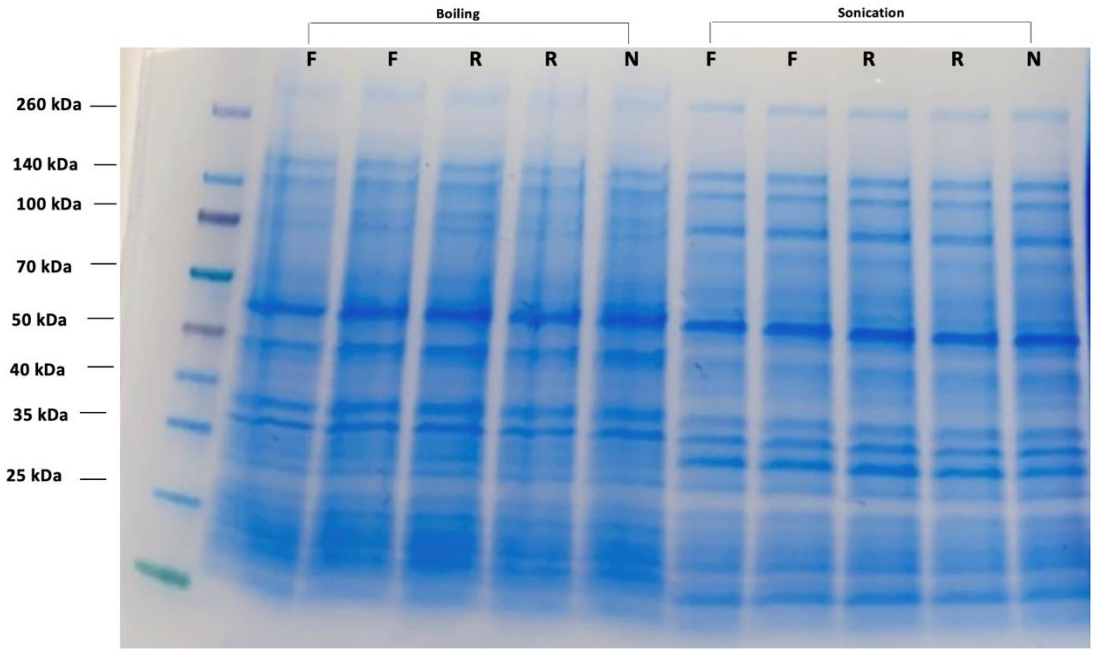

Figure 5.14 SDS-PAGE analysis of proteins from DH5α (pACYC184-His-traG).

The gel includes two samples of N-terminal tagged traG (F), two samples of C-terminal tagged traG (R), and one negative control sample (N). The negative control involved a version of TraG without any His tag. Proteins were extracted from each sample using two methods: boiling and sonication. The His-tagged proteins are expected to run at approximately 70 kD.

5.3.3.3 Western blotting to check the gene expression.

After the SDS-PAGE, Western Blotting was done using the procedure in Chapter two, Section 2.21.4. Proteins were transferred from the gel to a nitrocellulose membrane using the Trans-Blot Turbo Transfer System by Bio-Rad. The next step was to add the 6xHis monoclonal antibody (Clontech, Oxford, UK) primary antibody I added Goat Anti-Mouse IgG Antibody [HRP] (2BScientific, Oxfordshire, UK) as the secondary antibody to the blocking buffer (PBST) at a dilution ratio of 1:1000. This secondary antibody was used to detect the primary antibodies bound to the proteins on the Western blot membrane. To prepare the PBST blocking buffer, combine 5% skim milk powder with phosphate-buffered saline (PBS) in distilled water at a ratio of 1 tablet per 100 mL. Additionally, include 0.1% Tween 20 (Thermo-Fisher Scientific, Loughborough, UK) in the solution. The membrane

was washed in 20ml blocking buffer for 30 min. Then, the membrane was subjected to a washing process using PBST (Phosphate-Buffered Saline with Tween 20) washing buffer for 10 minutes, repeating the wash three times. The secondary antibody diluted in blocking buffer was added, and the membrane was incubated for three hours. The membrane was washed again to remove excess secondary antibodies, and the membrane was placed on a plastic surface with the protein side up. To image the membrane, a GE ImageQuant instrument was used and 2 ml of the activated ECL reagent (Thermo-Fisher Scientific, Loughborough, UK) was added to the membrane and incubated for 1 minute. The membrane was then placed on a tray and into the GE ImageQuant to image the proteins tagged with His_6, as depicted in Figure 5.16.

The SDS-PAGE and Western blotting procedures were repeated several times, producing consistent results. To verify the functionality of the Western system, the Western blotting procedure was repeated, utilizing a known His-tag protein as a positive control. The results depicted in the Figure 5.16 show a prominent band for the positive control, while no bands were observed for His-traG. One possible explanation for this consistency is that the expression of the *His-traG* might occur at levels below the detection point of Western blotting. To investigate this hypothesis, I decided to clone the *His_6-traG* gene into a pET28A high-expression plasmid.

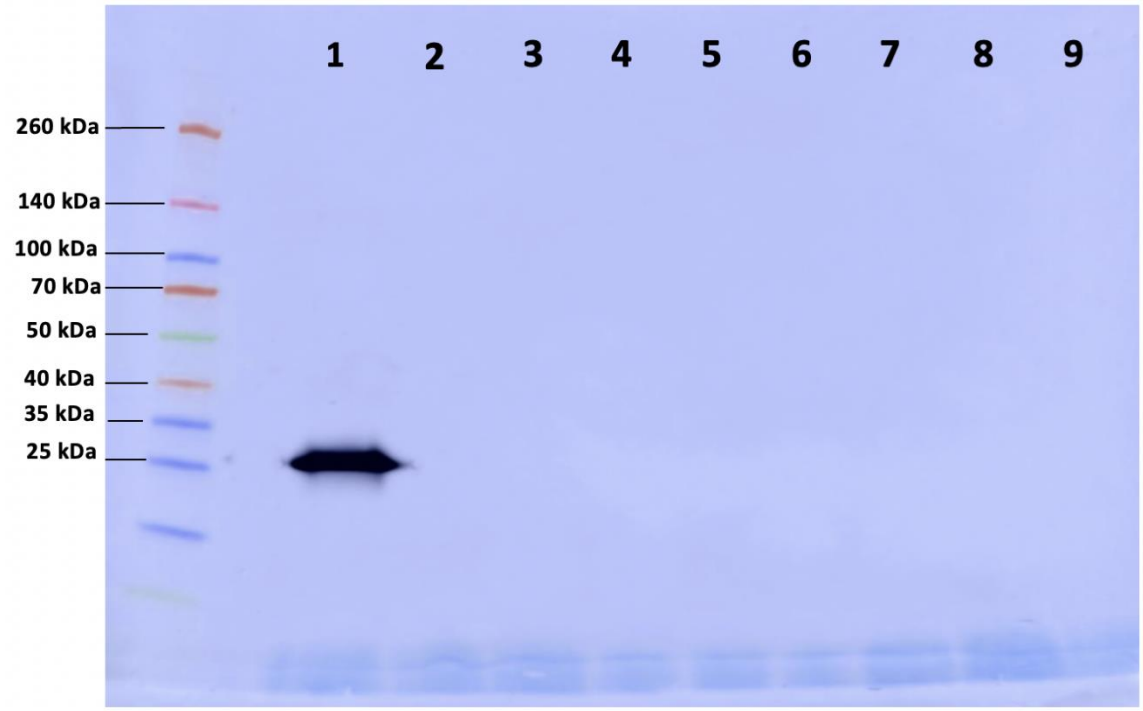

Figure 5.15 Western blotting to detect pACYC184-His-traG.

Sample 1: Positive control, containing His6-tagged Taq polymerase, to validate the efficacy of the Western blotting procedure. Samples 2 and 3: Negative controls, from bacteria containing only the empty vector, demonstrating absence of specific bands, thus verifying specificity of the antibody. Samples 4, 5, and 6: Bacteria with N-terminal tagged *traG* constructs. Samples 7, 8, and 9: Bacteria with C-terminal tagged *traG* constructs.

5.3.3.4 Cloning of His-*traG* into pET28A.

5.3.3.4.1 Amplifying *His-traG* gene from pACYC184- His-*traG* plasmid.

As described in the hypothesis, cloning the *His-traG* gene from pACYC184- His_6-*traG* plasmid into the pET28a expression vector was important to determine whether increasing the expression of the His_6-*traG* gene could facilitate the detection of this gene in Western blotting. To clone the His_6-*traG* gene, primers to amplify the His_6-*traG* from pACYC184-His_6-*traG* were designed with restriction sites for NcoI and NdeI using SnapGene software

(as shown in Chapter Two Table 2.6) and a gene map depicting pET28a before and after the insertion of the *His*$_6$-*traG* gene is presented in Figure 5.17. The *His*$_6$-*traG* was amplified using PCR with annealing at 59°C and then extension at 72°C for two minutes because the size of *His*$_6$-*traG* is 1987bp. The gene was purified after separating the bands by gel electrophoresis, as shown in Figure 5.18, and stored at -20°C for future work.

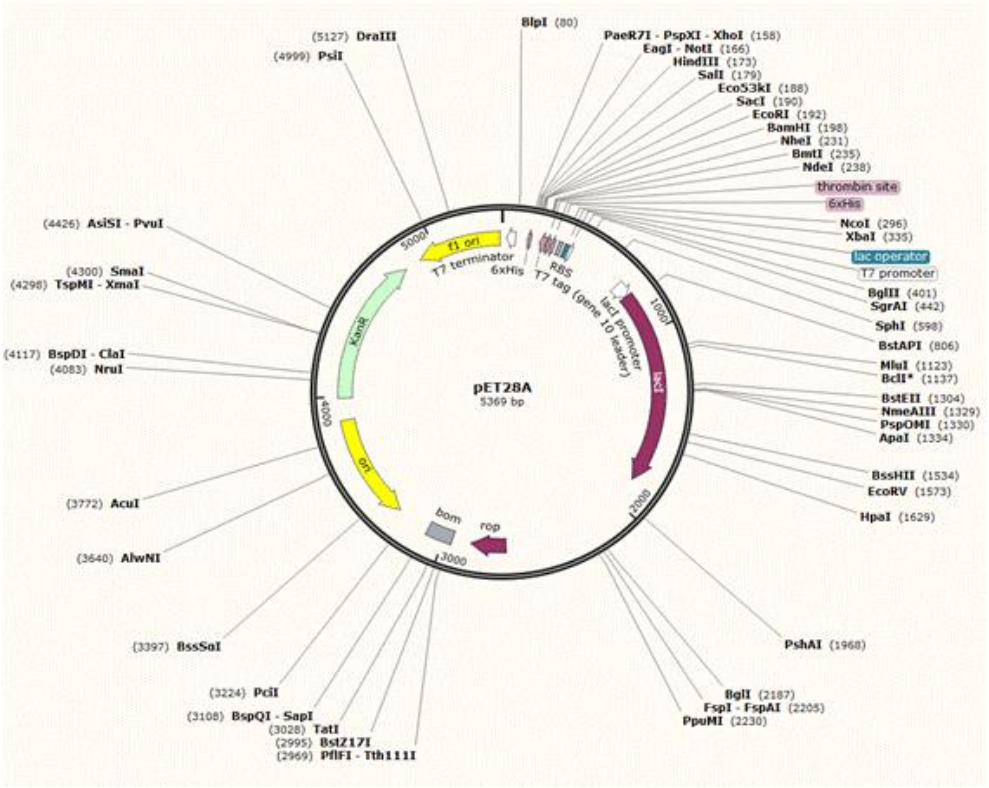

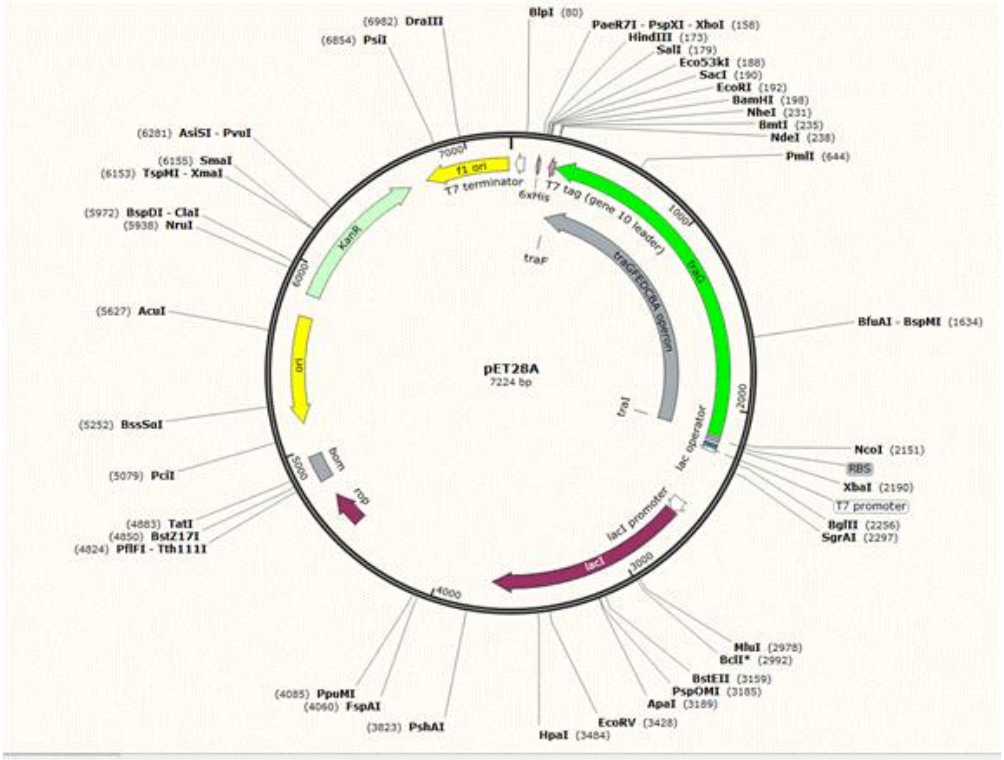

Figure 5.16 Gene map of the pET28a before and after the His$_6$-*traG* gene insertion.

The gene map provides a visual representation of the pET28a vector before and after cloning of the His6-traG gene fragment. Notable modifications in the gene map highlight the insertion of the His6-traG gene fragment within the vector, delineating the cloning process and illustrating the structural changes introduced into the vector during cloning.

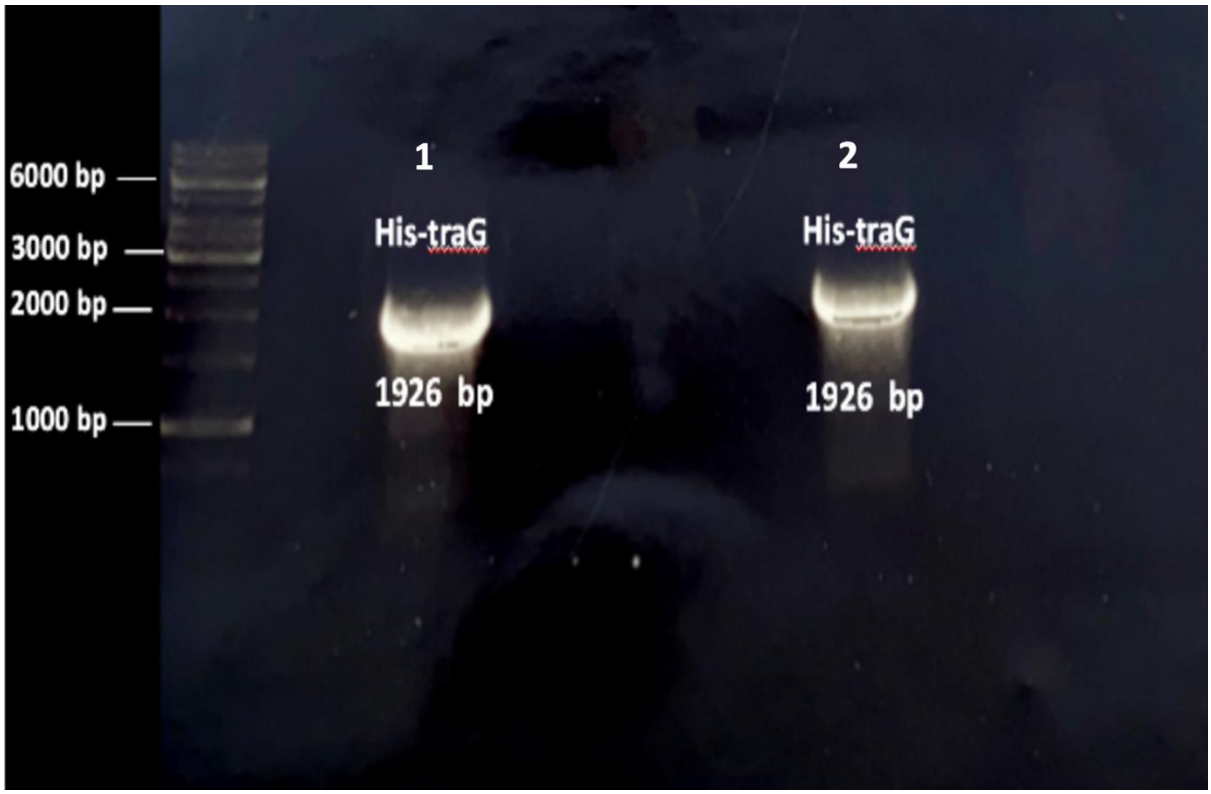

Figure 5.17 His$_6$-*traG* gene purified after separating by gel electrophoresis.

The PCR product of His$_6$-*traG* was generated using site-directed mutagenesis with Q5 polymerase. The gel electrophoresis image displays a distinct band in 1926 bp, corresponding to the expected size of His$_6$-*traG*.

5.3.3.4.2 Inserting the *His-traG* gene into the pET28a expression vector.

To insert the *His$_6$-traG* gene into pET28a, the purified *His$_6$-traG* gene and pET28a were digested with NcoI and NdeI restriction enzymes and ligated following the protocol in Chapter two sections 2.4 and 2.20. The plasmid DNA was then transformed and three transformant colonies were selected to be used in the SDS-PAGE and western blotting. A strain containing only the empty pET28a was employed as a negative control.

5.3.3.4.3 SDS-PAGE and western blotting to check expression of *His_6-traG* in pET28a.

Protein was isolated from samples as described in Chapter 2, Section 2.21.1. A volume of 15 µL from a strain sample with an OD_{600} of 0.6 was mixed with 5 µL of 4X protein loading buffer. The mixture was placed on ice, and three 10 second sonication bursts were employed. Samples were used for SDS-PAGE (Figure 5.15) and the rest were stored at -20°C.

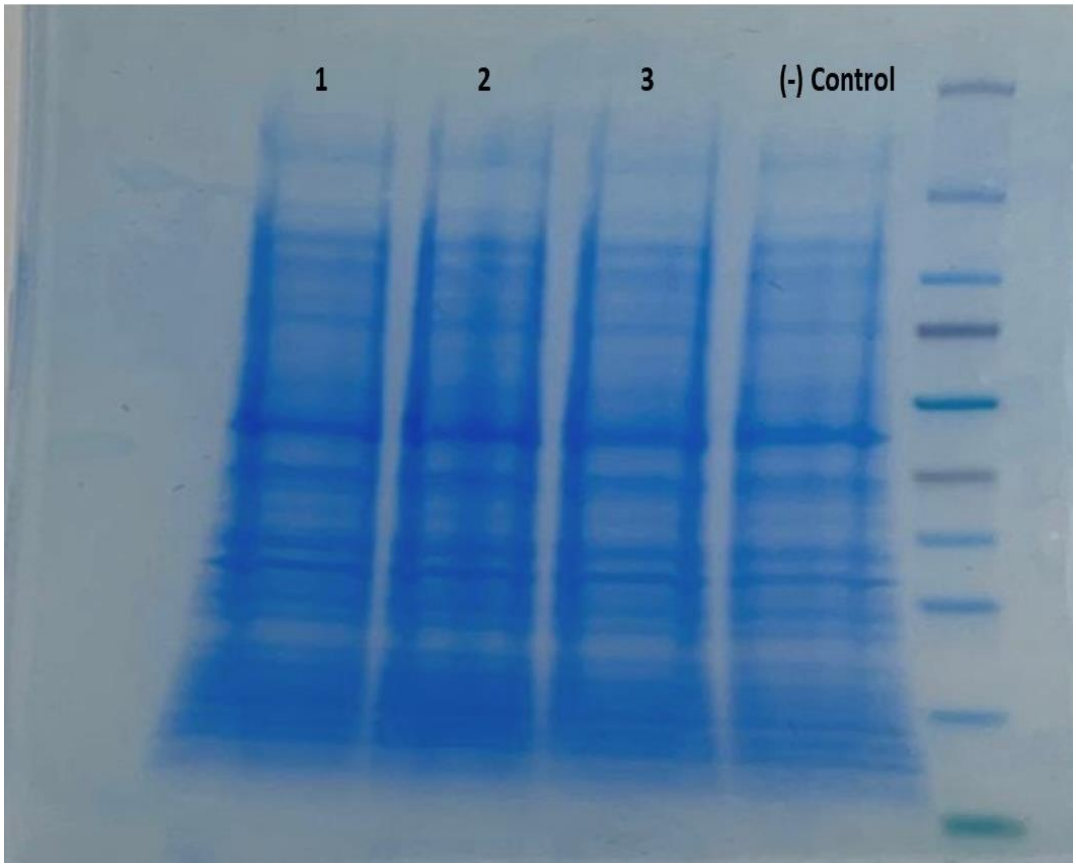

Figure 5.18 SDS-PAGE analysis of proteins from BL21(pET28a-His6-traG).

Samples were as follow: samples 1 and 2, N-terminal tagged *traG* variants; sample 3, C-terminal tagged *traG* variant; sample 4 is a negative control.

Following the SDS-PAGE, Western Blotting as described in Chapter two, Section 2.21.4 was employed, consistent with the methodology used in Section 5.3.3.3. Subsequently, the membrane was positioned on a tray and introduced

into the GE ImageQuant for protein imaging. The image in Figure 5.20 confirms the presence of His_6-*traG*. It was clear that *His_6-traG* in pET28a was detectable whether it was tagged at the N-terminus (F) or the C-terminus (R). This observation underscores and supports the earlier explanation that the challenge in detecting *His_6-traG* in pACYC184 was indeed due to its lower expression level.

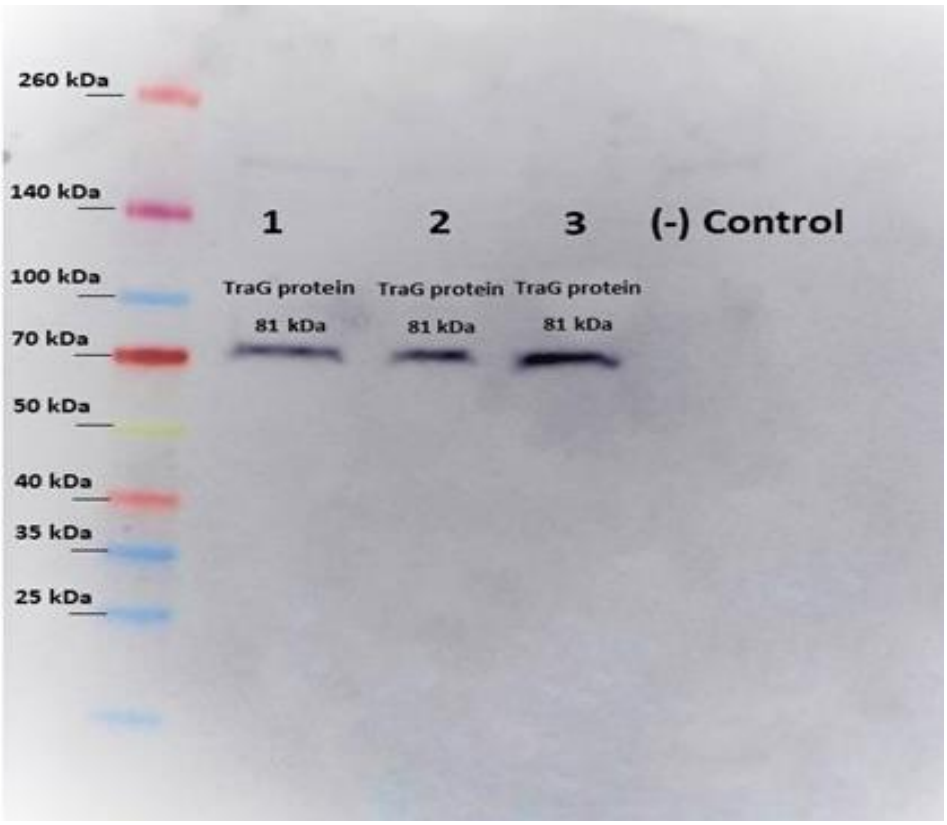

Figure 5.19 Western blotting of the gel shown in Figure 5.19.

Samples were as follow: samples 1 and 2, N-terminal tagged *traG* variants; sample 3, C-terminal tagged *traG* variant; sample 4 is a negative control.

5.3.4 Replacing *xylE* gene instead of *traG* to check the gene expression.

Due to the inability to determine the amount of *traG* expression in pACYC184-traG, conducting similar tests in pUB307 and pUBΔ+ was not meaningful. An alternative solution could be cloning the *xylE* reporter gene instead of *traG* in pACYC184-traG, pUB307 and pUBΔ+.

5.3.4.1 Inserting *xylE* instead of *traG* in pACYC184-traG.

To replace the *traG* ORF with the *xylE* ORF, primers to amplify the *xylE* gene from pGCMT1 plasmid but including the same sequences upstream and downstream of the start codon and stop codon as for *traG* were designed with restriction sites HindIII and XhoI using SnapGene software (as shown in Chapter two Table 2.6). A gene map of the pACYC184-traG before and after the *xylE* replacement was generated as shown in Figure 5.21 in order to facilitate the cloning of the *xylE* gene into pACYC184 plasmid instead of *traG*. The *xylE* gene was amplified using PCR with annealing at 60°C and the final extension at 72°C for 1 minute because the size of *xylE* is 924bp. The gene was purified after separating the bands by gel electrophoresis as shown in Figure 5.22 and stored at -20°C to use in future work.

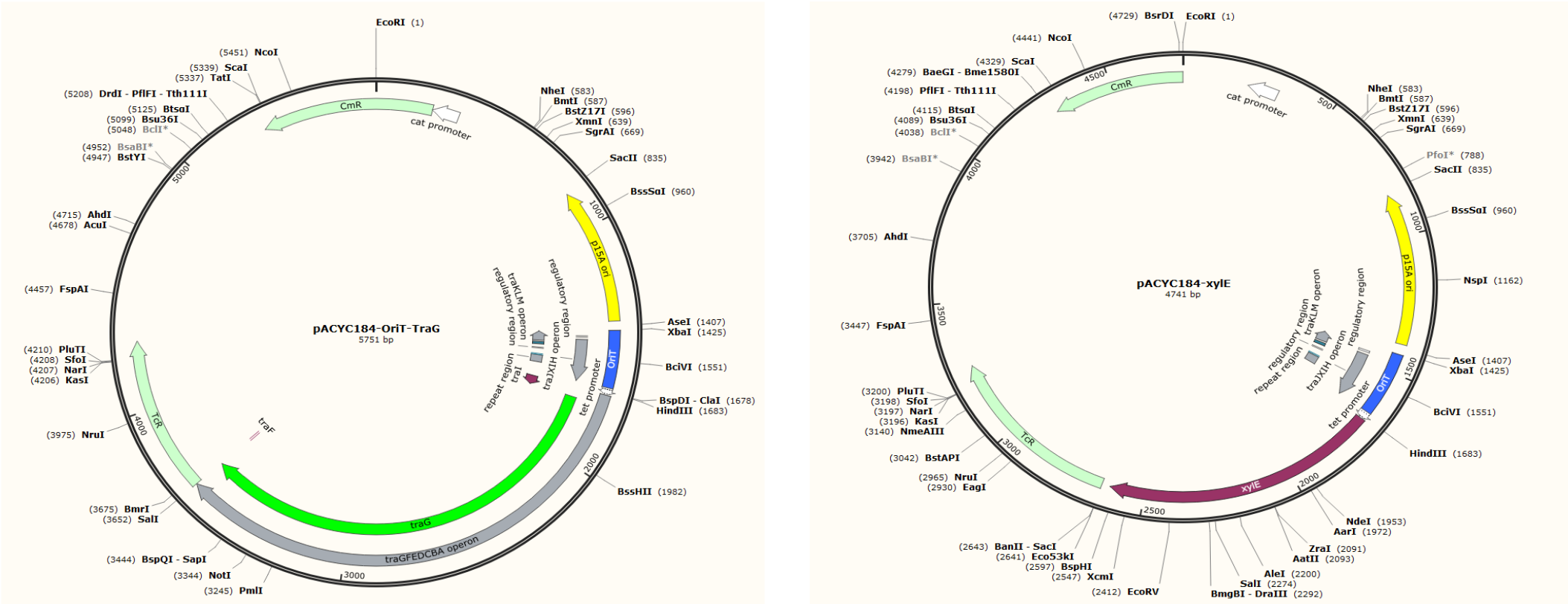

Figure 5.20 Gene map of the pACYC184-traG before and after the *xylE* insertion.

The gene map illustrates the pACYC184-traG vector both prior to and following the insertion of the xylE gene fragment. Key modifications are indicated, detailing the precise location of the xylE gene fragment within the vector. This map provides a visual representation of the cloning process, highlighting the structural changes that occur as a result of introducing the xylE gene fragment into the pACYC184-traG vector.

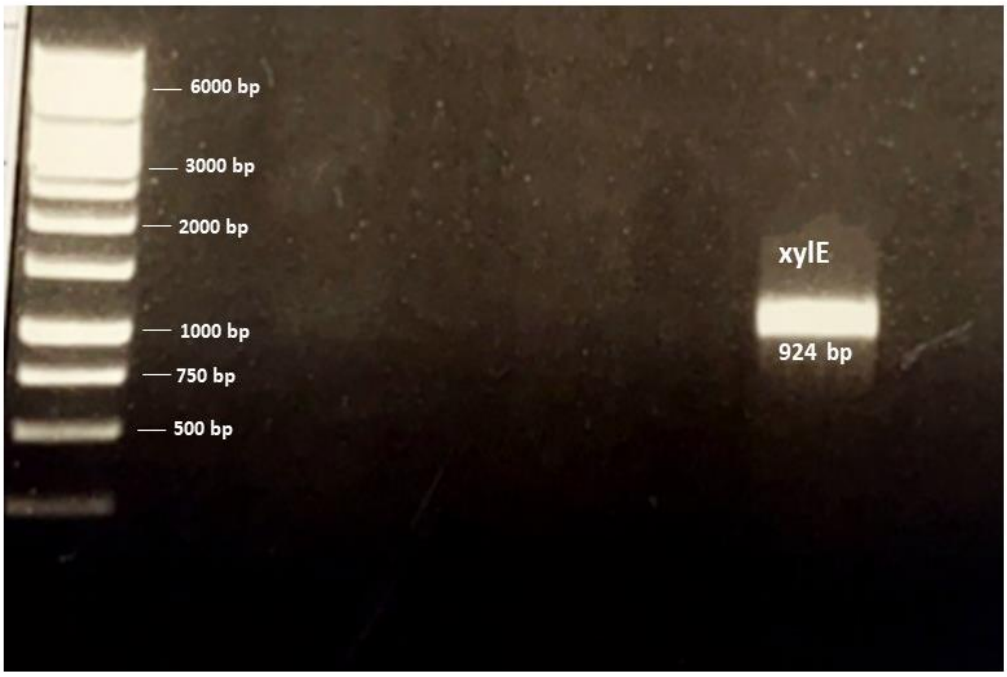

Figure 5.21 Gel electrophoresis of PCR product *xylE*.

The PCR product of *xylE* was subjected to gel electrophoresis, resulting in a distinct band observed at 924 bp. This band corresponds to the expected size of the *xylE* gene, confirming successful amplification of the target sequence.

To insert the *xylE* gene into the pACYC184 vector, the purified *xylE* gene was digested with HindIII and SalI restriction enzymes and the pACYC184-oriT-traG vector was digested with HindIII and XhoI for two hours at 37 °C. Subsequently, the digested fragments were ligated and transformed following the protocol in Chapter two sections 2.4 and 2.20. Plasmid DNA was isolated for the ten transformants and digested with HindIII and EcoRV, and then a gel was run to check the insertion (Figure 5.23.).

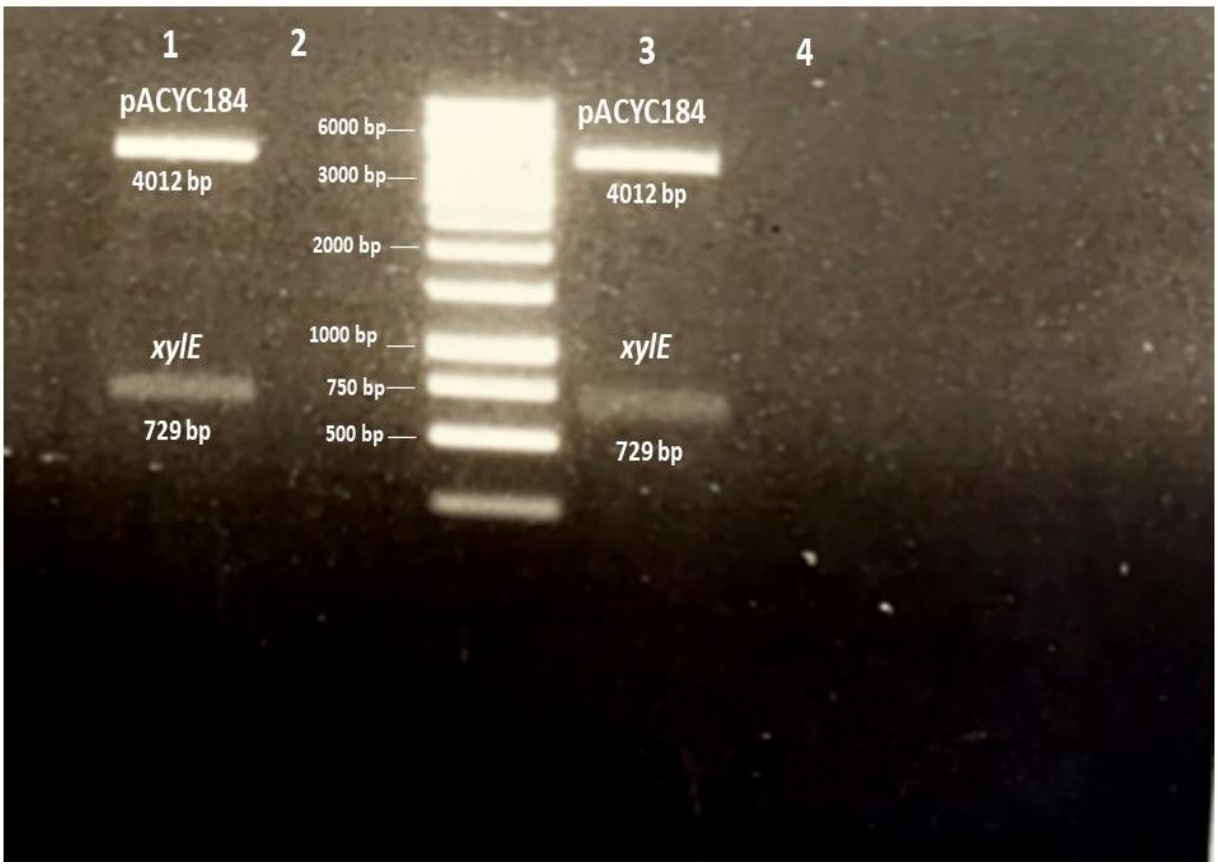

Figure 5.22 Gel electrophoresis of PCR product *xylE* gene inserted in the pACYC184 and digested with HindIII and EcoRV.

The gel electrophoresis analysis shows the PCR product of the *xylE* gene inserted into the pACYC184 vector and subsequently digested. The sizes of the pACYC184 vector and the *xylE* gene are noted to be 4012 bp and 729 bp, respectively. Distinct bands are observed on the gel, corresponding to the expected sizes of the digested fragments resulting from the insertion of the *xylE* gene into the pACYC184 vector. This analysis provides visual confirmation of successful gene insertion and digestion within the vector construct.

According to Figure 5.23, samples 1 and 3 contain the *xylE* gene. This can be observed from the appearance of a second band in the samples with a size of approximately 729 bp, which is the size of the *xylE* gene that digested with HindIII and EcoRV. The DNA of these strains was stored at -20°C for future use.

5.3.4.2 Replacing *xylE* gene instead of *traG* in pUB307.

Homologous recombination was employed to replace the *traG* ORF with the *xylE* ORF in pUB307, inserting *xylE* at the same genomic location where *traG* was originally situated. Primers were designed to create recombination homology arms specific to the target *traF* and *traI* in pUB307 with HindIII and XhoI restriction sites using SnapGene software (as shown in chapter two Table 2.6). A gene map of the pUB307 after the *xylE* insertion was generated (Figure 5.24). To initiate homologous recombination to insert *xylE* into pUB307, homology arms from pUB307 and *xylE* from pGCMT1 were amplified as shown in Figure 5.25 using PCR under the following conditions. The annealing was done at 59°C and the extension at 72°C for 1 minute because the size of *xylE* gene is 924bp. Subsequently, the individual homology arms were joined with *xylE* as shown in Figure 5.26 through SOEing PCR under the following conditions. The annealing was done at 59°C and the extension at 72°C for 2 minutes because the size of *xylE* flanked by the homology arms is 1900 bp

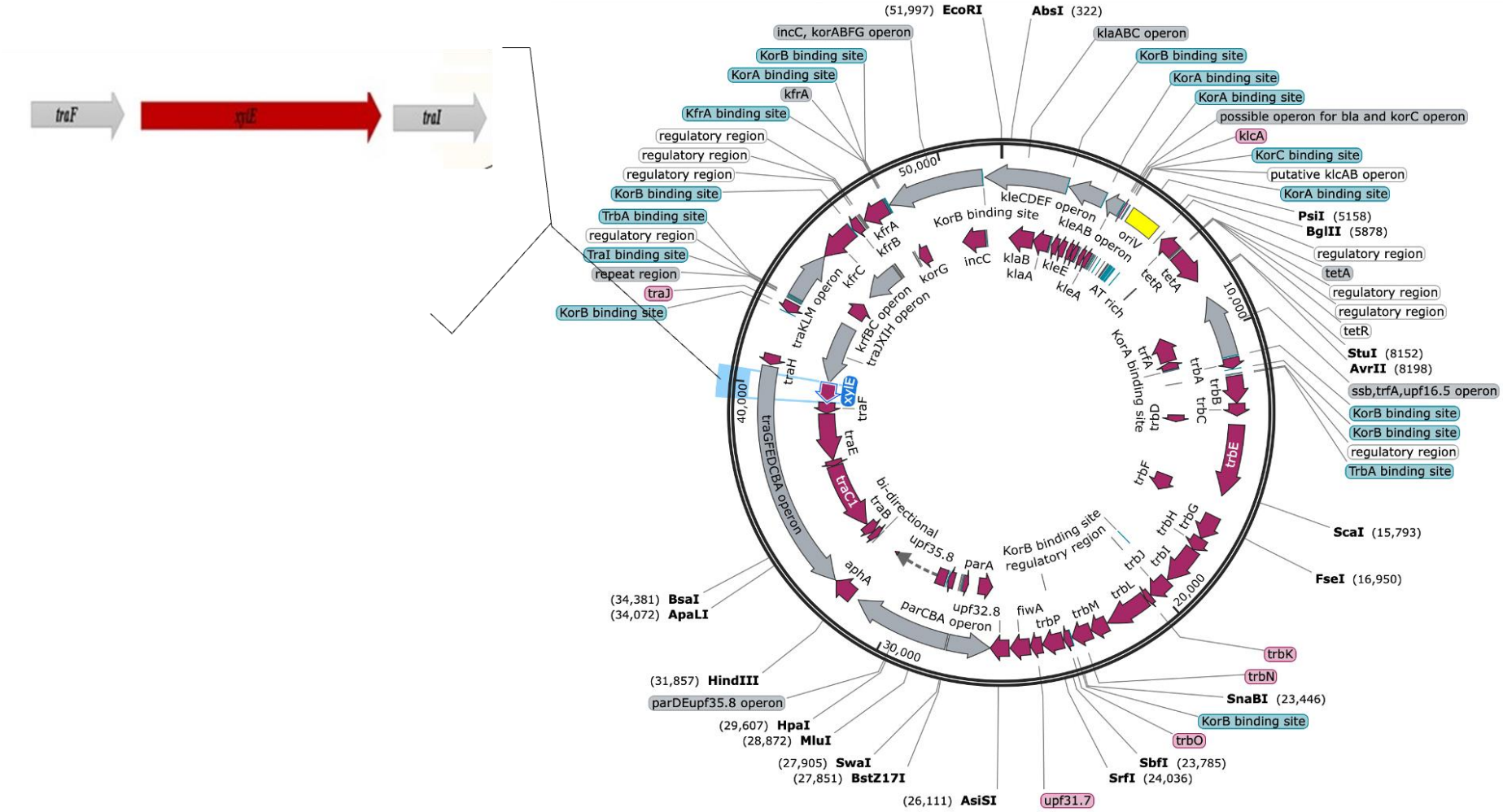

Figure 5.23. Map of pUB307 after the *xylE* replacement of *traG*.

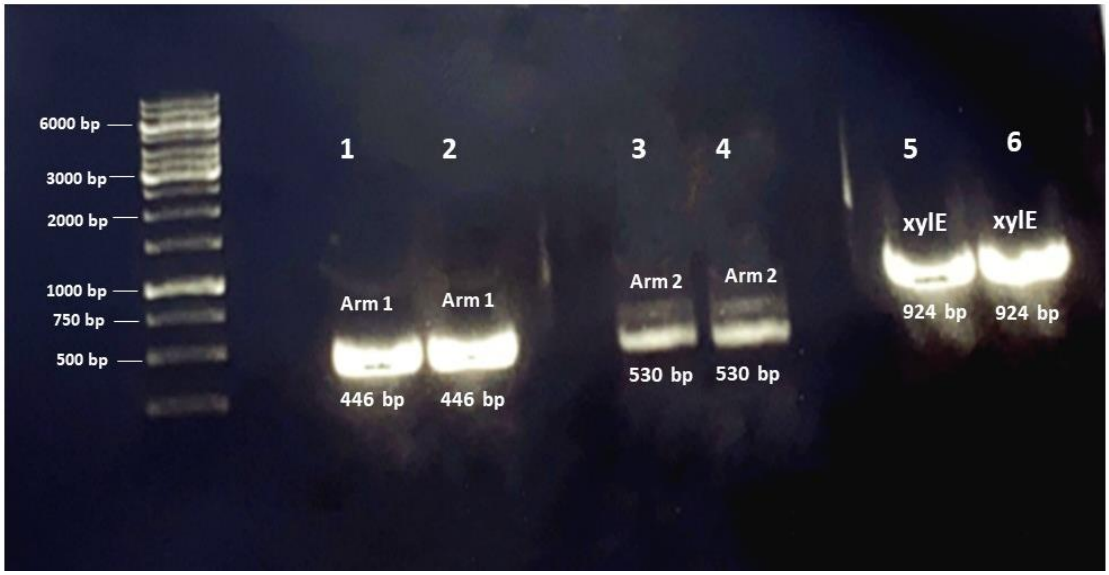

Figure 5.24 Gel electrophoresis of the PCR products of homology arm1, arm2 and *xylE* to insert *xylE* instead of *traG* in pUB307.

The gel shows distinct bands corresponding to PCR products of homology arm1 (446 bp), homology arm2 (530 bp), and xylE (924 bp) confirming successful amplification of these fragments.

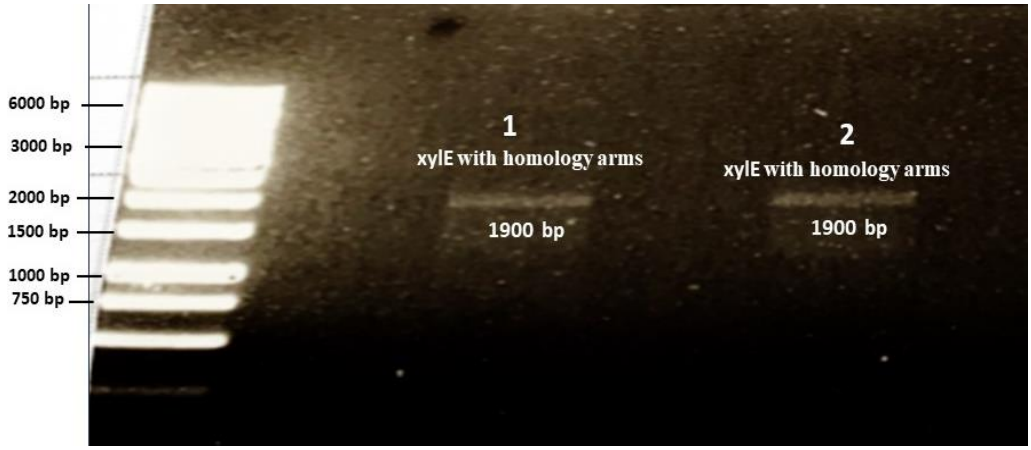

Figure 5.25 Gel electrophoresis of the PCR product of *xylE* and homology arms to insert *xylE* instead of *traG* in pUB307.

The gel reveals distinct bands corresponding to PCR products of *xylE* with homology arms, resulting in a size of 1900 bp confirming successful amplification of these fragments.

5.3.4.2.1 Inserting *xylE* with homology arms into pLAZ2 to generate a recombineering plasmid, enabling replacement of *xylE* for *traG* in pUB307.

To insert *xylE* with homology arms into pLAZ2, a Gene map of pLAZ2 before and after cloning the insertion was made, as shown in Figure 5.27. The product containing *xylE* with homology arms was digested with HindIII and XhoI, while was pLAZ2 was digested with HindIII and SalI for two hours at 37 °C. XhoI was chosen for digestion of the SOE'd PCR product due to the presence of a SalI site within the *xylE* gene sequence because it generates the same single stranded overhang as SalI. Subsequently, the digested fragments were ligated and transformed following the protocol in Chapter two sections 2.4 and 2.20. Plasmid DNA was isolated from ten transformants and digested with HindIII and SalI and analysed by gel electrophoresis (Figure 5.28). This analytical digest was chosen because the ligation between the XhoI-digested *xylE* with homology arms and SalI-digested pLAZ2 results in a junction that cannot be cleaved by either XhoI or SalI but the SalI site in *xylE* still allows this combination of enzymes to give a characteristic cleavage pattern.

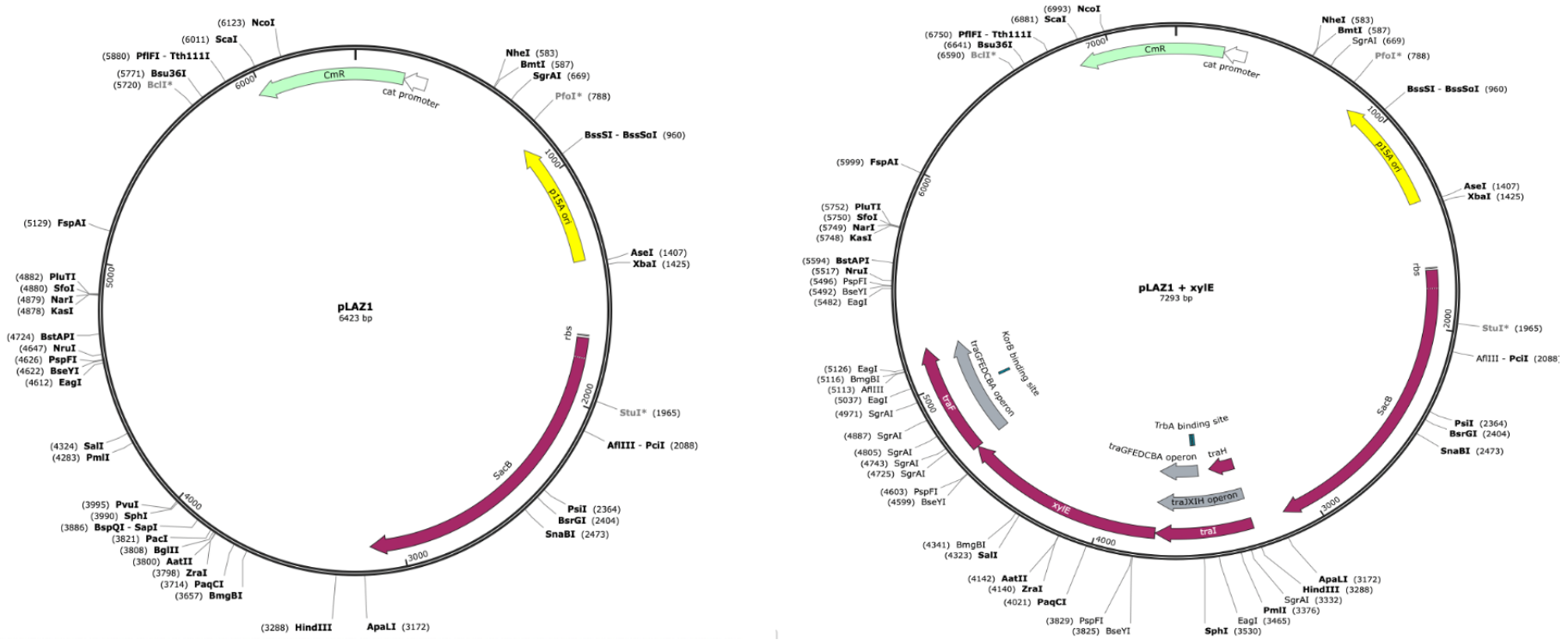

Figure 5.26 Map of pLAZ2 before and after cloning the *xylE* with homology arms to insert *xylE* instead of *traG* in pUB307.

Note that in pLAZ2 the HindIII site at 2946 and SalI site at 3982 are separated by 1036 bp while in the derivative the SalI site is now at 4319 thus giving an easily detactable change in size to 1337 bp.

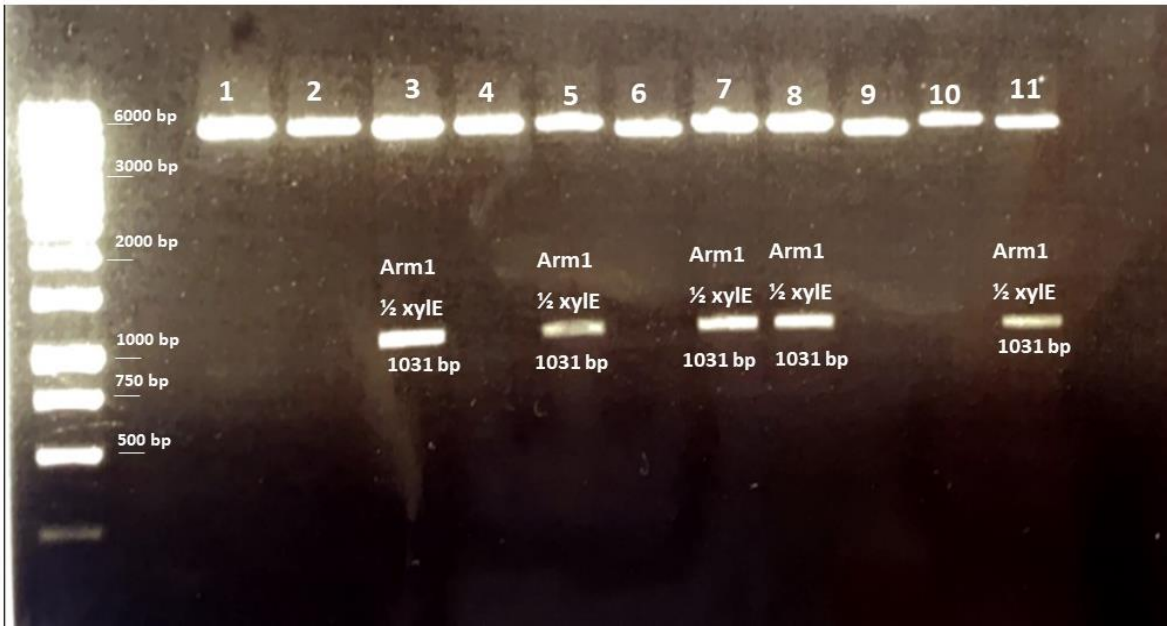

Figure 5.27 The pLAZ2 with *xylE* and homology arms digested with HindIII and SalI and analysed by gel electrophoresis.

The digestion of pLAZ2 containing *xylE* with homology arms using HindIII and SalI restriction enzymes should result in cleavage in the middle of the *xylE* gene and at the end of arm1, generating a fragment with a size of 1031 bp. As shown in Figure 5.28, samples 3, 5, 7, 8, and 11 give a fragment of the right size. The strains were stored at -20°C for future use.

5.3.4.2.2 Inserting *xylE* from recombineering pLAZ2-*xylE* with homology arms into pUB307 using homologous recombination.

To initiate homologous recombination aiming to insert *xylE* into pUB307, we employed the procedure outlined in Chapter two, Section 2.16. To identify potential insertions, PCR with outer primers corresponding to recombination homology arms (as detailed in Chapter two, Table 2.6) followed by gel electrophoresis was conducted to screen for colonies containing *xylE* as shown in Figure 5.29.

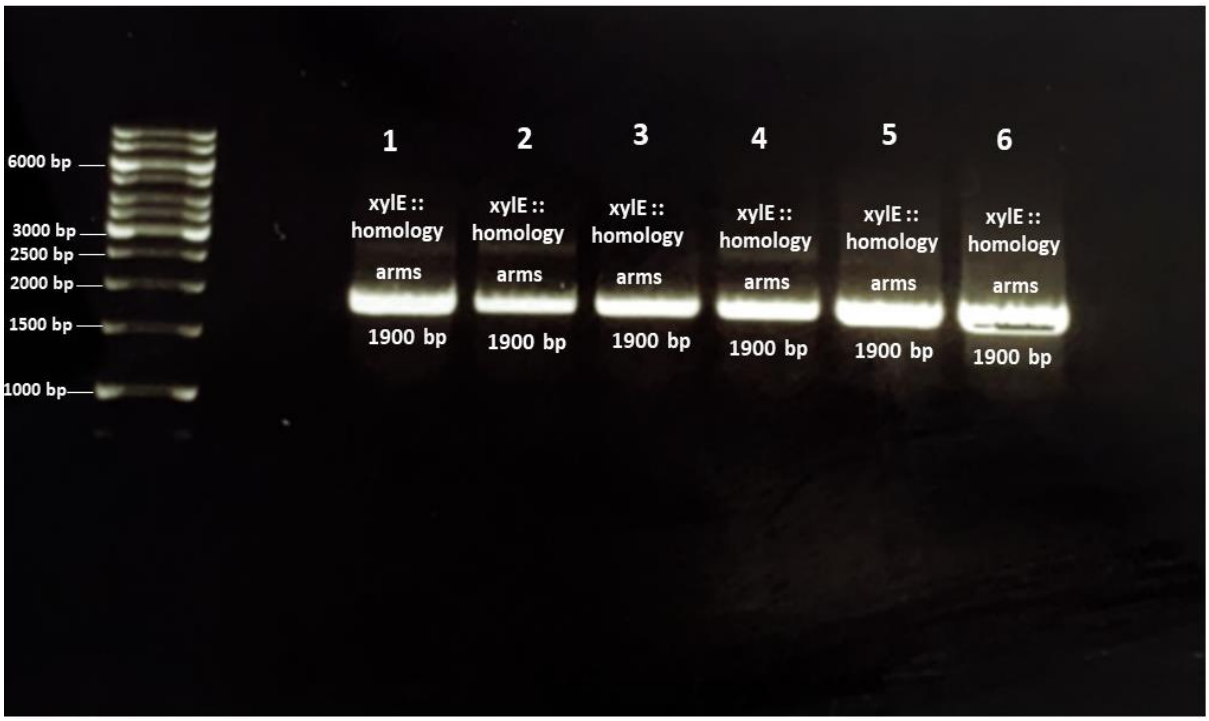

Figure 5.28 Gel electrophoresis of PCR products to check the insertion of *xylE* into pUB307.

All six samples appear to contain *xylE* based on a band of 1900 bp, corresponding to the size of *xylE* plus the homology arms. The strains were stored at -70°C for future use.

5.3.4.3. Replacing *tetp xylE* instead of *tetp traG* in pUBΔ+.

Homologous recombination was also used to integrate the *tetp-xylE* in place of *tetp-traG* within pUBΔ+, specifically at the genomic location where *tetp-traG* was reinserted in pUBΔ. Primers were designed to create recombination homology arms specific to the target *traM* and *kfrC* in pUBΔ+ with specific HindIII and XhoI restriction sites using SnapGene software (as shown in chapter two Table 2.6). A gene map of the pUBΔ+ after the *tetp-xylE* replacement has been generated is shown in Figure 5.30. Homology arms from pUBΔ+ and *xylE* from pGCMT1 were amplified as shows in Figure 5.31 using PCR with annealing at 59°C and extension at 72°C for 1 minute because the size of *xylE* gene is 924bp. Subsequently, the individual homology arms were joined with *xylE* as shown in Figure 5.32 by SOEing PCR with annealing at 59°C and extension at 72°C for 2 minutes because the size of *xylE* with the flanking homology arms is 2000 bp.

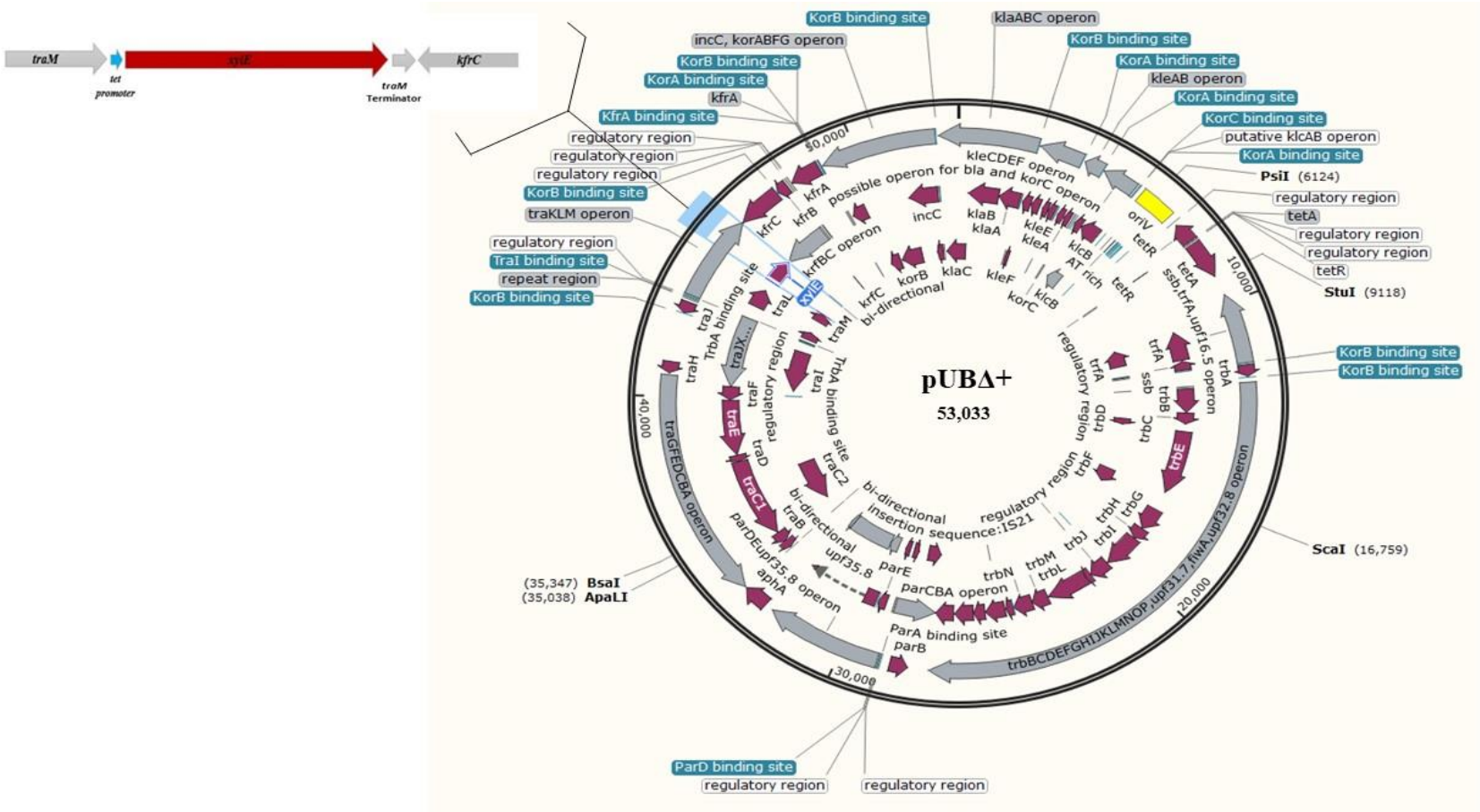

Figure 5.29 Gene map of pUBΔ+ after the *tetp-xylE* replacement.
The gene map illustrates the pUBΔ+ vector post-recombineering, where *xylE* replaces reinserted *traG*.

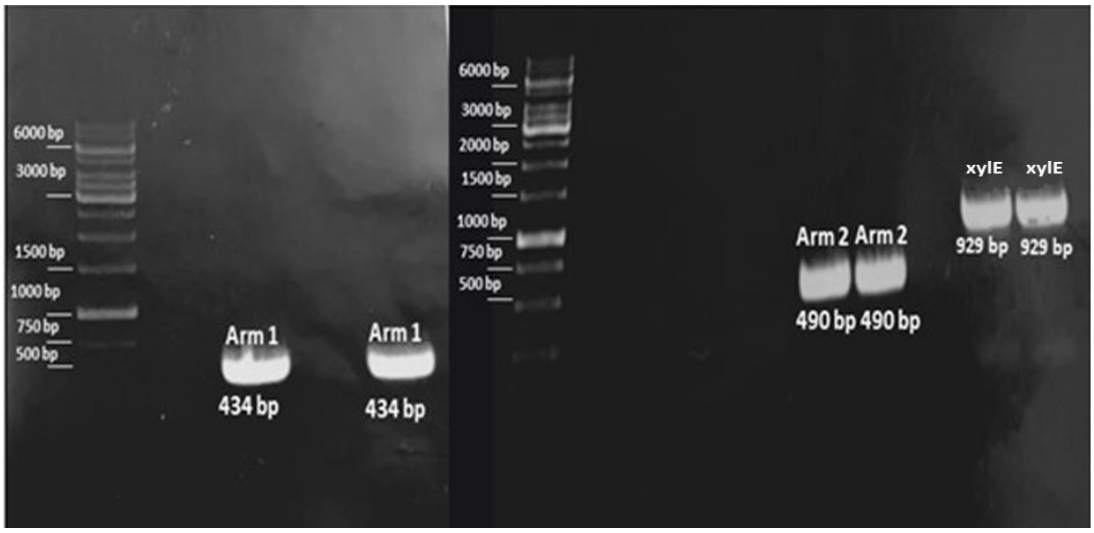

Figure 5.30 **Gel electrophoresis of PCR products corresponding to homology arm1, arm2, and *tetp-xylE*.**

Gel electrophoresis reveals distinct bands corresponding to PCR products of homology arm1 (434 bp), arm2 (490 bp), and Tetp-xylE (929 bp). The observed bands confirm successful amplification of these fragments, facilitating the characterization of genetic constructs.

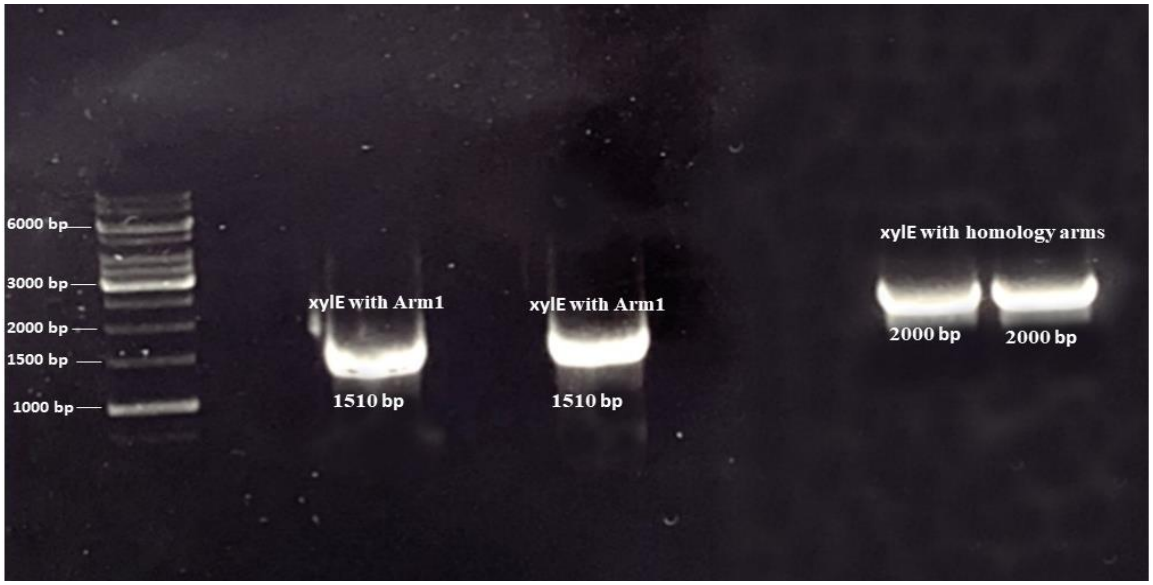

Figure 5.31 **Gel electrophoresis of the PCR products of *tetp-xylE* with homology arms to create a recombineering plasmid to insert *tetp-xylE* instead of *traG* in pUBΔ+.**

Gel electrophoresis reveals distinct bands corresponding to PCR products of *tetp-xylE* with homology arms, resulting in a size of 2000 bp confirming successful amplification of these fragments.

5.3.4.3.1 Inserting *tetp-xylE* with homology arms into pLAZ2 to generate a recombineering plasmid enabling the insertion of *tetp-xylE* for *traG* into pUBΔ+.

To insert the *tetp-xylE* with homology arms into the pLAZ2, a gene map before and after the insertion was made, as shown in Figure 5.33. The *tetp-xylE* with homology arms was digested with HindIII and XhoI and the pLAZ2 was digested with HindIII and SalI for two hours at 37°C. Subsequently, they were ligated and transformed using the protocol in Chapter two sections 2.4 and 2.20. Plasmid DNA was isolated from six transformants and digested with HindIII and SalI and analysed by gel electrophoresis (Figure 5.34).

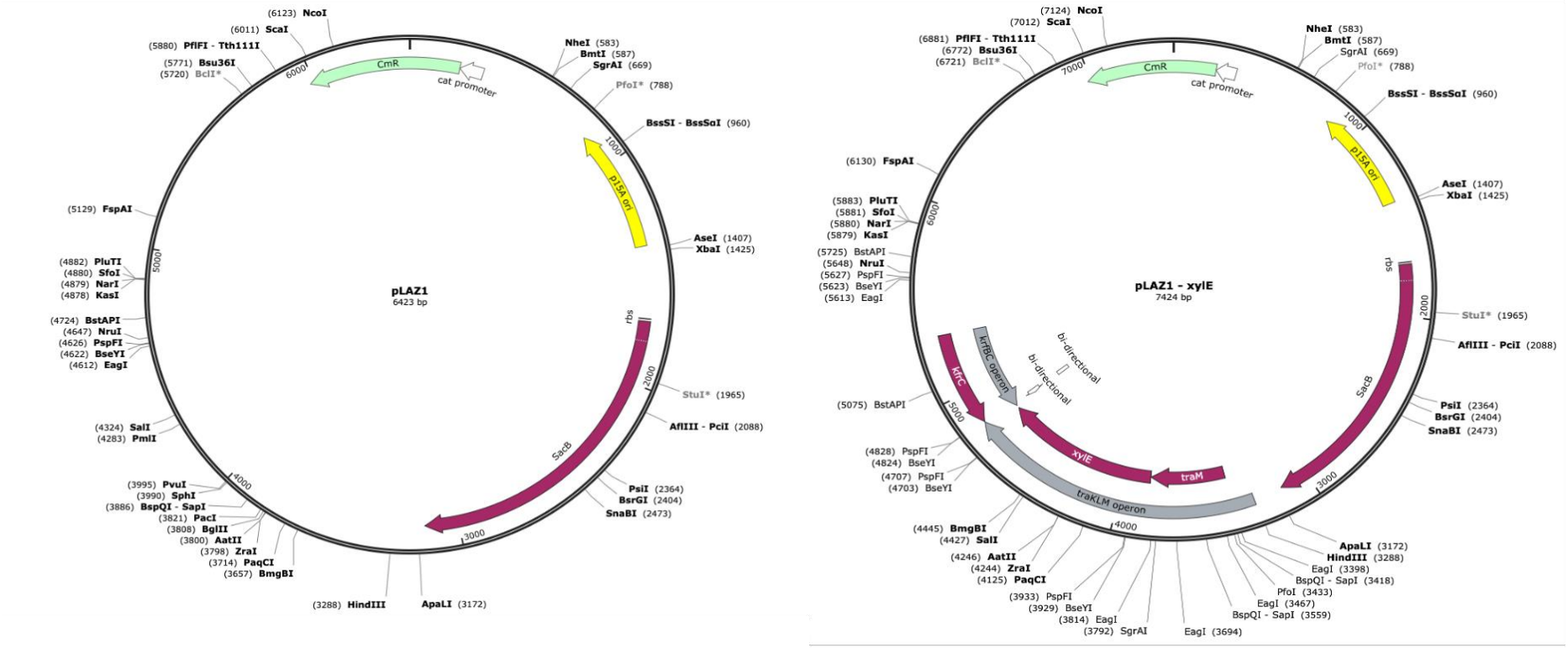

Figure 5.32 Gene map of pLAZ2 before and after cloning the tetp-xylE with homology arms to insert *xylE* instead of *traG* in pUBΔ+.

The gene map provides a visual representation of the pLAZ2 vector before and after cloning of the tetp-xylE gene fragment. Notable modifications in the gene map highlight the insertion of the *tetp-xylE* gene fragment within the vector, delineating the cloning process and illustrating the structural changes introduced into the vector during cloning.
`

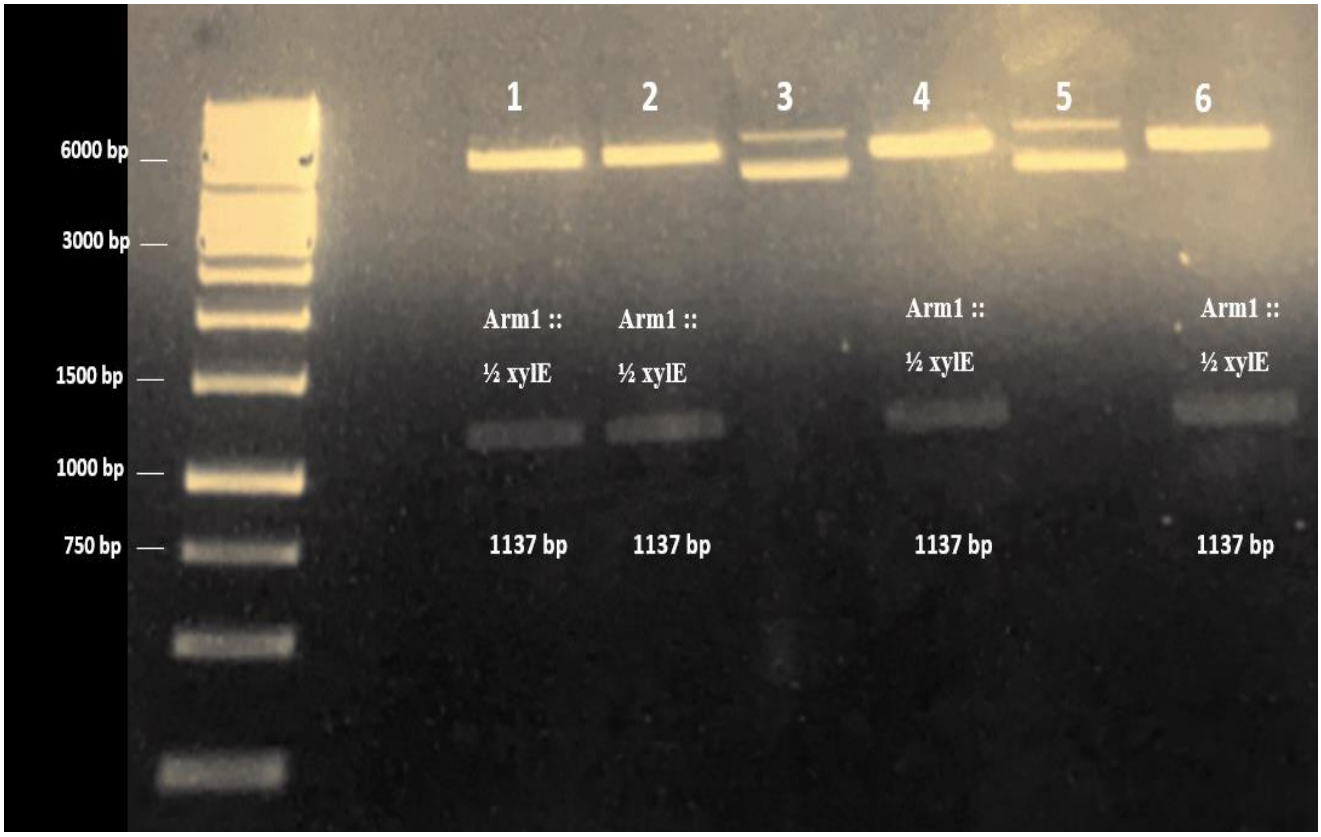

Figure 5.33 Electrophoretic analysis of clones of recombineering plasmid pLAZ2 with *tetp-xylE* and homology arms digested with HindIII and SalI.

The gel shows that samples 1, 2, 4, and 6 exhibit a band of about 1100 bp when digested with HindIII and SalI, consistent with the expected length of 1137 bp, corresponding to Homology Arm1 plus *tetp-xylE*,. The strains were stored at -70°C for future use.

5.3.4.3.2 Inserting *tetp-xylE* into pUBΔ+ using homologous recombination.

For homologous recombination to insert *tetp-xylE* into pUBΔtraG, the protocol in Chapter two Section 2.16 was utilized. To screen for potential insertion, PCR with recombination homology arms outer primers (as shown in chapter two, Table 2.6) was used to identify the colonies that had got *xylE* and gel was run to check the products as shown in figure 5.35.

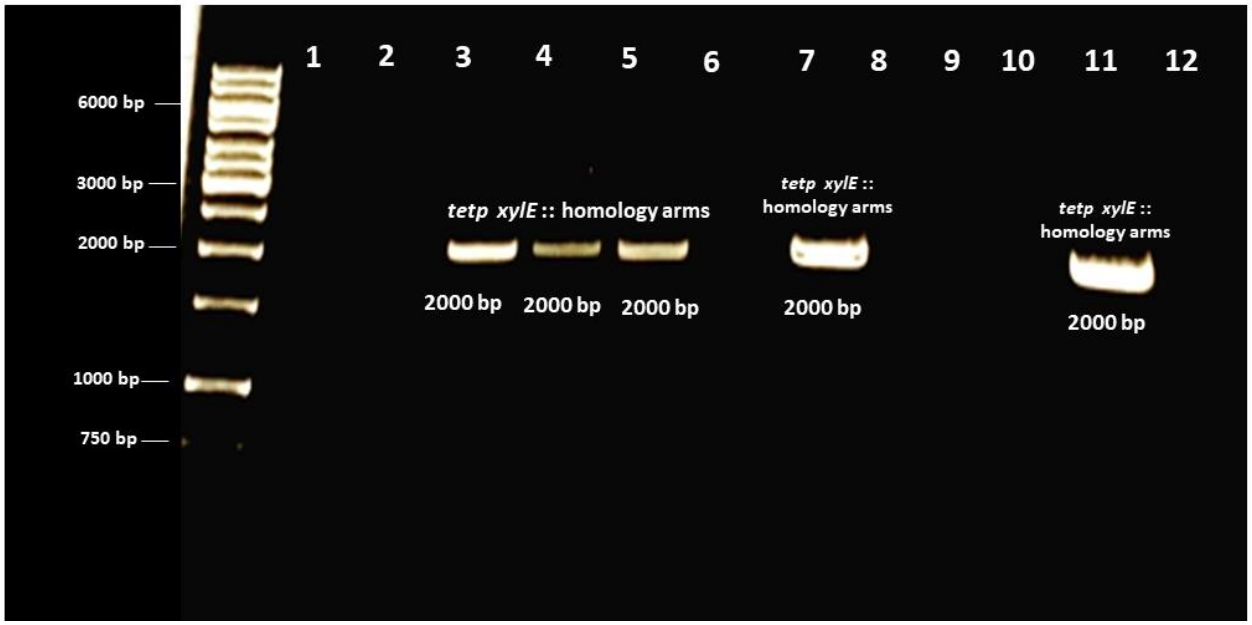

Figure 5.34 PCR product to check *tetp-xylE* insertion into pUBΔ+ running in an electrophoresis gel.

Samples 3, 4, 5, 7, and 11 apear to contain *tetp-xylE*, as evidenced by a band observed at 2000 bp. This band corresponds to the size of *xylE* plus the homology arm. The strains were stored at -70°C for future use.

5.3.5. The XylE assay to assess XylE protein activity.

The XylE assay is a biochemical assay used to measure the activity of the enzyme catechol 2,3-dioxygenase (XylE). This assay is commonly employed to assess the expression levels or activity of XylE, particularly in bacterial systems (Zukowski et al., 1983). The purpose of analysing XylE activity was to compare the expression of *xylE* when replacing *traG* in three different contexts: pUB307, pUBΔ+, and pACYC184-xylE. Additionally, the study investigated the influence of pUB307 on the *xylE* activity in recombineering plasmids pLAZ2-HA*traF-xylE*-HA*traI* and pLAZ2-HA*traM-xylE*-HA*kfrC*. The experimental proceedures followed the protocol outlined in Chapter Two, Section 2.17. Results from these assays are presented in Table 5.4 and Figure 5.36.

Table 5.4 Comparison of XylE activity[a] produced by the different strains constructed.

Plasmids in DH5α	Mean	SD	P value[b]
pUB307 :: *xylE* replacing *traG*	<0.1	0	0.008150
pUBΔ+ :: *tetp-xylE* replacing *tetp-traG*	3.367	1.159	
pACYC184 :: *tetp-xylE* replacing *tetp-traG*	7.106	0.711	0.008881
pLAZ *traI-xylE-traF*	4.917	0.682	0.00748
pLAZ *traI-xylE-traF* with pUB307	2.870	0.191	
pLAZ *traM-tetp-xylE-kfrC*	8.607	0.842	0.0560
pLAZ *traM-tetp-xylE-kfrC* with pUB307	7.083	0.519	

a. Units of the XylE assay is: micromoles of substrate converted per minute per milligram of protein (µmol/min/mg protein).
b. $p < 0.05$: Statistically significant $p < 0.01$: Highly statistically significant $p < 0.001$: Extremely statistically significant. Statistical significance determined using t-test in GraphPad.

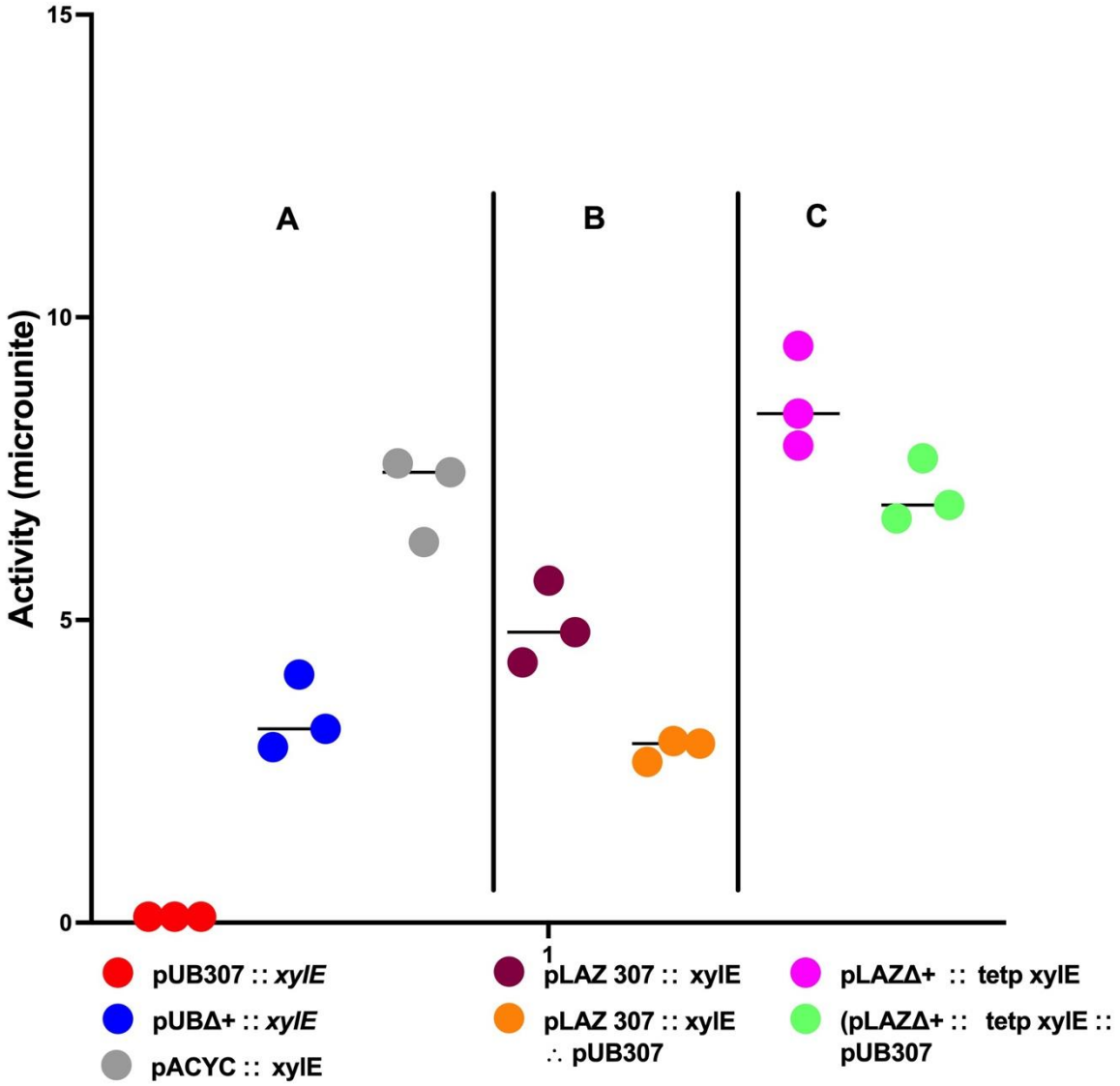

Figure 5.35 Comparison of *xylE* activity as a proxy for *traG* expression in the various contexts studied in this Thesis as shown in Table 5.4.

A. Expression in the three key contexts. Expression of *xylE*: integrated downstream of *traG*p in pUB307 (red dots); downstream of *tet*p in pUBΔ+ (blue dots); and downstream of *tet*p in pACYC184-xylE (grey dots).
B. Testing influence of trans-acting IncP functions (predicted TrbA) on *traG*p activity. Expression of *xylE* from *traG*p in pLAZ2*traI-xylE-traF* in the absence (brown dots) and presence (orange dots) of pUB307.
C. Testing influence of *trans*-acting IncP functions on *tet*p activity. Expression of *xylE* from *tet*p in pLAZ2*traM-tetp-xylE-kfrC* in the absence (magenta dots) and presence (green dots) of pUB307.

To validate that the absence of detectable XylE protein activity from pUB307 is not due to a deficiency in the sequence of the pUB307-xylE gene, sequencing was conducted. The same sample of pUB307 used in the XylE protein activity experiment was subjected to PCR amplification of the *xylE* gene, followed by sequencing. As shown in Figure 5.37, the sequencing results confirm the presence of a fully correct *xylE* gene in pUB307, consistent with the earlier confirmation presented in Figure 5.29 within this chapter

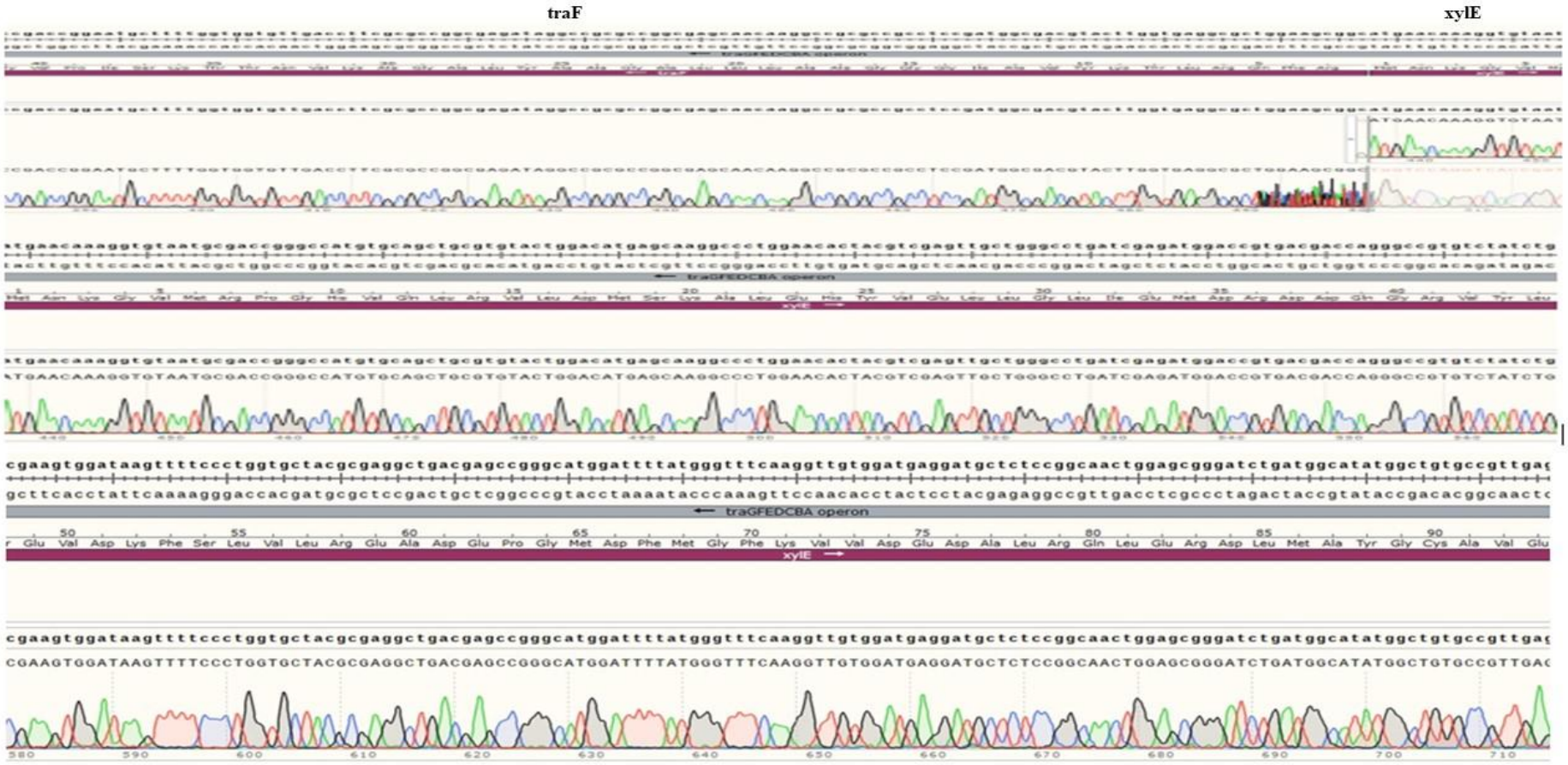

Figure 5.36 sequencing alignment of *xylE* gene with pUB307::xylE.

The pUB307 sample used for the XylE protein activity experiment was also subjected to PCR amplification and sequencing of the xylE gene. The sequencing results shown in this figure confirm that the xylE gene is fully intact within the pUB307 plasmid. This confirmation aligns with the earlier verification presented in Figure 5.29 of this chapter. Detailed sequence analysis reaffirmed the integrity and completeness of the xylE gene within the pUB307 plasmid, providing strong evidence of its correctness.

5.4 Discussion

The primary aim of this study was to address the fertility inhibition (FIR) challenge associated with pCURE plasmids, building upon earlier findings suggesting that F plasmids in the gut might hinder transfer. To achieve this, we focused on enhancing *traG* expression by strategically inserting *tetp-traG* within the *traKLM* transcriptional unit, just before the terminator following *traM*. This placement was chosen to avoid unintended overexpression of other transfer genes due to read-through from the upstream *tetp* promoter.

Our findings validated that the modified pCURE plasmid, with increased *traG* expression, effectively circumvents inhibition from F plasmids. This deliberate intervention not only demonstrates the potential for broad applicability but also ensures the integrity and core functionality of plasmid transferability. The precise insertion site of *tetp-traG* was critical, underscoring the importance of strategic genetic modifications.

5.4.1. Testing the capability of the pCURE plasmid with *tetp-traG* to escape different sources of inhibition.

The primary aim of this study was to address the fertility inhibition (FIR) challenge associated with pCURE plasmids, building upon earlier findings suggesting that F plasmids in the gut hight population in the gut (Getino et al., 2017), and it is able to inhibit transfer the transfer of numbers of plasmids incompatibility groups (Stephens et al., 2020). To achieve this, we focused on enhancing *traG* expression by strategically inserting *tetp-traG* within the *traKLM* transcriptional unit, just before the terminator following *traM*. This placement was chosen to avoid unintended overexpression of other transfer genes due to read-through from the upstream tetp promoter.

Our findings validated that the modified pCURE plasmid, with increased traG expression, effectively circumvents inhibition from F plasmids. This deliberate intervention not only demonstrates the potential for broad applicability but also ensures the integrity and core functionality of plasmid transferability. The precise insertion site of *tetp-traG* was critical, underscoring the importance of strategic genetic modifications.

5.4.2. Measuring *traG* gene expression in pUB307, pUBΔ+, and pACYC184-traG through the introduction of a Histidine tag.

To confirm the previous results and the hypothesis of this chapter, it was imperative to quantify the expression of the *traG* gene in pUB307, pUBΔ+, and pACYC184-*traG*, confirming a rise in pUBΔ+ in contrast to pUB307 and an increase in pACYC184-*traG* compared to both. The measurement of *traG* gene expression involved tagging *traG* with His_6, as detailed in the results of this chapter, Section 5.3.3.3. Only pACYC184-*traG* was initially tagged as a test case to assess the feasibility of measuring *traG* expression. If successful, the same protocol would be applied to the remaining plasmids.

However, upon tagging *traG* in pACYC184, we faced challenges in detecting *traG* in the western blotting. One possible explanation is that the expression of *traG* in pACYC184 may not be sufficient for the antibody detection. In other words, *traG* expression was not detected due to limited expression levels. Therefore, the tagging of pUBΔ+ and pUB307 was considered less than ideal, as their expression levels are expected to be lower than *traG* in pACYC184.

The process began with an attempt to evaluate the expression of *traG* in the pACYC184 plasmid. However, the absence of any observable bands corresponding to His-traG in western blotting, despite a clear band in the positive control, led us to suspect that the low expression of His-traG in pACYC184 might be the cause. To investigate this possibility, we cloned the His-traG gene from the pACYC184-His6-traG plasmid into the pET28a expression vector, which features the T7 promoter, a tightly regulated promoter. This approach aimed to determine whether increasing the expression of His-traG in pET28a could make it detectable in Western blotting analyses.

After replicating the Western blotting protocol utilized for pACYC184-His6-traG, this time with His-traG in pET28a, the results indicated detectable expression of His-traG in pET28a, as illustrated in Figure 5.20. This suggests that the expression level of His-TraG was indeed enhanced by cloning it into the pET28a vector, confirming our hypothesis regarding the low expression of His-traG in pACYC184.This finding serves as evidence that supports the hypothesis proposing that the level of *traG* expression in pACYC184 was undetectable by this method. An alternative approach for assessing *traG* expression is evaluating XylE protein activity.

5.4.2.1 The Xyle assay to assess *xylE* expression in pUB307, pUBΔ+, and pACYC184-xylE.

An alternative approach for assessing *traG* expression involved replacing the *xylE* gene for *traG* in pUB307, pUBΔ+, and pACYC184, followed by evaluating XylE protein activity in each case. The results showed that XylE activity in pUB307-xylE was undetectable, while it registered at 3.367 in pUBΔ+ :: xylE. This difference was statistically significant, as indicated in Table 5.4. and Figure 5.36. This finding supports the understanding of why

pUBΔ+ can overcome F inhibition while pUB307 cannot. The ability to overcome inhibition in pUBΔ+ is attributed to the increased expression of *traG*.

Furthermore, comparing pUBΔ+ activity with pACYC184-xylE which was statistically highly significant as shown in Table 5.5 and Figure 5.36, explains the ability of pACYC184-*traG* to escape pGBT30-*pifC* inhibition due to its high expression, in contrast to pUBΔ+ which, despite escaping F inhibition, fails to evade pGBT30-*pifC*. In conclusion, the variation in *traG* expression among pUB307, pUBΔ+, and pACYC184 plays a pivotal role in their ability to overcome F inhibition. In simpler terms, higher *traG* expression gives greater resistance to fertility inhibition. However, careful consideration should be given to the extent of *traG* expression increase, as excessively high expression may have a negative effect, counteracting its positive impact.

5.4.2.2 The effect of pUB307 on the *xylE* expression in recombineering plasmids pLAZ2 *traF-xylE-traI* and pLAZ2 *traM-xylE-kfrC*.

The results indicate that the presence of pUB307 leads to a statistically significant reduction in the expression of *xylE* in pLAZ2*traF-xylE-traI* with XylE activity being reduced from 4.917 down to 2.870 in the presence of pUB307 (Table 5.4). Conversely, the reduction in XylE activity for pLAZ2*traM-xylE-kfrC* from 8.607 to 7.083 upon the addition of pUBΔ307 was not statistically significant (Table 5.4). A plausible explanation for this is that in the presence of pUB307, TrbA represses the *traG* promoter, leading to decreased expression. In pLAZ2*traF-xylE-traI*, the *traF* homology arm contains the *traG* promoter. However, in pLAZ2*traM-xylE-kfrC, traG* is accompanied by the *tet*-promoter, which is not regulated by the TrbA repressor in pUB307.

This finding aligns with Zatyka et al., 1994 study, which concluded that the *traG* promoter is not repressed by relaxosome proteins but experiences repression from TrbA, encoded at the beginning of the *trb* operon encompassing the remaining transfer genes (Zatyka et al., 1994).

5.4.3 Highlights the potential significance of developing a targeted mutation in *traG*.

The exploration of developing a targeted mutation in *traG* to overcome *pifC* inhibition offers a promising opportunity to improve the performance of the pCURE system. Central to the success of this endeavor is the identification of the TraG-PifC interaction region that underlies fertility inhibition. This task requires a combination of protein structure modeling techniques and experimental validation of protein-protein interactions, serving as essential tools in pinpointing these critical regions.

Structural modeling of TraG and PifC can provide insights into their three-dimensional architecture and potential binding interfaces. Utilizing advanced computational approaches, such as AlphaFold, can predict the detailed structures of TraG and PifC with high accuracy, potentially identifying crucial interaction sites. Following these predictions, molecular docking simulations can be employed to further explore the potential binding interfaces between TraG and PifC. Subsequent experimental validation of these predicted interactions through techniques like co-immunoprecipitation assays or surface plasmon resonance can confirm the accuracy of the modeled complexes.

Once the crucial interaction regions are identified, targeted mutagenesis of TraG can be performed to disrupt these interactions while preserving essential functionality in plasmid transfer. This approach increases the likelihood of obtaining the desired mutant capable of

evading F inhibition and effectively performing its intended functional role within the CURE system.

In conclusion, this study demonstrates a significant advancement in the development of a CURE system by addressing the fertility inhibition challenge associated with pCURE plasmids. By strategically enhancing *traG* expression, we have overcome barriers to plasmid transfer and paved the way for more effective treatments for bacterial infections. While we developed tools and constructs aimed at exploring the molecular interactions between PifC and TraG, further research is required to fully elucidate these interactions. Nevertheless, our findings hold promise for the future of pCURE systems, offering a comprehensive solution with broad applicability and the potential to combat antibiotic resistance and improve patient outcomes.

Chapter 6: Discussion and Future Works

6.1 General comments

In recent years, microbial antibiotic resistance has emerged as a highly critical concern. The increase in microbial resistance over the recent years is a direct result of the widespread use of antibiotics for various purposes, including medical applications, agriculture, and other contexts (Bennett, 2008). Addressing the worldwide challenge of antibiotic resistance needs decisive measures, including the exploration and development of alternative therapies to antibiotics. One proposed strategy involves tackling multidrug-resistant infections by displacing the resistance plasmid from the bacteria that show resistance (Czaplewski et al., 2016b).

This Ph.D. thesis revolves around the notion of antimicrobial resistance plasmid curing through incompatibility, aiming to create effective technology to displace the antibiotic resistance plasmid from bacterial strains. The primary objective is to enable the curing plasmid pCURE-F-307 to transfer without being suppressed by other plasmids. This could enhance opportunity of the treatment options for antimicrobial resistance infections and to reduce the ongoing spread of the antimicrobial resistance plasmids.

The effectiveness of plasmid incompatibility in displacing IncF plasmids from host cells was demonstrated through the application of the pCURE2 curing plasmid (Hale et al., 2010). The subsequent development of this approach to get an efficient curing plasmid led to the generation of pCURE-K, pCURE-F-RK2, and pCURE-F-307 (Lazdins et al., 2020). In this study pCURE-F-307 was the focus of my research.

6.2 Discussion of key conclusions

6.2.1 Checking the fertility inhibition phenotype of plasmid F against RK2.

Before evaluating the impact of the F effect on RK2, it was important to examine various donor-to-recipient ratios for RK2 conjugative transfer to establish a standardized approach applicable to all transfer experiments in this study.

The efficiency of transfer showed differences across the three ratios examined in this investigation. The experiment was carried out by keeping the number of donors constant and increasing the number of recipients. The most favourable donor-to-recipient ratio as described in Chapter 3 section 3.3.1 was 1:10, followed by a 1:100 ratio, while the least effective transfer occurred at a 1:1 ratio. This finding contrasts with the conclusions reported by Hamilton et al. (2019), who conducted a study aiming to facilitate efficient inter-species conjugative transfer of a CRISPR nuclease for targeted bacterial elimination (Hamilton et al., 2019). They demonstrated the efficacy of plasmids utilizing the IncP RK2 conjugative system as carriers for a TevSpCas9 dual nuclease. In their assessment of th optimal donor-to-recipient ratio, *E. coli* served as the donor, and *S. enterica* as the recipient. Their findings showed that higher donor-to-recipient ratios (1:1, 10:1, and 50:1) led to a greater number of transconjugants per recipient compared to experiments utilizing lower donor-to-recipient ratios (1:5 or 1:10). However, if you want to eliminate all target organisms then it makes sense to outnumber the recipients whereas if the aim is to understand efficiency per donor it makes more sense to avoid limiting apparent transfers by the availability of recipients.

Initiating this study with the verification of the fertility inhibition phenotype of plasmid F against RK2 was crucial. Without confirming the inhibition of RK2 by the F plasmid, the entire study would lack significance and utility. In assessing the transfer efficiencies of two

distinct plasmids at designated time intervals, the methodology involved separate overnight culturing of the strains in Luria-Bertani (LB) broth at 37°C, followed by the preparation of 1:10 mixtures of donor and recipient strains. Five 20 µL spots of the donor-recipient mixture were then deposited onto LB agar plates to serve as controls and represent different time points during the mating process.

Mating was terminated at specific intervals (10, 30, 50, 180, and 240 minutes), with the LB agar spots excised and suspended in 1 ml of 0.85% (w/v) saline solution. Serial dilutions were made from 10^{-1} to 10^{-7}, and 20µL of each dilution was spotted onto selective plates, followed by overnight incubation at 37°C. The subsequent enumeration of colonies provided insights into the transfer efficiencies of the plasmids under investigation, offering a systematic understanding of bacterial conjugation dynamics over time.

The present investigation confirmed the adverse effect of the F' plasmid on the conjugative transfer of the IncP plasmid, consistent with earlier findings (Miller et al., 1985). Additionally, considering the feedback from the examiner, it is important to note that this method involves the creation of a biofilm where the movement of donors and recipients relative to each other is limited once the biofilm is formed.

Moreover, it would be beneficial to conduct experiments to evaluate transfer frequencies in liquid cultures to complement the findings from solid medium experiments. Addressing the separation of concerns related to transfer events from donor to recipient versus the growth of transconjugants post-transfer is also a critical aspect that can be explored further, aligning with existing literature that delves into determining transfer frequency while mitigating potential confounding factors.

The results of this study confirmed that the R388, R64, and F plasmids all possess the capability to inhibit RK2 transfer when present in the donor strain, individually and when two plasmids are concurrently present. In individual tests, R388 exhibited the highest inhibitory effect on RK2 transfer capability, followed by R64, while F demonstrated the least inhibition. However, upon combining F with other inhibiton sources, the most pronounced inhibition of RK2 transfer occurred with R64 and F together, surpassing the inhibition achieved by R388 in conjunction with F. One possible explanation for this observation is that both R64 and F plasmids generate PifC. In the presence of both plasmids, the cumulative amount of PifC is higher, thereby resulting in increased inhibition. However, in the presence of F and R388 the interaction between F and R388 has a negative impact on R388 as shown in Figure 6.1.

The PifC produced by F not only inhibits RK2 transfer but also has the ability to inhibit R388 transfer by targeting the TrwB coupling protein, which plays a role in the processing of conjugative DNA before the transfer of the R388 plasmid, as confirmed by (Miller et al., 1985). Since F limits the spread of R388, RK2 can evade this restriction by transferring into bacteria that have not yet acquired R388.

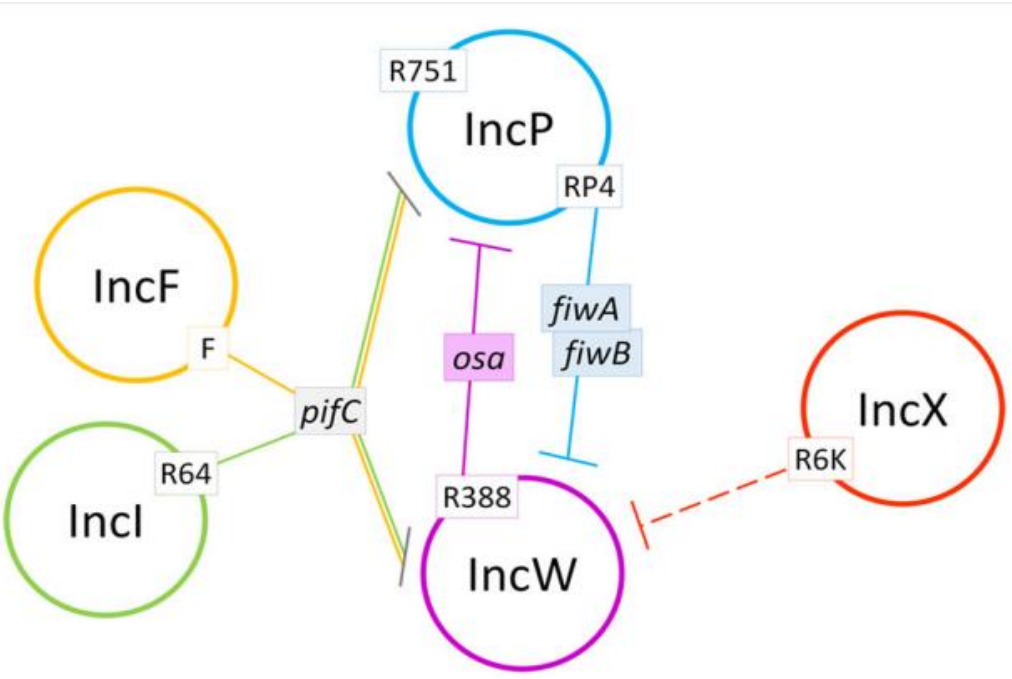

Figure 6.1 Plasmid interactions between plasmid incompatibility groups (Getino et al., 2017).

6.2.2 Getting a mutant of conjugative pCURE that is able to transfer without being suppressed by other plasmids.

The main goal of inserting the *traG* gene from pUB307 into the pACYC184 vector was to facilitate targeted mutagenesis specifically on the *traG* gene from pUB307, while preventing any unintended mutations in other segments of pUB307. The examination of the cloned pACYC184-traG vector revealed a remarkably intriguing and noteworthy outcome. The primary aim of the experiment was to check that F plasmid still inhibited transfer of pUB307 when *traG* was provided on the pACYC184-traG vector and subsequently compare these effects upon introducing a mutation into pACYC184-traG. Surprisingly, the pACYC184-traG exhibited the capability to overcome inhibition by the F plasmid even in the absence of any mutation as described in Chapter 4 section 4.3.2. This unexpected finding suggested a significant correlation between the expression level of *traG* and the ability to escape inhibition by the F plasmid. This phenomenon was investigated in Chapter Five of this study.

To generate a modified version of pUB307, homologous recombination was utilized to remove the *traG* gene. The experimental results confirmed the successful deletion of the *traG* gene from pUB307, leading to the creation of pUBΔ. The validation of the deletion involved assessing whether pUBΔ could transfer independently and comparing it with the transfer capability of pUBΔ in combination with pACYC184-oriT-traG. The findings indicated that pUBΔ could not autonomously undergo transfer, whereas successful transfer occurred when pACYC184-traG-oriT was present. This outcome provides strong support for the hypothesis of *traG* gene deletion, in line with the study by Álvarez-Rodríguez et al. (2020), which underscores the significant role of the TraG coupling protein in facilitating plasmid transfer during conjugation.

Furthermore, the inclusion of *oriT* in our constructs served a crucial purpose. By incorporating *oriT*, we aimed to aid in the isolation of mutants resistant to inhibition by PifC. Without *oriT*, the pACYC-traG plasmid would remain confined within the donor strain, leading to a scenario where only a one-step transfer, solely from the initial donor, would be possible. This limitation would significantly alter the dynamics within the population, as the ability for multi-step transfers would be compromised, thereby affecting the genetic exchange processes within bacterial communities. Therefore, the presence of *oriT* plays a vital role in not only facilitating mutant isolation but also in shaping the transfer dynamics and genetic dissemination patterns within bacterial populations.

Moving to the study focused on isolating a mutation in the *traG* gene, a specific base within a C-G base pair in the gene sequence was targeted for alteration to a T-A base pair through Hydroxylamine mutagenesis. The objective was to implement a modification that would

preserve the essential function of the *traG* gene while granting it the ability to evade inhibition from F.

To isolate a mutant able to escape *pifC* fertility inhibition, a procedure described in Chapter four, Section 4.3.7 was used. It was very encouraging that the procedure gave a strain that successfully escaped inhibition from PifC at t=10 minutes, in contrast to the wild-type *traG*. Further experiments were undertaken to examine the potential mutation, with a focus on identifying any sequence changes.

Upon conducting full-length plasmid sequencing for both the wild-type pACYC184-traG and the potential mutant pACYC184-traG, it was observed that the sequence of the potential mutant was identical to the starting monomeric plasmid but that it was trimer. Significantly, the quantity of plasmid DNA in the trimer was nearly double that of the monomer as shown in Chapter four, Section 4.3.10, Table 4.6. This observation could offer a reasonable explanation for the change in phenotype. The higher amount of DNA implies an increased copy number of the *traG* gene and thus raised *traG* expression, thereby enhancing its ability to escape inhibition. This finding aligns with the similar ability of pACYC-traG to escape PifC inhibition at 30 and 60 minutes when pUB037 was inhibited. Moreover, it supports the hypothesis that reinserting *traG* with high expression in pUB307 should enable it to escape inhibition.

6.2.3 Strategy for deriving pCURE plasmids that are resistant to fertility inhibition

The primary objective of this study was to develop a comprehensive solution for addressing the fertility inhibition resistance (FIR) challenge associated with pCURE plasmids. This goal

was accomplished by inserting *traG*, coupled with a tet-promoter to enhance *traG* expression, into the pCURE plasmid as explained in Chapter 5 section 5.3.1.4. The findings of this research affirm the ability of the modified pCURE plasmid, resulting in raised *traG* expression, to avoid inhibition from the F plasmid. This strategic approach offers several advantages, including its broad applicability and the potential for the pCURE plasmid to overcome multiple sources of inhibition such as R388 and R64 with a unified solution. Importantly, this strategy does not compromise the plasmid's transferability or its primary function. The findings align with those of (Willetts, 1980), who observed that increasing *traD* expression allowed it to overcome pJN7 inhibition as was discussed in Chapter five Section 5.4.1.

The outcomes of this study suggest that the proposed approach might be applicable to additional plasmids experiencing inhibition from different sources targeting their coupling proteins. Increasing the expression of the targeted gene, as shown in this study, presents a promising strategy for overcoming inhibitory challenges of this nature.

6.3 Future works

Despite the effectiveness of raising the expression of *traG* gene proved to be a comprehensive and effective solution, it is crucial to recognize that indiscriminate enhancements in expression may not consistently yield favourable outcomes. There can be instances where heightened expression negatively impacts gene functionality. For instance, in Chapter four, section 4.3.4, the introduction of IPTG to increase *pifC* gene expression had an adverse effect on the inhibitory capability of *pifC*.

Hence, it becomes imperative to carefully evaluate the consequences of raising *traG* expression. For instance, in this study, when *traG* expression was increased in pUBΔ+, it was successfully able to escape the inhibition from F. Notably, higher *traG* expression in bacteria with pACYC-traG demonstrated increased efficacy in escaping the inhibitory capabilities than pUBΔ+. To find the best expression level, necessitates testing different levels of *traG* expression, potentially involving the creation of a dose-response curve to identify an optimal level. This cautious approach should ensure a nuanced understanding of the impact of *traG* expression on the system, avoiding potential disadvantages and optimizing the desired outcome.

To enhance the mutagenesis process aimed at obtaining a mutant capable of escaping fertility inhibition, it is advisable to repeat the study using hydroxylamine mutagenesis. For this study, hydroxylamine mutagenesis was conducted at a temperature of 37°C. However, a critical adjustment could involve exploring a temperature range spanning from 30°C to 70°C degrees. This modification should identify the optimal reactivity of hydroxylamine, potentially amplifying its efficacy in inducing DNA damage (Chu et al., 2018).

A strategic use of this approach could involve manipulating both incubation time and temperature, with potential intervals of 16, 20, and 24 hours. This nuanced experimentation allows for a more comprehensive exploration of hydroxylamine mutagenesis, offering the opportunity to achieve a significant level of mutagenesis. By systematically varying these parameters, the study can uncover optimal conditions for enhancing the mutagenic potential of hydroxylamine. Consequently, this approach should increase the chance of obtaining the desired mutant capable of escaping F inhibition and effectively performing its intended functional role.

In order to engineer a targeted mutation in *traG* aimed at evading p inhibition, precise identification of the crucial TraG–PifC interaction region responsible for fertility inhibition through protein structure modeling and examination of their protein-protein interactions is essential. This would initially involve homology modeling TraG and PifC proteins using tools like SWISS-MODEL or Phyre2, followed by molecular docking simulations with software such as AutoDock or HADDOCK to predict binding sites. Then, the docked complexes would be analyzed to pinpoint key interaction residues, which would be further validated using experimental techniques like co-immunoprecipitation or surface plasmon resonance. This iterative process should build a comprehensive understanding of the structural basis of TraG-PifC interaction, facilitating the rational design of targeted mutations in TraG to disrupt or modulate this interaction and enable evasion of *pifC*-mediated fertility inhibition in bacterial conjugation (Schwede et al., 2003).

Schwede et al. (2003) introduced SWISS-MODEL, an automated protein homology-modeling server designed to facilitate the generation of three-dimensional protein models based on homologous structures. Their work aimed to provide a user-friendly and reliable tool for researchers. They outlined the methodology used by SWISS-MODEL, including sequence alignment, template selection, model building, and evaluation. Through rigorous assessment, they demonstrated the server's ability to produce high-quality protein models with accuracy and reliability comparable to other modeling methods. SWISS-MODEL's user-friendly interface and accessibility made it widely utilized in various fields such as structural biology, drug discovery, and protein engineering, empowering researchers worldwide with a powerful tool for predicting protein structures and advancing scientific understanding (Schwede et al., 2003).

This was a part of my PhD project when I started, and this is why Peter Winn was assigned as my co-supervisor. However, since Peter Winn left the university, and we discovered a new strategy to overcome inhibition by increasing *traG* expression, the project plan was revised (Schwede et al., 2003).

The research detailed in this thesis not only provides a comprehensive and universal solution for enhancing the efficacy of the curing plasmid pCURE-F-307 in overcoming fertility inhibition (FIR) but also lays the foundation for broader applications and potential advancements in genetic engineering. The significance of successfully addressing FIR lies in the ability to elevate the expression of the targeted gene. In simpler terms, increasing the expression of gene targeted by the inhibitory plasmid could be a general approach for any plasmid to overcome fertility inhibition.

Recently, our lab has taken a keen interest in creating a new pCURE plasmid using IncI2, specifically plasmid TP114. It is significant to explore whether IncI2 plasmids are susceptible to fertility inhibition and to assess the presence of the TraG homologue. If the TraG homologue is identified, it would be worthwhile to employ a similar strategy for this specific plasmid.

Importantly, the improved capacity of pUBΔ+ to overcome FIR should translate into an increased efficacy of pCURE-F-307 in displacing plasmids carrying antibiotic resistance genes, particularly those of the IncF type. This achievement assumes critical importance in the broader context of reducing the burden of antibiotic resistance, a paramount concern for the continued progress of medical sciences (Pitout and Laupland, 2008). The technology

described in this research appears as a promising component of the solution to address this global challenge, showcasing its potential to contribute significantly to the ongoing actions in mitigating antibiotic resistance and fostering sustainable medical practices.

Undertaking comprehensive and longterm studies with pCURE is very important to fully evaluate its effectiveness in providing plasmid displacement on a large scale within a population. These thorough investigations aim not only to uncover the future potential applications of pCURE but also to establish its suitability for human use. The critical step of addressing biosafety concerns is imperative before contemplating the transition of this technology into human applications.

References

ADAMCZYK, M. & JAGURA-BURDZY, G. 2003. Spread and survival of promiscuous IncP-1 plasmids. *Acta Biochim Pol,* 50**,** 425-53.

ALDERLIESTEN, J. B., DUXBURY, S. J. N., ZWART, M. P., DE VISSER, J., STEGEMAN, A. & FISCHER, E. A. J. 2020. Effect of donor-recipient relatedness on the plasmid conjugation frequency: a meta-analysis. *BMC Microbiol,* 20**,** 135.

ALOS, J.-I. 2014. Antibiotic resistance: A global crisis. *Enfermedades infecciosas y microbiologia clinica,* 33**,** 692-699.

ÁLVAREZ-RODRÍGUEZ, I., ARANA, L., UGARTE-URIBE, B., GÓMEZ-RUBIO, E., MARTÍN-SANTAMARÍA, S., GARBISU, C. & ALKORTA, I. 2020a. Type IV Coupling Proteins as Potential Targets to Control the Dissemination of Antibiotic Resistance. *Front Mol Biosci,* 7**,** 201.

ÁLVAREZ-RODRÍGUEZ, I., UGARTE-URIBE, B., DE LA ARADA, I., ARRONDO, J. L. R., GARBISU, C. & ALKORTA, I. 2020b. Conjugative Coupling Proteins and the Role of Their Domains in Conjugation, Secondary Structure and in vivo Subcellular Location. *Front Mol Biosci,* 7**,** 185.

AMBERG, D. C., BURKE, D. J. & STRATHERN, J. N. 2006. Hydroxylamine mutagenesis of plasmid DNA. *CSH Protoc,* 2006.

APPLEYARD, R. K. 1954. Segregation of New Lysogenic Types during Growth of a Doubly Lysogenic Strain Derived from Escherichia Coli K12. *Genetics,* 39**,** 440-52.

ASHBOLT, N. J., AMÉZQUITA, A., BACKHAUS, T., BORRIELLO, P., BRANDT, K. K., COLLIGNON, P., COORS, A., FINLEY, R., GAZE, W. H., HEBERER, T., LAWRENCE, J. R., LARSSON, D. G., MCEWEN, S. A., RYAN, J. J., SCHÖNFELD, J., SILLEY, P., SNAPE, J. R., VAN DEN EEDE, C. & TOPP, E.

2013. Human Health Risk Assessment (HHRA) for environmental development and transfer of antibiotic resistance. *Environ Health Perspect,* 121**,** 993-1001.

BAXTER, J. C. & FUNNELL, B. E. 2015. Plasmid partition mechanisms. *Plasmids: biology and impact in biotechnology and discovery***,** 133-155.

BEN, Y., FU, C., HU, M., LIU, L., WONG, M. H. & ZHENG, C. 2019. Human health risk assessment of antibiotic resistance associated with antibiotic residues in the environment: A review. *Environ Res,* 169**,** 483-493.

BENNETT, P. M. 2008. Plasmid encoded antibiotic resistance: acquisition and transfer of antibiotic resistance genes in bacteria. *Br J Pharmacol,* 153 Suppl 1**,** S347-57.

BERTANI, G. 1951. Studies on lysogenesis. I. The mode of phage liberation by lysogenic Escherichia coli. *J Bacteriol,* 62**,** 293-300.

BINGLE, L. E. & THOMAS, C. M. 2001. Regulatory circuits for plasmid survival. *Current Opinion in Microbiology,* 4**,** 194-200.

BIRNBOIM, H. & DOLY, J. 1979. A rapid alkaline extraction procedure for screening recombinant plasmid DNA. *Nucleic acids research,* 7**,** 1513-1523.

BLAIR, J. M., WEBBER, M. A., BAYLAY, A. J., OGBOLU, D. O. & PIDDOCK, L. J. 2015. Molecular mechanisms of antibiotic resistance. *Nat Rev Microbiol,* 13**,** 42-51.

BLATNY, J. M., BRAUTASET, T., WINTHER-LARSEN, H. C., HAUGAN, K. & VALLA, S. 1997. Construction and use of a versatile set of broad-host-range cloning and expression vectors based on the RK2 replicon. *Applied and environmental microbiology,* 63**,** 370-379.

BOYD, D. A., TYLER, S., CHRISTIANSON, S., MCGEER, A., MULLER, M. P., WILLEY, B. M., BRYCE, E., GARDAM, M., NORDMANN, P. & MULVEY, M. R. 2004. Complete nucleotide sequence of a 92-kilobase plasmid harboring the CTX-M-

15 extended-spectrum beta-lactamase involved in an outbreak in long-term-care facilities in Toronto, Canada. *Antimicrobial agents and chemotherapy,* 48**,** 3758-3764.

BOYD, E. F., HILL, C. W., RICH, S. M. & HARTL, D. L. 1996. Mosaic structure of plasmids from natural populations of Escherichia coli. *Genetics,* 143**,** 1091-100.

BOYER, H. W. & ROULLAND-DUSSOIX, D. 1969. A complementation analysis of the restriction and modification of DNA in Escherichia coli. *J Mol Biol,* 41**,** 459-72.

BRINGEL, F., FREY, L. & HUBERT, J.-C. 1989. Characterization, cloning, curing, and distribution in lactic acid bacteria of pLP1, a plasmid from Lactobacillus plantarum CCM 1904 and its use in shuttle vector construction. *Plasmid,* 22**,** 193-202.

BURKARDT, H.-J., RIESS, G. & PÜHLER, A. 1979. Relationship of group P1 plasmids revealed by heteroduplex experiments: RP1, RP4, R68 and RK2 are identical. *Microbiology,* 114**,** 341-348.

CAMPS, M. 2010. Modulation of ColE1-like plasmid replication for recombinant gene expression. *Recent Patents on DNA & Gene Sequences (Discontinued),* 4**,** 58-73.

CARATTOLI, A. 2009. Resistance plasmid families in Enterobacteriaceae. *Antimicrob Agents Chemother,* 53**,** 2227-38.

CARATTOLI, A. 2013. Plasmids and the spread of resistance. *International journal of medical microbiology,* 303**,** 298-304.

CHANG, A. C. & COHEN, S. N. 1978. Construction and characterization of amplifiable multicopy DNA cloning vehicles derived from the P15A cryptic miniplasmid. *J Bacteriol,* 134**,** 1141-56.

CHATTORAJ, D. K. 2000. Control of plasmid DNA replication by iterons: no longer paradoxical. *Molecular microbiology,* 37**,** 467-476.

CHEN, Z., YUAN, Y., HU, Q., ZHU, A., CHEN, F., LI, S., GUAN, X., LV, C., TANG, T. & HE, Y. 2024. SARS-CoV-2 immunity in animal models. *Cellular & Molecular Immunology***,** 1-15.

CHO, I., YAMANISHI, S., COX, L., METHÉ, B. A., ZAVADIL, J., LI, K., GAO, Z., MAHANA, D., RAJU, K., TEITLER, I., LI, H., ALEKSEYENKO, A. V. & BLASER, M. J. 2012. Antibiotics in early life alter the murine colonic microbiome and adiposity. *Nature,* 488**,** 621-6.

CHU, X. L., ZHANG, B. W., ZHANG, Q. G., ZHU, B. R., LIN, K. & ZHANG, D. Y. 2018. Temperature responses of mutation rate and mutational spectrum in an Escherichia coli strain and the correlation with metabolic rate. *BMC Evol Biol,* 18**,** 126.

COHEN, S. N., CHANG, A. C. & HSU, L. 1972. Nonchromosomal antibiotic resistance in bacteria: genetic transformation of Escherichia coli by R-factor DNA. *Proceedings of the National Academy of Sciences,* 69**,** 2110-2114.

COLLINS, L. A. & THUNE, R. L. 1996. Development of a Defined Minimal Medium for the Growth of Edwardsiella ictaluri. *Appl Environ Microbiol,* 62**,** 848-52.

COURVALIN, P. 2016. Why is antibiotic resistance a deadly emerging disease? *Clin Microbiol Infect,* 22**,** 405-7.

CZAPLEWSKI, L., BAX, R., CLOKIE, M., DAWSON, M., FAIRHEAD, H., FISCHETTI, V. A., FOSTER, S., GILMORE, B. F., HANCOCK, R. E. & HARPER, D. 2016a. Alternatives to antibiotics—a pipeline portfolio review. *The Lancet infectious diseases,* 16**,** 239-251.

CZAPLEWSKI, L., BAX, R., CLOKIE, M., DAWSON, M., FAIRHEAD, H., FISCHETTI, V. A., FOSTER, S., GILMORE, B. F., HANCOCK, R. E., HARPER, D., HENDERSON, I. R., HILPERT, K., JONES, B. V., KADIOGLU, A., KNOWLES, D., ÓLAFSDÓTTIR, S., PAYNE, D., PROJAN, S., SHAUNAK, S., SILVERMAN,

J., THOMAS, C. M., TRUST, T. J., WARN, P. & REX, J. H. 2016b. Alternatives to antibiotics-a pipeline portfolio review. *Lancet Infect Dis,* 16**,** 239-51.

DAVIES, J. & DAVIES, D. 2010. Origins and evolution of antibiotic resistance. *Microbiol Mol Biol Rev,* 74**,** 417-33.

DE OLIVEIRA, G. A., MARQUES, M. D. A., CRUZEIRO-SILVA, C., CORDEIRO, Y., SCHUABB, C., MORAES, A. H., WINTER, R., OSCHKINAT, H., FOGUEL, D. & FREITAS, M. S. 2016. Structural basis for the dissociation of α-synuclein fibrils triggered by pressure perturbation of the hydrophobic core. *Scientific reports,* 6**,** 37990.

DEL SOLAR, G., GIRALDO, R., RUIZ-ECHEVARRÍA, M. J., ESPINOSA, M. & DÍAZ-OREJAS, R. 1998. Replication and control of circular bacterial plasmids. *Microbiology and molecular biology reviews,* 62**,** 434-464.

FINERAN, P. C., BLOWER, T. R., FOULDS, I. J., HUMPHREYS, D. P., LILLEY, K. S. & SALMOND, G. P. 2009. The phage abortive infection system, ToxIN, functions as a protein–RNA toxin–antitoxin pair. *Proceedings of the National Academy of Sciences,* 106**,** 894-899.

FROST, L. S., IPPEN-IHLER, K. & SKURRAY, R. A. 1994. Analysis of the sequence and gene products of the transfer region of the F sex factor. *Microbiological reviews,* 58**,** 162-210.

GARCÍA-QUINTANILLA, M., PRIETO, A. I., BARNES, L., RAMOS-MORALES, F. & CASADESÚS, J. 2006. Bile-induced curing of the virulence plasmid in Salmonella enterica serovar Typhimurium. *Journal of bacteriology,* 188**,** 7963-7965.

GARCILLÁN-BARCIA, M. P. & DE LA CRUZ, F. 2008. Why is entry exclusion an essential feature of conjugative plasmids? *Plasmid,* 60**,** 1-18.

GERDES, K., CHRISTENSEN, S. K. & LØBNER-OLESEN, A. 2005. Prokaryotic toxin–antitoxin stress response loci. *Nature Reviews Microbiology,* 3**,** 371-382.

GETINO, M., PALENCIA-GÁNDARA, C., GARCILLÁN-BARCIA, M. P. & DE LA CRUZ, F. 2017. PifC and Osa, Plasmid Weapons against Rival Conjugative Coupling Proteins. *Front Microbiol,* 8**,** 2260.

GOMES, L., MONTEIRO, G. & MERGULHÃO, F. 2020. The Impact of IPTG Induction on Plasmid Stability and Heterologous Protein Expression by Escherichia coli Biofilms. *Int J Mol Sci,* 21.

GOODELL, J. W. 2020. COVID-19 and finance: Agendas for future research. *Finance research letters,* 35**,** 101512.

GORNALL, A. G., BARDAWILL, C. J. & DAVID, M. M. 1949. Determination of serum proteins by means of the biuret reaction. *J. biol. Chem,* 177**,** 751-766.

GRINSTED, J., BENNETT, P. M. & RICHMOND, M. H. 1977. A restriction enzyme map of R-plasmid RP1. *Plasmid,* 1**,** 34-7.

GROSS, P. 1985. Biologic activity of hydroxylamine: a review. *Crit Rev Toxicol,* 14**,** 87-99.

GROZDANOV, L., RAASCH, C., SCHULZE, J., SONNENBORN, U., GOTTSCHALK, G., HACKER, J. & DOBRINDT, U. 2004. Analysis of the genome structure of the nonpathogenic probiotic Escherichia coli strain Nissle 1917. *J Bacteriol,* 186**,** 5432-41.

GUBBINS, M. J., ARTHUR, D. C., GHETU, A. F., GLOVER, J. M. & FROST, L. S. 2003. Characterizing the structural features of RNA/RNA interactions of the F-plasmid FinOP fertility inhibition system. *Journal of Biological Chemistry,* 278**,** 27663-27671.

HAINES, A. S. 2001. *Studies on the active Partitioning system of the IncP-1 plasmids RK2 and R751*. University of Birmingham.

HALE, L., LAZOS, O., HAINES, A. & THOMAS, C. 2010. An efficient stress-free strategy to displace stable bacterial plasmids. *Biotechniques,* 48**,** 223-8.

HAMILTON, T. A., PELLEGRINO, G. M., THERRIEN, J. A., HAM, D. T., BARTLETT, P. C., KARAS, B. J., GLOOR, G. B. & EDGELL, D. R. 2019. Efficient inter-species conjugative transfer of a CRISPR nuclease for targeted bacterial killing. *Nat Commun,* 10**,** 4544.

HANAHAN, D. 1983. Studies on transformation of Escherichia coli with plasmids. *J Mol Biol,* 166**,** 557-80.

HAYES, F. & VAN MELDEREN, L. 2011. Toxins-antitoxins: diversity, evolution and function. *Critical reviews in biochemistry and molecular biology,* 46**,** 386-408.

HEDGES, R. & DATTA, N. 1973. Plasmids determining I pili constitute a compatibility complex. *Microbiology,* 77**,** 19-25.

HERSHFIELD, V., BOYER, H. W., YANOFSKY, C., LOVETT, M. A. & HELINSKI, D. R. 1974. Plasmid ColEl as a molecular vehicle for cloning and amplification of DNA. *Proc Natl Acad Sci U S A,* 71**,** 3455-9.

HOOPER, D., WOLFSON, J., MCHUGH, G., SWARTZ, M., TUNG, C. & SWARTZ, M. 1984. Elimination of plasmid pMG110 from Escherichia coli by novobiocin and other inhibitors of DNA gyrase. *Antimicrobial agents and chemotherapy,* 25**,** 586-590.

HOVI, M., SUKUPOLVI, S., EDWARDS, M. F. & RHEN, M. 1988. Plasmid-associated virulence of Salmonella enteritidis. *Microbial pathogenesis,* 4**,** 385-391.

HU, B., KHARA, P. & CHRISTIE, P. J. 2019. Structural bases for F plasmid conjugation and F pilus biogenesis in Escherichia coli. *Proc Natl Acad Sci U S A,* 116**,** 14222-14227.

JAGURA-BURDZY, G., IBBOTSON, J. P. & THOMAS, C. M. 1991. The korF region of broad-host-range plasmid RK2 encodes two polypeptides with transcriptional repressor activity. *J Bacteriol,* 173**,** 826-33.

KHAN, S. A. 2005. Plasmid rolling-circle replication: highlights of two decades of research. *Plasmid,* 53**,** 126-136.

KONIECZNY, I., BURY, K., WAWRZYCKA, A. & WEGRZYN, K. 2015. Iteron plasmids. *Plasmids: Biology and Impact in Biotechnology and Discovery***,** 13-32.

KONIECZNY, I. & HELINSKI, D. R. 1997. Helicase delivery and activation by DnaA and TrfA proteins during the initiation of replication of the broad host range plasmid RK2. *J Biol Chem,* 272**,** 33312-8.

KORNACKI, J., CHANG, C.-H. & FIGURSKI, D. 1993. kil-kor regulon of promiscuous plasmid RK2: structure, products, and regulation of two operons that constitute the kilE locus. *Journal of bacteriology,* 175**,** 5078-5090.

KRAUSE, M. & GUINEY, D. 1991. Identification of a multimer resolution system involved in stabilization of the Salmonella dublin virulence plasmid pSDL2. *Journal of bacteriology,* 173**,** 5754-5762.

LAMPKOWSKA, J., FELD, L., MONAGHAN, A., TOOMEY, N., SCHJØRRING, S., JACOBSEN, B., VAN DER VOET, H., ANDERSEN, S. R., BOLTON, D., AARTS, H., KROGFELT, K. A., WILCKS, A. & BARDOWSKI, J. 2008. A standardized conjugation protocol to asses antibiotic resistance transfer between lactococcal species. *Int J Food Microbiol,* 127**,** 172-5.

LANKA, E. & WILKINS, B. M. 1995. DNA processing reactions in bacterial conjugation. *Annual review of biochemistry,* 64**,** 141-169.

LAWLEY, T., KLIMKE, W., GUBBINS, M. & FROST, L. 2003. F factor conjugation is a true type IV secretion system. *FEMS microbiology letters,* 224**,** 1-15.

LAZDINS, A., MAURYA, A. P., MILLER, C. E., KAMRUZZAMAN, M., LIU, S., STEPHENS, E. R., LLOYD, G. S., HARATIANFAR, M., CHAMBERLAIN, M., HAINES, A. S., KREFT, J. U., WEBBER, M. A., IREDELL, J. & THOMAS, C. M. 2020. Potentiation of curing by a broad-host-range self-transmissible vector for displacing resistance plasmids to tackle AMR. *PLoS One,* 15**,** e0225202.

LEDERBERG, J. 1998. Plasmid (1952-1997). *Plasmid,* 39**,** 1-9.

LERMINIAUX, N. A., MACKENZIE, K. D. & CAMERON, A. D. S. 2020. Salmonella Pathogenicity Island 1 (SPI-1): The Evolution and Stabilization of a Core Genomic Type Three Secretion System. *Microorganisms,* 8.

LILLY, J. & CAMPS, M. 2015. Mechanisms of theta plasmid replication. *Microbiology spectrum,* 3**,** 10.1128/microbiolspec. plas-0029-2014.

LLOR, C. & BJERRUM, L. 2014. Antimicrobial resistance: risk associated with antibiotic overuse and initiatives to reduce the problem. *Ther Adv Drug Saf,* 5**,** 229-41.

LOPATKIN, A. J., MEREDITH, H. R., SRIMANI, J. K., PFEIFFER, C., DURRETT, R. & YOU, L. 2017. Persistence and reversal of plasmid-mediated antibiotic resistance. *Nat Commun,* 8**,** 1689.

LU, W., CHAI, Q., ZHONG, M., YU, L., FANG, J., WANG, T., LI, H., ZHU, H. & WEI, Y. 2013. Assembling of AcrB Trimer in Cell Membrane (vol 423, pg 123, 2012). *JOURNAL OF MOLECULAR BIOLOGY,* 425**,** 968-968.

MAKAROVA, K. S., HAFT, D. H., BARRANGOU, R., BROUNS, S. J., CHARPENTIER, E., HORVATH, P., MOINEAU, S., MOJICA, F. J., WOLF, Y. I. & YAKUNIN, A. F. 2011. Evolution and classification of the CRISPR–Cas systems. *Nature Reviews Microbiology,* 9**,** 467-477.

MATSON, S. W. & RAGONESE, H. 2005. The F-plasmid TraI protein contains three functional domains required for conjugative DNA strand transfer. *Journal of bacteriology,* 187**,** 697-706.

MILLER, J. F., LANKA, E. & MALAMY, M. H. 1985. F factor inhibition of conjugal transfer of broad-host-range plasmid RP4: requirement for the protein product of pif operon regulatory gene pifC. *J Bacteriol,* 163**,** 1067-73.

MILLER, J. H. 1972. Experiments in molecular genetics. *(No Title)*.

MRUK, I. & KOBAYASHI, I. 2014. To be or not to be: regulation of restriction–modification systems and other toxin–antitoxin systems. *Nucleic acids research,* 42**,** 70-86.

MULEC, J., STARCIC, M. & ZGUR-BERTOK, D. 2002. F-like plasmid sequences in enteric bacteria of diverse origin, with implication of horizontal transfer and plasmid host range. *Curr Microbiol,* 44**,** 231-5.

NI, B., DU, Z., GUO, Z., ZHANG, Y. & YANG, R. 2008. Curing of four different plasmids in Yersinia pestis using plasmid incompatibility. *Letters in applied microbiology,* 47**,** 235-240.

NICHOLAS, B. & AUDETTE, G. F. 2022. Solution characterization of the dynamic conjugative entry exclusion protein TraG. *Structural Dynamics,* 9.

NICOLA, M., ALSAFI, Z., SOHRABI, C., KERWAN, A., AL-JABIR, A., IOSIFIDIS, C., AGHA, M. & AGHA, R. 2020. The socio-economic implications of the coronavirus pandemic (COVID-19): A review. *Int J Surg,* 78**,** 185-193.

NORDMANN, P., NAAS, T. & POIREL, L. 2011. Global spread of carbapenemase-producing Enterobacteriaceae. *Emerging infectious diseases,* 17**,** 1791.

NORMAN, A., HANSEN, L. H. & SØRENSEN, S. J. 2009. Conjugative plasmids: vessels of the communal gene pool. *Philos Trans R Soc Lond B Biol Sci,* 364**,** 2275-89.

NOVICK, R. P. 1987. Plasmid incompatibility. *Microbiological reviews,* 51**,** 381-395.

O'NEILL, J. 2016. Tackling drug-resistant infections globally: final report and recommendations.

PANSEGRAU, W., LANKA, E., BARTH, P. T., FIGURSKI, D. H., GUINEY, D. G., HAAS, D., HELINSKI, D. R., SCHWAB, H., STANISICH, V. A. & THOMAS, C. M. 1994. Complete nucleotide sequence of Birmingham IncPα plasmids: compilation and comparative analysis. *Journal of molecular biology,* 239**,** 623-663.

PARTRIDGE, S. R., KWONG, S. M., FIRTH, N. & JENSEN, S. O. 2018. Mobile genetic elements associated with antimicrobial resistance. *Clinical microbiology reviews,* 31**,** 10.1128/cmr. 00088-17.

PERRY, J., WAGLECHNER, N. & WRIGHT, G. 2016. The Prehistory of Antibiotic Resistance. *Cold Spring Harb Perspect Med,* 6.

PITOUT, J. D. & LAUPLAND, K. B. 2008. Extended-spectrum β-lactamase-producing Enterobacteriaceae: an emerging public-health concern. *The Lancet infectious diseases,* 8**,** 159-166.

RIED, J. L. & COLLMER, A. 1987. An nptI-sacB-sacR cartridge for constructing directed, unmarked mutations in gram-negative bacteria by marker exchange-eviction mutagenesis. *Gene,* 57**,** 239-246.

ROSENFELD, R. & GROVER, N. 1993. Control of mini-R1 plasmid replication: a computer simulation. *Plasmid,* 29**,** 94-116.

RUIZ-MASÓ, J. A., MACHÓN, C., BORDANABA-RUISECO, L., ESPINOSA, M., COLL, M. & DEL SOLAR, G. 2015. Plasmid rolling-circle replication. *Plasmids: Biology and Impact in Biotechnology and Discovery***,** 45-69.

SANTINI, J. M. & STANISICH, V. A. 1998. Both the fipA gene of pKM101 and the pifC gene of F inhibit conjugal transfer of RP1 by an effect on traG. *J Bacteriol,* 180**,** 4093-101.

SASAKI, Y., TAKETOMO, N. & SASAKI, T. 1988. Factors affecting transfer frequency of pAM beta 1 from Streptococcus faecalis to Lactobacillus plantarum. *Journal of bacteriology,* 170**,** 5939-5942.

SCHÄGGER, H. & VON JAGOW, G. 1987. Tricine-sodium dodecyl sulfate-polyacrylamide gel electrophoresis for the separation of proteins in the range from 1 to 100 kDa. *Analytical biochemistry,* 166**,** 368-379.

SCHRÖDER, G., KRAUSE, S., ZECHNER, E. L., TRAXLER, B., YEO, H. J., LURZ, R., WAKSMAN, G. & LANKA, E. 2002. TraG-like proteins of DNA transfer systems and of the Helicobacter pylori type IV secretion system: inner membrane gate for exported substrates? *J Bacteriol,* 184**,** 2767-79.

SCHWEDE, T., KOPP, J., GUEX, N. & PEITSCH, M. C. 2003. SWISS-MODEL: an automated protein homology-modeling server. *Nucleic acids research,* 31**,** 3381-3385.

SCOTT FRIDKIN, M., BAGGS, J., MD, S. M., MD, P. M., RUBIN, P. M. A., MD, M. H. S., MD, G. D., MD, E. D., JAMES MEEK, M. & KIMBERLY, Y.-H. 2014. Vital signs: improving antibiotic use among hospitalized patients. *Morbidity and mortality weekly report,* 69**,** 194-200.

SELZER, G., SOM, T., ITOH, T. & TOMIZAWA, J.-I. 1983. The origin of replication of plasmid p15A and comparative studies on the nucleotide sequences around the origin of related plasmids. *Cell,* 32**,** 119-129.

SEN, D., YANO, H., SUZUKI, H., KRÓL, J. E., ROGERS, L., BROWN, C. J. & TOP, E. M. 2010. Comparative genomics of pAKD4, the prototype IncP-1δ plasmid with a complete backbone. *Plasmid,* 63**,** 98-107.

SHINTANI, M., TAKAHASHI, Y., YAMANE, H. & NOJIRI, H. 2010. The behavior and significance of degradative plasmids belonging to Inc groups in Pseudomonas within natural environments and microcosms. *Microbes Environ,* 25**,** 253-65.

STEPHENS, C., ARISMENDI, T., WRIGHT, M., HARTMAN, A., GONZALEZ, A., GILL, M., PANDORI, M. & HESS, D. 2020. F plasmids are the major carriers of antibiotic resistance genes in human-associated commensal Escherichia coli. *Msphere,* 5**,** 10.1128/msphere. 00709-20.

SUMMERS, D. 1998. Timing, self-control and a sense of direction are the secrets of multicopy plasmid stability. *Molecular microbiology,* 29**,** 1137-1145.

TAN, L., ZHANG, K. X., PECOT, M. Y., NAGARKAR-JAISWAL, S., LEE, P.-T., TAKEMURA, S.-Y., MCEWEN, J. M., NERN, A., XU, S. & TADROS, W. 2015. Ig superfamily ligand and receptor pairs expressed in synaptic partners in Drosophila. *Cell,* 163**,** 1756-1769.

THOMAS, C. M. 1981. Molecular genetics of broad host range plasmid RK2. *Plasmid,* 5**,** 10-19.

THOMAS, C. M. 2021. Plasmid Incompatibility. *In:* BELL, E. (ed.) *Molecular Life Sciences: An Encyclopedic Reference.* New York, NY: Springer New York.

TIEDJE, J. M., FANG, W., MANAIA, C. M., VIRTA, M., SHENG, H., LIPING, M., ZHANG, T. & EDWARD, T. 2019. Antibiotic resistance genes in the human-impacted environment: a one health perspective. *Pedosphere,* 29**,** 273-282.

TOUKDARIAN, A. E. & HELINSKI, D. R. 1998. TrfA dimers play a role in copy-number control of RK2 replication. *Gene,* 223**,** 205-11.

TREVORS, J. 1986. Plasmid curing in bacteria. *FEMS microbiology reviews,* 1**,** 149-157.

VAN EMBDEN, J., VELTKAMP, E., STUITJE, T., ANDREOLI, P. & NIJKAMP, H. 1978. Integration of a transposable DNA sequence which mediates ampicillin resistance into

Clo DF13 plasmid DNA: determination of the site and orientation of TnA insertions. *Plasmid,* 1**,** 204-217.

WAGNER, E. G. H. & SIMONS, R. W. 1994. Antisense RNA control in bacteria, phages, and plasmids. *Annual review of microbiology,* 48**,** 713-742.

WANG, X., LORD, D. M., CHENG, H.-Y., OSBOURNE, D. O., HONG, S. H., SANCHEZ-TORRES, V., QUIROGA, C., ZHENG, K., HERRMANN, T. & PETI, W. 2012. A new type V toxin-antitoxin system where mRNA for toxin GhoT is cleaved by antitoxin GhoS. *Nature chemical biology,* 8**,** 855-861.

WANG, Y. 2017. Spatial distribution of high copy number plasmids in bacteria. *Plasmid,* 91**,** 2-8.

WILKINS, B. M. 2002. Plasmid promiscuity: meeting the challenge of DNA immigration control. *Environmental Microbiology,* 4**,** 495-500.

WILLETTS, N. 1980. Interactions between the F conjugal transfer system and CloDF13::Tna plasmids. *Mol Gen Genet,* 180**,** 213-7.

WILLETTS, N. & SKURRAY, R. 1980a. The conjugation system of F-like plasmids. *Annu Rev Genet,* 14**,** 41-76.

WILLETTS, N. & SKURRAY, R. 1980b. The conjugation system of F-like plasmids. *Annual review of genetics,* 14**,** 41-76.

WILSON, G. G. & MURRAY, N. E. 1991. Restriction and modification systems. *Annual review of genetics,* 25**,** 585-627.

YANISCH-PERRON, C., VIEIRA, J. & MESSING, J. 1985. Improved M13 phage cloning vectors and host strains: nucleotide sequences of the M13mp18 and pUC19 vectors. *Gene,* 33**,** 103-19.

ZARGHAMPOOR, F., BEHZAD-BEHBAHANI, A., AZARPIRA, N., KHATAMI, S. R., FANIAN, M., AGHDAIE, M. H. & DEHBIDI, G. R. 2020. A single tube overlap

extension PCR method for splicing of multiple DNA fragments. *Avicenna journal of medical biotechnology,* 12**,** 37.

ZATYKA, M., JAGURA-BURDZY, G. & THOMAS, C. M. 1994. Regulation of transfer genes of promiscuous IncP alpha plasmid RK2: repression of Tra1 region transcription both by relaxosome proteins and by the Tra2 regulator TrbA. *Microbiology (Reading),* 140 (Pt 11)**,** 2981-90.

ZECHNER, E. L., LANG, S. & SCHILDBACH, J. F. 2012. Assembly and mechanisms of bacterial type IV secretion machines. *Philos Trans R Soc Lond B Biol Sci,* 367**,** 1073-87.

ZHANG, S., ABBAS, M., REHMAN, M. U., HUANG, Y., ZHOU, R., GONG, S., YANG, H., CHEN, S., WANG, M. & CHENG, A. 2020a. Dissemination of antibiotic resistance genes (ARGs) via integrons in Escherichia coli: A risk to human health. *Environ Pollut,* 266**,** 115260.

ZHANG, X., YAN, S., CHEN, J., TYAGI, R. & LI, J. 2020b. Physical, chemical, and biological impact (hazard) of hospital wastewater on environment: presence of pharmaceuticals, pathogens, and antibiotic-resistance genes. *Current Developments in Biotechnology and Bioengineering.* Elsevier.

ZUKOWSKI, M. M., GAFFNEY, D. F., SPECK, D., KAUFFMANN, M., FINDELI, A., WISECUP, A. & LECOCQ, J.-P. 1983. Chromogenic identification of genetic regulatory signals in Bacillus subtilis based on expression of a cloned Pseudomonas gene. *Proceedings of the National Academy of Sciences,* 80**,** 1101-1105.